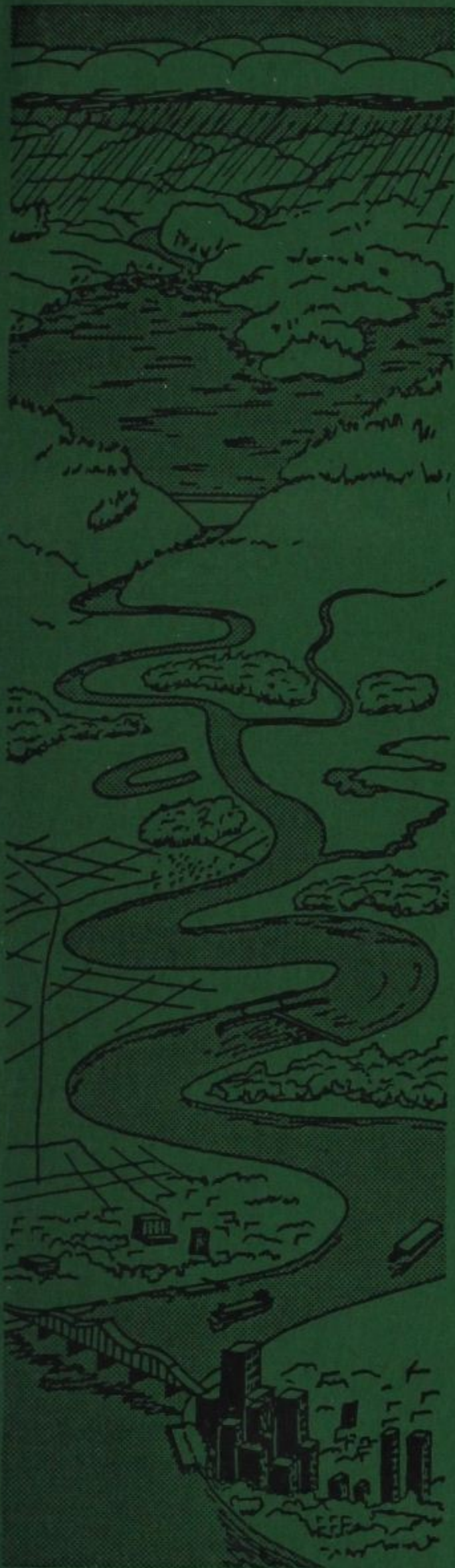




US Army Corps
of Engineers



JS-CE-C Property of the
United States Government
**ENVIRONMENTAL AND WATER QUALITY
OPERATIONAL STUDIES**



INSTRUCTION REPORT E-86-5

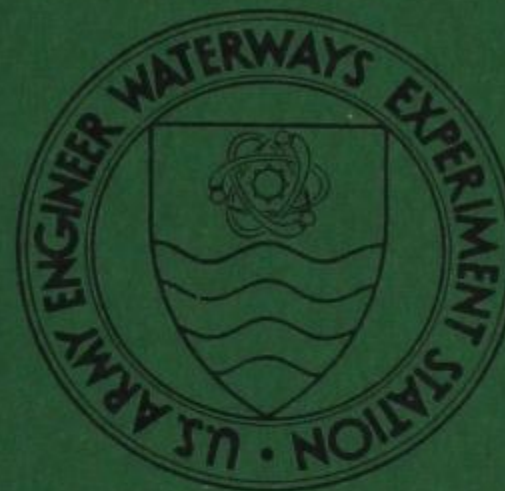
**CE-QUAL-W2: A NUMERICAL
TWO-DIMENSIONAL, LATERALLY AVERAGED
MODEL OF HYDRODYNAMICS AND WATER
QUALITY; USER'S MANUAL**

by

Environmental Laboratory, Hydraulics Laboratory

DEPARTMENT OF THE ARMY
Waterways Experiment Station, Corps of Engineers
PO Box 631, Vicksburg, Mississippi 39180-0631

BOOKS ARE ACCOUNTABLE PROPERTY CHARGED
TO AN INDIVIDUAL BY NAME. PLEASE DO
NOT LEND TO OTHERS WITHOUT CLEARING
YOURSELF.



August 1986

Final Report

Approved For Public Release; Distribution Unlimited

Library Branch
Technical Information Center
U.S. Army Engineer Waterways Experiment Station
Vicksburg, Mississippi

Prepared for DEPARTMENT OF THE ARMY
US Army Corps of Engineers
Washington, DC 20314-1000

Under CWIS Nos. 31593 and 31595
(EWQOS Work Units IA.4 and IC.2)

25210
14555744

TA 7
W34i
no. E-86-5

Unclassified

SECURITY CLASSIFICATION OF THIS PAGE (When Data Entered)

| REPORT DOCUMENTATION PAGE | | READ INSTRUCTIONS BEFORE COMPLETING FORM |
|--|--------------------------------|--|
| 1. REPORT NUMBER Instruction Report E-86-5 | 2. GOVT ACCESSION NO. | 3. RECIPIENT'S CATALOG NUMBER |
| 4. TITLE (and Subtitle) CE-QUAL-W2: A NUMERICAL TWO-DIMENSIONAL, LATERALLY AVERAGED MODEL OF HYDRODYNAMICS AND WATER QUALITY; USER'S MANUAL | | 5. TYPE OF REPORT & PERIOD COVERED Final report |
| | | 6. PERFORMING ORG. REPORT NUMBER |
| 7. AUTHOR(s) | 8. CONTRACT OR GRANT NUMBER(s) | |
| 9. PERFORMING ORGANIZATION NAME AND ADDRESS US Army Engineer Waterways Experiment Station Environmental and Hydraulics Laboratories PO Box 631, Vicksburg, Mississippi 39180-0631 | | 10. PROGRAM ELEMENT, PROJECT, TASK AREA & WORK UNIT NUMBERS CWIS Nos. 31593 and 31595 (EWQOS Work Units IA.4 and IC.2) |
| 11. CONTROLLING OFFICE NAME AND ADDRESS DEPARTMENT OF THE ARMY US Army Corps of Engineers Washington, DC 20314-1000 | | 12. REPORT DATE August 1986 |
| | | 13. NUMBER OF PAGES 318 |
| 14. MONITORING AGENCY NAME & ADDRESS (if different from Controlling Office) | | 15. SECURITY CLASS. (of this report) Unclassified |
| | | 15a. DECLASSIFICATION/DOWNGRADING SCHEDULE |
| 16. DISTRIBUTION STATEMENT (of this Report) Approved for public release; distribution unlimited. | | |
| 17. DISTRIBUTION STATEMENT (of the abstract entered in Block 20, if different from Report) | | |
| 18. SUPPLEMENTARY NOTES Available from National Technical Information Service, 5285 Port Royal Road, Springfield, Virginia 22161. | | |
| 19. KEY WORDS (Continue on reverse side if necessary and identify by block number) CE-QUAL-W2 (Computer program) Hydrodynamics Water quality--Mathematical models | | |
| 20. ABSTRACT (Continue on reverse side if necessary and identify by block number) This manual describes the two-dimensional, laterally averaged hydro- dynamic and water quality model CE-QUAL-W2 developed by the Environmental and Hydraulics Laboratories, US Army Engineer Waterways Experiment Station, and provides guidance in its use. The model was developed primarily for use in reservoirs but has applicability to lakes, rivers, and estuaries. | | |

(Continued)

20. ABSTRACT (Continued).

The manual is organized into four major parts with several appendixes. In Part I, CE-QUAL-W2 is introduced to the reader by summarizing its major usages, attributes, and historical development. Part II addresses model capabilities, assumptions, and limitations and supplies the basic information required to use the model. Part III outlines in detail the structure of CE-QUAL-W2, including the basic model equations and solution procedures. Part IV provides additional details of data assembly, presents literature values of various coefficients and constants, and discusses how to calibrate the model and interpret output.

The appendixes include: Appendix A, a description of various programming aspects; Appendix B, a glossary of variables and coefficients used in CE-QUAL-W2; and Appendix C, a description of the statistical and graphics routines.

PREFACE

This manual was sponsored by the Office, Chief of Engineers (OCE), US Army, as part of the Environmental and Water Quality Operational Studies (EWQOS) Program, Work Unit IA.4 (CWIS No. 31593), entitled "Improve and Verify Multidimensional Hydrodynamic Mathematical Models," and Work Unit IC.2 (CWIS No. 31595), entitled "Develop and Evaluate Multidimensional Reservoir Water Quality and Ecological Predictive Techniques." The OCE Technical Monitors for EWQOS were Mr. Earl Eiker, Dr. John Bushman, and Mr. James L. Gottesman.

The development and evaluation of the two-dimensional, laterally averaged hydrodynamic and water quality model CE-QUAL-W2, on which this manual is based, were conducted during the years 1978 to 1985 by the Environmental and Hydraulics Laboratories, US Army Engineer Waterways Experiment Station (WES). The developments in the water quality portions of the model were directed by the Environmental Laboratory (EL) under the general supervision of Dr. John Harrison, Chief of the EL, and Mr. Donald L. Robey, Chief of the Ecosystem Research and Simulation Division, and under the direct supervision of Mr. Mark S. Dortch, Chief of the Water Quality Modeling Group (WQMG). The developments in the hydrodynamic portions of the model were directed by the Hydraulics Laboratory (HL), WES, under the general supervision of Mr. Frank A. Herrmann, Jr., Chief of the HL, and Mr. John L. Grace, Chief of the Hydraulics Structures Division, and under the direct supervision of Mr. Jeffery P. Holland, Chief of the Reservoir Water Quality Branch (RWQB). Program Manager of EWQOS was Dr. J. L. Mahloch, EL.

CE-QUAL-W2 is based upon the hydrodynamic, thermal, and transport model GLVHT4 (Generalized Longitudinal-Vertical Hydrodynamics and Transport model version 4) developed under contract for WES by J. E. Edinger Associates, Inc. (JEEAI), Wayne, Pa. GLVHT4 is a later version of the LARM (Laterally Averaged Reservoir Model) code originally developed by JEEAI for the US Army Engineer Division, Ohio River. The Reservoir Water Quality Branch, Hydraulic Structures Division, Hydraulics

Laboratory, had the major responsibility for the developments that led to the GLVHT4 code.

This manual was prepared by Dr. James L. Martin of WQMG based partially upon reports by Mr. Edward M. Buchak and Dr. John E. Edinger of JEEA. Dr. Martin was principal author and technical editor of the manual. The section of Part IV of this manual dealing with coefficients for use with CE-QUAL-W2 was based upon reviews by Drs. Carol D. Collins and Joseph H. Wlosinski, WQMG. Appendix C was prepared by Dr. Stephen P. Schreiner, WQMG. Contributions and reviews of Messrs. Ross W. Hall, Jr., and Mark S. Dortch and Drs. Joseph H. Wlosinski and Stephen P. Schreiner (WQMG); Mr. Buchak and Dr. Edinger (JEEAI); and Mr. R. C. Berger, RWQB, are gratefully acknowledged. The manual was prepared for publication by Ms. Jessica S. Ruff, Information Products Division, WES.

This manual is published in loose-leaf format for convenience in periodic update. Revisions will be distributed automatically to all holders of record. It is the responsibility of each user to advise WES of address changes.

COL Allen F. Grum, USA, was the previous Director of WES. COL Dwayne G. Lee, CE, is the present Commander and Director. Dr. Robert W. Whalin is Technical Director.

This report should be cited as follows:

Environmental and Hydraulics Laboratories. 1986.
"CE-QUAL-W2: A Numerical Two-Dimensional, Laterally Averaged Model of Hydrodynamics and Water Quality; User's Manual," Instruction Report E-86-5, US Army Engineer Waterways Experiment Station, Vicksburg, Miss.

CONTENTS

| | <u>Page</u> |
|--|-------------|
| PREFACE | 1 |
| PART I: INTRODUCTION | 7 |
| Summary of Attributes | 8 |
| Background | 9 |
| PART II: BASIC STRUCTURE | 10 |
| General Comments | 10 |
| Model Capabilities | 10 |
| Hydrodynamic aspects | 10 |
| Water quality aspects | 11 |
| Hierarchical complexity | 12 |
| Interactions | 13 |
| Model Assumptions and Limitations | 13 |
| Theoretical assumptions | 13 |
| Two-dimensional assumption | 13 |
| Hydrodynamics and transport | 13 |
| Simplified biological/chemical relationships | 15 |
| Numerical considerations | 15 |
| Model Operations | 17 |
| Input data | 17 |
| Geometric schematization | 17 |
| Boundary conditions | 22 |
| Initial conditions | 24 |
| Hydraulic properties | 24 |
| Biological/chemical parameters | 25 |
| Computations | 26 |
| Output data | 28 |
| GRID | 28 |
| Time series | 28 |
| Depth profiles | 28 |
| Vector plots | 29 |
| Contours | 29 |
| Statistics | 29 |
| Diagnostics | 29 |
| Restart | 30 |
| Computer requirements | 30 |
| PART III: DETAILED STRUCTURE | 31 |
| General Comments | 31 |
| Laterally Averaged Water Body Dynamics | 31 |
| Basic relationships | 32 |
| Free surface wave equation | 35 |

| | <u>Page</u> |
|--|-------------|
| Numerical solution | 37 |
| Surface wave equation | 41 |
| Evaluation of F(I,K) terms | 44 |
| Computation of horizontal and vertical velocities | 46 |
| Constituent transport | 47 |
| Auxiliary operations | 49 |
| Wind shear and mixing | 49 |
| Wind shear in horizontal momentum | 49 |
| Vertical eddy viscosity and wind shear | 51 |
| Surface heat exchange | 54 |
| Evaporation | 56 |
| Density relationships | 57 |
| Ice cover relationships | 59 |
| Inflow and outflow boundary conditions | 61 |
| Constituent reactions and interactions | 62 |
| Conservative tracer | 63 |
| Inorganic suspended solids | 63 |
| Coliform bacteria | 67 |
| Total dissolved solids or salinity | 68 |
| Labile dissolved organic matter | 68 |
| Refractory dissolved organic matter | 70 |
| Algae | 70 |
| Detritus | 75 |
| Phosphorus | 77 |
| Ammonia-nitrogen | 80 |
| Nitrate-nitrogen | 81 |
| Dissolved oxygen | 83 |
| Sediments | 86 |
| Total inorganic carbon | 88 |
| Alkalinity | 91 |
| pH and carbonate species | 92 |
| Total iron | 97 |
| Temperature rate multipliers | 98 |
| PART IV: OPERATIONS | 100 |
| General Comments | 100 |
| General Procedure | 100 |
| Data Assembly | 102 |
| Time-varying boundary condition data | 104 |
| Input data description | 109 |
| General | 109 |
| Title cards | 109 |
| Geometry card | 111 |
| Branch geometry card | 112 |
| Water body parameter card | 114 |
| Time period card | 115 |
| delta-T and number of iterations cards | 116 |

| | <u>Page</u> |
|---|-------------|
| Snapshot card | 117 |
| Tapewrite card | 119 |
| Vertical profile card | 121 |
| Observation days card | 122 |
| Observation stations card | 123 |
| Segment print selector cards | 124 |
| Initial condition card | 125 |
| Constituent definition card | 126 |
| Constituent write cards | 127 |
| ITRIP card for constituents | 128 |
| Constituent update card | 129 |
| Constituent initial concentration card | 130 |
| Meteorological parameter card | 131 |
| Outlet card | 132 |
| Outlet segment location card | 133 |
| Outlet layer location card | 134 |
| Tributary card | 135 |
| Tributary location card | 136 |
| Withdrawal card | 137 |
| Withdrawal segment card | 138 |
| Withdrawal layer card | 139 |
| Bathymetry cards | 140 |
| Initial temperature cards | 141 |
| Initial constituent concentration cards | 142 |
| Constituent rate and parameters cards | 143 |
| Summary of CE-QUAL-W2 input deck | 153 |
| Coefficients for use in CE-QUAL-W2 | 154 |
| Card WP | 155 |
| Card RA | 158 |
| Card RB | 160 |
| Card RC | 160 |
| Card RD | 164 |
| Card RE | 177 |
| Card RF | 184 |
| Card RG | 185 |
| Card RH | 185 |
| Card RI | 187 |
| Card RJ | 192 |
| Card RK | 194 |
| Card RL | 195 |
| Card RM | 195 |
| Card RN | 196 |
| Card RO | 197 |
| Card RP | 198 |
| Card RQ | 199 |
| Card RR | 199 |
| Card RS | 199 |
| Card RT | 200 |

| | <u>Page</u> |
|---|-------------|
| Card RU | 200 |
| Card RV | 201 |
| Card RW | 201 |
| Card RX | 202 |
| Calibration Procedures | 202 |
| Water budget | 203 |
| Thermal structure | 204 |
| Water quality compartments | 206 |
| Confirmation | 208 |
| Output Interpretation | 208 |
| REFERENCES | 210 |
| APPENDIX A: PROGRAMMING ASPECTS | A1 |
| Outline of the Program | A1 |
| Algorithms | A26 |
| APPENDIX B: GLOSSARY OF VARIABLES | B1 |
| APPENDIX C: GRAPHICS AND STATISTICAL ROUTINES FOR CE-QUAL-W2 | C1 |
| Instructions for Contour Plotting | C3 |
| Instructions for Shaded Contour Plotting | C12 |
| Instructions for Vector Plotting | C13 |
| Instructions for Time Series Plotting | C16 |
| Instructions for Profile Plotting | C18 |
| Instructions for Statistical Routine | C20 |

CE-QUAL-W2: A NUMERICAL TWO-DIMENSIONAL, LATERALLY AVERAGED
MODEL OF HYDRODYNAMICS AND WATER QUALITY; USER'S MANUAL

PART I: INTRODUCTION

1. CE-QUAL-W2 is a numerical, two-dimensional, laterally averaged hydrodynamic and water quality model that describes the vertical and longitudinal distributions of thermal energy and selected biological and chemical materials in a water body through time. The primary criterion for selecting this model is the need to define water quality gradients in two dimensions. In nearly all Corps reservoirs, significant variations in water quality conditions occur along both the longitudinal and vertical axes. The capability of assessing the impact of reservoir design and operations on these gradients may be critical to a given water quality study. However, careful consideration should be given to the model selection and study objectives. For example, if release water quality is of primary concern, a one-dimensional model such as CE-QUAL-R1 (Environmental Laboratory 1985) may be appropriate. While the model was originally developed for reservoirs, its general structure also allows application to other systems, such as lakes, rivers, and estuaries.

2. CE-QUAL-W2 currently simulates the dynamics of up to 20 water quality constituents in addition to temperatures and circulation patterns. The model calculates in-pool water volumes, surface elevations, densities, vertical and longitudinal velocities, temperatures, and constituent concentrations as well as downstream release concentrations.

3. The model requires a data base that includes initial conditions, reservoir geometry, physical coefficients, biological and chemical reaction rates, and time sequences of hydrometeorological and inflowing water quality quantities. The proper application of the model is largely contingent upon the availability of a suitable data base of in-pool concentrations for model calibration and confirmation.

4. An interdisciplinary effort is recommended to acquire data, assemble the data base, compute, plot, and analyze results. A period of several months of intensive effort may be required for an application.

Summary of Attributes

5. The model CE-QUAL-W2 is a two-dimensional, laterally averaged hydrodynamics and transport model that includes the capability of simulating some important aspects of water quality. CE-QUAL-W2 is an unsteady free-surface model that handles variable density effects on the flow field. By solving the surface elevation implicitly, it removes the restriction of the Courant gravity wave criterion, permitting the use of longer time steps and the simulation of reasonable time periods for field applications (e.g., seasons and entire stratification cycles).

6. The simulation of biological and chemical constituents affecting water quality is a major attribute of CE-QUAL-W2. The model simulates the interaction of physical factors (such as flow and temperature regimes), chemical factors (such as nutrients), and an algal assemblage. The constituents are arranged in four levels of complexity, permitting flexibility in model application. The first level includes materials that are conservative, noninteractive, or do not affect other materials in the first level. The second level allows the user to simulate the interactive dynamics of oxygen-phytoplankton-nutrients. The third level allows simulation of pH and carbonate species. The fourth level allows simulation of total iron.

7. CE-QUAL-W2 also has the capability of including head or flow boundary conditions, branches, multiple lateral inflows and withdrawals, and other features that allow its application to a variety of situations. Some of these attributes are summarized below.

- a. Two-dimensional (laterally averaged) simulations of temperatures, constituents, and flow fields.
- b. Hydrodynamic computations influenced by variable water density caused by temperature and dissolved and suspended solids.
- c. Simulation of the interactions of numerous biological/chemical factors affecting water quality.
- d. Allowance for multiple inflow loadings and withdrawals.
 - (1) Tributaries.
 - (2) Point and nonpoint loading.

- (3) Precipitation.
- (4) Branch inflows.
- (5) Outflows through a dam.
- e. Allowance for multiple branches.
- f. Ice algorithm.
- g. Allowance for a sequence of time steps.
- h. Allowance for flow or head boundary conditions, making it suitable for reservoir and estuarine modeling.
- i. Simulation of circulation patterns.
- j. Restart capability.
- k. Inclusion of evaporation in water balance.
- l. Heat transfer computations.
- m. Variety of output options.

Background

8. This manual is a product of a program of evaluation and refinement of mathematical water quality models conducted at the US Army Engineer Waterways Experiment Station (WES). CE-QUAL-W2 is derived from the Generalized Longitudinal-Vertical Hydrodynamics and Transport (GLVHT) model that has been under development since 1975 as an efficient numerical model of rivers, reservoirs, and estuaries (Buchak and Edinger 1984). The early versions of this model were generally known as Laterally Averaged Reservoir Model (LARM). GLVHT has been successfully used to simulate temperature distributions and circulation in water bodies and has been applied in a variety of systems (Edinger and Buchak 1978; Edinger, Buchak, and Merritt 1983; Gordon 1980, 1983; Johnson et al. 1981). Primary modifications to this model included the addition of algorithms to simulate water quality constituents. These modifications were made relying heavily upon the established structure of the GLVHT model; thus, the basic programming and solution techniques remain intact. However, the number of modifications and improvements that have been incorporated requires that CE-QUAL-W2 be documented in detail to provide guidance on its use.

PART II: BASIC STRUCTURE

General Comments

9. The purpose of this section is to describe the basic structure of CE-QUAL-W2, its capabilities, and its limitations. CE-QUAL-W2 is a comprehensive reservoir water quality model. It deals with some of the major physical, chemical, and biological processes that occur within an impounded body of water. It is recommended that the user closely review this section and Part IV before attempting an application to determine if CE-QUAL-W2 is the appropriate tool for his particular needs and if sufficient data are available for model application.

10. Although a two-dimensional (2-D) model allows for a more realistic simulation of reservoir water quality, it must be emphasized that a 2-D model is somewhat more expensive and difficult to utilize, calibrate, and interpret than a one-dimensional (1-D) model. A 2-D model also requires some additional morphometric and field verification data. It is suggested that where a specific analysis does not require detailed consideration of longitudinal variations, a 1-D model may suffice and should be employed.

Model Capabilities

Hydrodynamic aspects

11. The structure of CE-QUAL-W2 permits time-varying hydrodynamic and transport simulations of reservoirs, estuaries, and other vertically stratified water bodies. An implicit computational scheme allows the use of relatively long time steps without the surface gravity wave restriction. It can be applied to a single continuous reach of a reservoir or more complex configurations, allowing computations in branches and tributaries.

12. Boundary conditions may be specified as either flows or heads. The head boundary condition permits the use of CE-QUAL-W2 where an open boundary is required. An example would be the modeling of a

single branch into a lake where the lake concentrations are not significantly impacted by the branch. This capability also permits application of the model to estuaries.

13. The fundamental basis of laterally averaged hydrodynamics has been firmly established. The numerical basis of the model is a finite difference solution of the free surface frictionally and internally damped longwave equation. The longwave equation results from substitution of the longitudinal momentum equation into the vertically integrated continuity equation. The finite differences are mapped onto a grid that allows for addition and subtraction of surface and headwater cells as the water surface changes.

14. The GLVHT model that forms the basis of CE-QUAL-W2 is considered to be an efficient numerical model and has been used successfully in over 20 practical applications (Buchak and Edinger 1984).

15. CE-QUAL-W2 allows simulation of hydrodynamics and temperature independently of water quality. However, water quality and hydrodynamics are not decoupled, requiring that they be run concurrently. This is due to the typically excessive storage required to save results of hydrodynamic simulations for later use in water quality.

Water quality aspects

16. The structure of CE-QUAL-W2 allows the simulation of up to 20 water quality constituents in addition to temperature, density, and flow velocity (see listing below). Many of the constituents are simulated primarily to include their effects upon other constituents of interest.

| <u>Level 1</u> | <u>Level 2</u> |
|------------------------------------|-------------------------------------|
| Conservative tracer | Labile dissolved organic matter |
| Inorganic suspended solids | Refractory dissolved organic matter |
| Coliform bacteria | Phytoplankton |
| Total dissolved solids or salinity | Detritus |
| | Phosphate-phosphorus |
| | Ammonia-nitrogen |
| | Nitrate-nitrogen |
| | Dissolved oxygen |
| | Organic sediments |

(Continued)

| Level 3 | Level 4 |
|----------------------------|------------|
| Dissolved inorganic carbon | Total iron |
| Alkalinity | |
| pH | |
| Carbon dioxide | |
| Bicarbonates | |
| Carbonates | |

17. Constituents that were selected are believed to represent the majority of the variability in the target constituents, such as dissolved oxygen. Further modifications may be expected in future versions as dictated by the need for particular applications.

18. Hierarchical complexity. The modeled constituents in CE-QUAL-W2 are arranged in four levels of complexity. The groupings are not arbitrary and are generally designed to be used in tandem rather than separately. However, as an option, the user may specify which of the 20 constituents are to be included in simulations. Any constituent may be "turned off" in cases where it is not considered to be important. However, this should be done with caution and only after complete familiarity with the model and the modeled system. As an example, it may not be necessary in a particular application to simulate total dissolved solids (TDS). However, TDS affects both the density and ionic strength of the water, thereby affecting both water movements and distributions of carbonate species. As a second example, the settling of suspended solids affects nutrient concentrations via adsorption and settling. Changes in nutrients can in turn impact a number of other parameters. In addition, suspended solids concentrations may affect water densities and heat exchange. Therefore, not including suspended solids in simulations may lead to erroneous conclusions regarding the processes of importance.

19. The fourth constituent level contains only total iron, which would appear to have best been included with level 1 constituents. However, it is included in a separate level to allow the possible future inclusion of other materials important during anoxic conditions. Total iron does interact with nutrients and should be included in simulations of level 2 constituents.

20. Interactions. A simplified description of the kinetic interactions between constituents is provided in Table 1. The majority of interactions are also influenced by temperature, and temperature rate multipliers are used to modify reaction kinetics. The model has been developed to provide the greatest possible flexibility at the least computational cost.

Model Assumptions and Limitations

21. The proper management of our water resources requires that we be able to promulgate cost-effective solutions to water quality problems. Mechanistic models, such as CE-QUAL-W2, are tools that allow assessment of impacts of changes in design and operation, with the advantage that they can be manipulated at less effort and expense than experimentation on the prototype. One cost associated with this advantage is that a number of simplifying assumptions must be made which place limitations on the use and interpretation of model results. The user must be aware of these limitations in order to avoid improper applications and inappropriate conclusions.

Theoretical assumptions

22. Two-dimensional assumption. The two-dimensional structure implies that lateral variations in flow, temperatures, or constituents are either negligible or can be adequately represented by an average value. If lateral gradients are large, this model may be inappropriate. Even in cases where this assumption is justifiable, exclusion of lateral definition may place limits on model applications.

23. Hydrodynamics and transport. The governing model equations (see Part III) are laterally and layer averaged with layer-averaged variables as the dependent variables. Eddy coefficients are used to model the influence of turbulence. The equations are written in the conservative form with the Boussinesq and hydrostatic approximations. Therefore, CE-QUAL-W2 is not a fully 2-D hydrodynamic model since the full vertical momentum equation is not used. Buoyancy effects are

Table 1

Internal Process Interactions for Variables in CE-QUAL-W2

| From | To | | | | | | | | | | | | | | | |
|------------------|--------|----|-----|---------|---------|-------|----------|---------|-----------|-----------|--------|---------------|------------|----------|------------|---------|
| | Tracer | SS | TDS | DOM (L) | DOM (R) | Algae | Detritus | Ortho-P | Ammonia-N | Nitrate-N | Oxygen | Inorg. carbon | Alkalinity | Sediment | Total iron | Surface |
| Tracer | F | | | | | | | | | | | | | | | |
| SS | | Y | | | | | | | | | | | | | | |
| TDS | | | F | | | | | | | | | | | | | |
| DOM (L) | | | | F | D | | | D | D | | | D | | | | |
| DOM (R) | | | | | F | | | D | D | | | D | | | | |
| Algae | | | | M | | Y | M | R | R | | P | R | | S | | |
| Detritus | | | | | | | Y | D | D | | | D | | S | | |
| Ortho-P | | A | | | | P | A | F | | | | | | | | A |
| Ammonia-N | | A | | | | P | A | | F | D | | | | | | A |
| Nitrate-N | | | | | | P | | | | F | | | | | | |
| Oxygen | | | | D | D | R | D | | D | | F | | | D | | X |
| Inorganic carbon | | | | | | P | | | | | | F | | | | X |
| Alkalinity | | | | | | | | | | | | | F | | | |
| Sediment | | | | | | | | D | D | | | D | | | | D |
| Total iron | | | | | | | | | | | | | | | | Y |
| Surface | | | | | | | | | | | X | X | | | | |

NOTES:

D = decay, decomposition, release
 F = diffusion and advection
 M = mortality
 P = photosynthesis
 R = respiration
 S = settling
 A = adsorption

Y = settling, diffusion, advection
 X = exchange at air/water interface
 SS = suspended solids
 DOM = dissolved organic matter
 (L) = labile
 (R) = refractory

included, but the model cannot resolve cases where appreciable vertical momentum occurs.

24. Simplified biological/chemical relationships. Aquatic ecosystems are extremely complex and variable. It is unreasonable and probably undesirable to attempt to model ecological systems by describing all concentrations and kinetics of all materials involved, even where they are known. Instead, a limited number of variables are used that will allow analysis while assuming that they still adequately described the desired aspects of the system's behavior. These variables represent an aggregation of a variety of functional groups. For example, CE-QUAL-W2 uses one algal compartment to represent the many hundreds of species that may occur in a reservoir. This aggregation imposes limits on applications. For example, changes resulting from algal succession and movement of "new actors" onto the stage cannot be simulated. The absence of functional groups also imposes limitations. For example, algal populations may be strongly impacted by grazing by zooplankton and higher order herbivores. However, these groups are presently not included in the model. Macrophyte production may also have an impact upon reservoir water quality, and this group is also not included in the model. Later modifications in the model structure may be expected in order to meet the needs of specific applications.

Numerical considerations

25. The numerical basis of the model is finite differencing of the governing equations. Upwind differencing is used for the advective momentum and constituent transport processes. The finite differences are mapped onto a grid consisting of longitudinal segments and vertical layers. This numerical structure imposes limitations upon model accuracy:

- a. The finite difference grid imposes limitations on model accuracy. The grid structure assumes that the complex morphometry of a reservoir or impoundment can be adequately represented by a simplified structure. The grid also serves to simulate a continuum using a number of discrete cells. A coarse discretization may result in inadequate resolution. Better resolution may be obtained

by use of a finer grid. However, the increased number of cells and smaller time step required result in increased computation times.

- b. The stability of the numerical scheme is affected by the flow field and grid size. The coupling of internal flow and the free surface computations removes the Courant surface gravity wave condition, which is often the most limiting stability requirement. The major remaining stability requirement is a result of flow and diffusion within a cell. The time step (Δt) limit may (similar to Roache 1982) be given by:

$$\Delta t \leq \frac{1}{2 \left(\frac{\alpha}{\Delta X^2} + \frac{\beta}{\Delta Z^2} \right) + \frac{|U|}{\Delta X} + \frac{|W|}{\Delta Z}}$$

where

α = longitudinal diffusion coefficient, m^2/sec

β = vertical diffusion coefficient, m^2/sec

ΔX = cell length, m

ΔZ = cell thickness, m

U = longitudinal velocity, m/sec

W = vertical velocity, m/sec

Often the diffusion is small relative to the advection terms, in which case the time step may be estimated by $\Delta t \leq V/Q^*$ where V is the cell volume, in cubic metres, and Q^* is the flow into a model cell, in cubic metres per second. Since flow fields may vary over simulations due to varying boundary conditions, provisions are included to allow multiple time steps.

- c. The scheme may be stable, allowing answers, yet produce unrealistic results. Local temperature inversions may occur if time steps are too large to allow completion of dispersive mixing relative to advection (Edinger and Buchak 1983). Diffusion may occur due to the numerical scheme, resulting in an erosion of gradients. This effect may be particularly pronounced when a disturbance occurs over relatively few model cells. Generally, better resolution is obtained by decreasing grid spacings. However, the cost is the decreased time steps and increased computational costs.

Model Operations

26. Basic model operations include data input, computations, and data output.

Input data

27. The initial task in applying CE-QUAL-W2 to a specific case (after determining that a 2-D model is required) is assembling the necessary data. These data include geometric schematization, initial and boundary conditions, hydraulic properties, biological/chemical parameters, and calibration and confirmation data. The data assembly, input formats, and typical values for model parameters are discussed in more detail in Part IV.

28. Geometric schematization. Data required in order to determine the computational grid may include bathymetric cross sections (y-z plane), a topographic plan (x-y plane), section-elevation view (x-z plane), and an elevation-area-volume table. These data will be used to develop the computation grid. The user should ensure that the imposed geometry is an adequate representation of the geometry and capacity of the real water body.

29. The computational grid consists of a series of vertical columns (segments) and horizontal rows (layers), with the number of cells being equal to the number of segments times the number of rows (Figure 1). The basic parameters used to define the grid are the longitudinal spacing (Δx , in metres), and the vertical spacing (h, in metres). The vertical spacing is constant throughout the grid. The horizontal spacing may vary with each branch. Each cell also has an associated width which represents an average value.

30. The branching capability of CE-QUAL-W2 allows the simulation of multiple branches or loops within a reservoir as well as the simple reservoir configuration. Data input includes the number of branches and the left and right active segment for each branch. Also specified is the segment where the branch leaves or enters the main stem (Branch 1) or another branch.

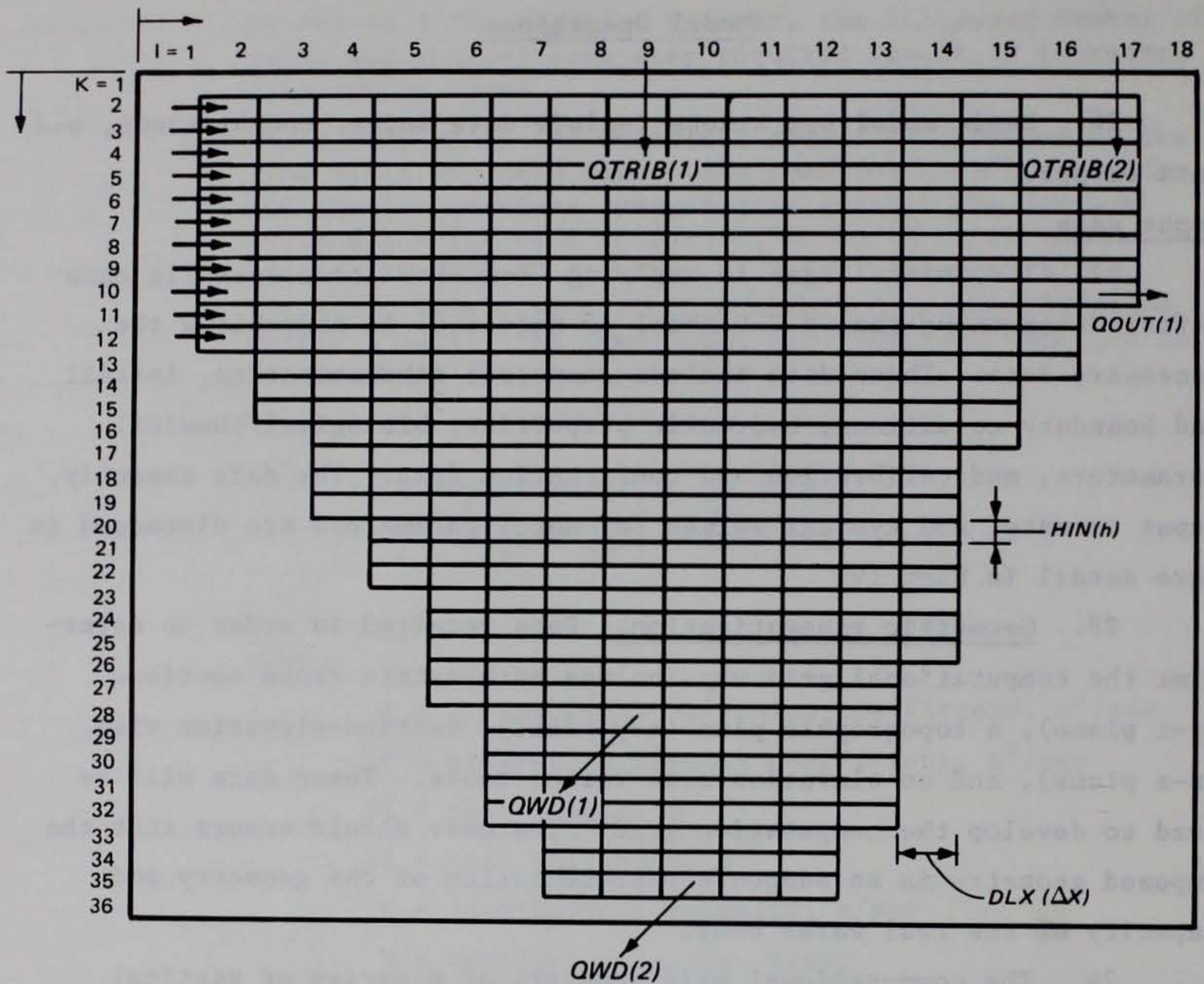


Figure 1. Grid structure used for Dillon Reservoir application of LARM (Buchak and Edinger 1982b)

31. Implicit in the geometric schematization is the identification of the branch center line. This may be defined as the dominant flow path, with its origin at the upstream boundary. All longitudinal distances are measured along the center line.

32. The choice of Δx and h is important to the success of the simulation. The bottom may be modeled more accurately if the ratio of $h/\Delta x$ is selected to match the overall reservoir slope. A selection of h and Δx should also be based on the disturbances that must be simulated to meet specific study objectives. Attention should be given to changes in width, depth, inflows, loadings, and other factors that may result in a disturbance. If it is obvious that the size of a disturbance is less than the finite difference grid's cell size, that

disturbance will be averaged over the cell, reducing both its magnitude and its driving force. For example, a simulated plume of material moving through the grid will be reduced in concentration due to numerical approximation as the thickness of the plume approaches the cell thickness. This can result in increased travel times if the driving density gradient is reduced.

33. The smallest wavelength of a disturbance that can be captured by a finite difference grid is $2\Delta x$ or, vertically, $2\Delta z$. Wavelengths approaching that limit are also subject to increased numerical dissipation, which will result in smearing of the disturbance. Decreasing cell sizes in relation to the size of the disturbance will usually result in increased resolution but at the cost of increased computational time due to both the increased number of cells and the smaller time step required as cells become smaller. Previous reservoir applications of the GLVHT model, which forms the basis of CE-QUAL-W2, have typically used Δx in the range of 1,000 to 2,000 m and h in the range of 1 to 2 m.

34. The widths must also be specified for each model cell and must represent an average value. Various techniques have been used to determine cell widths. These have included use of the Hydrologic Engineering Center code GEDA and the preprocessor code GIN to produce reservoir widths as a function of elevation at regular intervals from cross-sectional data for transects at irregular intervals of Δx (Buchak and Edinger 1982a). Alternatively, topographic maps for the reservoir may be used if they adequately represent existing morphometry. The segment boundaries, as determined by Δx , are first specified. A topographic contour for the elevation corresponding to the center of a model cell is then located. The area enclosed by the contour and within the segment boundary is then determined. That area, divided by the segment length Δx , represents the cell width. This process is repeated for each model cell. Calculated cell widths may require some refinement in order to approximate elevation area-capacity curves for a specific application. A model elevation area-capacity table is provided in the GRID output for comparison.

35. The computational grid extends from $I = 1$ to $I = \text{IMAX}$ and from $K = 1$ to $K = \text{KMAX}$ where IMAX and KMAX are the maximum number of longitudinal segments and vertical layers, respectively (Figure 2). The water body branches (one or more) are mapped onto this grid and extended from $I = \text{IL}$ (I left) to $I = \text{IR}$ (I right) longitudinally and from $K = 2$ to $K = \text{KB}$ (K bottom, $\text{KB} \leq \text{KMAX} - 1$). Each branch is also surrounded by boundary segments and layers so that these segments and layers, as well as the branch layers extending from KB to $\text{KMAX} - 1$, are not considered part of the active grid and are assigned cell widths of zero in the bathymetry data. These inactive cells are represented by clear areas in the single-branch example (Figure 1) and the three-branch example (Figure 2). Note that for multiple geometries, the requirement of boundary segments results in two boundary segments between active cells of adjacent branches.

36. The code automatically expands or contracts the grid to accommodate rising and falling water surfaces, so the selected grid should be large enough to contain the largest anticipated volume. The active grid consists of currently active and potentially active cells. Velocities, temperatures, and constituent concentrations are computed only for currently active cells. The number of currently active cells may vary with water surface elevation, and all potentially active cells must have a specified width. The current leftmost active boundary is defined by the parameter ILC (I Left Current) and the top as KT (K Top, Figure 2). The minimum value of both ILC and KT is two, indicating the water body is at its maximum volume. The grid must also satisfy the following rules:

- a. It must be at least two active cells deep at every segment.
- b. It must be at least three active cells long at every layer.
- c. Steps (up or down) in the water body bottom profile are permitted as long as each continuous layer is at least three cells long.
- d. Cell widths must not increase with depth.

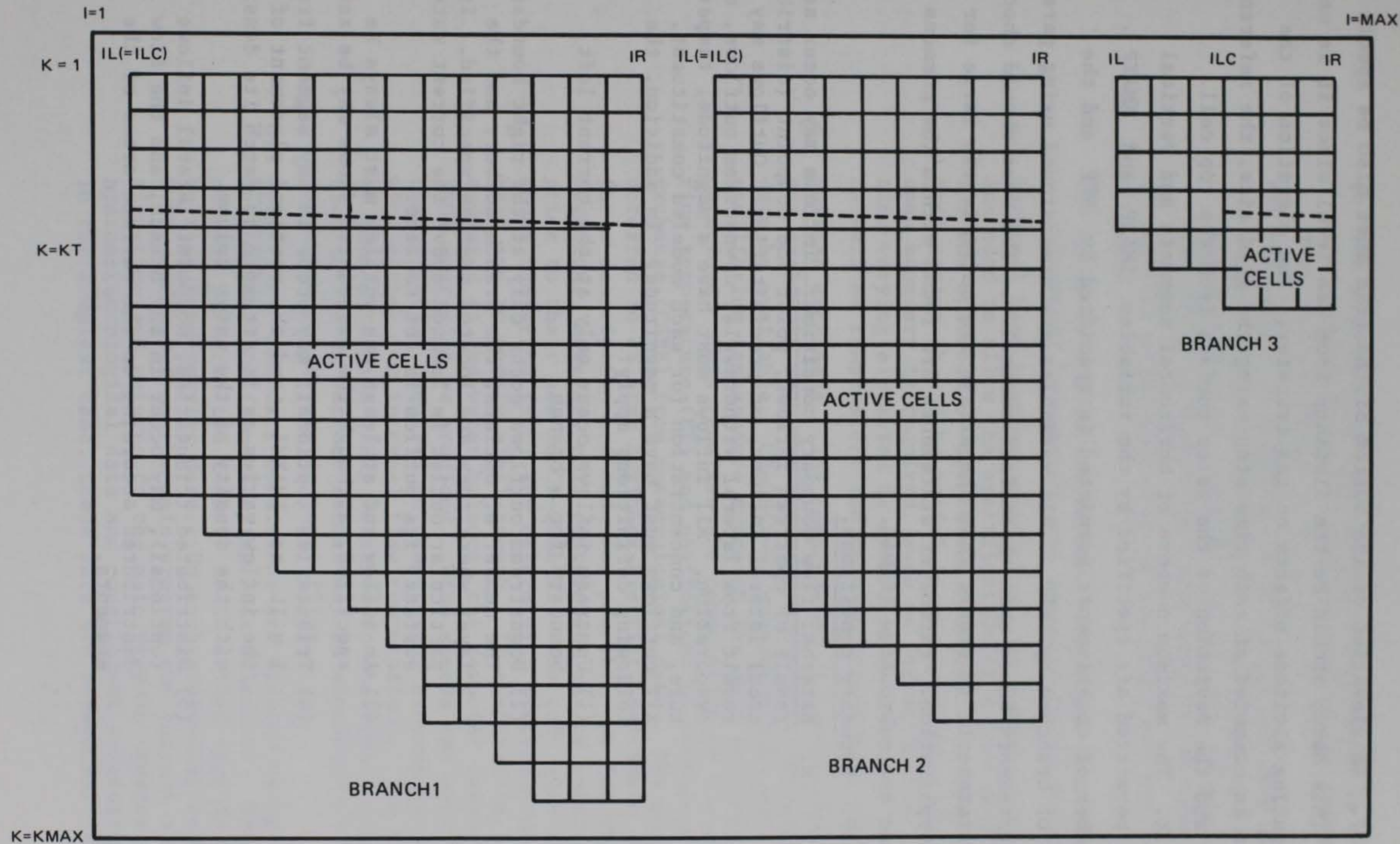


Figure 2. Grid representation of three-branch case

37. An elevation of the bottom of the grid must also be specified. This datum should be the distance from sea level since it is used in computing altitude effects on gas transfer. The elevation of the surface is computed at each time step using the grid size, the reference datum, and the deviation of the water surface from the top cell.

38. The maximum numbers of horizontal segments and vertical layers permitted are specified by the variables `IMAXP` and `KMAXP`. The number of constituents permitted is specified by `NCP` and the number of branches by `NBP`. All variables are dimensioned using parameter statements based upon these four variables. The user should check these statements to ensure that the arrays are sufficiently large for their application. Parameter statements are found within the commons file and the subroutine `TRIDAG`.

39. Boundary conditions.

a. External flow boundary condition. Inflows may occur as a result of upstream inflows, point and nonpoint (distributed) lateral inflows, or precipitation. Outflows may result from lateral withdrawals, downstream outflows, or evaporation. All inflows must have a magnitude, temperature, and concentration for each modeled constituent. All outflows must have a magnitude. In addition, the following definitions apply:

- (1) Upstream inflows occur only at the current left boundary for a branch.
- (2) Downstream outflows occur only at the right boundary. The number of outlets, the branch number, and the layer where they are located must be specified. If a particular outlet is located above the current water surface, its outflow is set to zero.
- (3) An inflow and at least one outflow must always be specified, although the associated flows may be zero.
- (4) Tributaries (optional) may occur in any segment from $I = IL$ to $IMAXM1$, and the vertical placement of the inflow varies as it attempts to match its density with the density of the water column.
- (5) Distributed tributaries, nonpoint lateral inflows (optional), may occur in any branch, and the flow is distributed according to the surface areas of the segments.

- (6) The magnitude of precipitation (optional) is distributed according to the surface area of the segments over all branches.
 - (7) The effect of evaporation is always included in heat budget computations; however, its inclusion in the water budget is optional. If it is to be included, the dewpoint temperature must also be provided.
 - (8) Lateral withdrawals may be specified for any active cell.
 - (9) Flows at boundaries between contiguous branches (internal boundaries) are computed by the model.
- b. External head boundary condition. An option is also included to allow the specification of a head condition for the upstream or downstream boundary of a branch. This option should be useful in an application where an open boundary is required, such as for estuaries. The time-varying elevation is specified at the open boundary as well as temperature and modeled constituent profiles.
- c. Surface exchanges. The computation of surface heat and gas exchanges requires that appropriate meteorological data be available. CE-QUAL-W2 presently utilizes the equilibrium temperature approach for heat exchange computations. This requires the computation of the equilibrium temperature (ET) and coefficient of surface heat exchange (CSHE) from meteorological data. The user is referred to US Army Engineer District, Baltimore (1977) for a description and code for possible use for this computation. However, unit conversions may be required prior to their use in CE-QUAL-W2. The code also requires solar radiation (SRO) for determining distributions of heat and to modify algal growth. If evaporation is to be computed in the water balance, the dewpoint temperature (TD) must also be provided. Wind speeds and wind direction are also required to compute gas exchange as well as wind stress for internal flow computations. The effects of wind direction (PHI) relative to the branch orientation (PHIO) on surface stress may be simulated by including these parameters in input files.
- d. TVDS file. Boundary conditions are updated using the subroutine TVDS (Time Varying Data Selector). This subroutine performs two tasks. It is called once in order to read time-varying data. On each succeeding call, TVDS receives from the main program the current simulation time and returns to the main program updates for hydrometeorological data and constituent concentrations. In the simplest case, these data are constants. For

time-varying boundary conditions, the parameters can be supplied at any time interval. Daily or more frequent data are recommended if available. These data are passed both through the parameters specified in the call and through the commons file. There is no general format for this subroutine since it often requires modification for a specific application. The user is referred to Part IV for a more detailed description of this subroutine. The commons file and call parameters may require modification to ensure that all required parameters are passed to the main program.

40. Initial conditions. Initial conditions must be selected in order to start each simulation. These conditions may be provided in the control file or from a previous simulation using the restart file.

- a. Control file specification. Initial conditions that are specified in the control file include the starting time of the simulation, the water surface elevation, temperatures, and modeled constituent concentrations. Temperatures and constituent concentrations may be specified by either single values, for an isoclinal field, or by reservoir-wide vertical distribution. The flow field is always initialized to zero by the code. The solution technique is such that the applied boundary conditions quickly force an internally compatible flow field.
- b. Restart specification. An option is available, through the subroutine RSRTWR, to have the flow field, temperatures, and constituent concentrations written to a data file at the end of a simulation period. This file may then be used to provide the initial conditions for subsequent simulations. This allows long simulations to be broken into easily managed units.

41. Hydraulic properties.

- a. Dispersion coefficients. Input data include the specification of AX , DX , and DCX , the horizontal dispersion coefficients for momentum, temperature, and constituents, respectively. These parameters are space and time invariant. Vertical dispersion coefficients are computed internally and are space and time variant.
- b. Chezy coefficient. The Chezy coefficient is also space and time invariant. Boundary friction varies spatially with the amount of bottom area exposed, as well as temporally with the flow field.
- c. Density. The flow field is impacted by water densities. The water density is calculated in the function DNST and is based upon water temperatures. The effects of TDS or salinity and inorganic suspended solids are also included

if they are simulated. The choice of TDS or salinity in simulations is indicated by the parameter IWT.

- d. Solar radiation absorption. The distribution of solar radiation in the vertical dimension is controlled by the parameters BETA and GAMMA. BETA represents the fraction of solar radiation absorbed at the water's surface, and GAMMA is an attenuation rate. These parameters do not affect overall heat exchange, which is summarized in the parameters ET and CSHE. They do affect the vertical placement of heat resulting from solar radiation, which can impact density stratification and flow patterns. If algae are included in simulations, self-shading effects due to solids (inorganic suspended solids, algae, and detritus) are added to a baseline value (EXCO) to estimate the total attenuation coefficient. The self-shading attenuation is determined by the concentrations of inorganic suspended solids and organic suspended solids (algae and detritus) through the parameters EXTINS and EXTINP, respectively. EXCO is the attenuation coefficient due only to pure water and dissolved solids.
- e. Time steps. Internal flows affect the time step that can be used for simulations. A provision is made to allow specification of a number of time period pairs for a specific application. Each pair consists of the time step (Δt) and the number of iterations at the specified Δt . This allows the use of small time steps during periods of high velocities and longer time steps during quiescent conditions.
- f. Sheltering coefficients. Sheltering coefficients (variable EWC) function to reduce measured wind speeds for a particular branch, thereby reducing surface wind stress. This may be necessary where wind directions are not available and are known to change or where topography or seasonal changes in vegetation reduce wind effects. The sheltering coefficient is coupled to the time step specification, allowing different coefficients for different periods during the simulation.

42. Biological/chemical parameters.

- a. Constituent field. CE-QUAL-W2 can simulate up to 20 water quality constituents in addition to temperatures and flow fields. The selection of the constituent field is indicated by the variable NC, representing the number of constituents, and ITRIP, which may be used to "turn off" a particular constituent. For example, the four constituents in the first constituent level are the conservative tracer, inorganic suspended solids, coliform bacteria, and either salinity or TDS as specified by IWT. These constituents are assigned numbers 1 to 4,

respectively. To simulate only coliform bacteria, it is necessary to set the number of constituents to be modeled at 3 (NC = 3) with ITRIP values of 0, 0, 1. This may be repeated to form any desired combination of the constituents included in the model. However, caution should be exercised in using this option since many of the constituents are interrelated. For example, suspended solids affect densities, solar radiation absorption, and nutrient adsorption. To arbitrarily remove this constituent from simulations may result in erroneous conclusions regarding the processes of importance.

- b. Update intervals. The model CE-QUAL-W2 further separates the sources and sinks into those due to external loadings (such as inflows, FORTRAN variable HNC) and those due to constituent kinetics (internal transformation, variable CSS). This is because the time steps for model solution are relatively small, generally less than 0.5 hr. However, the time scale required for biological processes may be much more coarse than that required for hydrodynamics and transport. A provision is made for the user to specify the frequency at which the constituent kinetics are updated. This may allow a considerable savings in computer time. For example, the constituent kinetics are sensitive to temperature, but the temperature variations that may occur in an hour may have a negligible effect on biological rates. It may then be possible to update temperature rates less frequently than hydrodynamics without affecting computed trends. The number of iterations between updates of constituent kinetics is NUPDC and for temperature rate multipliers, NUPDRT.
- c. Constants and kinetic rates. Although the constituent interactions are very simplified in CE-QUAL-W2, there remain a number of parameters which must be defined to describe the system. Of these, more than half deal with temperature rate multipliers. The remainder include: stoichiometric coefficients, decay rates, settling rates, growth rates, adsorption coefficients, rates of sediment oxygen demand and nutrient release, algal growth, excretion, respiration rates, and others. The user is referred to Part IV for a detailed description of the parameters and their possible values.

Computations

43. The computations performed by CE-QUAL-W2 are summarized in the overall program outline (Figure 3). A detailed description of the model is provided in Part III. Detailed descriptions of the

1. Set up the computation
 - 1.1 Introduce the computation
 - 1.2 Read control and geometric data, initialize variables
 - 1.3 Read initial condition data
 - 1.4 Write control data
 - 1.5 Complete geometric computations
 - 1.6 Initialize variables and arrays branch by branch
 - 1.7 Write initial condition data to TAPE6 (through subroutine GRID)
2. Integrate the equations through time
 - 2.1 Access time-varying boundary condition data
 - 2.2 Update hydrodynamic and transport source arrays for the entire grid
 - 2.3 Calculate hydrodynamic and transport source for each branch
 - 2.4 Compute hydrodynamics and transport, branch by branch
 - 2.4.1 Compute branch-related constants
 - 2.4.2 Compute longitudinal momentum terms
 - 2.4.3 Compute the water surface elevation
 - 2.4.4 Compute longitudinal velocities
 - 2.4.5 Compute vertical velocities
 - 2.4.6 Transport heat
 - 2.4.7 Update constituent rate terms (through subroutines)
 - 2.4.8 Transport constituents
 - 2.4.9 Compute densities (through function DNST)
 - 2.4.10 Record the maximum value of Z_1
 - 2.5 Perform layer and segment additions and subtractions
 - 2.6 Exchange time-dependent variables and arrays
 - 2.7 Summarize and write results
3. Terminate the computation

Figure 3. Overall outline of CE-QUAL-W2

computations and programming aspects are provided in Appendix A. A glossary of variables is provided as Appendix B.

Output data

44. The model CE-QUAL-W2 can quickly produce an overwhelming quantity of numerical data. Adequate means of interpreting model predictions are an essential requirement which can greatly affect time needed for applications and, possibly, the ultimate success or failure of the modeling effort. A variety of visual and statistical tools have been provided to allow ease of interpretation of the large amount of data generated by CE-QUAL-W2. Detailed descriptions of the use of options and output examples are provided in Part IV and Appendix C.

45. GRID. The subroutine GRID provides a variety of numerical data. The amount of information printed to files is specified by the user. The output may include the initial information in the input data set for verification as well as a water body area and capacity table. During a simulation, at time intervals specified by the user, data on time-varying inflow rates and tributary concentrations, water surface elevations, and current snapshots of vertical velocities, horizontal velocities, density deviations, temperatures, and constituent concentrations for the 2-D grid are provided. An option is available for a short-form version where information is provided at only a selected number (less than seven) of vertical segments (all layers) and may be printed on an 8-1/2- by 11-in. page.

46. Time series. Time series plots are X-Y plots of variations for a predicted variable in the outflow through time, and for changes in surface elevation through time.

47. Depth profiles. This option provides vertical profiles of temperature and constituent concentrations at particular segments over time. The time intervals can be the same as those for the GRID output information described above. Alternatively, they can be specified for only specific dates, such as those where field data are available. Several profiles can also be overlaid simultaneously, allowing comparison of particular simulation results or comparison of predicted to measured data.

48. Vector plots. Flow vectors are computed from the horizontal and vertical flows and are plotted on the 2-D grid. A self-adjusting time scale, based upon the magnitude of flows, determines the length of the resulting vectors. Vector diagrams provided at user-specified time intervals allow examination of changes in circulation patterns.

49. Contours. Three formats of contour plots are available. Variations in reservoir water quality can be conceptualized as a 3-D wedge where the three axes are the vertical, horizontal, and time. Contour plots are available as slices of the wedge in any of three directions. A slice can be taken which represents the reservoir at a particular time, showing the longitudinal and vertical gradients of any selected constituent. A slice may also be taken across the face of the wedge, which allows contours of constituents at a particular vertical segment through time. A third view available is a slice at a particular horizontal layer showing variations in that layer through time. For each of the three views, lines of constant constituent magnitude are graphed over a specified range of values. These three views allow the user an easily interpretable visual aid in identifying spatial and temporal variations. As an option, any of the three views may also have printed the predicted values or those from different data sources. This allows a means of confirming trends. A final option is the use of shadings to represent variations in values or concentrations rather than isopleths. The shading option allows an immediate visual interpretation which may be useful for some applications.

50. Statistics. The statistical package is primarily intended for comparisons of simulations with each other or with measured observations to aid model calibration and interpretation of the successes of calibration and confirmation. Statistics provided include the observed and predicted means, T statistic, reliability index, and normalized mean error. These statistics are provided for each comparison date and as grand values for all dates of comparison.

51. Diagnostics. The diagnostic file is available for user-defined diagnostics. The file currently prints all dates where the grid size is expanded or contracted due to rising or falling water levels. A

calculated time step based upon the net flow into model cells is also provided to aid in selection of time period (DLT, NIT) pairs for a specific application. The actual time step required may be considerably less than that provided in this file.

52. Restart. Restart files allow the model predictions for temperatures, constituents, and flow fields to be written to a file at the end of a period of simulation. This file can then be used to provide the initial conditions for subsequent simulations. This allows relatively long simulations to be broken into discrete, easily managed units.

Computer requirements

53. CE-QUAL-W2 contains 5,788 lines of code (including blank lines, comments, etc.) in the source program. Hydrodynamic and temperature simulations require approximately 0.0022 sec per model cell per time iteration on a VAX11/750 computer system. This time requirement is increased approximately 10 percent by each water quality constituent included in simulations. The DeGray application of CE-QUAL-W2 required 2.1 megabytes of virtual memory at run time where all real variables were double-precision and arrays were dimensioned according to $IMAXP = 32$, $KMAXP = 36$, $NBP = 3$, and $NCP = 20$.

PART III: DETAILED STRUCTURE

General Comments

54. The fundamental structure of CE-QUAL-W2 is based upon the laterally averaged equations of fluid motion. These can be developed from the general three-dimensional and time-varying equations (Buchak and Edinger 1982b; Edinger and Buchak 1975, 1980). A major portion of the model coding is based upon the numerical solution of these equations to describe hydrodynamics and transport. This is essential since the variations that may occur in water quality are influenced largely by physical processes.

55. Many of the tasks performed by the code are auxiliary to the main program in that they act on state variables without modifying the solution scheme. For example, formulations for wind stress serve to modify or define that variable without altering the overall solution scheme that includes the effects of wind stress. This is also true of the water quality routines. They serve to modify or define variables, such as sources or sinks for a given constituent, without modifying the scheme for solving the governing equations.

56. The next section provides a detailed description of the laterally averaged equations, solution techniques, and auxiliary functions. These operations form a basis for the model coding. A detailed outline of the resulting coding and descriptions of algorithms are provided in Appendix A.

Laterally Averaged Water Body Dynamics

57. The laterally averaged equations of fluid motion can be derived from the three-dimensional equations of fluid motion as illustrated in Buchak and Edinger (1982b) and Edinger and Buchak (1975, 1980). There are six unknowns and six equations, including: (a) the free water surface elevation η ; (b) the pressure P ; (c) the horizontal velocity U ; (d) the vertical velocity W ; (e) the constituent

C ; and (f) the density ρ . The six equations are: (a) the free surface wave equation; (b) the hydrostatic pressure; (c) horizontal momentum; (d) continuity; (e) constituent transport; and (f) an equation of state relating density and constituents including temperature, TDS (or salinity), and inorganic suspended solids.

Basic relationships

58. The laterally averaged equation for horizontal momentum balance is:

$$\begin{aligned} \partial UB/\partial t + \partial UUB/\partial x + \partial WUB/\partial z = \\ - 1/\rho \partial BP/\partial x + \partial(BA_x \partial U/\partial x)/\partial x + \partial B\tau_x/\partial z \end{aligned} \quad (1)$$

where

U = x-direction, laterally averaged velocity, $m \text{ sec}^{-1}$

B = water body width, m

t = time, sec

x and z = Cartesian coordinates: x is along the lake center line at the water surface, positive to the right; z is positive downward from the x -axis, m

W = z -direction, laterally averaged velocity, $m \text{ sec}^{-1}$

ρ = density, $kg \text{ m}^{-3}$

P = pressure, $N \text{ m}^{-2}$

A_x = x -direction momentum dispersion coefficient, $m^2 \text{ sec}^{-1}$

τ_x = shear stress per unit mass resulting from the vertical gradient of U , $m^2 \text{ sec}^{-2}$

The first term represents the time rate of change of horizontal momentum, and the second and third terms are horizontal and vertical advection of momentum. The first term on the right-hand side (RHS) of Equation 1 is the force imposed by the horizontal pressure gradient; the second term on the RHS is the horizontal dispersion of momentum; and the third term on the RHS is the force due to shear stresses. The vertical equation of motion reduces to the hydrostatic approximation:

$$\partial P/\partial z = \rho g \quad (2)$$

where g is the acceleration due to gravity, $m \text{ sec}^{-2}$

59. The equation of continuity becomes:

$$\partial UB/\partial x + \partial WB/\partial z = qB \quad (3)$$

where q is the lateral boundary inflow or outflow (reverse sign) per unit volume, per second.

60. Vertically integrated continuity gives the free water surface relationship of:

$$\partial \bar{B}\eta/\partial t = \partial/\partial x \int_{\eta}^h UBdz - \int_{\eta}^h qBdz \quad (4)$$

where

\bar{B} = time and spatially varying surface width, m

η = free water surface location, m

h = total depth

61. The constituent transport becomes:

$$\begin{aligned} \partial BC/\partial t + \partial UBC/\partial x + \partial WBC/\partial z - \partial (BD_x \partial C/\partial x)/\partial x \\ - \partial (BD_z \partial C/\partial z)/\partial z = C_q B + SB \end{aligned} \quad (5)$$

where

C = laterally averaged constituent concentration, $mg \ell^{-1}$

D_x = x-direction temperature and constituent dispersion coefficient, $m^2 \text{ sec}^{-1}$

D_z = z-direction temperature and constituent dispersion coefficient, $m^2 \text{ sec}^{-1}$

C_q = lateral inflow or outflow mass flow rate of constituent per unit volume, $mg \ell^{-1} \text{ sec}^{-1}$

S = source/sink term for constituent concentration

Each constituent, such as temperature, suspended solids, or dissolved oxygen, has a balance as in Equation 5 with specific source and sink, or flux, terms. The first term in Equation 5 represents the time rate of change of constituent concentration; the second and third terms are the horizontal and vertical advection of constituents; the third and fourth terms are the horizontal and vertical diffusion of constituents. The first term on the RHS is the lateral inflow/outflow of constituents, and the second term on the RHS represents kinetic source/sink rates for constituents.

62. The equation of state is

$$\rho = R(C) \quad (6)$$

The equation of state includes each constituent such as temperature, TDS (or salinity), and suspended solids that have significant effects on density.

63. Equations 1-6 constitute six equations to be solved for the six unknowns of U , P , W , η , C , and ρ . Lateral averaging eliminates the lateral momentum balance, the lateral velocity component, and the Coriolis acceleration. The computational problem is reduced to six equations in six unknowns and, most important, to two coordinate directions. The reduction to two coordinate directions is the main feature that reduces computational time and storage over the three-dimensional (3-D) case.

64. The laterally averaged horizontal pressure gradient in the horizontal momentum balance includes density driving force. It can be expanded to:

$$\partial(BP)/\partial x = B(\partial P/\partial x) + P(\partial B/\partial x) \quad (7)$$

The second term $P(\partial B/\partial x)$ represents the static force of the fluid on the x projection of the lateral boundary, which in turn is cancelled by the force of the boundary on the fluid. Thus, $B(\partial P/\partial x)$ represents the internal fluid horizontal pressure gradient. The horizontal

pressure gradient is evaluated from Equation 2 to give:

$$B(\partial P/\partial x) = -\rho_{\eta} Bg(\partial \eta/\partial x) + Bg \int_{\eta}^z (\partial \rho/\partial x) dz \quad (8)$$

at any depth z , where ρ_{η} is the density at the surface. The horizontal pressure gradient is divided into the two components: the surface slope and the vertical integral of the horizontal density gradient. The first term is known as the barotropic gradient and the second as the baroclinic gradient. The horizontal density gradient is the major driving force for the density circulation exhibited in many water bodies.

Free surface wave equation

65. The basic characteristics of the longitudinal and vertical free water surface hydrodynamics can be examined through evaluation of the water surface relationship, Equation 4. The vertical integral of the horizontal flow required in Equation 4 can be determined from the algebraic forward time difference of the local acceleration of horizontal momentum in Equation 1. Formulation of the forward time difference of UB , called $U'B'$, is the first step in evaluating the numerical equations. It gives:

$$U'B' = UB - B\Delta t/\rho \partial P/\partial x + F_x \Delta t + \Delta t B \partial \tau_x / \partial z \quad (9)$$

where

$$F_x = \partial(BA_x \partial U/\partial x)/\partial x - \partial(UUB)/\partial x - \partial(WUB)/\partial z \quad (10)$$

The vertical integrals of the various terms in Equations 9 and 10 can be further evaluated for insertion into the vertical integral of the flow required in the free water surface balance, Equation 4.

66. The vertical integral of the horizontal pressure gradient can be evaluated from Equation 8 to give:

$$1/\rho_{\eta} \int_{\eta}^h (B\partial P/\partial x) dz =$$

$$-\partial\eta/\partial x g \int_{\eta}^h B dz + g/\rho_{\eta} \int_{\eta}^h \left[B \int_{\eta}^z (\partial\rho/\partial x) dz \right] dz \quad (11)$$

The first term on the RHS results from the fact that $\partial\eta/\partial x$ is a function only of x and is constant over z . The integral of width B over depth is the total cross-sectional area across which the surface slope contribution to the horizontal pressure gradients acts. The second term is the force due to the horizontal density gradient.

67. The vertical integral of the horizontal shear stress can be expanded from the derivations of $B\partial\tau_x/\partial z$ to give:

$$\int_{\eta}^h (B\partial\tau_x/\partial z) dz = B_h \tau_h - B_{\eta} \tau_{\eta} - \int_{\eta}^h \tau_x (\partial B/\partial z) dz \quad (12)$$

The first term is the column bottom shear evaluated at $z = h$ and can be evaluated from bottom velocity friction relationships. The surface shear $B_{\eta} \tau_{\eta}$ is the surface wind shear component parallel to the x axis. The third term is the wall or bottom shear due to the horizontal projection of the sloping sides of the water body ($\partial B/\partial z$). It is evaluated as bottom shear over the projected width ∂B at each elevation. The internal velocity shear cancels out of the vertical integration.

68. Collecting the various terms of Equation 9 into Equation 4 gives the surface elevation equation of:

$$\begin{aligned}
& \frac{\partial \bar{B}\eta}{\partial t} - g\Delta t \left(\frac{\partial}{\partial x} \int_{\eta}^h B dz \right) = \frac{\partial}{\partial x} \int_{\eta}^h UB dz \\
& - g\Delta t / \rho_{\eta} \left(\frac{\partial}{\partial x} \int_{\eta}^h \left[B \int_{\eta}^z (\partial \rho / \partial x) dz \right] dz \right. \\
& \left. + \left(\frac{\partial}{\partial x} \right) \left[B_h \tau_h - B_{\eta} \tau_{\eta} - \int_{\eta}^h \tau_x (\partial B / \partial z) dz \right] \Delta t \right. \\
& \left. + \left(\frac{\partial}{\partial x} \right) \left(\int_{\eta}^h F_x dz \right) \Delta t - \left(\int_{\eta}^h qB dz \right) \right.
\end{aligned} \tag{13}$$

With the η or surface coordinate terms collected on the left-hand side (LHS), Equation 13 is the water surface equation of the integrated water body. Equation 13 is, therefore, a numerical form of the frictionally dampened longwave equation for an irregular geometry, stratified water body.

Numerical Solution

69. The numerical procedure for solving for the six unknowns on each time step is to compute first the water surface elevations from Equation 13. With new values of η , new values of U can be computed from Equation 9. With new U values, the vertical velocity component W is found from continuity, Equation 3. The new constituent distribution is computed from the constituent balance, Equation 5. Using new U and W values, the water surface elevation equation (Equation 13) can be solved for η simultaneously. This substitution makes the solution spatially implicit in η at the same time level and eliminates the

Courant gravity wave speed criterion that $\Delta x/\Delta t > \sqrt{gH_{\max}}$, which leads to short computational Δt in deep water bodies.

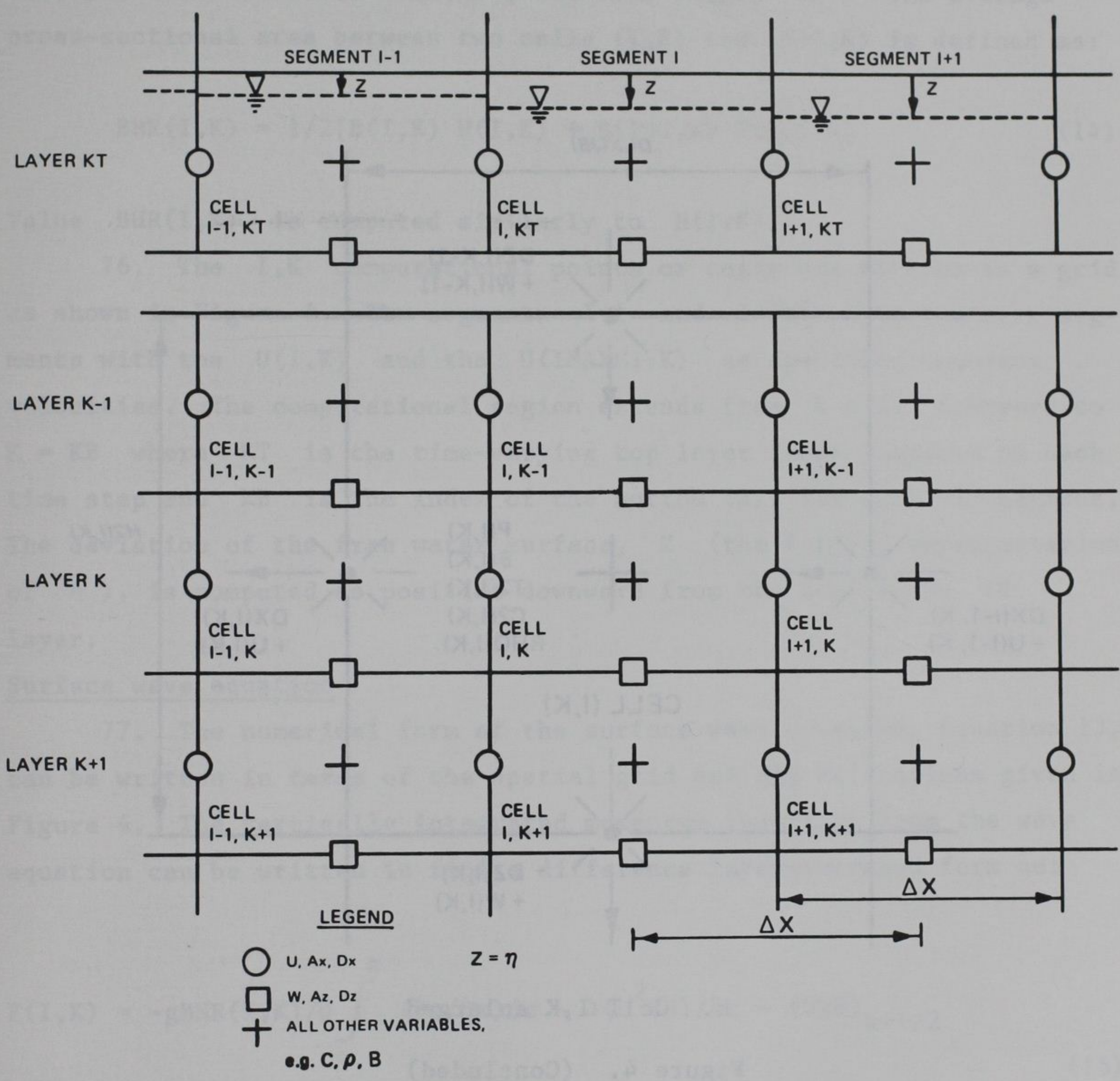
70. With the laterally averaged equations of motion expressed in an algebraic form, it is necessary to devise a finite difference coding for numerical computations. The coding not only includes the finite difference form of the equations but also the logic and algorithms needed to carry out the computations. These procedures are discussed in Appendix A.

71. The variables are located on a physical space and computational grid, as shown in Figure 4. It is called a space-staggered grid since certain variables are at one location and the remainder are displaced $\Delta x/2$ or $\Delta z/2$. There is a rational basis for choosing the grid locations which can be seen by using imaginary control volumes about a point.

72. The constituent concentration C is surrounded by a cell that has the U and W at the boundaries. Therefore, the U and W can transport C into and out of this cell with no spatial averaging of velocities necessary to determine the change in C over time. Similarly, the W is computed for the same volume using the U values.

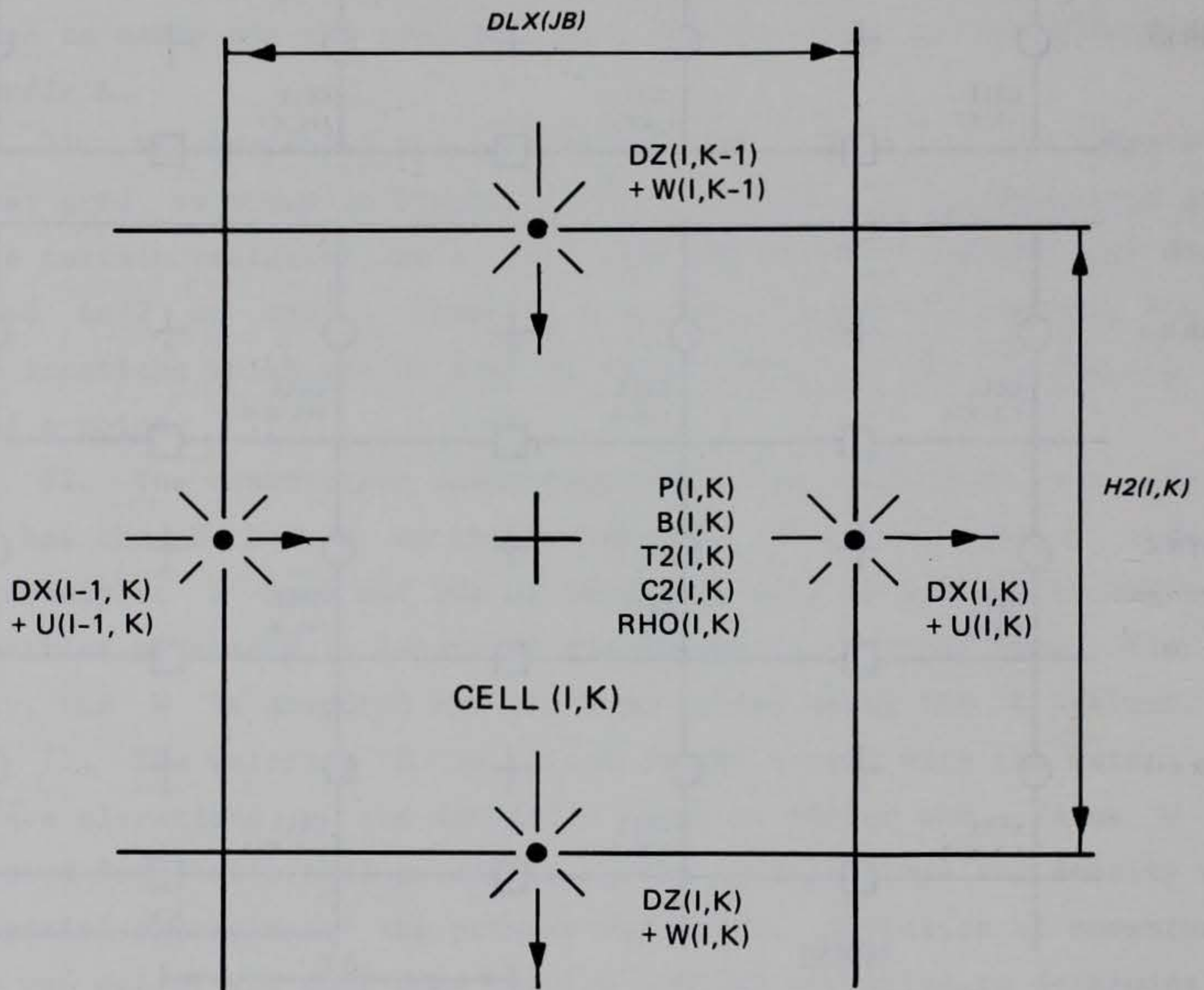
73. The velocity U is surrounded by a cell with the water surface elevations η and densities known at either end. Value U is computed from horizontal gradients of the surface slope and density with no spatial averaging of the primary variables. Advection of momentum into and out of the cell does require spatial averaging to determine the fluxes and the ends of the cell, but the variable U being computed remains centered.

74. For purposes of finite differencing, the variables are referenced to the computational point (I,K) using the space-staggered scheme shown in Figure 4. The velocity components $U(I,K)$ and $W(I,K)$ and the internal shear stress $\tau_x(I,K)$ are placed at the boundaries of an imaginary cell surrounding the (I,K) point. The variables $Z(I)$, $P(I,K)$, $\rho(I,K)$, $B(I,K)$, and $C(I,K)$ are placed at the center of the



a. Space-staggered grid structure

Figure 4. Location convention for variables on finite difference grid (Continued)



b. Cell I,K enlarged

Figure 4. (Concluded)

cell. The dispersion coefficients $AX(I,K)$, $DX(I,K)$, $DXC(I,K)$, $AZ(I,K)$, and $DZ(I,K)$ are defined at the cell boundaries.

75. The geometry is specified as in Figure 4 by a cell width $B(I,K)$, cell thickness $H(I,K)$, and cell length Δx . The average cross-sectional area between two cells (I,K) and $(I+1,K)$ is defined as:

$$BHR(I,K) = 1/2[B(I,K) H(I,K) + B(I+1,K) H(I+1,K)] \quad (14)$$

Value $BHR(I,K)$ is computed similarly to $H(I,K)$.

76. The I,K computational points or cells are arrayed in a grid as shown in Figure 4. The segments $I=1$ and $I=IMAX$ are boundary segments with the $U(1,K)$ and the $U(IMAXM1,K)$ as specified boundary velocities. The computational region extends from $K = KT$ downward to $K = KB$ where KT is the time-varying top layer index computed on each time step and KB is the index of the bottom cell for each I segment. The deviation of the free water surface, Z (the Fortran representation of η), is computed as positive downward from the top of the KT layer.

Surface wave equation

77. The numerical form of the surface wave equation, Equation 13, can be written in terms of the spatial grid and its definitions given in Figure 4. The vertically integrated momentum functions from the wave equation can be written in finite difference layer-averaged form as:

$$F(I,K) = -gBHR(I,K)/\rho \int_{\eta}^z (\partial\rho/\partial x) dz - \partial(U^2BH)/\partial x - (UWB)_{k+1/2} \quad (15)$$

$$+ (UWB)_{k-1/2} + \partial[BHA_x (\partial U/\partial x)]/\partial x - (\tau_x^B)_{k+1/2} + (\tau_x^B)_{k-1/2}$$

where, when computing $Z'(I)$, the new value of η at time step $N + 1$, the terms in $F(I,K)$ are evaluated from parameters available at time step N . The terms making up $F(I,K)$ are, respectively, the

density gradient component of the horizontal pressure gradient; the gradient of horizontally advected momentum; the vertical advection of momentum out of the K layer; the vertical advection of momentum into the K layer; the horizontal dispersion of momentum; the horizontal shear stress on the bottom of the K layer, and the horizontal shear stress on the top of the K layer.

78. The surface wave equation can be written in time-backward, spatially implicit tridiagonal form as:

$$A(I)Z'(I-1) + V(I)Z'(I) + C(I)Z'(I+1) = D(I) \quad (16)$$

where the tridiagonal matrix coefficients $A(I)$, $V(I)$, and $C(I)$ include the reservoir geometry summed over a cross section as:

$$A(I) = -g(\Delta t^2/\Delta x) \sum_k BHR(I-1,K) \quad (17)$$

$$V(I) = \Delta x B(I,KT) + g(\Delta t^2/\Delta x) \left[\sum_k BHR(I-1,K) + \sum_k BHR(I,K) \right] \quad (18)$$

$$C(I) = -g(\Delta t^2/\Delta x) \sum_k BHR(I,K) \quad (19)$$

The $A(I)$ geometry is the cross-sectional area between the $I-1$ and I segments, and the $C(I)$ geometry is the cross-sectional area between the I and $I+1$ segments. The geometry in $V(I)$ is the sum of the two cross sections. The tridiagonal coefficient $D(I)$ includes the overall dynamics, inflows, and outflows as:

$$D(I) = \Delta x B(I,KT)Z(I) + \Delta t^2 \sum_k [F(I,K) - F(I-1,K)] \quad (20)$$

$$+ \Delta t \sum_k [U(I,K)BHR(I,K) - U(I-1,K)BHR(I-1,K)] - \Delta t \sum_k Q'(I,K)$$

where $Q'(I,K)$ is the lateral boundary inflow or outflows at cell I,K . Equation 16 is solved using the Thomas tridiagonal algorithm.

79. The surface deviation, Equation 16, results from substitution of the vertically integrated momentum balance into the vertically integrated continuity balance. Substitution of these terms into the vertically integrated continuity equation is analogous to algebraically cross differentiating the vertically integrated continuity and momentum balances to arrive at the classical surface-longwave equation and finite differencing the latter implicitly forward in time. Thus, Equation 16 is the implicit finite difference form of the frictionally dampened longwave equation.

80. Equation 16 applies throughout the grid that represents the water body, including boundary regions where there is zero flux. To incorporate longitudinal flow-type boundary conditions, $D(I)$ is modified by subtracting the total inflow or adding the total outflow (times the time step) for the left and right boundaries, respectively. This method avoids the use of the applied boundary velocity U , computed as:

$$U(ILC-1,K) = QIN(JB)/BHR(ILC-1,K) \quad (21)$$

or

$$U(IR,K) = QOUT(J)/BHR(IR,K) \quad (22)$$

where $QIN(JB)$ and $QOUT(J)$ are the inflow and outflow, respectively. These applied velocities are derived variables and their use in the longwave equation leads to accumulating errors, which the direct use of $QOUT(J)$ and $QIN(JB)$ avoids.

81. Head-type boundary conditions are incorporated into the solution by using the off-diagonal coefficients $A(ILC)$ and/or $C(IR)$ with the applied boundary elevations at the upstream and/or downstream ends, respectively, of the active finite difference grid. These terms are ordinarily ignored by the Thomas algorithm; however, here they are

subtracted from the RHS expression $D(I)$ in the solution for $Z(ILC)$ and/or $Z(IR)$. There are two cases in which the head-type boundary conditions are used. These are open water boundaries, for which the external head, or elevation, is known from an observation record, and the boundaries of branches, where the applied head is generated by the solution to the surface wave equation in a joining branch. The first case is the common estuary case. The second case is represented by multistemmed lakes; reservoirs or estuaries; canals and cuts; and deltas. In applications to these geometries, the numerical solution is applied to each branch in turn, with the internal boundary conditions permitting the joining of the branches to form the water body. Since branch computations are performed sequentially, the precision of calculation could be aided by proper numbering of the branches so that water surface elevations are calculated using only information from the present time step.

Evaluation of $F(I,K)$ terms

82. The forcing function in the wave equation $F(I,K)$ in Equation 15 must be evaluated before the water surface elevations are computed at the new time step. All of the terms in $F(I,K)$ are therefore evaluated for variables computed from the past time step. The new time step data entering the wave equation are the boundary inflows, outflows, and surface heights. Many of the terms entering $F(I,K)$, including the longitudinal and vertical advection of momentum, the longitudinal dispersion of momentum, and the horizontal shears, also enter the horizontal momentum balance for the computation of $U(I,K)$ and are therefore evaluated as separate arrays.

83. The contribution of the horizontal density gradient to horizontal momentum is an integral over depth from a fixed reference surface of a horizontal density gradient. It applies at the I to $I+1$ boundary or where $U(I,K)$ and $F(I,K)$ are located. It is first computed using the vertical integration of pressure as:

$$P(I,K) = P(I,K-1) + \text{RHO}(I,K) * G * H2(I,K) \quad (23)$$

and

$$\begin{aligned} \text{HPG}(I,K) &= 0.5 * \text{DLXR} * \text{BR}(I,K) * (\text{H2}(I+1,K) \\ &* (\text{P}(I+1,K-1) + \text{P}(I+1,K)) - \text{H2}(I,K) \\ &* (\text{P}(I,K-1) + \text{P}(I,K))) \end{aligned} \quad (24)$$

to form $\text{HPG}(I,K)$, the horizontal pressure gradient. The second integral is formed when compiling the tridiagonal coefficients in Equation 20.

84. The horizontal advection of momentum is computed around the transport of the quantity $U(I,K)$ by velocities at $I+1/2$ and $I-1/2$ which are found by spatial averaging. Upwind differencing is used to evaluate the horizontal advection of momentum terms:

$$\begin{aligned} \text{ARR} &= 0 \\ \text{UR} &= (\text{U}(I+1,K) + \text{U}(I,K))/2 \\ \text{IF}(\text{UR.GT.0.}) \text{ARR} &= 1 \\ \text{AL} &= 0 \\ \text{UL} &= (\text{U}(I,K) + \text{U}(I-1,K))/2 \\ \text{IF}(\text{UL.GT.0.}) \text{AL} &= 1 \\ \text{ADMX}(I,K) &= (\text{BH2}(I+1,K) * \text{UR} * (\text{ARR} * \text{U}(I,K) + (1. - \text{ARR}) \\ &* \text{U}(I+1,K)) - \text{BH2}(I,K) * \text{UL} * (\text{AL} * \text{U}(I-1,K) \\ &+ (1. - \text{AL}) * \text{U}(I,K)))/\text{DLX}(\text{JB}) \end{aligned} \quad (25)$$

The horizontal advection of momentum is also applied at the I to $I+1$ interface.

85. The vertical advection of horizontal momentum is evaluated using upwind differencing for the transport of the I to $I+1$ interface quantity:

$$\begin{aligned} \text{AB} &= 0 \\ \text{WB} &= (\text{W}(I+1,K) + \text{W}(I,K))/2 \\ \text{IF}(\text{WB.GT.0.}) \text{AB} &= 1 \\ \text{ADMZ}(I,K) &= (\text{BR}(I,K) + \text{BR}(I,K+1)) \\ &* \text{WB} * (\text{AB} * \text{U}(I,K) + (1. - \text{AB}) * \text{U}(I,K+1))/2 \end{aligned} \quad (26)$$

86. The horizontal shears are evaluated at the cell upper and lower interfaces based on the velocity gradient relationships of:

$$ST(I,K) = ST(I,K) + AZ(I,K-1) * 0.5 * (BR(I,K-1) + BR(I,K)) * (U(I,K-1) - U(I,K))/H2(I,K) \quad (27)$$

and

$$SB(I,K) = ST(I,K+1) + GC2 * (BR(I,K) - BR(I,K+1)) * U(I,K) * ABS(U(I,K)) \quad (28)$$

where $ST(I,K)$ initially consists of the vertical attenuation of wind shear. The $AZ(I,K)$ is evaluated at the top and bottom interface. Evaluation of AZ as a function of density gradients and wind shear is discussed as an auxiliary function.

87. The longitudinal dispersion of momentum is computed at the I and $I+1$ interface using a second-order central difference as follows:

$$DM(I,K) = (AX/DLX2) * 0.5 * (H2(I,K) + H2(I+1,K)) * (BR(I+1,K) * U(I+1,K) - 2.0 * BR(I,K) * U(I,K) + BR(I-1,K) * U(I-1,K))$$

where $AX(I,K)$ is located at the position of $U(I,K)$.

Computation of horizontal and vertical velocities

88. The horizontal velocity component is computed from Equation 9. The pressure and horizontal pressure gradients are computed again immediately after the surface displacements are obtained from the wave equation and the surface layer thicknesses are updated. The horizontal velocity component is then computed from the term and the horizontal pressure gradient, the advection of momentum, the horizontal dispersion of momentum, and shear components developed for the wave equation. The horizontal velocity equation is:

$$\begin{aligned}
 U(I,K) = & (BHR2(I,K) * U(I,K) + DLT * (-ADMX(I,K) \\
 & - ADMZ(I,K) + ADMZ(I,K-1) - HPG(I,K) + DM(I,K) \\
 & + ST(I,K) - SB(I,K))) / BHR1(I,K)
 \end{aligned}
 \tag{29}$$

where the horizontal pressure gradient HPG(I,K) is updated for the new Z(I) . Many of the other terms were previously evaluated when determining F(I,K) .

89. The vertical velocity components are computed from Equation 3 by integrating continuity from the bottom upward as:

$$\begin{aligned}
 WT1 &= W(I,K+1) * BB(I,K+1) \\
 WT2 &= ((BHR1(I,K+1) * U(I,K+1)) - (BHR1(I-1,K+1) \\
 & * U(I-1,K+1))) / DLX(JB) - Q(I,K+1) / DLX(JB) \\
 W(I,K) &= (WT1 + WT2) / BB(I,K)
 \end{aligned}
 \tag{30}$$

where

$$BB(I,K) = (B(I,K) + B(I,K+1)) / 2
 \tag{31}$$

and Q(I,K) is the lateral inflow and outflow to cell I,K .

90. The top cell W(I,KT) is computed separately from the surface change in elevation to maintain continuity in the surface layers and to correct for truncation errors accumulated from summing over the whole water column. Value W(I,KT) is used in the transport computation.

Constituent transport

91. The constituent transport relationship is solved explicitly for N constituents with values of C(I,K,JC) in the adjacent cell formulation of:

$$\begin{aligned}
 T1(I,K) = & (TCC(I,K) * T2(I,K) + TCL(I,K) * T2(I-1,K) \\
 & + TCR(I,K) * T2(I+1,K) + TCT(I,K) * T2(I,K-1) \\
 & + TCB(I,K) * T2(I,K+1) + HNT(I,K) / DLX(JB)) \\
 & * DLT / BHR1(I,K)
 \end{aligned}
 \tag{32}$$

where the coefficients are determined from the general form of the transport equation. They are solved once during a time step for

temperature. The transport coefficients $TCR(I,K)$, $TCL(I,K)$, and $TCC(I,K)$ are recomputed prior to constituent transport to allow a different value of horizontal dispersion for constituents. The transport coefficients are then applied across all constituents. The transport coefficients are:

$$\begin{aligned}
 TCR(I,K) &= DLX1 * BHR1(I,K) \\
 &\quad * ((-1. + US(I,K)) * U(I,K) + DX(I,K)/DLX(JB)) \\
 TCL(I+1,K) &= TCR(I,K) + DLX1 * BHR1(I,K) * U(I,K) \\
 TCB(I,K) &= -W(I,K) * BB(I,K) * (1. - WS(I,K)) \\
 &\quad + DZ(I,K) * 2. * BB(I,K)/(H2(I,K) + H2(I,K+1)) \\
 TCT(I,K+1) &= TCB(I,K) + W(I,K) * BB(I,K) \tag{33} \\
 TCC(I,K) &= BH2(I,K)/DLT \\
 &\quad + DLX1 * BHR2(I-1,K) \\
 &\quad * ((1. - US(I-1,K)) * U(I-1,K) - DX(I-1,K)/DLX(JB)) \\
 &\quad + DLX1 * BHR2(I,K) \\
 &\quad * (-US(I,K) * U(I,K) - DX(I,K)/DLX(JB)) \\
 &\quad - W(I,K) * BB(I,K) * WS(I,K) \\
 &\quad + W(I,K-1) * BB(I,K-1) * (1. - WS(I,K-1)) \\
 &\quad - DZ(I,K) * 2. * BB(I,K)/(H2(I,K) + H2(I,K+1)) \\
 &\quad - DZ(I,K-1) * 2. * BB(I,K-1)/(H2(I,K-1) + H2(I,K))
 \end{aligned}$$

where

$$US = 0 \quad \text{if } U < 0$$

$$US = 1 \quad \text{if } U > 0$$

$$WS = 0 \quad \text{if } W < 0$$

$$WS = 1 \quad \text{if } W > 0$$

92. The sources and sinks for heat are included in the term $HNT(I,K)$. The sources and sinks for other constituents are represented by the sum of two terms $HNC(I,K,JC)$ and $CSS(I,K,JC)$. The $HNC(I,K,JC)$ term includes all external sources and sinks, such as loadings due to inflows and withdrawals. The term $CSS(I,K,JC)$ includes all internal sources and sinks such as those due to constituent reactions and interactions. This allows the updating of internal sources and sinks at different frequencies than the hydrodynamics without affecting numerical stability.

Auxiliary Operations

93. The auxiliary functions are relationships that describe processes that are independent of the computational scheme and can be changed or revised as knowledge advances or as needed for specific applications. The auxiliary functions include the descriptions of the turbulent dispersion process, the constituent reactions and interactions, heat budget, and ice relationships.

Wind shear and mixing

94. Longitudinal-vertical, numerical hydrodynamic models require evaluation of wind shear and vertical mixing over the depth of the water column. There are a number of wind shear and mixing problems that arise with longitudinal-vertical, numerical models.

95. First, there is the anomaly that with fixed grid, movable surface models, the same wind shear applied only at the surface would be absorbed in a variable thickness layer and could lead to extreme velocities and velocity gradients. Leendertse and Liu (1977), in the 3-D models, have had to limit wind shear as a function of layer depth. Bloss and Harleman (1979) have had to decay wind energy as a function of depth in a 1-D, vertical model. Second, in 2-D models, it is necessary to evaluate vertical eddy viscosity and vertical eddy diffusivity as functions of wind speed, and especially for winds normal to the axis of the model. Also, in branched longitudinal-vertical models it is necessary to account for different wind effects on different branches, not only due to wind direction but also due to wind shading and fetch.

Wind shear in horizontal momentum

96. In 2-D longitudinal-vertical models, wind shear enters the longitudinal momentum balance through the vertical transport of horizontal momentum. The instantaneous horizontal and vertical velocity can be written as:

$$u = U + u' + u'' \quad (34)$$

$$w = W + w' + w'' \quad (35)$$

where U and W are the time-averaged mean velocity components, u' and w' are the turbulent velocity fluctuations about the mean generated by velocity shear, and u'' and w'' are the velocity components of wind waves propagated downward from the water surface. The time mean of the vertical transport of momentum becomes:

$$\langle uw \rangle = UW + \langle u'w' \rangle + \langle u''w'' \rangle \quad (36)$$

where $\langle u'w' \rangle + \langle u''w'' \rangle$ makes up the longitudinal shear stress. The turbulent transport is related to the mean velocity as:

$$\langle u'w' \rangle = -A_z \partial U / \partial z \quad (37)$$

where A_z is the vertical eddy viscosity.

97. Averaged over time, the decay of shear due to the velocity fluctuations by analogy to wind wave decay (Kinsman 1979) becomes:

$$\langle u''w'' \rangle = \tau_{wx} e^{-2kz} \quad (38)$$

where

τ_{wx} = surface shear due to wind along the x-axis of the model

k = the wave number

and the surface shear due to wind mixing along the x-axis of the model is evaluated from

$$\tau_{wx} = \rho_a / \rho_w W^2 C_d \cos(\theta_1 - \theta_2) \quad (39)$$

where

ρ_a = density of air, kg m^{-3}

ρ_w = density of water, kg m^{-3}

C_d = drag coefficient

W = sheltered wind speed, m sec^{-1}

θ_1 = wind direction relative to north

θ_2 = branch orientation relative to north

and the sheltered wind speed is the product of the measured wind speed and the sheltering coefficients. The drag coefficient C_d varies with wind speed. The wave number k is evaluated by

$$k = \frac{4\pi^2}{gT_w^2} \quad (40)$$

where the wind wave period T_w is determined by the empirical expression of Wiegel (1964).

$$T_w = 6.95 \times 10^{-2} F^{0.233} |W|^{0.534} \quad (41)$$

where the fetch F is equal to one-half the branch length. The horizontal shear over depth then becomes:

$$\tau_x = -A_z \frac{\partial U}{\partial z} + \tau_{wx} e^{-2kz} \quad (42)$$

Thus, the wind shear decays with depth and generates horizontal velocities directly through the horizontal momentum balance, and the momentum is dissipated through the vertical eddy viscosity.

Vertical eddy viscosity and wind shear

98. The vertical eddy viscosity for longitudinal-vertical dynamics can be formulated by analogy to the 3-D case for which:

$$A_z = K(\ell^2/2)[(\partial U/\partial z)^2 + (\partial V/\partial z)^2]^{1/2} e^{-Cz} \quad (43)$$

where K is taken to be 0.1, ℓ is the vertical length scale taken as the layer thickness Δz for finite differences, C is a constant, and

Ri is the local Richardson number, as determined by $Ri = (g \partial\rho/\partial z) / (\rho(\partial U/\partial z)^2)$. Upper and lower bounds are imposed on Ri, which in turn impose limits on A_z .

99. In a longitudinal-vertical model, the lateral velocity V and its gradient $\partial V/\partial z$ are due to the lateral component of wind shear and average laterally to zero, but not necessarily the square $(\partial V/\partial z)^2$. It is assumed that the cross wind shear τ_{wy} generates lateral wave components v'' such that $\langle w''v'' \rangle = \tau_{wy} e^{-2kz}$. Further, by analogy let:

$$A_z^2 (\partial V/\partial z)^2 = \left(\tau_{wy} e^{-2kz} \right)^2 \quad (44)$$

giving, for the cross wind shear

$$(\partial V/\partial z)^2 = \left(\tau_{wy} e^{-2kz/A_z} \right)^2 \quad (45)$$

where the surface shear due to the lateral cross-current fluctuations is given by

$$\tau_{wy} = \rho a / \rho_w W^2 C_d \sin(\theta_1 - \theta_2) \quad (46)$$

Thus, the eddy viscosity with cross wind shear becomes:

$$A_z = K(\ell^2/2) \left[(\partial U/\partial z)^2 + \left(\tau_{wy} e^{-2kz/A_z} \right)^2 \right]^{1/2} e^{-CRi} \quad (47)$$

In numerical form, A_z can be iterated from Equation 45 by using the previous time step value to evaluate the cross wind shear contribution.

100. The above formulation of wind shear in horizontal momentum and evaluation of A_z leads to wind-driven surface currents that are 3 to 10 percent of the surface wind velocity, with the higher values appearing at higher wind speeds. This is in accordance with the few

attempts to relate wind speed and surface current velocity from field data that appear in the literature. With the formulation, the surface current does not reach abnormal values as it does for the case of wind shear applied only to the surface and as the thickness of the surface layer decreases. The depth of the wind-driven surface layer increases with wind speed, and the mass transport due to wind appears to be insensitive to the finite difference layer thickness.

101. The Quabbin application of the GLVHT model (Buchak and Edinger 1982a) with three interconnected arms showed the importance of wind shading geographically over each arm as well as the importance of variable fetch as it affects the wind wave decay. In this case, there were significant differences in temperature profiles between the three arms at a given time that were attributable to fetch and wind shading.

102. The need to identify the geographical distribution of wind shading, fetch, and angle of an arm segment axis relative to the wind leads to great flexibility in characterizing wind conditions on real water bodies. Presently, wind speed and direction as a function of time are known at best for one or two stations in reservoir research studies, and at worst in the usual applied case from a distant airport anemometer. More effort is required to characterize the variability of wind speed, direction, and resulting wind waves throughout geometrically complex reservoirs before fixed rules can be established for assigning wind shading and fetch to reservoir segments. In the interim, it is possible to proceed to new case applications using the experience of past applications.

103. The wind wave formulation is presently based on the significant wave height and period. It is obvious that there is a whole spectrum of wind wave components u'' and v'' and hence a whole spectrum of wind wave decay rates that produce a spectrum of wind shears. It is presently not known if the major portion of the wind shear is propagated by the waves making up the significant wave height and period portion of the wind wave spectrum. The present formulation provides the basis for further theoretical investigations.

104. The vertical eddy diffusivity D_z is assumed to be a fraction (0.14) of the vertical eddy viscosity. The maximum and minimum allowable values for A_z , and hence D_z , are calculated internally and are influenced by a specified low value (AZMIN) and an upper value which is computed from $\Delta x^2 / \Delta t$. The longitudinal eddy viscosity A_x and diffusivity D_x are presently considered constants.

Surface heat exchange

105. Surface heat exchange can be formulated as a source/sink term using the explicit transport computation (Equation 32) as long as the integration time step is shorter than the time step of the meteorological data update. The surface heat exchange processes that depend on water surface temperatures are computed using previous time step data for water surface temperature and are therefore lagged from the transport processes by the integration time step.

106. The net heat exchange at the water surface is composed of seven processes:

- a. Shortwave solar radiation.
- b. Reflected shortwave radiation.
- c. Longwave atmospheric radiation.
- d. Reflected longwave radiation.
- e. Heat transfer due to conduction.
- f. Back radiation for the water surface.
- g. Heat loss due to evaporation.

107. After some linearization, these processes may be incorporated into a single thermal equation quantifying net heat exchange (Edinger and Geyer 1965).

$$H_s = K(T_e - T_s) \Delta x B \quad (48)$$

where

H_s = net rate surface heat transfer, $^{\circ}\text{C m}^3 \text{sec}^{-1}$

K = coefficient of surface heat exchange, m sec^{-1}

T_e = equilibrium temperature, $^{\circ}\text{C}$

T_s = surface temperature, $^{\circ}\text{C}$

Δx = segment length, m

B = segment width, m

The equilibrium temperature is defined as that temperature at which the net rate of heat exchange between the water surface and the atmosphere is zero. The coefficient of heat exchange is the rate of transfer at the air/water interface. The equilibrium temperature approach has the advantage of extending, without modification, through the range of conditions under which ice forms. The term-by-term method of computing surface heat exchange can easily be incorporated into the code. As with the other auxiliary functions described in this section, the particular form of surface heat exchange computations adopted does not affect the structure of the code. The seven individual heat exchange processes can be computed and their magnitudes added to the heat transport source/sink array, HNT.

108. The components of surface heat exchange, with the exception of shortwave radiation, are immediately absorbed at the water surface or in the top approximately 0.6 m. However, shortwave radiation penetrates the surface and decays exponentially with depth according to Beer's Law. These processes may be expressed as:

$$H_s = [K(T_e - T_s) - (1-\beta)\psi]\Delta x B \quad (49)$$

$$H_i = (1-\beta)\psi e^{-\lambda Z_i} \Delta x B_i \quad (50)$$

where

H_s = heat transfer into or out of the surface layer, $^{\circ}\text{C m}^3 \text{sec}^{-1}$

H_i = heat absorption in layer i , $^{\circ}\text{C m}^3 \text{sec}^{-1}$

β = percentage of incoming solar radiation absorbed in the surface layer

ψ = shortwave radiation reaching the surface, $^{\circ}\text{C m sec}^{-1}$

λ = attenuation coefficient, m^{-1}

Z_i = depth, m

Δx = segment length, m

B = segment width, m

The shortwave radiation reaching the surface is removed successively from the bottom of the top cell in the computations and passed into the top of the next lower cell. The attenuation coefficient λ is assigned a single value (GAMMA) when algae are not included in simulations. If algae are included, a base value (EXCO) is used which represents the attenuation due to pure water plus dissolved components. This coefficient is then modified by suspended solids concentrations (inorganic suspended solids, algae, and detritus) to allow simulation of the effects of self-shading on temperature distributions and light available for algal growth (see Part IV).

109. The heat exchange variables should be computed as a side computation and accessed through the subroutine TVDS (see Part IV). Caution should be exercised in the use of temperature estimates for the surface temperature-dependent terms. The computation of heat exchange variables is described by US Army Engineer District, Baltimore (1977). Also, note that heat units ($W m^{-2}$) are converted to model units by dividing by the specific heat of water ($J kg^{-1} ^\circ C^{-1}$) and its density ($kg m^{-3}$).

Evaporation

110. Heat losses due to evaporation are always included in terms for net heat exchange. However, the computation of the effects of evaporation rates on the water budget is included as a user option. The rate of evaporation is computed from (Edinger, Brady, and Geyer 1974).

$$Q_e = \beta_e (T_s - T_d) f(W) B \Delta x / \rho L_e \quad (51)$$

where

- Q_e = evaporation rate, $m^3 sec^{-1}$
- T_s = water surface temperature, $^\circ C$
- T_d = dewpoint temperature, $^\circ C$
- $f(W)$ = evaporative wind speed function, $W m^{-2} mm Hg^{-1}$
- B = width of the surface layer, m
- Δx = segment length, m

ρ = density of water, kg m^{-3}

L_e = latent heat of vaporization, W sec kg^{-1}

and β_e is the slope of the chord between T_s and T_d on the saturated water vapor pressure curve $\text{mm Hg } ^\circ\text{C}^{-1}$ which is computed from

$$\beta_e = 0.35 + 0.015T_a + 0.0012T_a^2 \quad (52)$$

where T_a is the average of T_s and T_d .

111. Five wind speed functions are included in CE-QUAL-W2 which may be selected by the user. These are the functions described by Brady, Graves, and Geyer (1969); Harbeck, Koberg, and Hughes (1959); Jacoby et al. (1977); Meyer (1928); and Morton (1965). The default expression is Brady, Graves, and Geyer (1969). Others may be accessed by commenting out this expression and activating the desired one. The different formulations result from the empirical determination of $f(W)$ for different sized and shaped water bodies, and various formulations were tested by Edinger, Brady, and Geyer (1974). The evaporative wind speed function used to calculate heat exchange must be consistent with the function used to compute evaporation rate.

Density relationships

112. The accurate depiction of hydrodynamics requires that water densities be accurately predicted. Water densities are affected by variations in temperatures and solids concentrations, according to the following relation:

$$\rho = \rho_T + \Delta\rho_s \quad (53)$$

where

ρ = water density, kg m^{-3}

ρ_T = water density as a function of temperature, kg m^{-3}

$\Delta\rho_s$ = density increment due to solids, kg m^{-3}

113. A variety of formulations have been proposed to describe water density variations due to temperature. The following relationship described by Gill (1982) is used in CE-QUAL-W2:

$$\begin{aligned} \rho_T = & 999.8452594 + 6.793952 \times 10^{-2} T - 9.095290 \times 10^{-3} T^2 \\ & + 1.001685 \times 10^{-4} T^3 - 1.120083 \times 10^{-6} T^4 \\ & + 6.536332 \times 10^{-9} T^5 \end{aligned} \quad (54)$$

where T water temperature, °C.

114. Density increments may also result from solids concentrations, both suspended and dissolved. For most applications, dissolved solids data will be in the form of total dissolved solids (TDS). However, for some applications, salinity may be specified. The density increment for dissolved solids is calculated for either of these variables, with the choice specified by the variable IWT. The density increment due to TDS is given by (Ford and Johnson 1983)

$$\begin{aligned} \Delta\rho_{TDS} = & C_{TDS} (8.221 \times 10^{-4} - 3.87 \times 10^{-6} T^{-6} \\ & + 4.99 \times 10^{-8} T^2) \end{aligned} \quad (55)$$

where C_{TDS} is the TDS concentration in $g\ m^{-3}$ and that for salinity (Gill 1982)

$$\begin{aligned} \Delta\rho_{SL} = & C_{SL} (0.824493 - 4.0899 \times 10^{-3} T + 7.6438 \times 10^{-5} T^2 \\ & - 8.2467 \times 10^{-7} T^3 + 5.3875 \times 10^{-9} T^4) \\ & + C_{SL}^{1.5} (-5.72466 \times 10^{-3} + 1.0227 \times 10^{-4} T \\ & - 1.6546 \times 10^{-6} T^2) + 4.8314 \times 10^{-4} C_{SL}^2 \end{aligned} \quad (56)$$

where C_{SL} is salinity in $kg\ m^{-3}$. The density increment for suspended solids is given by (Ford and Johnson 1983)

$$\Delta\rho_{SS} = C_{SS}(1 - 1/SG) \times 10^{-3} \quad (57)$$

where

C_{SS} = suspended solids concentration, $g\ m^{-3}$

SG = specific gravity of suspended solids

Assuming a specific gravity of 2.65, the above relationship is simplified to

$$\Delta\rho_{SS} = 0.00062 C_{SS} \quad (58)$$

The total density increment due to solids is then

$$\Delta\rho_S = (\Delta\rho_{SL} \text{ or } \Delta\rho_{TDS}) + \Delta\rho_{SS} \quad (59)$$

Ice cover relationships

115. The onset and loss of ice cover, as well as ice thickness, play an important role in the heat transport of water bodies in northern climates. At high latitudes, the ice cover might remain until late spring or early summer and prevent warming due to absorption of shortwave solar radiation.

116. The ice model is based on the processes which include an ice cover with ice-to-air heat exchange, conduction through the ice thickness, and conduction between the underlying water and a "melt temperature" layer on the bottom of the ice (Ashton 1979). The overall heat balance for the water to ice-to-air system is:

$$\rho_i L \Delta h / \Delta t = h_{ia}(T_i - T_e) - h_{wi}(T - T_m) \quad (60)$$

where

ρ_i = density of ice, $kg\ m^{-3}$

L = latent heat of ice, $J\ kg^{-1}$

$\Delta h / \Delta t$ = change in ice thickness h with time, $m\ sec^{-1}$

h_{ia} = ice-to-air coefficient of surface heat exchange, $W\ m^{-2}\ ^\circ C^{-1}$

T_i = ice temperature, °C

T_e = equilibrium temperature of ice-to-air heat exchange, °C

h_{wi} = coefficient of water-to-ice heat exchange through the melt layer, $W m^{-2} °C^{-1}$

T = water temperature below ice, °C

T_m = melt temperature (0° C), °C

The ice-to-air coefficient of surface heat exchange h_{ia} and its equilibrium temperature T_e are computed the same as for water surface heat exchange in Edinger, Brady, and Geyer (1974) because the heat balance of the thin ice surface water layer is the same as the net rate of surface heat exchange. The coefficient of water-to-ice exchange h_{wi} depends on the turbulence and water movement under the ice and their effect on the melt layer thickness. It is known to be a function of water velocity for rivers and streams but must be empirically adjusted for reservoirs.

117. The ice temperature in the overall ice heat balance is computed from equating the rate of surface heat transfer between the ice and the air to the rate of heat conduction through the ice as:

$$h_{ia}(T_i - T_e) = k_i(T_i - T_m)/h \quad (61)$$

where k_i is the molecular heat conductivity of ice, $W m^{-1} °C^{-1}$. When solved for the ice temperature T_i and inserted in the overall ice heat balance, the ice thickness relationship becomes:

$$\rho_i L \Delta h / \Delta t = (T_m - T_e) / (h/k_i + 1/h_{ia} - h_{wi}(T - T_m)) \quad (62)$$

from which the ice cover thickness can be computed for each longitudinal surface segment of the GLVHT model. Heat from the water to the ice transferred by the last term is removed in the water temperature transport computations.

118. The coefficient h_{wi} is divided by ρC_p to convert the water-to-ice exchange coefficient from $W/(m^2 °C)$ to $°C m^3 sec^{-1}/(m^2 °C)$. In SI (metric) units, $\rho = 1,000 kg m^{-3}$, $C_p = 4,186 W sec$

$$\text{kg}^{-1} \text{ } ^\circ\text{C}^{-1} \quad \text{and} \quad 1/(\rho C_p) = 2.389 \times 10^{-7} \text{ } ^\circ\text{C} \text{ m}^3 \text{ sec}^{-1} \text{ W}^{-1} .$$

Inflow and outflow boundary conditions

119. Inflows and outflows are specified either as lateral flows normal to the longitudinal-vertical plane or as velocities at the longitudinal boundaries. The boundary velocities are computed from the inflows and outflows or the specified external head and contribute to horizontal momentum fluxes. The vertical distribution of velocities must be specified as a boundary condition. Associated with the velocity distributions is the constituent distribution which may influence horizontal density gradients and momentum.

120. Lacking specific velocity distribution data, the simplest velocity inflow boundary distribution is a uniform velocity computed from the inflow rate and cross section. The uniform velocity distribution is usually redistributed by the hydrodynamic computations themselves over the cross section within one or two model segment lengths of the inflow location. This is the normally encountered inflow velocity case for shallow headwaters.

121. Deeper upstream segments and significant density anomalies of the inflow relative to the main water body can result in distorted inflow velocity profiles. A uniform distribution of a dense inflow can cause artificially large density flows in the headwater and reverse circulation and inflow mixing as the flow becomes established. Such flows may require redistribution over the cross section with more of the flow near the bottom layers for denser flows and more near the top for lighter flows to give a more realistic inflow profile.

122. Outflows from reservoirs are usually from ports that are within a layer or two in thickness. Tests have shown that single-layer outflows produce up-reservoir velocity withdrawal envelopes similar to those found in selective withdrawal schemes. It has not been necessary to use any selective withdrawal scheme to represent withdrawals from an outflow except in the case of an intake that extended through many layers.

123. Because of grid resolution, lateral averaging, and hydrostatic approximation for the vertical momentum equation, CE-QUAL-W2 should not be expected to accurately resolve withdrawal velocity distributions for the outlets. To correct for this, the outlet specifications (location and percentage of total flow) for CE-QUAL-W2 should be calibrated against a known or predicted withdrawal distribution. Predicted withdrawal distributions can be obtained from physical and mathematical selective withdrawal models, e.g., SELECT (Bolan and Grace 1973) and WESSEL (Thompson and Bernard 1985).

Constituent reactions and interactions

124. The constituent transport relationships described in the previous section efficiently compute the transport of all constituents with their unit volume reaction and interaction rates expressed in the source and sink terms. All sources and sinks for water temperature are contained in the term $HNT(I,K)$. The sources and sinks for biological and chemical constituents are divided into two separate terms, $HNC(I,K,JC)$ and $CSS(I,K,JC)$. The term $HNC(I,K,JC)$ contains all external sources and sinks for constituents that are transported, such as are due to external loadings, and are evaluated in the main body of the program. The term $CSS(I,K,JC)$ represents internal sources and sinks due to constituent reactions and interactions. These terms are computed in a series of subroutines for all nonconservative materials that are subjected to transport. This division of terms allows internal sources and sinks to be updated at different frequencies than hydrodynamics and transport, which is consistent with the coarser time scales often associated with biological and chemical processes as opposed to hydrodynamics. This also allows a savings in computational time. The frequency at which $CSS(I,K,JC)$ is updated is specified by the parameter $NUPDC$.

125. The source and sink term $CSS(I,K,JC)$ represents a mass rate of change of constituent JC due to all reactions and interactions for cell I,K , in units of grams per second, where concentrations are expressed as milligrams per litre. The reactions and interactions can be

depicted graphically by considering each constituent as a compartment. Mass transfer rates between compartments may be represented by arrows, with a gain (or source) represented by an arrow leading to the compartment and a loss (or sink) by an arrow leading away. The process rate equation for a particular constituent can be developed directly from such a graphical representation. Both graphical and mathematical descriptions of the process rates for each constituent are provided.

126. All biological and chemical reaction rates are affected by temperature. This effect is expressed in a series of temperature rate multipliers computed in the subroutine RMULT. Due to the number of rate multipliers that must be computed, this computation may significantly add to computational time required for simulations. However, the temperature variations that may occur over short periods of time may not appreciably affect reaction rates. A provision is made to specify the frequency at which the temperature rate multipliers are updated, through the parameter NUPDRT, allowing a savings in simulation times.

127. Constituent concentration values are not allowed to become negative. Additionally, some constituent concentrations are not allowed to become zero to avoid division by zero errors. A check is made at the end of the time loop, and concentrations are modified if they fall below zero or a set minimum value.

128. A cross reference is provided for the terms in the compartmental rate equations and their FORTRAN equivalent (Table 2). All rate terms used in model equations are in units of 1 sec^{-1} . These rates are converted internally from the rates in units of 1 day^{-1} provided in the control file (see Part IV).

129. Conservative tracer. A conservative constituent has been included to allow simulation of dye studies, movements of conservative materials through the water body, and as an aid in the calibration and testing of flow regimes. As a conservative material, this constituent has no internal sources or sinks and the rate term $\text{CSS}(I,K,1)$ is set to zero.

130. Inorganic suspended solids. Inorganic suspended solids concentrations are important in any simulation or reservoir water quality

Table 2

Computer Cross Reference

| <u>Equation</u> | <u>Computer Code</u> | <u>Equation</u> | <u>Computer Code</u> |
|-----------------|----------------------|-----------------|-----------------------------|
| β | FFACT | ω_3 | SETL(1) |
| γ_{11} | RTMLT1(1,I,K) | ω_4 | FESETL |
| γ_{12} | RTMLT1(2,I,K) | A_1 | ADSRBP |
| γ_{13} | RTMLT1(3,I,K) | A_2 | ADMAXP |
| γ_{14} | RTMLT1(4,I,K) | A_3 | ADSRBN |
| γ_{15} | RTMLT1(5,I,K) | A_4 | ADMAXN |
| γ_{16} | RTMLT1(6,I,K) | A_e | PEXCR(1) |
| γ_{17} | RTMLT1(7,I,K) | A_g | PMAX(1) |
| γ_{18} | RTMLT1(8,I,K) | A_{kt} | B(I,KT)*DLX(JB) |
| γ_{21} | RTMLT2(5,I,K) | A_m | PMORT(1) |
| γ_{22} | RTMLT2(6,I,K) | A_r | PRESP(1) |
| γ_{23} | RTMLT2(7,I,K) | A_s | (B(I,K-1) - B(I,K))*DLX(JB) |
| γ_{24} | RTMLT2(8,I,K) | C_i | CW(I,K,i) |
| Δz | H2(I,K) | D_c | DMC02 |
| δ_P | BIOD | D_o | DM02 |
| δ_N | BION | F | B(I,K)/B(I,K-1) |
| δ_C | BIOC | H | EL |
| δ_{OF} | O2FAC | I_o | SRM |
| δ_{OR} | O2RESP | I_s | PISAT(1) |
| δ_{ON} | O2NH3 | K_a | CNH3DK |
| δ_{OD} | O2DET | K_c | COLIDK |
| δ_{OM} | O2DOM | K_d | DOMDK |
| δ_s | SFC02 | K_{dt} | DETUDK |
| θ | Q10COL | K_e | AEXCR(I,K,1) |
| ϕ_1 | XL | K_g | AMU(I,K,1) |
| ϕ_2 | XP | K_m | ANPM(I,K,1) |
| ϕ_3 | XN | K_n | CN03DK |
| ω_1 | SSETL | K_r | RFRDK |
| ω_2 | DSETL | K_{rs} | ART(I,K,1) |

(Continued)

Table 2 (Concluded)

| <u>Equation</u> | <u>Computer Code</u> | <u>Equation</u> | <u>Computer Code</u> |
|-----------------|----------------------|-----------------|----------------------|
| K_s | SEDDK | S_1 | SOD(I) |
| K_t | DOMRFR | S_2 | XP4REL |
| P_1 | ALDIGO | S_3 | CNREL |
| P_2 | PS2P04(1) | S_4 | FEREL |
| P_3 | PS2N(1) | V | BH2(I,K)*DLX(JB) |
| | | W_a | WA |

because of their influence on both the density and light regimes. Increased suspended solids reduce light penetration in the water column and, therefore, may influence temperature distributions. Nearly all biological and chemical rates are temperature dependent. Nutrient concentrations are also affected by solids concentrations through the mechanisms of adsorption and settling. Light and nutrient availability largely control algal production. With reference to Figure 5, the rate equation for inorganic suspended solids is given by

$$CSS(I,K,2) = \omega_1 V C_2 / \Delta z \quad (63)$$

where

ω_1 = settling velocity, m sec⁻¹

V = cell volume, m³

C_2 = suspended solids concentration, g m⁻³

Δz = cell thickness, m

131. In the finite difference representation of suspended solid concentrations, the solids settled from layer K-1 of segment I serve as a source for the layer below it, K. However, only a given fraction (F) is allowed to settle to the K layer as determined by the ratio of their widths, $B(I,K)/B(I,K-1)$. The remaining portion (1-F) is assumed

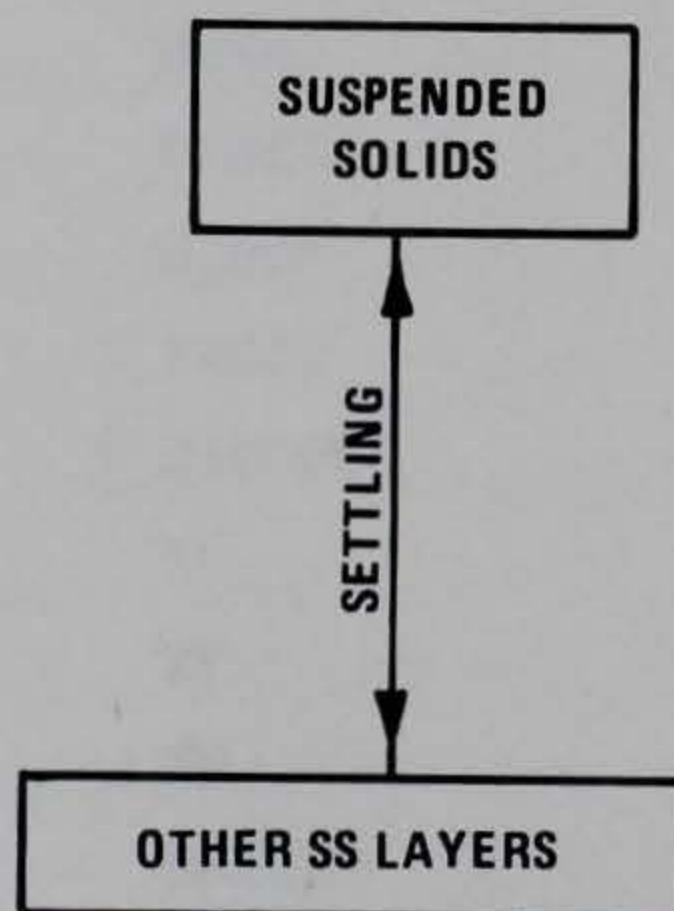


Figure 5. Internal flux for inorganic suspended solids

to be lost to sediments. No provision is made to accumulate sediment inorganic solids or to allow resuspension. In addition, lateral averaging results in homogeneous solids concentrations in the lateral dimension, while in reality concentrations may decrease with distance away from the dominant flow path. No provision is made to include this effect in simulations. The rate term for inorganic suspended solids is evaluated in the subroutine SOLIDS.

132. Coliform bacteria. The abundance of coliform bacteria has traditionally been used as an indicator of pathogen contamination. Standards and criteria have been formulated and promulgated based upon coliform concentrations to indicate the safety of water for drinking or recreational purposes. Predictions of coliform bacteria are, therefore, important because of their impact on project purposes such as recreation and water supply.

133. Total coliforms, fecal coliforms, or fecal streptococci can be simulated with this compartment. This compartment is independent of all other compartments except temperature. With reference to Figure 6, the rate equation for coliforms is

$$CSS(I,K,3) = -K_c \theta^{(T-20)} V C_3 \quad (64)$$

where

K_c = the death rate, sec^{-1}

θ = temperature factor (Q10)

T = water temperature, $^{\circ}\text{C}$

V = cell volume, m^3

C_3 = coliform concentration, g m^{-3}

and the rate term is evaluated in the subroutine COLIFORM.

134. The Q10 formulation arises from a doubling of the reaction rate with each 10° increase in temperature. This doubling rate has not been found at lower temperatures (Hargrave 1972b) and is quite variable for various reactions (Giese 1968). Modeling coliform bacteria is discussed in detail in Zison et al. (1978).

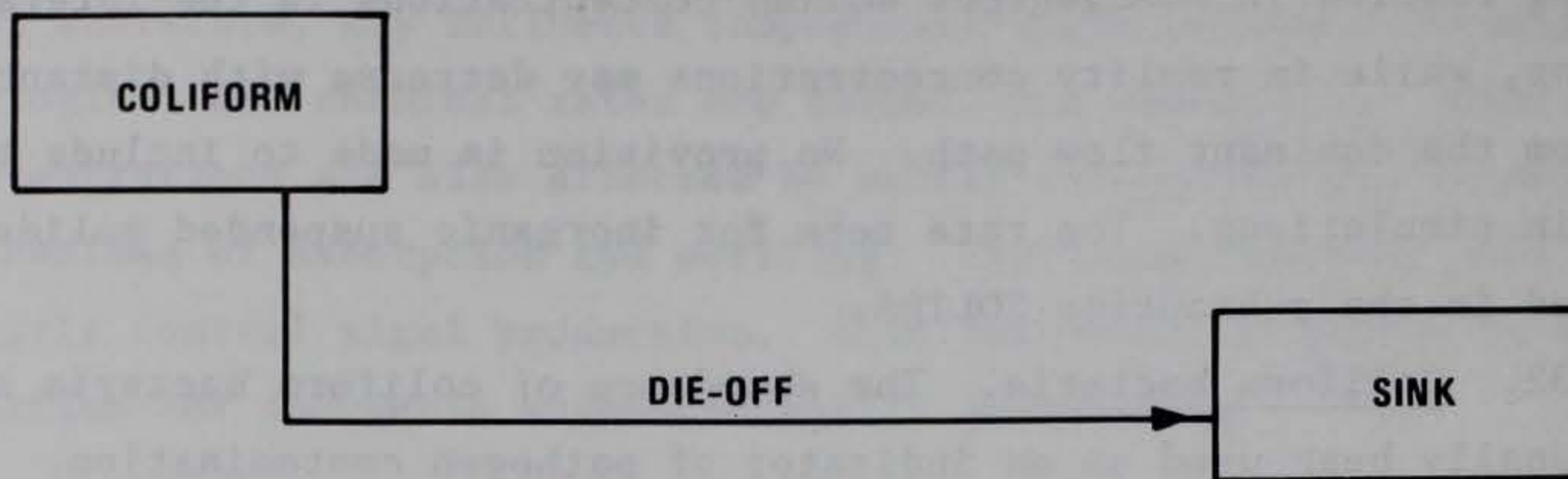


Figure 6. Internal flux for coliform bacteria

135. Total dissolved solids or salinity. Dissolved solids concentrations affect both the density of water and its ionic strength, thereby affecting water movements, pH, and the distribution of carbonate species. The simulation of dissolved solids may be important for many applications. Dissolved solids are treated as a conservative material; therefore, the process rate term $CSS(I,K,4)$ is set to zero.

136. It is expected that dissolved solids will normally be expressed as TDS in the majority of CE-QUAL-W2 applications. However, some applications may require simulation of salinity rather than TDS. Provisions are made to allow the user to use either TDS or salinity in simulations, with the choice indicated by the parameter IWT. The choice is then reflected in the expressions used to compute density arrays and ionic strength. If TDS is used in simulations, it should be provided in units of grams per cubic metre, while salinity should be in units of kilograms per cubic metre.

137. Labile dissolved organic matter. Because of the importance of dissolved oxygen in reservoirs, it is imperative to include as model variables all constituents that exert an oxygen demand. This demand is often measured in rivers as the biochemical oxygen demand (BOD), which includes, for example, microbial respiration and metabolism of various organic and inorganic compounds. In reservoirs, however, production of these materials occurs as well as decomposition, requiring that the major constituents or components of BOD be modeled on an individual basis. One of these constituents is dissolved organic matter (DOM),

which is composed of labile and refractory components. In CE-QUAL-W2, DOM is represented in two separate compartments because of the different decomposition rates of the two groups.

138. With reference to Figure 7, the rate equation for labile DOM is given by

$$CSS(I,K,5) = K_e VC_7 + (1 - P_1)K_m VC_7 - \gamma_{11}K_d VC_5 - K_t VC_5 \quad (65)$$

where

- V = volume, m^3
- K_e = algal excretion rate, sec^{-1} (see Equation 74)
- K_m = algal mortality rate, sec^{-1} (see Equation 75)
- K_d = labile DOM decay rate, sec^{-1}
- K_t = transfer rate from labile to refractory DOM, sec^{-1}
- P_1 = pattern coefficient for algal mortality
- γ_{11} = temperature rate multiplier
- C_7 = algal concentration, $g\ m^{-3}$
- C_5 = labile DOM concentration, $g\ m^{-3}$

and the rate terms are evaluated in subroutine ORGNICS. Where applications only require simulation of dissolved oxygen and BOD, this compartment would best represent BOD. Labile DOM is assumed not to decay if dissolved oxygen concentrations fall below a minimum value (OXYLIM). The decay is stopped by setting its rate multiplier equal to zero.

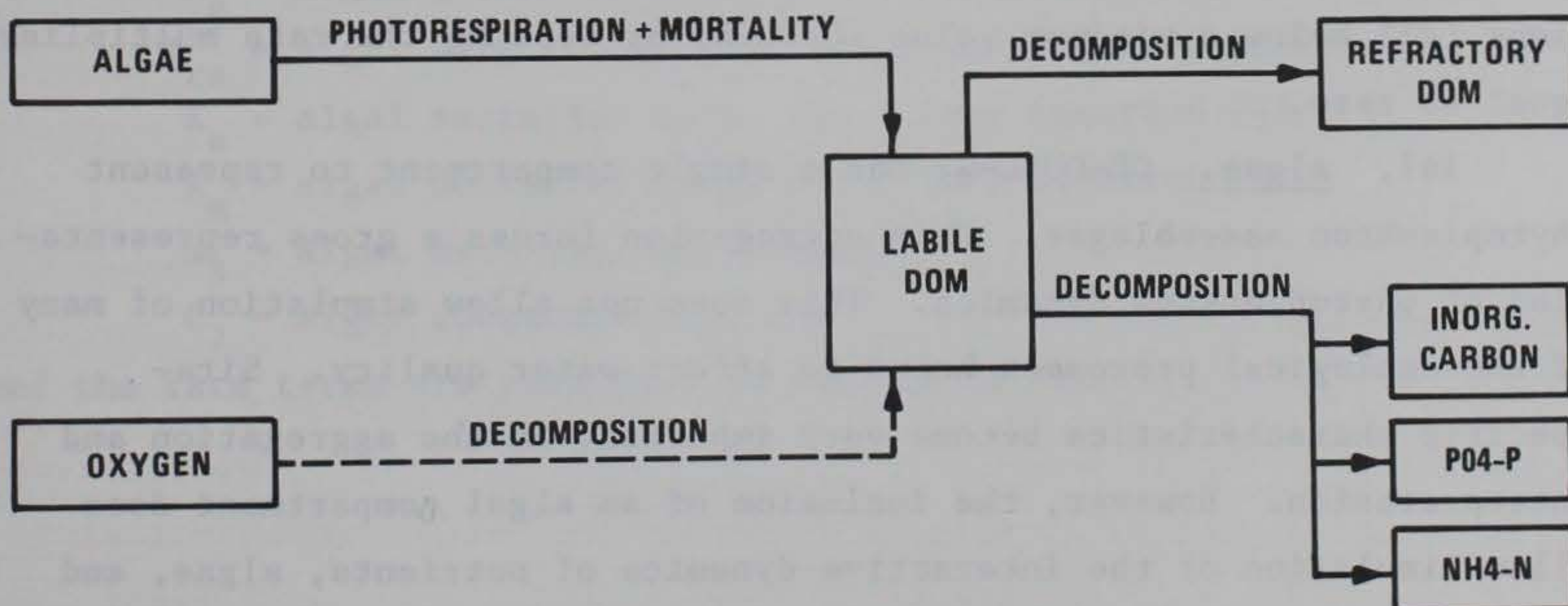


Figure 7. Internal flux between labile DOM and other compartments

139. Refractory dissolved organic matter. Refractory DOM is composed of recalcitrant compounds that decompose at a relatively slow rate in the aquatic environment, exerting oxygen demands over long periods of time. The majority of DOM present in a reservoir, especially in the hypolimnion, may consist of refractory compounds. The majority of allochthonous DOM may also consist of refractory components, and the partition of labile and refractory compounds is represented by the parameter DOMCNT. Internally, refractory compounds may be produced from the decomposition of labile DOM.

140. With reference to Figure 8, the rate equation for refractory DOM is given by

$$\text{CSS}(I,K,6) = K_t VC_5 - \gamma_{11} K_r VC_6 \quad (66)$$

where

$$\begin{aligned} V &= \text{volume, m}^3 \\ K_t &= \text{transfer rate from labile DOM, sec}^{-1} \\ C_5 &= \text{concentration of labile DOM, g m}^{-3} \\ \gamma_{11} &= \text{temperature rate multiplier} \\ K_r &= \text{decay rate, sec}^{-1} \\ C_6 &= \text{concentration of refractory DOM, g m}^{-3} \end{aligned}$$

and the rate terms are evaluated in subroutine REFRACT. Decay of refractory DOM is not allowed to occur if dissolved oxygen concentrations fall below a minimum value (OXYLIM) by setting the rate multiplier equal to zero.

141. Algae. CE-QUAL-W2 has a single compartment to represent phytoplankton assemblages. This aggregation forces a gross representation of phytoplankton dynamics. This does not allow simulation of many of the ecological processes known to affect water quality. Site-specific characteristics become very important in the aggregation and interpretation. However, the inclusion of an algal compartment does allow simulation of the interactive dynamics of nutrients, algae, and dissolved oxygen. Proper aggregation can also provide insight into potential problems associated with algal biomass magnitudes and timing

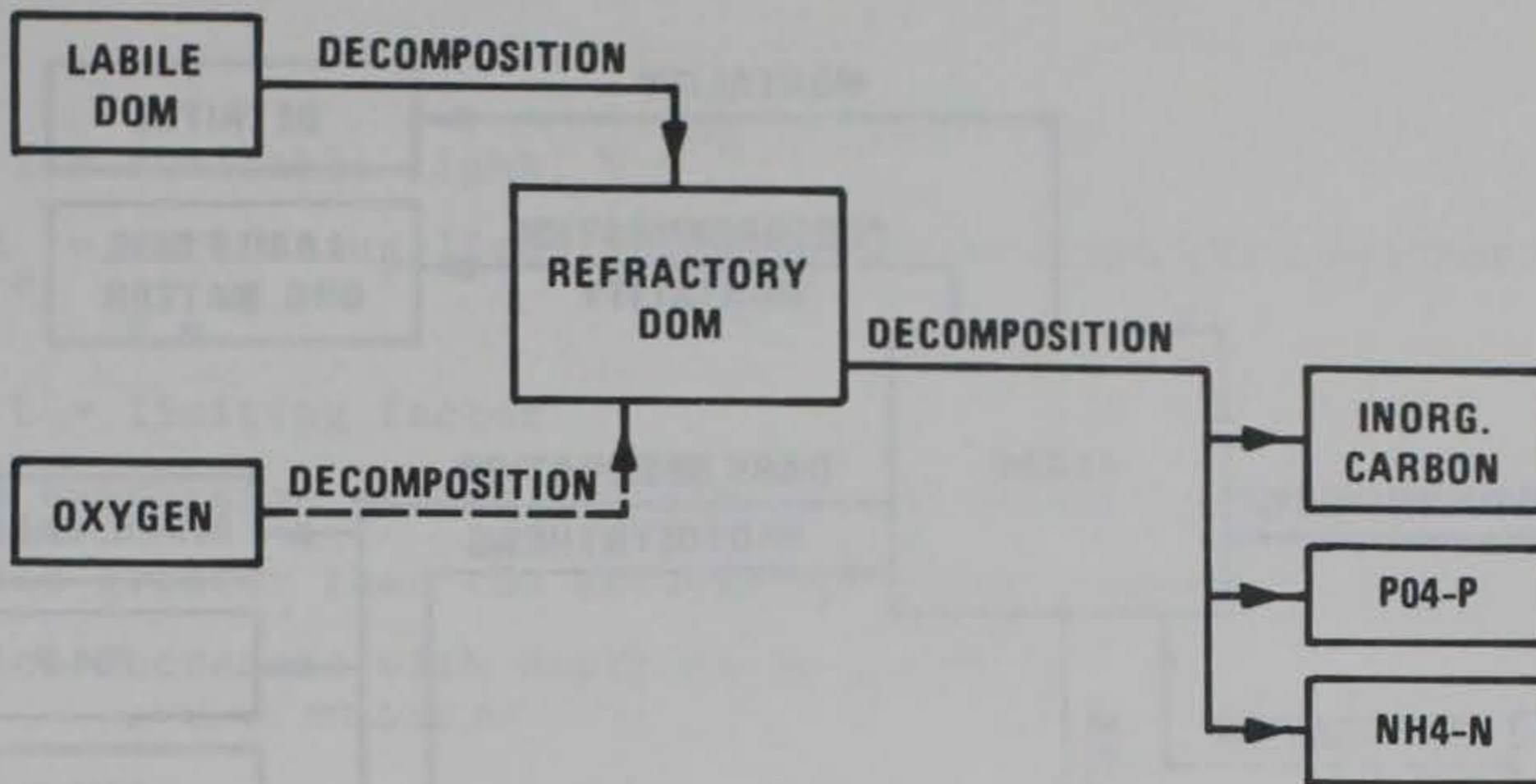


Figure 8. Internal flux between refractory DOM and other compartments

of blooms. Large phytoplankton populations may result in large variations in dissolved oxygen concentrations and contribute to undesirable aesthetic conditions.

142. With reference to Figure 9, the rate equation for algae is given by

$$CSS(I,K,7) = K_g VC_7 - K_{rs} VC_7 - K_e VC_7 - K_m VC_7 - \omega_3 VC_7 / \Delta z \quad (67)$$

where

v = volume, m^3

Δz = cell thickness, m

K_g = algal growth rate, sec^{-1} (see Equation 68)

K_{rs} = algal dark respiration rate, sec^{-1} (see Equation 73)

K_e = algal excretion rate, sec^{-1} (see Equation 74)

K_m = algal mortality rate, sec^{-1} (see Equation 75)

ω_3 = algal settling rate, $m sec^{-1}$

C_7 = algal concentration, $g m^{-3}$

and the rate terms are evaluated in subroutine PHYTO.

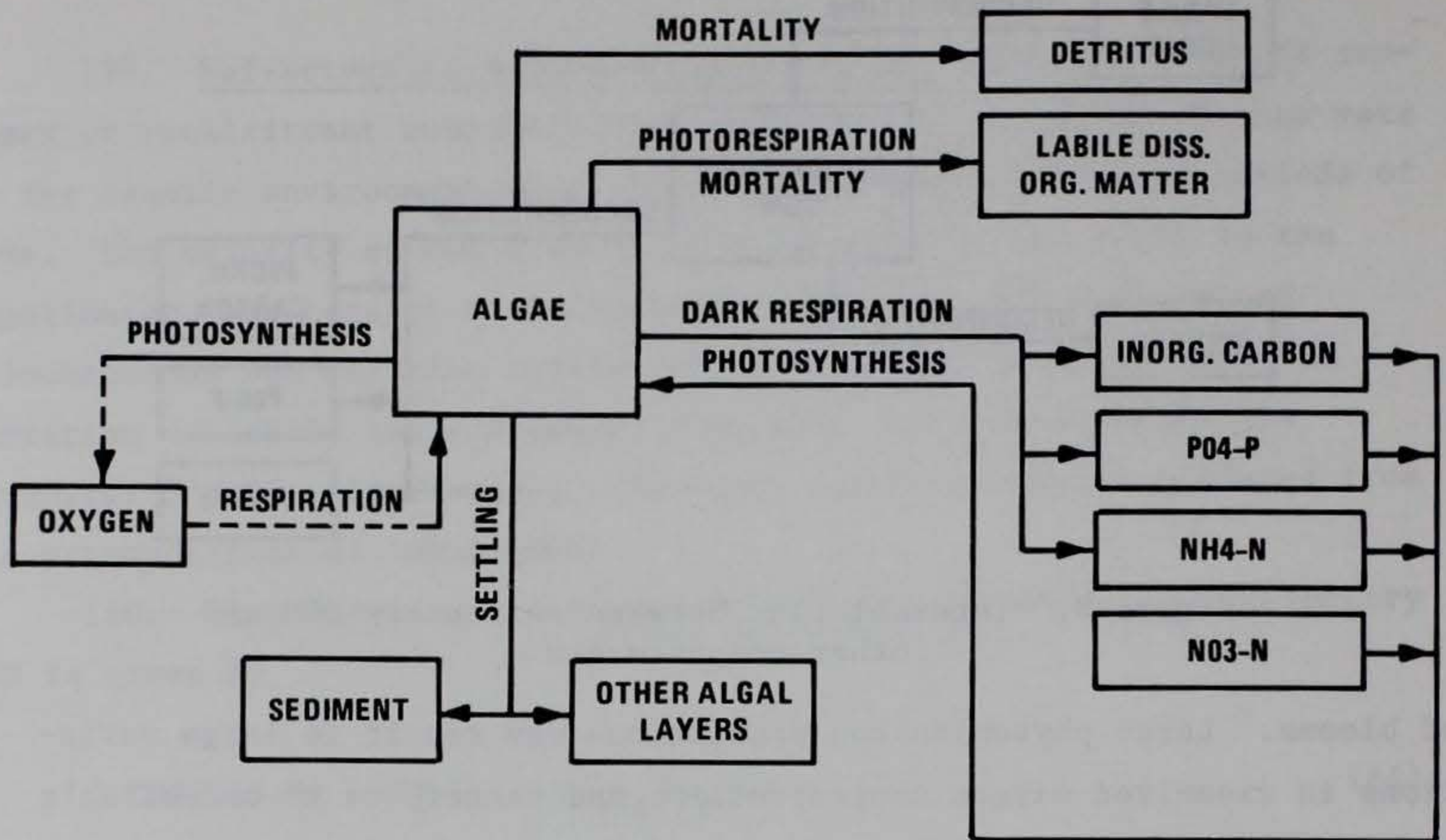


Figure 9. Internal flux between algae and other compartments

143. The algal growth rate (K_g) is computed by modifying a maximum growth rate (A_g) by environmental factors due to temperature, light, and the availability of nutrients, as is given by

$$K_g = \gamma_{15} \gamma_{21} \text{MIN}(\phi_i) A_g \quad (68)$$

where

- γ_{15} = temperature rate multiplier for ascending limb of curve
- γ_{21} = temperature rate multiplier for descending limb of curve
- ϕ_i = rate multiplier for limiting factor i
- A_g = maximum algal growth rate, sec^{-1}

144. The rate multipliers for algal growth are computed based upon available light (ϕ_1), phosphorus (ϕ_2), and nitrogen (ϕ_3). The rate multiplier for light is based upon the Steele (1962) function

$$L = \frac{I}{I_s} \exp \left(- \frac{I}{I_s} + 1 \right) \quad (69)$$

where

I = available light, $W m^{-2}$

I_s = saturating light intensity at maximum photosynthetic rate,
 $W m^{-2}$

L = limiting factor

The above expression allows for simulation of photoinhibition at light intensities greater than the saturation value. However, light penetration decreases with depth as is given by

$$I = (1-\beta)I_0 e^{-\alpha z} \quad (70)$$

where

I_0 = solar radiation at the water surface, $W m^{-2}$

α = attenuation coefficient, $l m^{-2}$

z = depth, m

β = fraction of I_0 absorbed at the water surface

The average effect of light on algal growth in a particular model cell can be obtained by combining the above two expressions and integrating over the cell depth to obtain (Chapra and Reckhow 1983)

$$\phi_1 = \frac{e^1}{\alpha \Delta z} [\exp(-\lambda_2) - \exp(-\lambda_1)]$$

where

$$\lambda_1 = \frac{(1-\beta) I_0}{I_s} e^{-\alpha d} \quad (71)$$

$$\lambda_2 = \frac{(1-\beta) I_0}{I_s} e^{-\alpha(d + \Delta z)}$$

d = depth at top of the model cell, m

and it should be noted that the units used for solar radiation in computing algal growth (watts per square metre) differ from those used in heat exchange computations (degrees Centigrade per metre per second).

145. The fraction of solar radiation βI_0 is added directly to the surface layer or to the layers occurring in the first 0.6 m of the water column. The attenuation coefficient α consists of a baseline value (EXCO) to which the self-shading effects of inorganic and organic (algae and detritus) suspended solids are added, as determined by multiplying their concentrations by the coefficients EXTINS and EXTINP, respectively.

146. The rate multipliers limiting algal growth due to concentrations of phosphorus (ϕ_2) and nitrogen (ϕ_3) are computed using the Monod relationship

$$\phi_i = \frac{C_i}{P_i + C_i} \quad (72)$$

where

C_i = concentration of phosphorus or nitrate + ammonia-nitrogen, $g\ m^{-3}$

P_i = half-saturation coefficient, $g\ m^{-3}$

147. Algal dark respiration is computed using the rising limb of the temperature function

$$K_{rs} = \gamma_{15} A_r \quad (73)$$

where A_r is the maximum dark respiration rate, per second.

148. Algal photorespiration (excretion) is evaluated using an inverse relation to the light rate multiplier

$$K_e = (1 - \phi_1) A_e \quad (74)$$

where A_e is a maximum excretion rate constant, per second. Excretion rates increase at both low and high light intensities, with excretion products contributing to labile DOM.

149. Algal mortality is described by

$$K_m = \gamma_{15} A_m \quad (75)$$

where A_m is the maximum mortality rate, per second. This mortality rate represents both natural and predator mortality. Algal growth is assumed not to occur in the absence of light or where temperatures are less than the minimum required for growth (T_1) or greater than the maximum (T_4). Algal growth is now allowed to exceed the limit imposed by nutrient supply at a given time step. Algal excretion is not allowed to exceed algal growth rates.

150. As with suspended solids, algae that settle from a model cell serve as a source for the layer below. However only a fraction (F) is allowed to settle to the next layer, where F is determined by the ratio of cell widths. The remaining fractions ($1-F$) are passed to the sediments. Unlike inorganic solids, however, the algae that are passed to the sediments accumulate within that compartment. This is also the case for detritus.

151. Detritus. Detritus represents particulate organic material suspended in the water column but capable of settling to the bottom. Through decomposition processes, detritus serves as a source of the chemical nutrients nitrogen, phosphorus, and carbon. Microbial processes are included in the model through the decomposition of organic matter. Detritus, therefore, serves as a surrogate, implicitly simulating microbial decomposition of particulate organic matter and mineralization of nutrients. A stoichiometric relationship is used to release ammonium-nitrogen, phosphorus, and carbon, and an oxygen demand is exerted as detritus decomposes. When detritus settles to the bottom, it is converted to organic sediment.

152. With reference to Figure 10, the rate equation for detritus is given by

$$CSS(I,K,8) = P_1 K_m VC_7 - K_{dt} \gamma_{14} VC_8 - \omega_2 VC_8 / \Delta z \quad (76)$$

where

- V = cell volume, m^3
- P_1 = partition coefficient for algal mortality
- K_m = algal mortality rate, sec^{-1} (see Equation 75)
- C_7 = algae concentration, $g\ m^{-3}$
- K_{dt} = detritus decay rate, sec^{-1}
- ω_2 = detritus settling rate, m/sec
- C_8 = detritus concentration, $g\ m^{-3}$
- Δz = model cell thickness, m
- γ_{14} = temperature rate multiplier

and the rate terms are evaluated in subroutine DETRITS. The settling of detritus and its accumulation in organic sediments is handled identically to the algal compartment.

153. Detritus is assumed not to decay where the dissolved oxygen concentrations are below a minimum value given by the variable OXYLIM. Decay is stopped by setting its rate multiplier equal to zero where this condition occurs. In reality, the decay would be expected to continue but at a much slower rate. That decay process would use different biochemical pathways which are not modeled in CE-QUAL-W2.

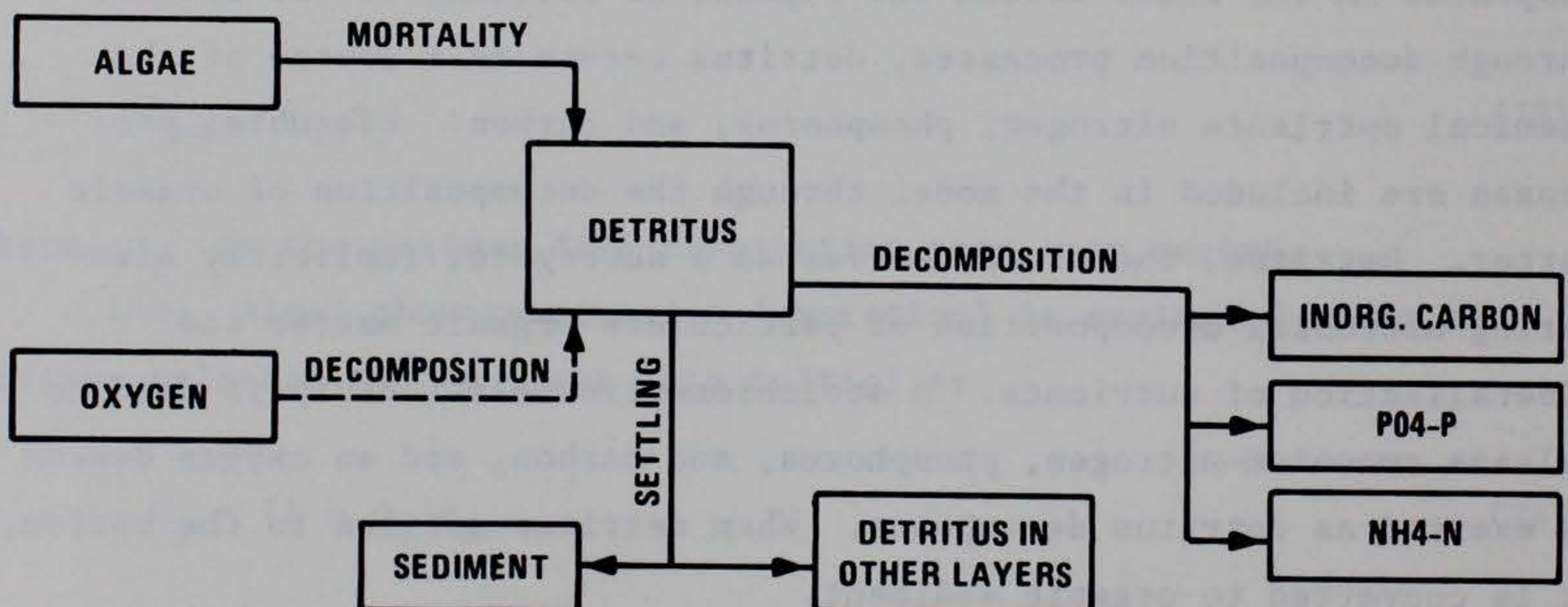


Figure 10. Internal flux between detritus and other compartments

154. Phosphorus. Phosphorus is an important element in aquatic ecosystems since it serves as one of the primary nutrients for phytoplankton. In addition to serving as a nutrient for plants, phosphorus is extremely important in all biological organisms for its various forms of energy storage. The formation of high-energy bonds in compounds such as ATP provides the energy for many life processes. Algae, through photosynthesis, are able to convert inorganic elements such as phosphorus, nitrogen, carbon, hydrogen, and oxygen into organic compounds such as carbohydrates, lipids, and proteins. In many fresh waters, phosphorus is considered to be the element that limits the maximum production of phytoplankton biomass (Schindler 1971; Schindler et al. 1973; Vollenweider 1968, 1976). Phosphorus, therefore, is an important compartment in the model.

155. Phosphorus is assumed to be in a completely available form as orthophosphate (PO_4) for uptake by phytoplankton. Measurements of soluble reactive phosphorus most closely fit the form used in the model.

156. With reference to Figure 11, the rate equation for phosphorus is given by

$$\begin{aligned}
 \text{CSS}(I,K,9) = & (K_{rs} - K_g) \delta_P \text{VC}_7 + K_d \delta_P \gamma_{11} \text{VC}_5 + K_{dt} \delta_P \gamma_{14} \text{VC}_8 \\
 & + K_r \delta_P \gamma_{11} \text{VC}_6 + K_s \delta_P \gamma_{16} \gamma_{26} C_{13} + S_2 \gamma_{18} \gamma_{24} A_s \\
 & - VA_1 A_2 (\omega_1 C_2 + \omega_2 C_8 + \omega_3 C_7 + \beta \omega_4 C_{20}) C_9 / \Delta z
 \end{aligned} \tag{77}$$

where

- V = volume, m^3
- Δz = model cell thickness, m
- A_s = sediment area, m^2
- A_1 = adsorption coefficient, $m^3 g^{-1}$
- A_2 = maximum mass of phosphorus adsorbed per mass of solids
- δ_P = stoichiometric coefficient for phosphorus
- γ_{ii} = temperature rate multipliers
- ω_i = settling velocities, $m \text{ sec}^{-1}$

- β = adsorption increment for iron
 K_{rs} = algal dark respiration rate, sec^{-1} (see Equation 73)
 K_g = algal growth rate, sec^{-1} (see Equation 68)
 K_d = labile DOM decay rate, sec^{-1}
 K_{dt} = detritus decay rate, sec^{-1}
 K_s = sediment decay rate, sec^{-1}
 S_2 = anaerobic sediment release rate, $\text{g m}^{-2} \text{sec}^{-1}$
 K_r = refractory DOM decay rate, sec^{-1}
 C_6 = refractory DOM concentration, g m^{-3}
 C_7 = algae concentration, g m^{-3}
 C_5 = labile DOM concentration, g m^{-3}
 C_8 = detritus concentration, g m^{-3}
 C_{13} = organic sediment mass, g
 C_2 = inorganic suspended solids concentration, g m^{-3}
 C_9 = phosphorus concentration, g m^{-3}
 C_{20} = total iron concentration, g m^{-3}

and the rate terms are evaluated in subroutine PHOSPHR.

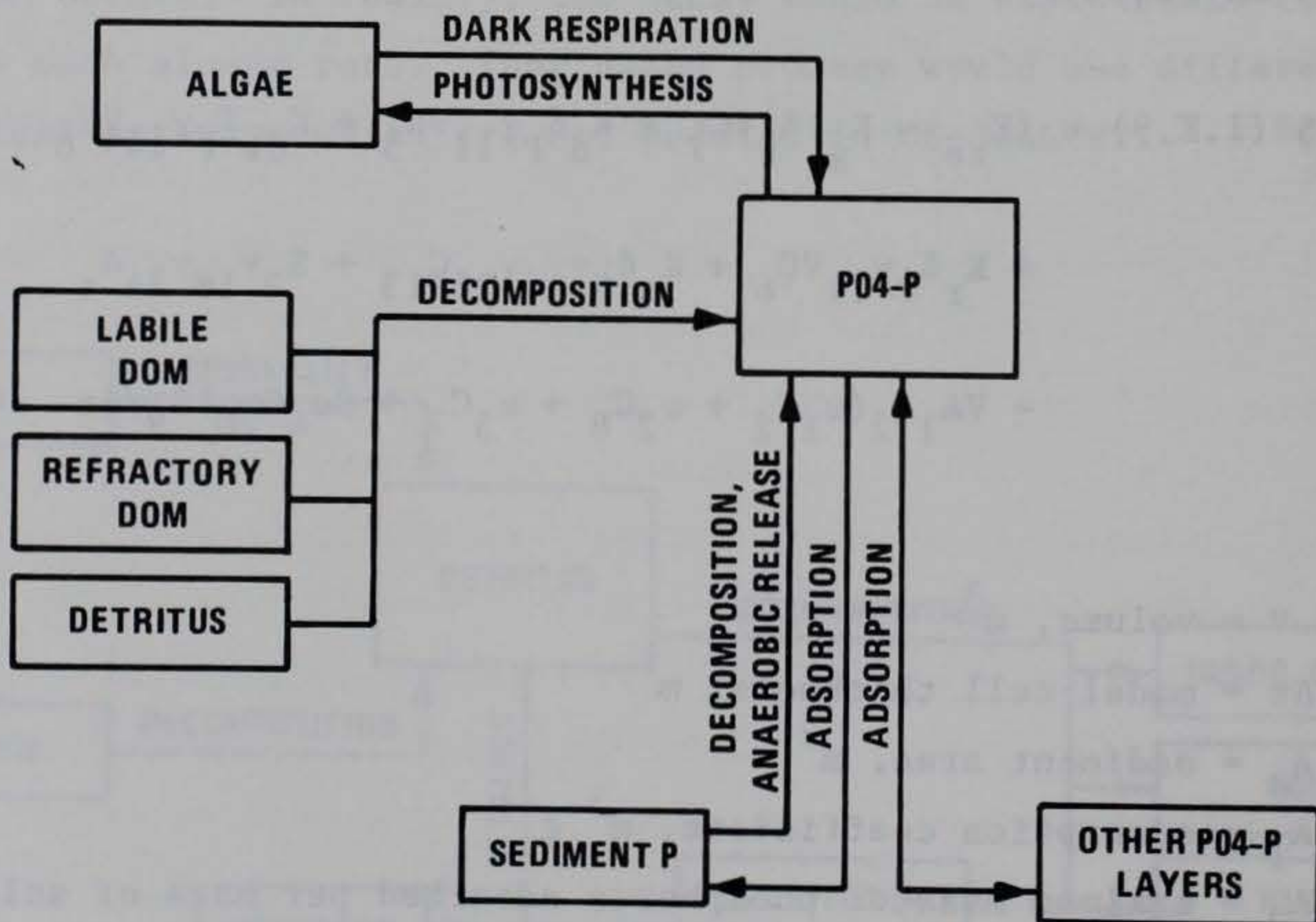


Figure 11. Internal flux between phosphorus and other compartments

157. The contribution to the phosphorus compartments from algae, detritus and DOM is apparent from examination of the rate equations and compartmental diagrams. However, the effects due to settling and contribution from sediments require some additional explanation.

158. Phosphorus tends to become associated with particulates and is lost when these materials settle. This loss may be rapid in the upper end of reservoirs (riverine and transition zones) due to the greater concentrations and size distributions of allochthonous particulates. The loss occurs at a slower rate in the lacustrine zone as phosphorus becomes associated with autochthonous particulates which may settle at a slower rate. This tendency for phosphorus to be become associated with particulates (be adsorbed) can be described by a Langmuir isotherm. Since phosphorus concentrations are generally small, only the linear region of the isotherm is utilized and is represented by the products of $A_1 A_2 C$ solids C_9 . The adsorbed solids then settle at a rate equal to the settling velocity of the solids, as is described in the above equation. The settling of phosphorus is handled similarly to inorganic suspended solids in that the fraction F is allowed to settle to the next lower cell while the fraction $1-F$ is lost to the sediment. Adsorption is not allowed to occur if dissolved oxygen concentrations are less than a minimum value.

159. The sediment contribution of phosphorus to overlying waters can be simulated in two ways. One, a sediment compartment is provided which accumulates organic materials (detritus and algae) and then allows them to decay. This is modeled as a first-order process. However, in many cases, sediment phosphorus releases depend upon the age of sediments, chemistry, and other factors that are not adequately represented by the sediment compartment alone. Alternatively, the sediment can be assigned a release rate for phosphorus (S_2), which is independent of sediment concentrations and models the sediments as a "black box" using a zero-order rate. Sediment release of phosphorus using the zero-order rate term is only allowed to occur if the dissolved oxygen concentration of the overlying water is less than a minimum value (OXYLIM). The choice of the two methods is indicated by the ITRIP

value for the sediment compartment and the value of the zero-order sediment release rate.

160. Ammonia-nitrogen. Ammonium-nitrogen is a nutrient that is used by algae during photosynthesis to form proteins. Un-ionized ammonia is an important compound in aquatic systems since it can be highly toxic to aquatic organisms. (Refer to Hutchinson (1957) and Trussell (1972) for information concerning these compounds.)

161. With reference to Figure 12, the rate equation for ammonia-nitrogen is given by

$$\begin{aligned}
 \text{CSS}(I,K,10) = & K_{rs} \delta_N \text{VC}_7 - K_g \delta_N \text{VC}_7 \frac{C_{10}}{C_{10} + C_{11}} + K_d \delta_N \gamma_{11} \text{VC}_5 \\
 & + K_r \delta_N \gamma_{11} \text{VC}_6 + K_{dt} \delta_N \gamma_{14} \text{VC}_8 + K_s \delta_N \gamma_{18} \gamma_{24} C_{13} \\
 & + S_3 \gamma_{17} \gamma_{27} A_s + K_n \gamma_{13} \text{VC}_{11} - K_a \gamma_{12} \text{VC}_{10} \\
 & - VA_3 A_4 (\omega_1 C_2 + \omega_2 C_8 + \omega_3 C_7 + \beta \omega_4 C_{20}) C_{10} / \Delta z
 \end{aligned} \tag{78}$$

where

- V = volume, m^3
- A_s = sediment area, m^2
- Δz = cell thickness, m
- A_3 = adsorption coefficient, $m^3 g^{-1}$
- A_4 = maximum mass of ammonia adsorbed per mass of solids
- δ_N = stoichiometric coefficient for nitrogen
- γ_{ii} = temperature rate multipliers
- ω_i = settling velocities, $m \text{ sec}^{-1}$
- β = adsorption increment for iron
- K_{rs} = algae dark respiration rate, sec^{-1} (see Equation 73)
- K_g = algae growth rate, sec^{-1} (see Equation 68)
- P_t = correction factor for particulate ammonia-nitrogen

- K_d = labile DOM decay rate, sec^{-1}
 K_r = refractory DOM decay rate, sec^{-1}
 K_{dt} = detritus decay rate, sec^{-1}
 K_s = sediment decay rate, sec^{-1}
 S_3 = sediment ammonia release rate, $\text{g m}^{-2} \text{sec}^{-1}$
 K_n = nitrate-nitrogen decay rate, sec^{-1}
 K_a = ammonia-nitrogen decay rate, sec^{-1}
 C_2 = suspended solids concentration, g m^{-3}
 C_5 = labile DOM, g m^{-3}
 C_6 = refractory DOM, g m^{-3}
 C_7 = algae concentration, g m^{-3}
 C_8 = detritus concentration, g m^{-3}
 C_{10} = ammonia-nitrogen concentration, g m^{-3}
 C_{11} = nitrate-nitrogen concentration, g m^{-3}
 C_{13} = sediment mass, g
 C_{20} = total iron concentration, g m^{-3}

and the rate terms are evaluated in subroutine AMMONIA. As with phosphorus, the zeroth order sediment release only occurs when dissolved oxygen is less than a minimum value (OXYLIM). Below this value, adsorption, detritus decay, and DOM decay are set equal to zero. Either a zero- or first-order process may be used for sediment phosphorus release, as with phosphorus. The settling of adsorbed ammonia-nitrogen is handled identically to phosphorus.

162. Nitrate-nitrogen. This compartment represents nitrite plus nitrate-nitrogen. Nitrite is an intermediate product in nitrification between ammonium and nitrate. Nitrate is used by algae and macrophytes during photosynthesis.

163. Nitrogen may be the limiting nutrient for algae in systems with high phosphorus loadings. Some species of blue-green algae are capable of fixing atmospheric nitrogen for use in photosynthesis. Nitrogen fixation has been coded in the model, so simulations of assemblages dominated by nitrogen-fixing blue-green algae should be interpreted cautiously.

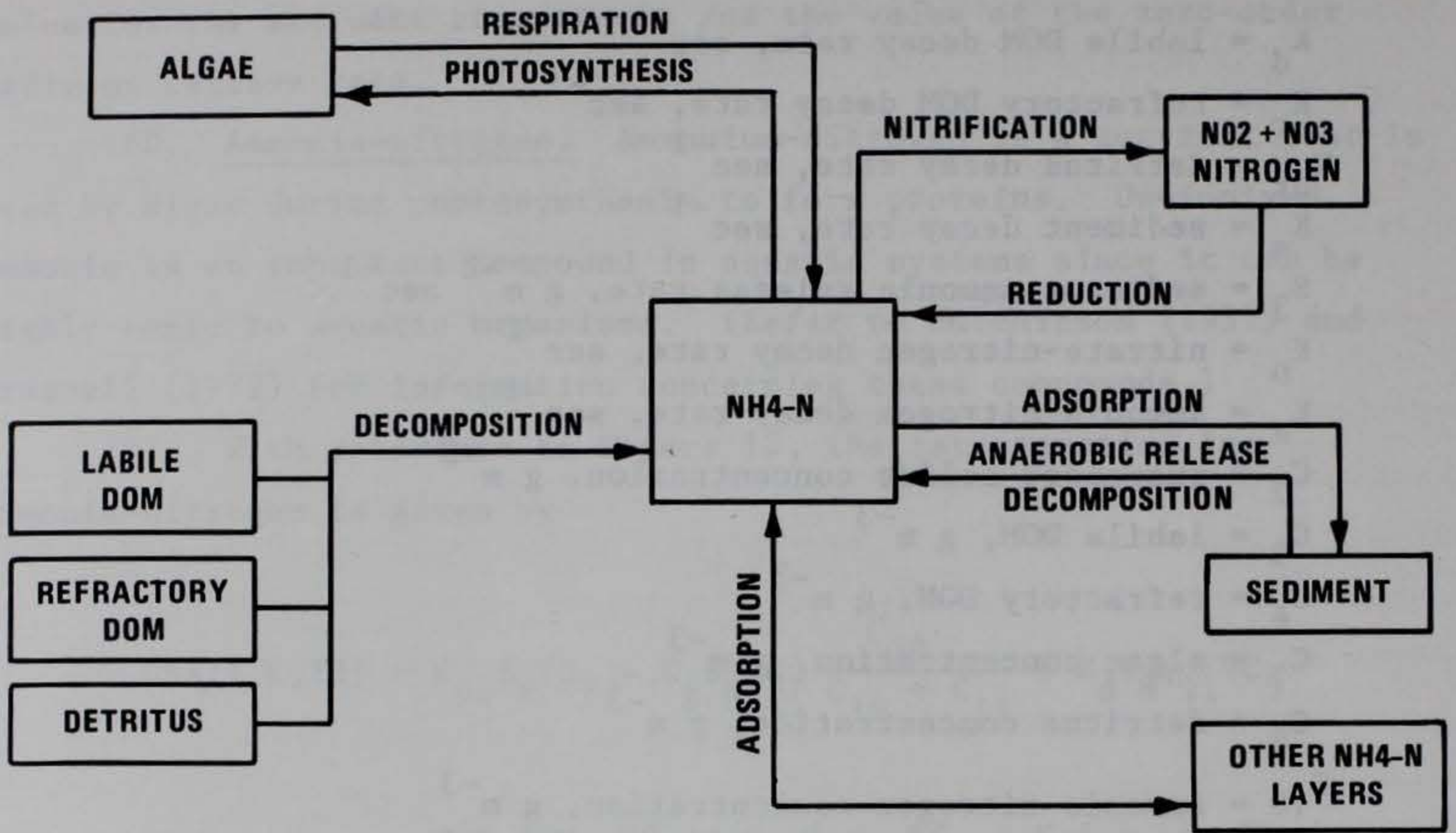


Figure 12. Internal flux between ammonia-nitrogen and other compartments

164. With reference to Figure 13, the rate equation for nitrate-nitrogen is given by

$$\begin{aligned}
 \text{CSS}(I,K,11) = & K_a \gamma_{12} V C_{10} - K_n \gamma_{13} V C_{11} \\
 & - K_g \delta_N V C_7 \left(1 - \frac{C_{10}}{C_{10} + C_{11}} \right)
 \end{aligned}
 \tag{79}$$

where

V = volume, m^3

γ_{17} = temperature rate multiplier for ascending portion of curve

δ_N = stoichiometric coefficient for nitrogen

K_a = ammonia decay (nitrification) rate, sec^{-1}

K_n = nitrate-nitrogen decay (reduction, denitrification) rate, sec^{-1}

K_g = algae growth rate, sec^{-1} (see Equation 68)

C_7 = algae concentration, $g\ m^{-3}$
 C_{10} = ammonia-nitrogen concentration, $g\ m^{-3}$
 C_{11} = nitrate-nitrogen concentration, $g\ m^{-3}$

and the rate terms are evaluated in subroutine NITRATE. Nitrification is only allowed to occur if oxygen is present, and nitrate reduction is allowed only if dissolved oxygen is less than a specified minimum value (OXYLIM).

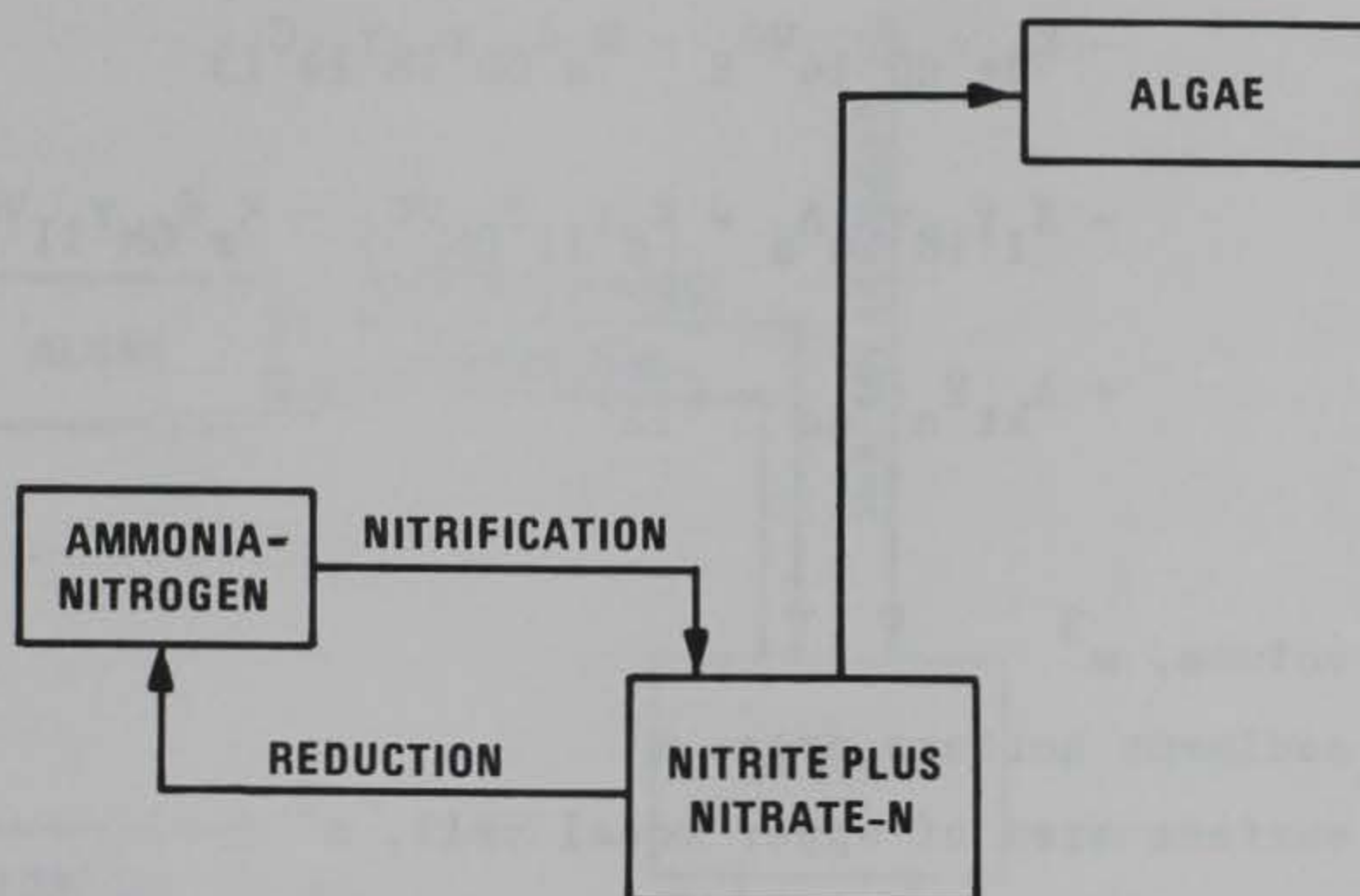


Figure 13. Internal flux between nitrate + nitrite-nitrogen and other compartments

165. Dissolved oxygen. Oxygen is one of the most important elements in aquatic ecosystems. It is essential for higher forms of life, controls many chemical reactions through oxidation, and is a surrogate variable indicating the health or general condition of aquatic systems.

166. CE-QUAL-W2 is both an aerobic and anaerobic model. Inclusion of descriptions for anaerobic release of phosphorus and ammonia permits the simulation to continue through anaerobic periods until aerobic conditions again occur. Knowledge about potential anaerobic periods is very useful since it provides information on potential problems. Simulations can be used to identify the possibilities for both metalimnetic and hypolimnetic oxygen depletion and its impact on various water control management alternatives. If a single variable were to be measured in aquatic systems that would provide

maximum information about the system state, it would be dissolved oxygen.

167. With reference to Figure 14, the rate equation for dissolved oxygen is given by

$$\begin{aligned}
 \text{CSS}(I,K,12) = & K_g \delta_{OF}^{VC_7} - K_{rs} \delta_{OR}^{VC_7} - K_a \delta_{ON} \gamma_{12}^{VC_{10}} \\
 & - K_{dt} \delta_{OD} \gamma_{14}^{VC_8} - K_s \delta_{OD} \gamma_{18} \gamma_{24} C_{13} \\
 & - S_1 \gamma_{18} \gamma_{24} A_s - K_d \gamma_{11} \delta_{OM}^{VC_5} - K_r \delta_{OM} \gamma_{11}^{VC_6} \\
 & + A_{kt} E_o (C_{so} - C_{12})
 \end{aligned}
 \tag{80}$$

where

- V = volume, m^3
- A_s = sediment surface area, m^2
- A_{kt} = surface area of upper model cell, m^2
- δ_{oi} = oxygen stoichiometric coefficients
- γ_{ii} = temperature rate multiplier
- K_g = algal growth rate, sec^{-1} (see Equation 68)
- K_{rs} = algal dark respiration rate, sec^{-1} (see Equation 73)
- K_a = ammonia decay (nitrification) rate, sec^{-1}
- K_{dt} = detritus decay rate, sec^{-1}
- K_d = labile DOM decay rate, sec^{-1}
- K_r = refractory DOM decay rate, sec^{-1}
- K_s = sediment decay rate, sec^{-1}
- S_1 = rate of sediment oxygen demand, $g\ m^{-2}\ sec^{-1}$
- E_o = interfacial exchange rate for oxygen, $m\ sec^{-1}$
- C_7 = algae concentration, $g\ m^{-3}$
- C_5 = labile DOM concentration, $g\ m^{-3}$
- C_6 = refractory DOM concentration, $g\ m^{-3}$
- C_8 = detritus concentration, $g\ m^{-3}$
- C_{10} = ammonia-nitrogen concentration, $g\ m^{-3}$
- C_{12} = dissolved oxygen concentration, $g\ m^{-3}$

C_{13} = sediment mass, g

C_{so} = saturation dissolved oxygen concentration, $g\ m^{-3}$ (see Equation 84)

and the rate terms are evaluated in subroutine OXYGEN. Decay rates are allowed to occur only if dissolved oxygen concentrations are not equal to zero. This is accomplished by setting temperature rate multipliers equal to zero.

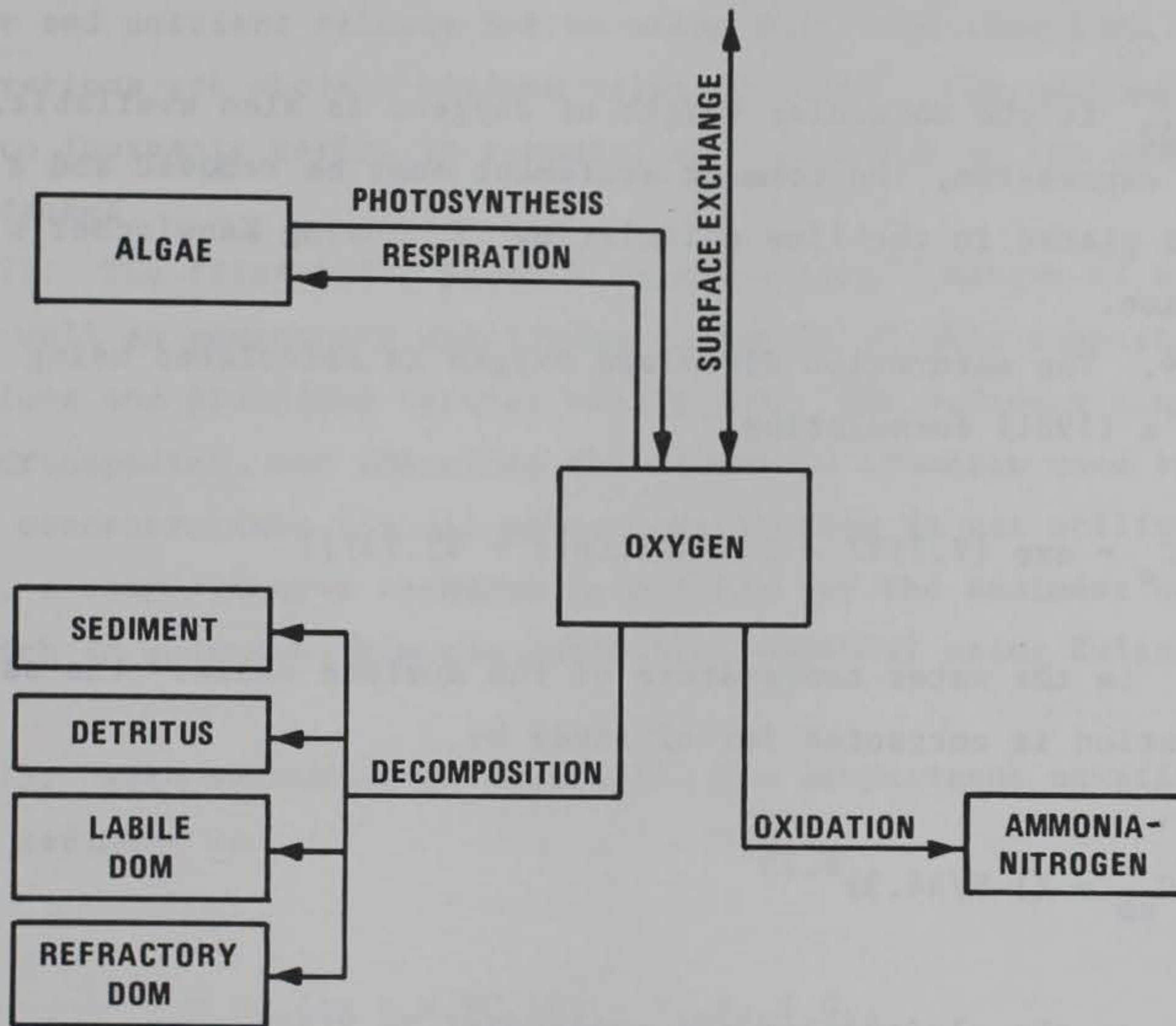


Figure 14. Internal flux between dissolved oxygen and other compartments

168. The interfacial exchange rate is computed according to Kanwischer's (1963) formulation

$$E_o = \frac{D_o}{\left[200 - 60(W_a)^{1/2} \right]} * 1 \times 10^{-6} \quad (81)$$

where D_o is the molecular diffusivity of dissolved oxygen and W_a the wind speed ($m\ sec^{-1}$). In using this equation, W_a is limited to $11\ m\ sec^{-1}$ to avoid instabilities. An alternative expression from Mackay (1980, as reported in Chapra and Reckhow 1983),

$$E_o = 6.4185 \times 10^{-6} \frac{W_a^{1.5}}{M_{O_2}^{0.5}} \quad (82)$$

where M_{O_2} is the molecular weight of oxygen, is also available. To use this expression, the comment statement must be removed and a comment statement placed in the line calculating E_o using Kanwischer's formulation.

169. The saturation dissolved oxygen is calculated using Mortimer's (1981) formulation

$$C_s = \exp \{7.7117 - 1.31403[\ln(T + 45.93)]\} \quad (83)$$

where T is the water temperature of the surface cells. The saturation concentration is corrected for altitude by

$$C_{so} = (1-H/44.3)^{5.25} \quad (84)$$

where H is the altitude of the reservoir, in kilometres.

170. Sediments. Organic sediment contributions to nutrients and dissolved oxygen demands may be simulated in two ways in CE-QUAL-W2. The first method is through the use of constant, or zero-order, releases and demands. This method has been frequently used to model sediment demands and release rates. It has the advantage that it does not depend upon sediment concentrations and does not require a separate sediment compartment to allow accumulations. The second method is to use a sediment compartment to accumulate organic sediments and allow their decay, and hence nutrient releases and oxygen demand, to be dependent upon

concentrations, a first-order process. Either of these methods, or a combination of them, may be used to simulate effects of organic sediments upon water quality. However, caution must be exercised to avoid errors if both pathways are used.

171. The zero-order process involves specifying a sediment oxygen demand and a release rate for phosphorus and ammonia-nitrogen. These rates are dependent upon temperature. Sediment oxygen demand is assumed to occur and nutrient release not to occur only when dissolved oxygen concentrations are above a minimum value (OXYLIM). The sediment contribution to inorganic carbon is computed as a fraction of the sediment oxygen demand.

172. The first-order process requires specification of a decay rate as well as parameters specifying inclusion of this compartment in simulations and providing initial conditions. The sediment compartment is not transported, and therefore the transport equation used to solve for new concentrations for all other constituents is not utilized. Instead, a compartmental equation is written for the sediment compartment which is solved within the subroutine SEDIMENT using Eulerian scheme.

173. With reference to Figure 15, the compartment equation for organic sediment is

$$\frac{d C_{13}}{dt} = \omega_2 V C_8 / \Delta z + \omega_3 V C_7 / \Delta z - \gamma_{18} \gamma_{28} K_s C_{13} \quad (85)$$

where

- V = volume, m^3
- Δz = model cell thickness, m
- ω_2 = detritus settling velocity, $m \text{ sec}^{-1}$
- ω_3 = algae settling velocity, $m \text{ sec}^{-1}$
- γ_{18} = sediment rate multiplier for ascending limb of curve
- γ_{28} = sediment rate multiplier for descending limb of curve
- K_s = sediment decay rate, sec^{-1}
- C_7 = algae concentration, $g \text{ m}^{-3}$

C_8 = detritus concentration, $g\ m^{-3}$

C_{13} = sediment mass, g

As was discussed in the sections dealing with algae and detritus, the material accumulated in the sediment is all material settled out of the bottom-most cell of a segment. For other cells, the amount accumulated is $1-F$ of the material settled out of the cell while the fraction F is passed to the layer below. The fraction F is computed from the ratio of cell widths as $B(I,K)/B(I,K-1)$.

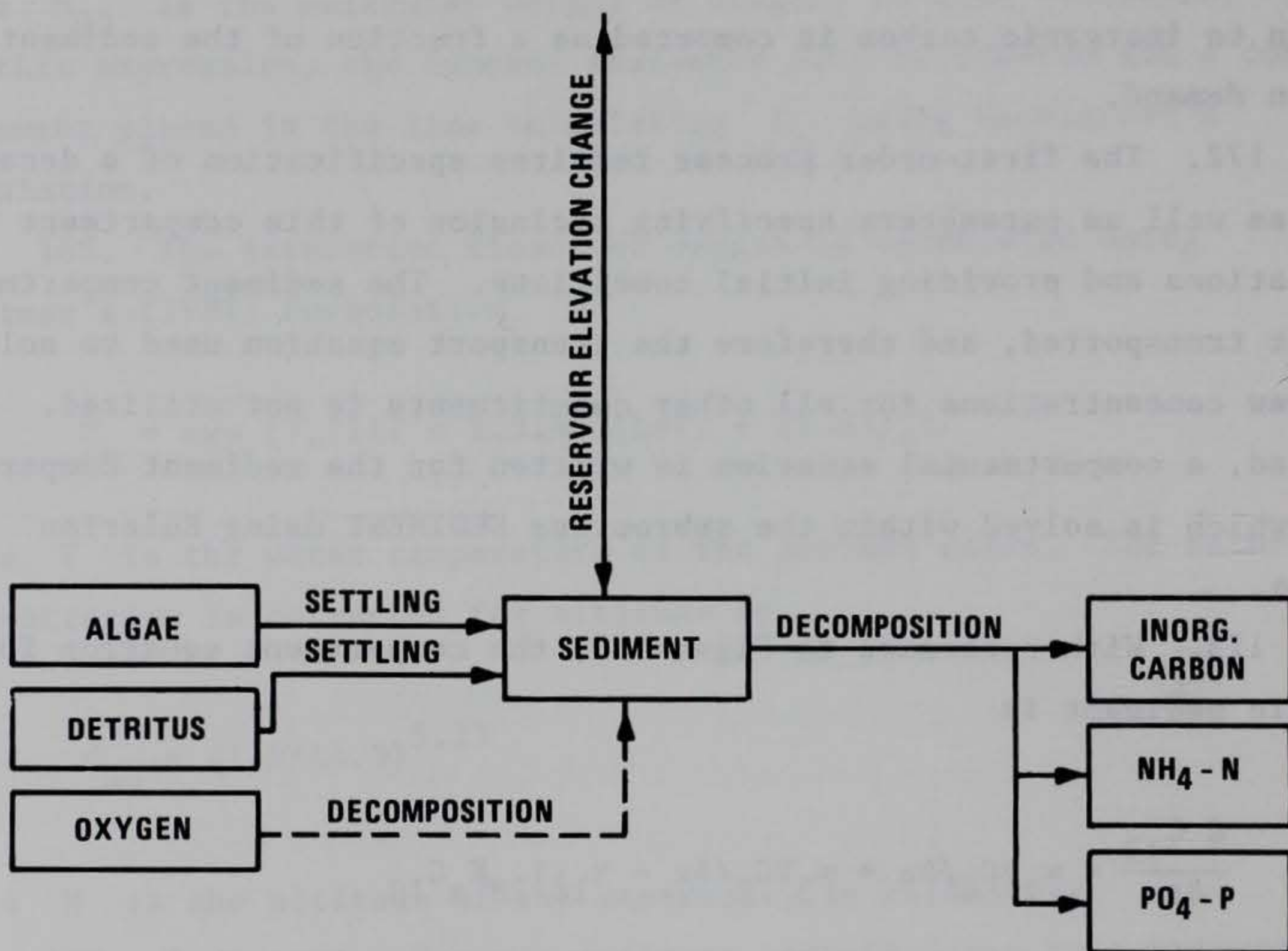


Figure 15. Flux between organic sediments and other compartments

174. Total inorganic carbon. Carbon, hydrogen, and oxygen are the most abundant elements in living matter and form the essential backbone of organic material. Inorganic carbon, modeled by this compartment, also directly influences pH.

175. With reference to Figure 16, the rate equation for total inorganic carbon is given by

$$\begin{aligned}
 \text{CSS}(I,K,14) = & (K_{rs} - K_g) \delta_C \text{VC}_7 + K_{dt} \delta_C \gamma_{14} \text{VC}_8 + K_s \gamma_{18} \gamma_{28} \delta_C C_{13} \\
 & + K_d \gamma_{11} \delta_C \text{VC}_5 + K_r \gamma_{11} \delta_C \text{VC}_6 + S_1 \gamma_{18} \gamma_{28} \delta_s A_s \\
 & + A_{kt} E_c (C_{sc} - C_{17})
 \end{aligned} \tag{86}$$

where

- V = model cell volume, m^3
- A_s = sediment surface area, m^2
- A_{kt} = surface area of top cell, m^2
- γ_{ii} = temperature rate multipliers
- δ_C = stoichiometric coefficients for carbon
- K_{rs} = algal dark respiration rate, sec^{-1} (see Equation 73)
- K_g = algal growth rate, sec^{-1} (see Equation 68)
- K_{dt} = detritus decay rate, sec^{-1}
- K_s = sediment decay rate, sec^{-1}
- K_d = labile DOM decay rate, sec^{-1}
- K_r = refractory DOM decay rate, sec^{-1}
- S_1 = sediment oxygen demand, $\text{g m}^{-2} \text{sec}^{-1}$
- E_c = inorganic carbon interfacial exchange rate, m sec^{-1}
- C_5 = labile DOM concentration, g m^{-3}
- C_6 = refractory DOM concentration, g m^{-3}
- C_7 = algae concentration, g m^{-3}
- C_8 = detritus concentration, g m^{-3}
- C_{13} = sediment mass, g
- C_{14} = inorganic carbon concentration, g m^{-3}
- C_{17} = carbon dioxide concentration, g m^{-3}
- C_{sc} = carbon dioxide saturation concentration, g m^{-3}
(see Equation 89)

and the rate terms are evaluated in subroutine CARB.

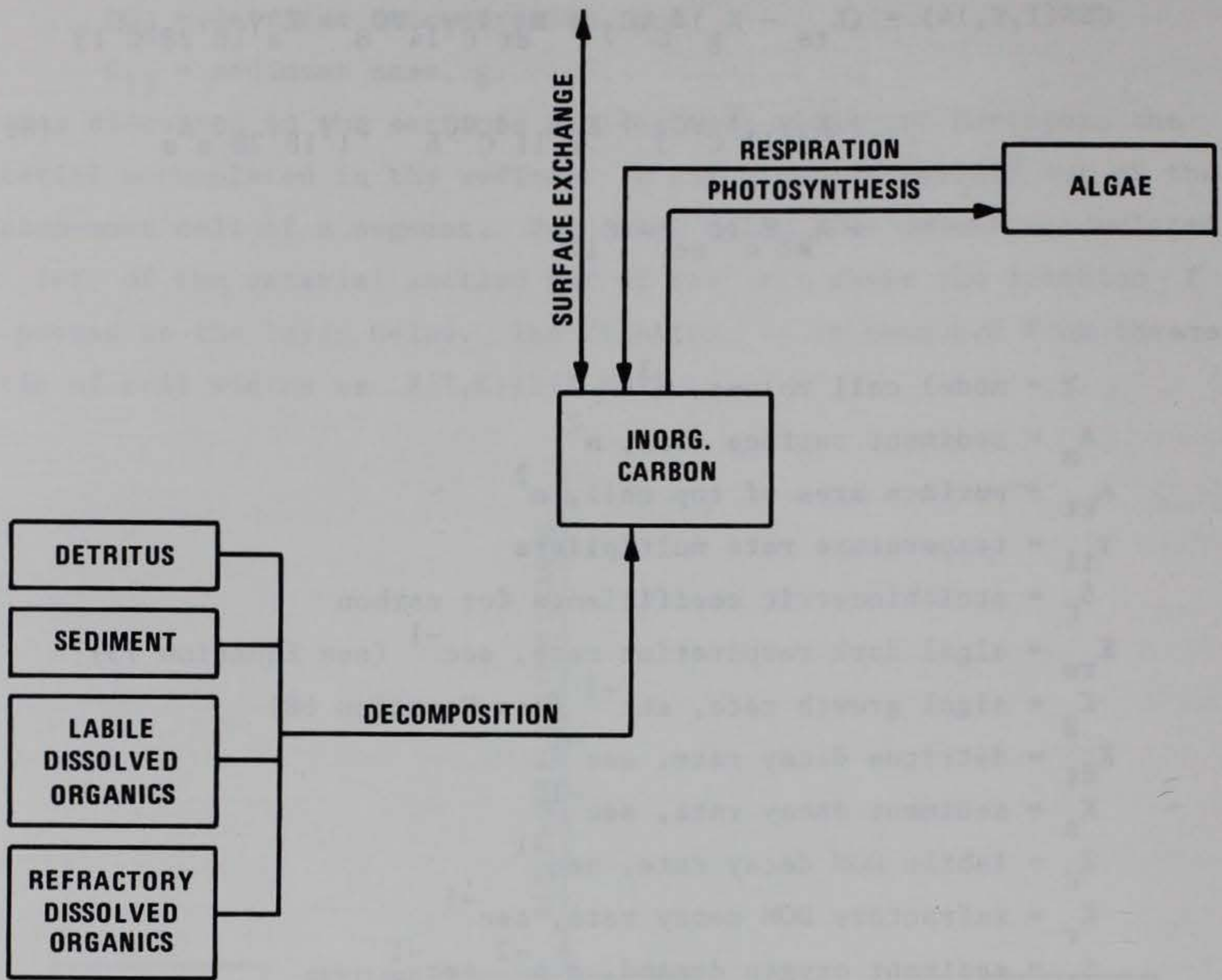


Figure 16. Internal flux between inorganic carbon and other compartments

176. The rate of interfacial exchange is computed using Kanwischer's (1963) formulation

$$E_c = \frac{D_c}{[200 - 60(W_a)^{1/2}] \times 10^{-6}} \quad (87)$$

where D_c is the molecular diffusivity of carbon dioxide and W_a the wind speed, in metres per second. An alternative expression from Mackay (1980, in Chapra and Reckhow 1983),

$$E_c = 6.4185 \times 10^{-6} \frac{W_a^{1.5}}{M_{CO_2}^{0.5}} \quad (88)$$

where M_{CO_2} is the molecular weight of carbon dioxide, is also available as a hardwired option. To use this option, comment statements must be placed in front of coding for Kanwischer's expression and removed from Mackay's.

177. The concentration of carbon dioxide for the interfacial exchange rate is determined from total inorganic carbon and alkalinity in subroutine PHCO2. The saturation concentration of carbon dioxide is determined from

$$C_{sc} = 0.286 \exp(-0.0314 T) P_a \quad (89)$$

where P_a is an altitude correction factor and T is the water temperature of the surface cell ($^{\circ}C$). The altitude correction is determined from

$$P_a = (1 - H/44.3)^{5.25} \quad (90)$$

(Mortimer 1981) where H is the elevation of the reservoir from sea level, in kilometres.

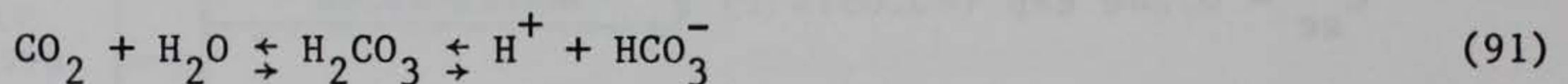
178. Alkalinity. Alkalinity provides an indication of the buffering capacity of aquatic systems, and therefore their resistance to pH changes resulting from acidic or alkaline loadings. The alkalinity is assumed to be conservative in CE-QUAL-W2, and its internal rate term $CSS(I,K,15)$ is set equal to zero. Alkalinity, along with total inorganic carbon, is used to determine pH and distributions of carbonate species in subroutine PHCO2.

179. In reality, alkalinity variations are common in most aquatic systems. Whittings, or large precipitations of carbonates, may occur. Sediment release of carbonates may increase alkalinity in the anoxic

zones of many reservoirs. Where description of these effects is desired, an additional compartment for alkalinity must be added to simulate nonconservative variations.

180. pH and carbonate species. The pH and carbonate species are computed using water temperature, TDS (or salinity), alkalinity, and total inorganic carbon concentrations using basic carbonate relationships. The carbonate species computed include (constituent number in parentheses) carbon dioxide (17), bicarbonates (18), and carbonates (19). The pH (constituent 16) and carbonate species are computed in subroutine PHCO2. These materials are not subject to transport and are computed at each water quality update interval.

181. The calculations performed by PHCO2 are based on the carbonate-bicarbonate equilibrium reaction (Stumm and Morgan 1981):



182. These equilibria express the source of bicarbonate and carbonate ions, alkaline constituents of fresh waters, and the dissolution of atmospheric CO_2 in water. The contribution of calcium and magnesium carbonate to the alkalinity is not overly expressed. The equilibrium state in terms of the equilibrium constants K_1 is:

$$K_1 = \frac{[\text{H}^+][\text{HCO}_3^-]}{[\text{H}_2\text{CO}_3]} \quad (94)$$

$$K_2 = \frac{[H^+][CO_3^{=}]}{[HCO_3^-]} \quad (95)$$

$$K_w = \frac{[H^+][OH^-]}{[H_2O]} \quad (96)$$

where

[X] = molar concentration of X

[H₂O] = unity (by definition)

183. The alkalinity imparted to the water can be defined as

$$[ALK] = [HCO_3^-] + 2[CO_3^{=}] + [OH^-] - [H^+] \quad (97)$$

in which, on a molecule-by-molecule basis, the excess of negative charges over positive charges is expressed. In addition, by viewing the abundance of bicarbonate and carbonate ions as arising from the dissolution of carbonic acid, the following concentration condition prevails:

$$[H_2CO_3] + [HCO_3^-] + [CO_3^{=}] = \text{CONST} = C_T \quad (98)$$

184. By combining Equations 94, 95, and 98, the quantities $[HCO_3^-]$ and $[CO_3^{=}]$ can be expressed in terms of $[H^+]$ and the constant C_T . In addition, Equation 96 allows for the quantity $[OH^-]$ to be expressed in terms of $[H^+]$. When these expressions are installed in Equation 97, the result is:

$$[ALK] = \frac{C_T [H^+] K_1}{[H^+] K_1 + K_1 K_2 + [H^+]^2} \frac{[H^+] + 2K_2}{[H^+]} + \frac{K_w}{[H^+]} - [H^+] \quad (99)$$

185. CE-QUAL-W2 interprets the constant C_T as moles per litre of total inorganic carbon and regards the quantity [ALK] as known. Equation 99 is iteratively solved in subroutine PHCO2 until the value of $[H^+]$ converges. The negative logarithm of $[H^+]$ is, by definition, pH.

186. Once Equation 99 has been solved for $[H^+]$, the abundance of $[H_2CO_3]$ is calculated as

$$[H_2CO_3] = \frac{C_T}{1 + \frac{K_1}{[H^+]} + \frac{K_1 K_2}{[H^+]^2}} \quad (100)$$

and is the same as that of $[CO_2]$. The concentration of bicarbonates is computed from

$$[HCO_3^-] = \frac{C_T}{1 + \frac{[H^+]}{K_1} + \frac{K_2}{[H^+]}} \quad (101)$$

and carbonate from

$$[CO_3^{=}] = \frac{C_T}{1 + \frac{[H^+]}{K_1 K_2} + \frac{[H^+]}{K_2}} \quad (102)$$

which are converted to concentration units of grams per cubic metre prior to being printed.

187. The equilibrium constants used in the preceding equations are obtained by first expressing a thermodynamic temperature dependence for a related constant, K_i^* :

$$\log K_i^* = a + \frac{b}{T} + cT + d \log T \quad (103)$$

The constants a , b , c , and d are given as follows:

| | <u>a</u> | <u>b</u> | <u>c</u> | <u>d</u> |
|---------|----------|----------|-----------|----------|
| K_w^* | 35.3944 | -5242.39 | -0.00835 | 11.8261 |
| K_1^* | 14.8435 | -3404.71 | -0.032786 | 0 |
| K_2^* | 6.4980 | -2902.39 | -0.02379 | 0 |

The relation between K_i and K_i^* is obtained from the definition of the activity of a chemical species.

$$\{X\} = \gamma[X] \quad (104)$$

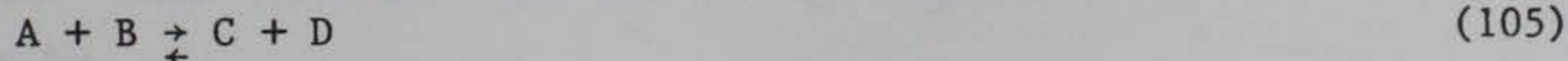
where

$\{X\}$ = activity of species X in moles per litre

γ = dimensionless activity coefficient

$[X]$ = concentration in moles per litre

For the reaction



the equilibrium constant K^* is

$$K^* = \frac{\{C\} \{D\}}{\{A\} \{B\}} \quad (106)$$

thus,

$$K^* = \frac{\gamma_C [C] \gamma_D [D]}{\gamma_A [A] \gamma_B [B]} = \frac{\gamma_C \gamma_D}{\gamma_A \gamma_B} K \quad (107)$$

$$K = \frac{\gamma_A \gamma_B}{\gamma_C \gamma_D} K^* \quad (108)$$

The activity coefficients are obtained from an extension of Debye-Huckel theory as:

$$\text{Log } \gamma = \frac{-AZ^2\sqrt{I}}{1 + 0.33a\sqrt{I}} + k_1 + k_2 I + k_3 I^2 \quad (109)$$

where

I = ionic strength

Z = ionic charge

A = approximately 0.5 for water at 25° C

a = ionic size parameter

k_i = empirical coefficients

The ionic strength is approximated (Sawyer and McCarty 1967) as

$$I = 2.5 \times 10^{-5} \times \left[\frac{\text{TDS}}{\text{mg}/\ell} \right] \quad (110)$$

or, in the case of salinity,

$$I = 0.00147 + 0.019885 S + 0.000038 S^2 \quad (111)$$

where S is the salinity (in kilograms per cubic metre). The values of the other parameters as used by CE-QUAL-W2 are:

| | <u>z</u> | <u>a</u> | <u>k₁</u> | <u>k₂</u> | <u>k₃</u> |
|-------------------------------|----------|----------|----------------------|----------------------|----------------------|
| HCO ₃ ⁻ | 1 | 4 | 0.0047 | 0.042 | -0.0093 |
| CO ₃ ⁼ | 2 | 4.5 | 0.0121 | 0.0972 | -0.0207 |

188. The activity coefficients for [H⁺], [OH⁻], [H₂CO₃], and [H₂O] are treated as special cases:

$$[\text{H}^+] \quad \gamma = 1$$

$$[\text{H}_2\text{O}] \quad \gamma = 1$$

$$[\text{H}_2\text{CO}_3] \quad \gamma = 0.07551$$

$$[\text{OH}^-] \quad \gamma = 0.07551$$

189. Total iron. Total iron is included in the model primarily as a result of its effect on nutrient concentrations through the processes of adsorption and settling. Iron is commonly released from anoxic sediments and may largely influence nutrient dynamics in many reservoirs. Iron may also contribute to dissolved oxygen depletions. However, simulation of only total iron does not allow inclusion of its effect on dissolved oxygen.

190. With reference to Figure 17, a rate equation for total iron is given by

$$\text{CSS}(I,K,20) = S_4 \gamma_{18} \gamma_{28} A_s - V \omega_4 C_{20} / \Delta z$$

where

$$V = \text{volume, m}^3$$

$$A_s = \text{sediment area, m}^2$$

$$\Delta z = \text{cell thickness, m}$$

$$\gamma_{18} = \text{temperature rate multiplier for ascending portion of curve}$$

γ_{28} = temperature rate multiplier for descending portion of curve

ω_4 = settling velocity, m sec^{-1}

S_4 = sediment release rate, $\text{g m}^{-2} \text{sec}^{-1}$

C_{20} = total iron concentration, g m^{-3}

and the rate terms are evaluated in subroutine FETOT.

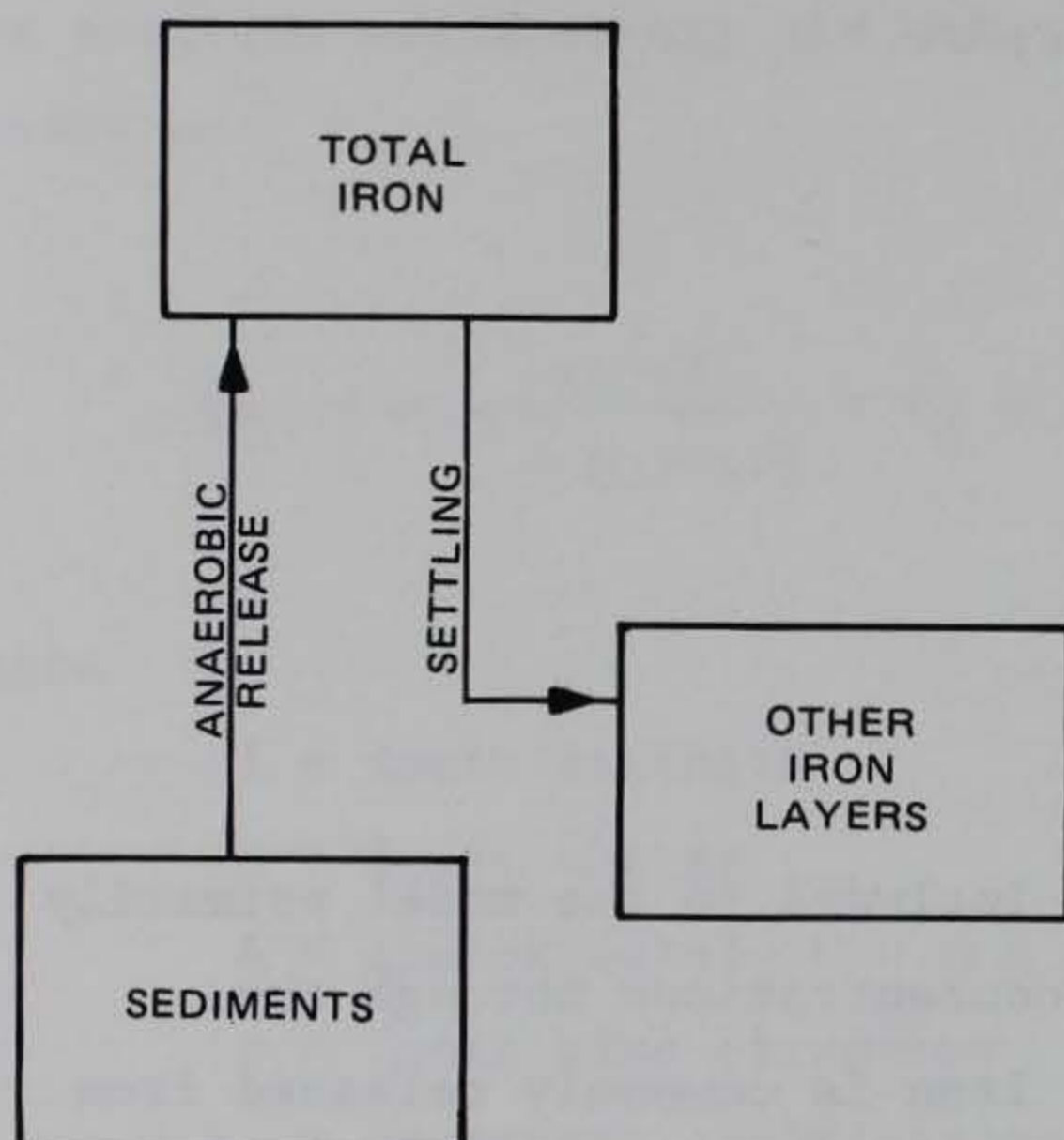


Figure 17. Internal flux between total iron and other compartments

191. Temperature rate multipliers. Most biological and chemical rates are temperature dependent. Subroutine RMULT calculates the temperature dependence for all such rates. It is called after the temperature solution so that the temperature of the current computational interval is used.

192. A representative rate multiplier function is shown in Figure 18 with its K and T parameters. The shape of the curve represents, in general, how biological process rates exhibit an optimum range and diminish (asymmetrically) at higher and lower temperatures. Curvature details differ from process to process. CE-QUAL-W2 uses a mathematical representation of Figure 18 that allows a broad range of curves to be represented (Thornton and Lessem 1978).

$$\lambda_{ii} = \begin{cases} 0 & T \leq T_1 \\ \frac{K_1 \exp [\gamma_1(T - T_1)]}{1 + K_1(\exp [\gamma_1(T - T_1)] - 1)} \times \frac{K_4 \exp [\gamma_2(T_4 - T)]}{1 + K_4(\exp [\gamma_2(T_4 - T)] - 1)} & T_1 < T < T_4 \\ 0 & T \geq T_4 \end{cases} \quad (112)$$

where

$$\gamma_1 = \frac{1}{T_2 - T_1} \ln \frac{K_2(1 - K_1)}{K_1(1 - K_2)}$$

$$\gamma_2 = \frac{1}{T_4 - T_3} \ln \frac{K_3(1 - K_4)}{K_4(1 - K_3)}$$

The user supplies temperatures T_1 to T_4 and multiplier factors K_1 to K_4 . Temperatures T_1 and T_4 represent mortality limits, and T_2 and T_3 are used to define the optimum range. The maximum reaction rates supplied by the user are multiplied by λ_{ii} to determine rates corresponding to the water temperature of a model cell.

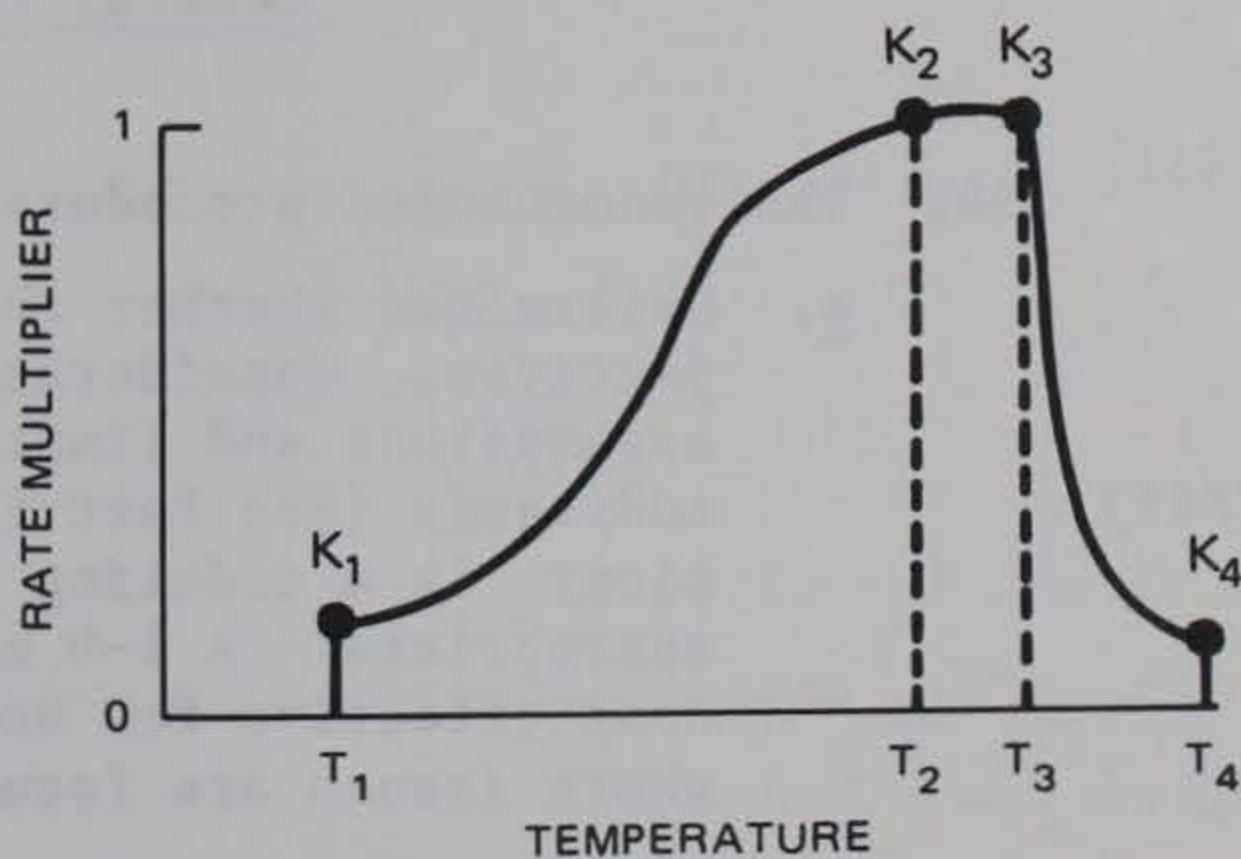


Figure 18. The temperature rate multiplier

PART IV: OPERATIONS

General Comments

193. As suggested in the opening paragraphs of this manual, the tasks of data assembly, calibration, and analysis are major tasks whose time and labor requirements should not be underestimated.

194. Adequate data preparation and analyses require a thorough knowledge of the site and its specific characteristics. Familiarization with the reservoir, its general ecology, watershed, dam, outlet structure, project operation, and measured data are essential. Many site-specific characteristics are not discernible from topographic maps alone. In addition, the location of sampling stations may heavily influence water quality results.

195. Involvement of a multidisciplinary team is recommended for the modeling effort. Expertise may be required in the areas of hydrodynamics, project operation, limnology, and aquatic biology. Decisions made throughout a model application may require knowledge in these areas. Within Part IV, the general procedures for model application are outlined. Next, data assembly is presented, followed by model calibration, confirmation, and output interpretation.

General Procedure

196. The recommended procedure for any modeling study is:
- a. Determined whether the model can address the study objectives. Consideration must be given to the model assumptions and limitations and to the factors the model addresses (see Part II). The user must answer the question: Is a modeling study required and is this appropriate? A 1-D model may suffice and may be more cost effective for some applications, such as those where issues are focused on release water quality.
 - b. Compile the necessary information to run the model. Review the next sections and Part II to determine data requirements for CE-QUAL-W2.

- c. Determine whether sufficient data are available to run the model. This is a difficult question to answer and is largely influenced by the study objectives.
- d. Assemble data. This topic is discussed in the following sections and in Part II.
- e. Check out model. A run should be made to determine if the program compiles and executes correctly and if the data deck and output forms are in the correct formats. A sample data deck and printout should be used for this.
- f. Determine time step. The first actual model simulation will probably be run with a single low and constant time step. However, the information obtained in those simulations can be used to estimate a series of time steps for future simulations which may result in a considerable savings in computation time. No single criterion has been found to provide reliable estimates of time step requirements for numerical stability. However, criteria that may be used to estimate time steps from TAPE 6 (GRID) and TAPE 61 (DIAGNOS) output include the following:

$$\Delta t < \Delta x/U \quad (113)$$

$$\Delta t < \Delta z/W \quad (114)$$

$$\Delta t < \Delta x/\sqrt{g H \Delta \rho / \rho} \quad (115)$$

$$\Delta t < V/Q^* \quad (116)$$

$$\Delta t < \frac{1}{2} \frac{\Delta x^2}{D_x} \quad (117)$$

$$\Delta t < \frac{1}{2} \frac{\Delta z^2}{D_z} \quad (118)$$

where

Δt = time step, sec

Δx = segment length, m

Δz = layer thickness, m

- H = reservoir depth, m
- g = gravitational constant, m sec^{-2}
- ρ = water density, kg m^{-3}
- $\Delta\rho$ = maximum water density difference from surface to bottom, kg m^{-3}
- U = horizontal velocity, m sec^{-1}
- W = vertical velocity, m sec^{-1}
- D_x = horizontal diffusion, m sec^{-2}
- D_z = vertical diffusion, m sec^{-2}

Relatively small time steps may be required for stability during periods of high flows, while longer time steps may be used during more quiescent conditions. The speed at which a wave travels through a branch may also be limiting, and the multiple-branch case may be more limiting than the single-branch case.

- f. Calibrate model. The calibration procedures for CE-QUAL-W2 are discussed in detail in a later section.
- g. Perform confirmation. The confirmation procedures are discussed in detail in a later section.
- h. Interpret output. This step is also discussed in detail in a later section. The step involves addressing the study objectives and comparing management alternatives.

Data Assembly

197. The data required by CE-QUAL-W2 consist of geometric schematization, initial and boundary conditions, hydraulic properties, and biological and chemical parameters. Before assembling these data sets, it is suggested that the user review this section and Part II to determine if sufficient data are available to use the model. All of the necessary information to run the model is included in the control file, with the exception of time-varying boundary condition data.

198. The calibration and confirmation data are required in order to assess the adequacy of model calibration and confirmation. These data are not utilized in the performance of simulations. They are contained in external files and may be used by auxiliary graphics and statistical programs to allow comparison of measured and simulated results.

The data requirements for these tasks and the process of calibration and confirmation will be discussed in more detail in later sections. The format of these external files for compatibility with graphics programs is discussed in Appendix C.

199. The control file sets the stage for simulations by providing all necessary information to define the geometry of the system, define constants and parameters, and establish initial conditions. The information contained in the control file was discussed in Part II. The following section provides specific information concerning the format and data supplied for each card image of the control file. A section providing general guidelines for values of coefficients and parameters follows the control file description.

Time-varying boundary condition data

200. The time-varying boundary condition data consist of time sequences of meteorological, hydrological, and water quality values required during the simulation. These are supplied through the subroutine TVDS (Time Varying Data Selector), which reads external files containing time-varying data and supplies updated values during the course of the simulation. As the amount of time-varying data varies considerably with applications, there is no general format to this subroutine. It must be modified to suit the needs of each specific application. However, some guidance can be provided in its use.

201. Time-varying data are required for all external processes affecting the system. The amount of time-varying data needed varies with options selected in the input data deck. If inflows are specified, their corresponding temperature and constituent concentrations must also be specified. If head boundary conditions are used, the water surface elevation, temperature, and constituent profiles at the boundary are required. Data are also required for heat exchange and wind. A summary of the FORTRAN variables required for each condition or process is provided in Table 3.

202. A typical TVDS listing is provided as Figure 19. In this example, only variables affecting heat exchange, wind, and evaporation are defined. However, a similar structure would be used if other variables must be defined or if more than one external file must be read.

203. The first statement in the subroutine is the INCLUDE in the VAX version, which contains the common blocks. The common statements should be examined to ensure that all variables of interest are defined and dimensioned. A dimension statement then follows for the array(s) containing the time-varying data. A series of comment cards generally follow describing the particular application.

204. In the simplest case, for steady-state conditions, the dimension statement would not be required and it would now only be necessary to assign values to variables. In a second case, time-varying data may be calculated from user-supplied equations. In the case where time-varying data are contained in external files, the TVDS subroutine

Table 3
TVDS FORTRAN Variables

| Process | FORTRAN Variables | | |
|------------------------------------|-------------------|-------------|---------------|
| Flow boundary conditions | | | |
| Precipitation | PRECIP, | TPRCEP, | CPRECP(JC) |
| Inflow | QIN(JB), | TIN(JB), | CIN(JB,JC) |
| Tributaries (lateral inflows) | QTRIB(JT), | TTRIB(JT), | CTRIB(JT,JC) |
| Distributed tributaries (nonpoint) | QDSTRB(JB), | TDSTRB(JB), | CDSTRB(JB,JC) |
| Outlets | QOUT(JO) | | |
| Withdrawals | QWD(JW) | | |
| Head boundary conditions | | | |
| Upstream head | ELL(JB), | TL(K,JB), | CL(K,JB,JC) |
| Downstream head | ELR(JB), | TR(K,JB), | CR(K,JB,JC) |
| Heat exchange | ETM, CSHE, SRO | | |
| Wind | PHI, WA | | |
| Evaporation | TD | | |

NOTES: JB = 1, NB; JC = 1, NC; JO = 1, NOUT; JT = 1, NTRIB;
 JW = 1, NWD; K = 1, KMAX.

generally performs two tasks. The first task is to read external files into arrays and the second is to update variables using that array at the appropriate simulation time. The external files containing time-varying data must include the data associated with the updates to determine when particular values should be used. Update values should be provided on a daily, or more frequent, basis and do not have to be at regular intervals.

205. When TVDS is first called (IFLAG = 0), external file(s) containing time-varying data (TAPE 51 to TAPE 54) are read into the array(s) defined in the dimension statement and the total number of updates counted. This is accomplished in lines 18 to 45 of Figure 19. If the units of the input file are not compatible with those of CE-QUAL-W2, they should be converted at this time. In the example provided in Figure 19, the time units in the input file were in Julian day.hour and


```

1 C *****
2 C *
3 C *           S U B R O U T I N E   T V D S           *
4 C *
5 C *****
6
7     SUBROUTINE TVDS(IFLAG,ABTM)
8     INCLUDE 'XCQR.COM.FOR'
9 C
10    DIMENSION TVD(5000,9)
11
12 C  DEGRAY RESERVOIR
13 C  CADDO RIVER:QIN(1)-BRANCH 1
14 C  NO TRIBUTARIES, DISTRIBUTED INFLOWS
15 C  NO WITHDRAWALS
16 C  NO PRECIPITATION
17
18    IERFL=0
19    IF (IFLAG.EQ.1) GO TO 1000
20 C
21 C  #####
22 C  # READ TIME VARYING BOUNDARY DATA FROM EXTERNAL FILES (ON INITIAL #
23 C  # CALL TO TVDS, IFLAG=0) #
24 C  #####
25 C
26 C  _____
27 C  | INPUT HYDROMETEOROLOGICAL DATA ARRAY FROM FILE 54 |
28 C  _____
29
30    NR=0
31    DO 100 I=1,5000
32        READ(54,10,END=110)RJD,(TVD(I,J),J=2,9)
33 10    FORMAT(F7.2,F8.1,2E8.3,F8.2,F8.1,F8.1,F8.2,F8.1)
34
35 C  CONVERT DATES FROM JULIAN DAY.HOUR TO ABTM (YEAR*1000+JULIAN DAY+HOUR/24)
36        J=RJD
37        CONVERT=(RJD-J)*100./24.
38        IF (CONVERT.GT.1) CONVERT=1.0
39        TVD(I,1)=J+CONVERT+79000.
40        NR=NR+1
41
42 100  CONTINUE
43 110  ISTART54=2
44
45    RETURN

```

Figure 19. Example listing of a TVDS subroutine (Continued)


```

46 C
47 C #####
48 C # UPDATE TIME VARYING BOUNDARY CONDITION DATA ON SECOND #
49 C # AND SUBSEQUENT CALLS TO TVDS (IFLAG=1) #
50 C #####
51
52 C _____
53 C | UPDATE HYDROMETEOROLOGICAL DATA |
54 C _____
55
56 1000 IFILE=54
57 IF (ABTM.LT.TVD(1,1).OR.ABTM.GT.TVD(NR,1)) THEN
58     IFLAG=-1
59     WRITE(6,80)IFILE,ABTM
60     RETURN
61 END IF
62 C
63 N=ISTART54
64 DO 2000 I=N,NR
65
66 IF (ABTM.GE.TVD(I-1,1).AND.ABTM.LT.TVD(I,1)) THEN
67     PHI=2.0 HRDWIRE
68     ETM=TVD(I-1,2) ETM
69     CSHE=TVD(I-1,3) CSHE
70     SRO=TVD(I-1,4) SRO
71     QIN(1)=TVD(I-1,5)*1.68 HRDWIRE
72     QOUT(5)=0.10*TVD(I-1,7)
73     QOUT(6)=0.20*TVD(I-1,7)
74     QOUT(7)=0.40*TVD(I-1,7)
75     QOUT(8)=0.20*TVD(I-1,7)
76     QOUT(9)=0.10*TVD(I-1,7)
77
78 C             CONVERT WIND FROM KM/HR TO M/S
79     WA=TVD(I-1,8)*1000./3600. WA
80     TD=TVD(I-1,9) TD
81 C
82 C
83     IERFL=1
84     GO TO 2030
85 END IF
86 ISTART54=ISTART54 + 1
87 2000 CONTINUE
88
89 2030 IF (IERFL.NE.1) THEN
90     IFLAG=-1
91     WRITE(6,80)IFILE,ABTM
92 END IF
93
94 RETURN
95 80 FORMAT('FILE ',I8,'*****READIT ERROR AT',F15.9,'DAYS*****')
96 END
97

```

Figure 19. (Concluded)

were converted to absolute time units (year * 1,000 + Julian day + hours/24) in lines 36 to 40.

206. In subsequent calls to TVDS (IFLAG = 1), the required variables are assigned updated values. Prior to accomplishing this, an error flag (IERFL) is set equal to zero. A check is usually made here (line 66, Figure 19) to see if the starting time of the simulation is less than the first date for which data are available or greater than the last date. If it is, indicating that no data are available, the error flag is not reset, and error message is written to TAPE 6 and execution is halted. If not, a loop over the update file is conducted until a case is found where the simulation time is either equal to a date in the file or between two dates for which data are available. Once the proper data are selected, the selected variables are updated. If no updates occur, the error flag is not reset, an error message is written, and execution is halted.

Input data description

207. General. Descriptions for each of the cards (or card images) used as input to CE-QUAL-W2 are presented on the following pages. There are three data types: character, real (may be left or right justified), and integer (must be right justified). There are 11 data fields per card (with constituent parameters using a slightly different format as noted later):

| <u>Field</u> | <u>Length</u> | <u>Columns</u> |
|--------------|---------------|----------------|
| 0 | 2 | 1-2 |
| 1 | 6 | 3-8 |
| 2 | 8 | 9-16 |
| 3 | 8 | 17-24 |
| 4 | 8 | 25-32 |
| 5 | 8 | 33-40 |
| 6 | 8 | 41-48 |
| 7 | 8 | 49-56 |
| 8 | 8 | 57-64 |
| 9 | 8 | 65-72 |
| 10 | 8 | 73-80 |

This format is similar to that used in the Hydrologic Engineering Center codes.

208. Title cards (required). Title cards may be used to identify applications, simulations, or other parameters as required. These cards do not affect the computation.

CARD T1 - The text input with this card appears in the header with each velocity, temperature, and constituent field snapshot, as well as in the overall header printed once for each simulation.

| <u>Field</u> | <u>Parameter</u> | <u>Value</u> | <u>Description</u> |
|--------------|------------------------|--------------|---|
| 0 | AID | T1 | character: card identification |
| 1-9 | TITLE (1,J), J=1,18 | | character: simulation identification text |

CARD T2 - The text input with this card always appears in the overall simulation header and appears in the first snapshot header if IFORM = 1 .

| <u>Field</u> | <u>Parameter</u> | <u>Value</u> | <u>Description</u> |
|--------------|------------------|--------------|---|
| 0 | AID | T2 | character: card identification |
| 1-9 | TITLE (2) | | character: simulation identification text |

CARD T3 - The text input using this card always appears in the overall simulation header and appears in the first snapshot if IFORM = 1 .

| <u>Field</u> | <u>Parameter</u> | <u>Value</u> | <u>Description</u> |
|--------------|------------------------|--------------|---|
| 0 | AID | T3 | character: card identification |
| 1-9 | TITLE (3,J), J=1,18 | | character: simulation identification text |

CARD T4 - The text input using this card always appears in the overall simulation header and appears in the first snapshot if IFORM = 1 .

| <u>Field</u> | <u>Parameter</u> | <u>Value</u> | <u>Description</u> |
|--------------|------------------------|--------------|---|
| 0 | AID | T4 | character: card identification |
| 1-9 | TITLE (4,J), J=1,18 | | character: simulation identification text |

209. Geometry card (required).

CARD GE - The geometry card specifies the overall grid size (the number of segments and layers), the thickness of the individual cells, the location of the grid relative to the reference datum, the number of branches, and the water body type.

| <u>Field</u> | <u>Parameter</u> | <u>Value</u> | <u>Description</u> |
|--------------|------------------|--------------|---|
| 0 | AID | GE | character: card identification |
| 1 | IMAX | ≥5 | integer: number of I-segments |
| 2 | KMAX | ≥4 | integer: number of K-layers |
| 3 | HIN(1,1) | + | real: layer thickness, m |
| 4 | DTM | -,0,+ | real: distance from reference <u>DaTuM</u> (mean sea level) to lower grid boundary, m |
| 5 | NB | 1 ≤ NB ≤ 6 | integer: number of branches |
| 6 | IWT | 0 | integer: freshwater water body, total dissolved solids represented by constituent 4 |
| | | 1 | integer: saline water body, salinity represented by constituent 4 |

NOTES: CE-QUAL-R2 requires a grid with $IMAX \geq 5$ and $KMAX \geq 4$. A typical grid has $IMAX$ in the 10 to 36 range and $KMAX$ in the 15 to 31 range. The grid size, number of branches, and number of constituents should be within the range of the PARAMETER statements in the Commons file and the subroutine TRIDAG.

The value of $HIN(1,1)$ is the 0.5- to 3-m range. Variable $HIN(1,1)$ is read as the cell height for cell $I=1$, $K=1$, and then applied to all other cells.

210. Branch geometry card (one BG CARD for each branch).

CARD BG - The branch geometry card specifies the location of the branch on the grid, branch boundary conditions, the length of individual cells, and the orientation of the branch.

| <u>Field</u> | <u>Parameter</u> | <u>Value</u> | <u>Description</u> |
|--------------|------------------|--------------------------------|---|
| 0 | AID | BG | character: card identification, Branch Geometry |
| 1 | IBC(1,JB) | + | integer: left-hand active segment of the branch |
| 2 | IBC(3,JB) | + | integer: right-hand active segment of the branch |
| 3 | ILS(JB) | -1 | integer: upstream head (external) boundary condition |
| | | 0 | integer: upstream flow (external) boundary condition |
| | | + | integer: main stem or other branch segment where the branch leaves the main stem or another branch; upstream head (internal) boundary condition |
| 4 | IES(JB) | -1 | integer: downstream head (external) boundary condition |
| | | 0 | integer: downstream flow (external) boundary condition |
| | | + | integer: main stem or other branch segment where the branch enters the main stem or another branch; downstream head (internal) boundary condition |
| 5 | DLX (JB) | + | real: ΔX , branch segment length, m |
| 6 | PHIO(JB) | $0 \leq \text{PHIO} \leq 2\pi$ | real: the angle between the positive x-axis (branch center line in the flow direction) and the north, in radians |

NOTES: The main stem is defined as the first branch coded into the grid. Two inactive segments always separate it from the next branch in the grid and that branch from the next, etc. Branches are numbered by the code, with the main stem referred to as "BRANCH 1."

The branch DLX may differ from another branch DLX.

The branch may not enter or leave itself.

The boundary condition data that TVDS is required to supply for each of the boundary condition types are as follows.

| <u>Type</u> | <u>Data required</u> |
|----------------------------|----------------------|
| Upstream flow - external | QIN, CIN |
| Upstream head - external | ELL, TL, CL |
| Upstream head - internal | -- |
| Downstream flow - external | QOUT |
| Downstream head - external | ELR, TR, CR |
| Downstream head - internal | -- |

Variables CIN(JB,JC) , CL , and CR are required for the no-constituent case.

One QIN is needed for each branch for which ILS = 0 , although QIN values may be 0. The QOUT for the case of IES = 0 is optional.

211. Water body parameter card (required).

CARD WP - The WP card specifies certain hydrodynamic parameters, including horizontal dispersion coefficients for momentum, heat, and constituents, as well as GAMMA and BETA, which affect depth variations of solar radiation absorption and attenuation.

| <u>Field</u> | <u>Parameter</u> | <u>Value</u> | <u>Description</u> |
|--------------|------------------|--------------|--|
| 0 | AID | WP | character: card identification for <u>Water body Parameters</u> |
| 1 | AX | + | real: X-direction momentum dispersion coefficient, $m^2 \text{ sec}^{-1}$ |
| 2 | DXI | + | real: X-direction heat dispersion coefficient, $m^2 \text{ sec}^{-1}$ |
| 3 | DXS | + | real: X-direction constituent dispersion coefficient, $m^2 \text{ sec}^{-1}$ |
| 4 | CHZY | + | real: <u>CHeZY</u> resistance coefficient, $m^{0.5} \text{ sec}^{-1}$ |
| 5 | BETA | + | real: fraction of incident solar radiation absorbed at the water surface |
| 6 | GAMMA | + | real: solar radiation attenuation coefficient, m^{-1} |

NOTES: The parameter GAMMA includes all factors affecting solar radiation attenuation. The parameter is used only when constituents in Levels I and II are not simulated; otherwise, the extinction coefficient is determined by EXCO, EXTINS, EXTINP, and suspended solids concentrations (inorganic, algae, and detritus). The user should ensure that NC > 7 and ITRIP(2), ITRIP(7), and ITRIP(8) are equal to one to include self-shading effects.

212. Time period card (required).

CARD TM - The TM card specifies the number of time period pairs for the specific application. Each pair consists of the delta-T (DLT) in seconds and the number of iterations (NIT) at the specified DLT .

| <u>Field</u> | <u>Parameter</u> | <u>Value</u> | <u>Description</u> |
|--------------|------------------|--------------|---|
| 0 | AID | TM | character: card identification, <u>Time</u> |
| 1 | NP | NP ≤ 50 | integer: <u>Number</u> of DLT and NIT Pairs to be read from following <u>DN</u> cards |

213. delta-T and number of iterations cards (required).

CARD DN - Each DN card specifies the delta-T in seconds and the number of steps to be iterated through at that delta-T. One DN card is required for each period (NP) specified on the TM card. An effective wind coefficient for each branch must also be specified for each time period pair.

| <u>Field</u> | <u>Parameter</u> | <u>Value</u> | <u>Description</u> |
|--------------|----------------------|--------------|--|
| 0 | AID | DN | character: card identification, <u>Delta-T</u> and <u>Number of iterations</u> |
| 1 | DLTO(J) | + | real: delta-t, computation time step, sec |
| 2 | NIT(J,1) | + | integer: <u>Number of I</u> terations at the specified delta-T |
| 3-8 | EWC(J,JB) JB=1,NB | + | real: effective wind coefficient for each branch ($1 \leq NB \leq 6$) |

214. Snapshot card (required).

CARD SN - This card specifies the form and frequency of snapshots printed to TAPE 6 and set a series of output write switches that define which of the velocity, temperature, density, and constituent fields and algal limiting factors will be written in the snapshots.

| <u>Field</u> | <u>Parameter</u> | <u>Value</u> | <u>Description</u> |
|--------------|------------------|--------------|--|
| 0 | AID | SN | character: card identification, <u>S</u> Snapshot print specification, TAPE 6 |
| 1 | IFORM | 0 | integer: snapshot output shortened (cell widths and volume-area-elevation tables suppressed) and compressed to fit an 8-1/2-in. page width; output is for the nine segments specified on the IO card |
| | | 1 | integer: normal snapshot output using entire 132-column, 14-in. page width; output is for the 17 segments specified on the I1 and I2 cards |
| 2 | TBPR | + | real: <u>T</u> ime to <u>B</u> egin <u>P</u> rinting, ABTM compatible time, year * 1,000 + Julian day + hours/24. |
| 3 | FOPR | + | real: <u>F</u> requency <u>O</u> f <u>P</u> rinting, hours; snapshots are printed every FOPR hours, beginning at TBPR |
| 4 | IWRITE(1) | 0 | integer: U (horizontal velocity) WRITE switch off |
| | | 1 | integer: U (horizontal velocity) WRITE switch on |
| 5 | IWRITE(2) | 0 | integer: W (vertical velocity) WRITE switch off |
| | | 1 | integer: W (vertical velocity) WRITE switch on |
| 6 | IWRITE(3) | 0 | integer: T (temperature field) WRITE switch off |
| | | 1 | integer: T (temperature field) WRITE switch on |
| 7 | IWRITE(4) | 0 | integer: RHO (density field) WRITE switch off |

(Continued)

| <u>Field</u> | <u>Parameter</u> | <u>Value</u> | <u>Description</u> |
|--------------|------------------|--------------|--|
| 7 | IWRITE(4) | 1 | integer: RHO (density field) WRITE switch on |
| 8 | IWRITE(5) | 0 | integer: C (constituent field) WRITE switch off |
| | | 1 | integer: C (constituent field) WRITE switch on |
| 9 | IWRITE(6) | 0 | integer: LIMIT (algal growth limitation factor) WRITE switch off |
| | | 1 | integer: LIMIT (algal growth limitation factor) WRITE switch on |

NOTES: The six IWRITE switches control whether the following CE-QUAL-W2 variables are printed in the snapshots:

| | | | | | | |
|-----------|-----|------|-----|-----|-----|-------|
| IWRITE: | (1) | (2) | (3) | (4) | (5) | (6) |
| VARIABLE: | U | W,AZ | T | RHO | C | LIMIT |

Each switch must be set to either 0 (off) or 1 (on). The format of the output is specified by the IFORM parameter, which determines whether output is specified for the nine segments defined by the IO card or for the 17 segments defined by the I1 and I2 cards. The frequency of printing is controlled by TBPR and FORP. The IWRITE switches 3 (temperature) and 4 (RHO) also control whether or not these variables are to be printed to files for vertical profiles (IVPR) and contouring (ITCON), if these options are selected on the TW card.

215. Tapewrite card (required).

CARD TW - This card contains a series of on/off switches which control whether, and at what frequency, output is written to TAPE 61, TAPE 62, TAPE 63, TAPE 64, TAPE 65 and TAPE 66.

| <u>Field</u> | <u>Parameter</u> | <u>Value</u> | <u>Description</u> |
|--------------|------------------|--------------|---|
| 0 | AID | TW | character: card identification, tape write specifications for TAPE 61- TAPE 66 |
| 1 | IDIAG | 0 | <u>I</u> nteger: the printing of delta-T and user-inserted <u>D</u> IAGNostics is suppressed |
| | | 1 | <u>I</u> nteger: user-inserted <u>D</u> IAGNostics are written to TAPE 61 |
| 2 | IRSW | 0 | <u>I</u> nteger: <u>R</u> e <u>S</u> tart <u>W</u> rite switch off, no restart conditions written to TAPE 62 |
| | | 1 | <u>I</u> nteger: <u>R</u> e <u>S</u> tart <u>W</u> rite switch on, restart conditions written to TAPE 62 |
| 3 | ITSR | 0 | <u>I</u> nteger: <u>T</u> ime <u>S</u> eries <u>R</u> esults of user-specified variables not written to TAPE 63 |
| | | 1 | <u>I</u> nteger: <u>T</u> ime <u>S</u> eries <u>R</u> esults of user-specified variables written to TAPE 63 |
| 4 | IVPR | 0 | <u>I</u> nteger: <u>V</u> ertical <u>P</u> rofile results of specified variables at user-specified locations not written to TAPE 64 |
| | | 1 | <u>I</u> nteger: <u>V</u> ertical <u>P</u> rofile results of specified variables at user-specified locations written to TAPE 64 |
| 5 | ICIRC | 0 | <u>I</u> nteger: <u>C</u> IRCulation data for vector plots not written to TAPE 65 |
| | | 1 | <u>I</u> nteger: <u>C</u> IRCulation data for vector plots written to TAPE 65 |
| 6 | ICNTR | 0 | <u>I</u> nteger: <u>C</u> o <u>N</u> Tou <u>R</u> ing information not written to TAPE 66. |
| | | 1 | <u>I</u> nteger: <u>C</u> o <u>N</u> Tou <u>R</u> ing information written to TAPE 66. |
| 7 | TBPL | + | real: <u>T</u> ime to <u>B</u> egin <u>P</u> lot, year/days |
| 8 | FOPL | + | real: <u>F</u> requency <u>O</u> f <u>P</u> lotting, hours |

(Continued)

| <u>Field</u> | <u>Parameter</u> | <u>Value</u> | <u>Description</u> |
|--------------|------------------|--------------|--|
| 9 | TBTS | + | real: <u>T</u> ime to <u>B</u> egin <u>T</u> ime <u>S</u> eries out- put, year/days |
| 10 | FOTS | + | real: <u>F</u> requency <u>O</u> f <u>T</u> ime <u>S</u> eries, hours |

NOTES: CE-QUAL-W2 has seven output files (tapes) available:

- TAPE 6 - Control file, bathymetry, and snapshots: Receives snapshot output according to the form, interval, and switch parameters on the snapshot card.
- TAPE 61 - Diagnostics: Receives temporary diagnostic values as inserted in the code by the user if IDIAG is set equal to 1.
- TAPE 62 - Restart: Restart conditions are written if IRSW = 1 .
- TAPE 63 - Time series results: Receives time series histories, at FOTS intervals for water surface elevations (EL) and outflow concentrations as specified by IWRITE(3) and ICTRIP(J) designators if ITSR = 1 .
- TAPE 64 - Vertical profile results: Receives computed temperatures (if IWRITE(3) = 1), densities (if IWRITE(4) = 1), and constituent concentrations (if ICTRIP(J) = 1) for OD dates and OS segments if IVPR = 1 .
- TAPE 65 - Circulation plot file: receives circulation data required to produce vector plots at FOPL intervals beginning with TBPL if ICIRC = 1 .
- TAPE 66 - Contour plot file: Receives information for contour plots of temperatures (if IWRITE(3) = 1), densities (if IWRITE(4) = 1, card SN), and the constituent J (if ICTRIP(J) = 1) if ITCON = 1 (card VP). Contouring information provided only at FOPL intervals if ITCON = 1 and only for OD dates if ITCON = 0 .

216. Vertical profile card (required).

CARD VP - The vertical profile card permits the user to define the total number of days for which observed temperature data are available and the total number of stations (CE-QUAL-W2 grid segments) at which the observations apply.

| <u>Field</u> | <u>Parameter</u> | <u>Value</u> | <u>Description</u> |
|--------------|------------------|--------------|--|
| 0 | AID | VP | character: card identification |
| 1 | NOBDAY | + | integer: <u>Number of OB</u> servati <u>on</u> <u>DAYs</u> in survey data |
| 2 | NOBSTA | + | integer: <u>Number of OB</u> servati <u>on</u> <u>STAtions</u> in survey data |
| 3 | ITCON | 0 | integer: write to TAPE 66 (contours) for every OD date following TBPL |
| | | 1 | integer: write to TAPE 66 (contours) at every FOPL hours beginning at TBPL |

NOTE: TAPE 64 (Vertical Profile) output, controlled by the IVPR on/off switch on the TW card, generally is produced for the purpose of validating CE-QUAL-W2 results by comparing them to observations at specific locations and on specific days.

217. Observation days card (required if NOBDAY > 0).

CARD OD - This card specifies the target days on which vertical temperature profile data are to be written to TAPE 64.

| <u>Field</u> | <u>Parameter</u> | <u>Value</u> | <u>Description</u> |
|--------------|-----------------------|--------------|---|
| 0 | AID | OD | character: card identification, observation days |
| 1-10 | TTP(I), I=1,NOBDAY | + | real: <u>T</u> arget of <u>T</u> imes of <u>P</u> rofiles, ABTM compatible time: year * 1,000 + Julian day of observation. One vertical profile will be written to TAPE 64 for each segment specified on CARD OS and for each date in the TTP array |

NOTE: TAPE 64 write statements are activated by the IVPR switch on CARD TW.

218. Observation stations card (required if NOBDAY > 0).

CARD OS - This card specifies the stations, or segments along the water body, for which vertical profile data are to be written to TAPE 64.

| <u>Field</u> | <u>Parameter</u> | <u>Value</u> | <u>Description</u> |
|--------------|-----------------------|----------------------|---|
| 0 | AID | OS | character: card identification, observation stations |
| 1-10 | ITP(I), I=1,NOBSTA | $1 \leq \text{IMAX}$ | integer: I-segments targeted for observation stations |

219. Segment print selector cards (required). These cards permit the user to select which segment results are to be printed for IFORM = 0 and IFORM = 1. Nine segments may be selected for IFORM = 0 (short form) and 17 segments for IFORM = 1 (long form).

CARD I0

| <u>Field</u> | <u>Parameter</u> | <u>Value</u> | <u>Description</u> |
|--------------|---|-----------------------|--------------------------------|
| 0 | AID | I0 | character: card identification |
| 1-9 | I0(I), I=1,9 or I=1,IMAX if IMAX < 9 | $1 \leq I0 \leq IMAX$ | integer: segment number |

CARD I1

| <u>Field</u> | <u>Parameter</u> | <u>Value</u> | <u>Description</u> |
|--------------|---|-----------------------|--------------------------------|
| 0 | AID | I1 | character: card identification |
| 1-10 | I1(I), I=1,10 or I=1,IMAX if IMAX < 10 | $1 \leq I1 \leq IMAX$ | integer: segment number |

| <u>Field</u> | <u>Parameter</u> | <u>Value</u> | <u>Description</u> |
|--------------|---|-----------------------|--------------------------------|
| 0 | AID | I2 | character: card identification |
| 1-7 | I1(I), I=11,17 or I=11,IMAX if IMAX < 17 | $1 \leq I1 \leq IMAX$ | integer: segment number |

NOTES: If $IMAX < 9$, I0 cards may contain less than nine values and do not have to be filled to complete the card requirements.
 If $IMAX < 10$, I1 cards may contain less than 10 values and do not have to be filled to complete the card requirements.
 If $11 < IMAX < 17$, I2 cards may contain less than seven values and do not have to be filled to complete the card requirements.

220. Initial condition card (required).

CARD IC - This card defines the starting time and the corresponding initial water surface elevation, temperature, and ice thickness.

| <u>Field</u> | <u>Parameter</u> | <u>Value</u> | <u>Description</u> |
|--------------|------------------|--|---|
| 0 | AID | IC | character: card identification, <u>I</u> nitial <u>C</u> onditions |
| 1 | IRSR | 0 | <u>I</u> nteger: <u>R</u> e <u>S</u> tart <u>R</u> ead switch off, no restart conditions read |
| | | 1 | <u>I</u> nteger: <u>R</u> e <u>S</u> tart <u>R</u> ead switch on, restart conditions from previous simulation read from TAPE 59 |
| 2 | ABTM | 1. < ABTM ≤ (Year * 1,000.) + 366. | real: <u>A</u> bsolute <u>T</u> ime, simulation starting time, 1,000. * Year + Julian day + hours/24 |
| 3 | EL | -,0,+ | real: initial water surface <u>E</u> levation, m (must be compatible with DTM; referenced to mean sea level) |
| 4 | TI | -1. | real: vertical profile of temperature read from <u>T</u> I cards which follow BA cards |
| | | 0. ≤ TI ≤ 100 | real: initial temperature, °C |
| 5 | RIIT | 0,+ | Real: <u>I</u> nitial <u>I</u> ce <u>T</u> hickness, m (not required if ICE = 0 (MP card)) |

NOTE: For the case of externally given, right-hand boundary elevation (ZR) for the primary branch (main stem), KT and ZI are computed by the code and the values entered on the IC card are not used and may be omitted.

221. Constituent definition card (required).

CARD CD - This card specifies the number of water quality constituents to be simulated and also permits these transport computations to be turned off for a particular simulation.

| <u>Field</u> | <u>Parameter</u> | <u>Value</u> | <u>Description</u> |
|--------------|------------------|--------------|---|
| 0 | AID | CD | character: card identification, <u>Constituent Definition</u> |
| 1 | NC | | integer: <u>Number of Constituents</u> to be simulated. Note: if NC > 0, <u>CONSTITUENT INITIAL CONCENTRATION CARD</u> is required. |
| 2 | ICC | 0 | <u>Integer: Constituent transport Computations suppressed</u> |
| | | 1 | <u>Integer: Constituent Transport Computations performed</u> |

NOTE: The user generally will complete a hydrodynamic and temperature simulation to his satisfaction (ICC = 0) before going on to the water quality constituent computations (ICC = 1).

222. Constituent write cards (required).

CARD CW - These cards permit the user to select which constituents are to be printed to files for contouring and vertical profiles if IVPR = 1 and/or ITCON = 1 on the TW card, with the exception of temperature and density which are designated by IWRITE(3) and IWRITE(4) on the SN card.

| <u>Field</u> | <u>Parameter</u> | <u>Value</u> | <u>Description</u> |
|--------------|----------------------|--------------|--|
| 1-10 | ICTRIP(J) J=1, NC | 0 | Constituent J WRITE to TAPES 64 and 66 off |
| | | 1 | Constituent J WRITE to TAPES 64 and 66 on |

NOTES: An ICTRIP designation is required for all constituents simulated.

223. ITRIP card for constituents (required if constituents simulated).

CARD IT - These cards, along with the number of constituents (NC) parameter of the CD card, set the constituent field. An ITRIP designation is required for all constituents simulated from 1 to NC and indicates if particular constituents are to be included in simulations.

| <u>Field</u> | <u>Parameter</u> | <u>Value</u> | <u>Description</u> |
|--------------|---------------------|--------------|---|
| 0 | AID | IT | character: card identifier |
| 1-10 | ITRIP(J) J=1, NC | 0 | integer: constituent J is not included in simulations |
| | | 1 | integer: constituent J is to be included in simulations |

NOTES: For example, to simulate only coliform bacteria (constituent number 3), NC could be set equal to 3, ITRIP(1) and ITRIP(2) set equal to 0, and ITRIP(3) set equal to 1. Constituents should be removed from the field only after detailed consideration of the possible impacts of that removal upon other constituents and their interactions.

224. Constituent update card (required).

CARD UD - This card indicates the frequency at which temperature rate multipliers and/or internal sources and sinks for constituents are updated.

| <u>Field</u> | <u>Parameter</u> | <u>Value</u> | <u>Description</u> |
|--------------|------------------|--------------|---|
| 0 | AID | UD | character: card identifier |
| 1 | NUPDC | + | integer: <u>N</u> umber of iterations between <u>UPD</u> ating <u>C</u> onstituent internal sources and sinks |
| 2 | NUPDRT | + | integer: <u>N</u> umber of iterations between <u>UPD</u> ating <u>R</u> ate multipliers for <u>T</u> emperature |

NOTES: The constituent internal sources and sinks are defined by the array CSS, while the temperature rate multipliers are defined in the arrays RTMLT1 and RTMLT2. Caution must be exercised in selection of the update intervals. However, the discretionary use of update intervals does allow a savings in computation time.

225. Constituent initial concentration card (optional: required if NC > 0).

CARD CC - These cards contain the initial concentration for each of the NC constituents specified on CARD CD.

| <u>Field</u> | <u>Parameter</u> | <u>Value</u> | <u>Description</u> |
|--------------|--------------------|--------------|--|
| 0 | AID | CC | character: card identification, <u>Con-</u> <u>stituent Concentration</u> |
| 1 | CI(JC), JC=1,NC | -1. | real: vertical profile of constituents read from CI cards which follow TI and SI cards |
| | | CI(JC) ≥ 0. | real: initial concentrations for each of NC constituents |

NOTE: A CC card is required for each constituent (JC ≤ NC) if
ITRIP(JC) = 1 .

226. Meteorological parameter card (required).

CARD MP - This card specifies whether evaporation is included in the water budget computations.

| <u>Field</u> | <u>Parameter</u> | <u>Value</u> | <u>Description</u> |
|--------------|------------------|--------------|--|
| 0 | AID | MP | character: card identification, meteorological parameter |
| 1 | IEVAP | 0 | <u>I</u> nteger: <u>E</u> VAPoration rates not computed and not included in water budget computations |
| | | 1 | <u>I</u> nteger: <u>E</u> VAPoration rates computed and included in water budget computations |
| 2 | ICE | 0 | <u>I</u> nteger: <u>I</u> CE computations not performed |
| | | 1 | <u>I</u> nteger: <u>I</u> CE computations performed |
| 3 | IPRECP | 0 | <u>I</u> nteger: <u>P</u> RECIpitation not included in heat and water budgets |
| | | 1 | <u>I</u> nteger: <u>P</u> RECIpitation included in heat and water budgets; values for amount of precipitation, temperature, and constituent concentrations must be specified in TVDS |

NOTE: Evaporation rates are sometimes given in the inflow record as $QIN_{net} = QIN - QET$. This is the case for which IEVAP should be set to zero. The contribution of evaporation to surface heat exchange is always considered, regardless of the value of IEVAP.

227. Outlet card (required).

CARD OU - This card specifies the number of reservoir outlets.

At least one outlet is required.

| <u>Field</u> | <u>Parameter</u> | <u>Value</u> | <u>Description</u> |
|--------------|------------------|------------------------------|--|
| 0 | AID | Ou | character: card identification, <u>OUTlets</u> |
| 1 | NOUT | $1 \leq \text{NOUT} \leq 10$ | integer: <u>Number of OUTlets</u> located at right grid boundary |

NOTES: For each outlet specified, a flow needs to be supplied by the subroutine TVDS. At least one outlet is required, although its flow may be set to zero.

A single outlet spanning a number of layers may be specified by breaking the single outlet into several and dividing the outflow among them.

228. Outlet segment location card (required).

CARD OJ - This card specifies the branch number for each outlet from the reservoir.

| <u>Field</u> | <u>Parameter</u> | <u>Value</u> | <u>Description</u> |
|--------------|-----------------------|-------------------------------|--|
| 0 | AID | OJ | character: card identification, outlet branch |
| 1-10 | JBOUT(J), J=1,NOUT | $1 \leq \text{JBOUT} \leq 10$ | integer: <u>J</u> -Branch number in which <u>OUTlet</u> is located |

NOTES: The outlet specified for a particular branch is always placed at cell IR, KOUT. Outlets are permitted only for the downstream flow type of boundary condition (IES = 0).

229. Outlet layer location card (required).

CARD OK - This card specifies the vertical location of outlets from the reservoir.

| <u>Field</u> | <u>Parameter</u> | <u>Value</u> | <u>Description</u> |
|--------------|---------------------|-----------------------|---|
| 0 | AID | OK | character: card identification, <u>K</u> -layer location of <u>O</u> utlets |
| 1-10 | KOUT(J), J=1,NOU | $1 \leq KOUT \leq 10$ | integer: <u>K</u> -layer number of <u>O</u> utlets |

NOTE: If $KOUT(J) < KT$ at any particular time, the associated $QOUT(J)$ is not considered in the water or heat budget computations.

230. Tributary card (required).

CARD TR - This card specifies the number of reservoir tributaries.

| <u>Field</u> | <u>Parameter</u> | <u>Value</u> | <u>Description</u> |
|--------------|------------------|-------------------------------|---|
| 0 | AID | TR | character: card identification, <u>TR</u> ibutaries |
| 1 | NTRIB | $0 \leq \text{NTRIB} \leq 10$ | integer: Number of reservoir <u>TR</u> IBu- taries; if <u>N</u> TRIB > 0, the following card, <u>TR</u> IBUTARY LOCATION CARD, is required |
| 2 | IDSTRB | 0 | <u>I</u> nteger: <u>D</u> i <u>S</u> tributed <u>TR</u> i <u>B</u> utaries option not used |
| | | 1 | <u>I</u> nteger: <u>D</u> i <u>S</u> tributed <u>TR</u> i <u>B</u> utaries option used; variables <u>O</u> DSTRB , <u>T</u> DSTRB , and <u>C</u> DSTRB supplied for each branch by TVDS; this flow is distributed among the segments in each branch proportional to their surface areas; the distributed tributary option may be used to handle unged tributaries to complete the water budget |

NOTE: For each tributary, inflow temperatures and constituent concentrations need to be supplied by subroutine TVDS.

231. Tributary location card (required if NTRIB > 0).

CARD TL - This card gives the reservoir segment numbers at which tributary inflows enter and is required if NTRIB > 0.

| <u>Field</u> | <u>Parameter</u> | <u>Value</u> | <u>Description</u> |
|--------------|-----------------------|---|--|
| 0 | AID | TL | character: card identification, <u>T</u> ributary <u>L</u> ocations |
| 1 | ITRIB(J) J=1,NTRIB | $2 \leq \text{ITRIB}(J) \leq \text{IMAX}-1$ | integer: <u>I</u> -segment number at which each <u>T</u> ributary enters |

NOTE: Tributary flows are entered in the segment specified here and at a layer that corresponds to their density, which is computed by CE-QUAL-W2 and is shown on the output as KTRIB . Tributaries above the current upstream boundary segment (ILC) on any particular time step are combined with the upstream inflow.

232. Withdrawal card (required).

CARD WD - This card specifies the number of withdrawals from the reservoir.

| <u>Field</u> | <u>Parameter</u> | <u>Value</u> | <u>Description</u> |
|--------------|------------------|-----------------------------|---|
| 0 | AID | WD | character: card identification, <u>With-Drawals</u> |
| 1 | NWD | $0 \leq \text{NWD} \leq 10$ | integer: <u>Number of reservoir With-Drawals</u> ; if $\text{NWD} > 0$, the following cards, WI and WK, are required |

NOTE: For each withdrawal, an outflow rate needs to be supplied by subroutine TVDS.

233. Withdrawal segment card (required if NWD > 0).

CARD WI - This card specifies the longitudinal location (segment) for each withdrawal and is required if NWD > 0.

| <u>Field</u> | <u>Parameter</u> | <u>Value</u> | <u>Description</u> |
|--------------|--------------------|---|---|
| 0 | AID | WI | character: card identification, <u>Withdrawal I</u> -segment |
| 1-10 | IWD(J), J=1,NWD | $2 \leq \text{IWD}(J),$ $\leq \text{IMAX}-1$ | integer: <u>I</u> -segment number for each NWD <u>WithDrawals</u> |

NOTE: The layer number for each withdrawal is specified on the WK card, which follows.

234. Withdrawal layer card (required if NWD > 0).

CARD WK - This card specifies the vertical location (layer) for each withdrawal and is required if NWD > 0.

| <u>Field</u> | <u>Parameter</u> | <u>Value</u> | <u>Description</u> |
|--------------|--------------------|---|---|
| 0 | AID | WK | character: card identification, <u>With</u> - <u>drawal</u> <u>K</u> -layer |
| 1-10 | KWD(J), J=1,NWD | $2 \leq \text{KWD}(J),$ $\leq \text{KMAX}-1$ | integer: <u>K</u> -layer number for each of NWD <u>With</u> <u>Drawals</u> |

NOTES: The segment number for each withdrawal is specified on the preceding card. Each individual withdrawal must have its segment and layer specified in the same field on the WI and WK cards, respectively.

A single withdrawal spanning a number of layers may be specified by breaking it into several. Withdrawals above the current upstream boundary segment (IL) or above the current water surface layer (KT) are ignored.

235. Bathymetry cards (required).

CARDS BA - These cards contain the cell widths for each of the $IMAX * KMAX$ cells, which are taken from cross-section drawings and represent an average value for each cell.

| <u>Field</u> | <u>Parameter</u> | <u>Value</u> | <u>Description</u> |
|--------------|-----------------------------------|------------------|--|
| 0 | AID | BA | character: card identification, <u>B</u> athymetry |
| 1-10 | (B(I,K), K=1,KMAX I=1,IMAX) | $B(I,K) \geq 0.$ | real: cell widths, m (left to right and top to bottom, filling each BA card) |

NOTES: For the grid boundary segments ($I = 1$ and $I = IMAX$) and boundary layers ($K = 1$ and $K = KMAX$), B must be set to zero; inactive cells also are identified by setting their widths to zero.

The read statement for these cards is:

```
READ(5,1070) ((B(I,K),K=1,KMAX),I=1,IMAX)
```


236. Initial temperature cards.

CARDS TI - These cards specify the initial temperature field and are required if the TI parameter on the IC card is -1.

| <u>Field</u> | <u>Parameter</u> | <u>Value</u> | <u>Description</u> |
|--------------|---------------------|-----------------------------------|---|
| 0 | AID | TI | character: card identification |
| 1-10 | TIVP(K) K=1,KMAX | $0. \leq \text{TIVP(K)} \leq 40.$ | real: initial temperature vertical profile |

NOTE: The values specified here yield an initial temperature field that is vertically stratified but longitudinally homogeneous over the entire grid.

237. Initial constituent concentration cards.

CARDS CI - These cards specify the initial constituent concentration field and are required for each constituent JC if the CI parameter on the IC card is -1, and $ITRIP(JC) = 1$.

| <u>Field</u> | <u>Parameter</u> | <u>Value</u> | <u>Description</u> |
|--------------|------------------------------------|----------------------------------|--|
| 0 | AID | CI | character: card identification |
| 1-10 | CIVP(K,JC), JC=1,NC K=1,KMAX | $0. \leq CIVP(JC,K) \leq 1,000.$ | real: initial constituent concentration vertical profile |

NOTE: The values specified here yield an initial constituent concentration field for each constituent, one at a time, that is vertically stratified but longitudinally homogeneous.

238. Constituent rate and parameters cards. Descriptions for each of the constituent parameter card images used as input to CE-QUAL-W2 are presented on the following pages. These card images differ in several respects from the format of the previous cards. First, the arrangement of data fields differs, as is shown below. Secondly, all cards are arranged in an alphanumeric order, beginning with the letter R and ending with a letter indicating the location of the card in the card sequence, RA, RB, RC, etc. All cards are required if $NC \geq 12$; only RA is required if $2 \leq NC \leq 4$; and no cards are required if $NC < 2$. However, all rate cards may be appended to the deck. There are three data types, as in previous cards: character, real (may be left or right justified), and integer (must be right justified). There are 10 data fields per card:

| <u>Field</u> | <u>Length</u> | <u>Columns</u> |
|--------------|---------------|----------------|
| 0 | 2 | 1-2 |
| 1 | 8 | 3-10 |
| 2 | 8 | 11-18 |
| 3 | 8 | 19-26 |
| 4 | 8 | 27-34 |
| 5 | 8 | 35-42 |
| 6 | 8 | 43-50 |
| 7 | 8 | 51-58 |
| 8 | 8 | 59-66 |
| 9 | 8 | 67-74 |

NOTE: All rate terms on the following cards are in base and referenced to 20° C.

CARD RA

| <u>Field</u> | <u>Parameter</u> | <u>Value</u> | <u>Description</u> |
|--------------|------------------|--------------|---|
| 0 | AID | RA | character: card identification |
| 1 | Q10COL | + | real: Q10 coefficient for coliform bacteria |
| 2 | TCOLDK | + | real: coliform bacteria mortality rate, day ⁻¹ |
| 3 | TSSETL | + | real: inorganic suspended solids settling rate, m day ⁻¹ |

CARD RB

| <u>Field</u> | <u>Parameter</u> | <u>Value</u> | <u>Description</u> |
|--------------|------------------|--------------|--|
| 0 | AID | RB | character: card identification |
| 1 | DMO2 | + | real: air/water interface molecular diffusion coefficient for dissolved oxygen, $m^2 \text{ sec}^{-1}$ |
| 2 | DMCO2 | + | real: air/water interface molecular diffusion coefficient for carbon dioxide, $m^2 \text{ sec}^{-1}$ |

CARD RC

| <u>Field</u> | <u>Parameter</u> | <u>Value</u> | <u>Description</u> |
|--------------|------------------|--------------|--|
| 0 | AID | RC | character: card identification |
| 1 | EXCO | + | real: attenuation coefficient for solar radiation exclusive of suspended solids effects, m^{-1} |
| 2 | EXTINS | + | real: self-shading coefficient due to inorganic suspended solids, $m^3 m^{-1} g^{-1}$ |
| 3 | EXTINP | + | real: self-shading coefficient due to organic suspended solids (algae + detritus) $m^3 m^{-1} g^{-1}$ |
| 4 | ALDIGO | + | real: fraction of algal biomass lost by mortality to the detritus compartment; the remainder goes to labile organic matter |

CARD RD

| <u>Field</u> | <u>Parameter</u> | <u>Value</u> | <u>Description</u> |
|--------------|------------------|--------------|--|
| 0 | AID | RD | character: card identifier |
| 1 | TPMAX(1) | + | real: algal maximum growth rate, day^{-1} |
| 2 | TSETL(1) | + | real: algal settling rate, day^{-1} |
| 3 | PS2P04(1) | + | real: algal half-saturation coefficient for phosphorus, $g m^{-3}$ |
| 4 | PS2N(1) | + | real: algal half-saturation coefficient for nitrogen, $g m^{-3}$ |

CARD RE

| <u>Field</u> | <u>Parameter</u> | <u>Value</u> | <u>Description</u> |
|--------------|------------------|--------------|---|
| 0 | AID | RE | character: card identifier |
| 1 | PISAT(1) | + | real: algal light saturation intensity at maximum photosynthetic rate, $W m^{-2}$ |
| 2 | TPEXCR(1) | + | real: algal maximum excretion or photo-respiration rate, day^{-1} |
| 3 | TPMORT(1) | + | real: algal mortality rate, day^{-1} |
| 4 | TPRESP(1) | + | real: algal dark respiration rate, day^{-1} |

CARD RF

| <u>Field</u> | <u>Parameter</u> | <u>Value</u> | <u>Description</u> |
|--------------|------------------|--------------|---|
| 0 | AID | RF | character: card identifier |
| 1 | ALG1T1 | + | real: lower temperature bound for algal growth, $^{\circ}C$ |
| 2 | ALG1T2 | + | real: lower temperature bound for maximum algal growth, $^{\circ}C$ |
| 3 | ALG1T3 | + | real: upper temperature bound for maximum algal growth, $^{\circ}C$ |
| 4 | ALG1T4 | + | real: upper temperature bound for algal growth, $^{\circ}C$ |

CARD RG

| <u>Field</u> | <u>Parameter</u> | <u>Value</u> | <u>Description</u> |
|--------------|------------------|--------------|---|
| 0 | AID | RG | character: card identifier |
| 1 | ALG1K1 | + | real: rate multiplier corresponding to ALG1T1 |
| 2 | ALG1K2 | + | real: rate multiplier corresponding to ALG1T2 |
| 3 | ALG1K3 | + | real: rate multiplier corresponding to ALG1T3 |
| 4 | ALG1K4 | + | real: rate multiplier corresponding to ALG1T4 |

CARD RH

| <u>Field</u> | <u>Parameter</u> | <u>Value</u> | <u>Description</u> |
|--------------|------------------|--------------|--|
| 0 | AID | RH | character: card identifier |
| 1 | TDSETL | + | real: detritus settling rate, m day^{-1} |
| 2 | DETT1 | + | real: lower temperature bound for detritus decay, $^{\circ}\text{C}$ |
| 3 | DETT2 | + | real: lower temperature bound for maximum rate of detritus decay, $^{\circ}\text{C}$ |
| 4 | DETK1 | + | real: rate multiplier corresponding to DETT1 |
| 5 | DETK2 | + | real: rate multiplier corresponding to DETT2 |

CARD RI

| <u>Field</u> | <u>Parameter</u> | <u>Value</u> | <u>Description</u> |
|--------------|------------------|--------------|--|
| 0 | AID | RI | character: card identifier |
| 1 | TDOMDK | + | real: maximum labile DOM decay rate, day^{-1} |
| 2 | TNH3DK | + | real: maximum ammonia-nitrogen decay (nitrification) rate, day^{-1} |
| 3 | TNO3DK | + | real: maximum nitrate-nitrogen decay (denitrification) rate, day^{-1} |
| 4 | TDETDK | + | real: maximum detritus decay rate, day^{-1} |

CARD RJ

| <u>Field</u> | <u>Parameter</u> | <u>Value</u> | <u>Description</u> |
|--------------|------------------|--------------|--|
| 0 | AID | RJ | character: card identifier |
| 1 | TRFRDK | + | real: maximum refractory DOM decay rate, day^{-1} |
| 2 | TDOMRF | + | real: maximum rate at which labile DOM decomposes to refractory DOM, day^{-1} |
| 3 | DOMCNT | + | real: the fraction of influent DOM that is labile |
| 4 | TSEDDK | + | real: maximum sediment decay rate, day^{-1} |

CARD RK

| <u>Field</u> | <u>Parameter</u> | <u>Value</u> | <u>Description</u> |
|--------------|------------------|--------------|---|
| 0 | AID | RK | character: card identifier |
| 1 | DOMT1 | + | real: lower temperature bound of labile DOM decay, °C |
| 2 | DOMT2 | + | real: lower temperature bound of maximum labile DOM decay, °C |
| 3 | DOMK1 | + | real: rate multiplier corresponding to DOMT1 |
| 4 | DOMK2 | + | real: rate multiplier corresponding to DOMT2 |

CARD RL

| <u>Field</u> | <u>Parameter</u> | <u>Value</u> | <u>Description</u> |
|--------------|------------------|--------------|---|
| 0 | AID | RL | character: card identifier |
| 1 | NH3T1 | + | real: lower temperature bound of ammonia-nitrogen decay (nitrification), °C |
| 2 | NH3T2 | + | real: lower temperature bound of maximum ammonia-nitrogen decay, °C |
| 3 | NH3K1 | + | real: rate multiplier corresponding to NH3T1 |
| 4 | NH3K2 | + | real: rate multiplier corresponding to NH3T2 |

CARD RM

| <u>Field</u> | <u>Parameter</u> | <u>Value</u> | <u>Description</u> |
|--------------|------------------|--------------|---|
| 0 | AID | RM | character: card identifier |
| 1 | NO3T1 | + | real: lower temperature bound of nitrate-nitrogen decay (denitrification), °C |
| 2 | NO3T2 | + | real: lower temperature bound of maximum nitrate-nitrogen decay, °C |
| 3 | NO3K1 | + | real: rate multiplier corresponding to NO3T1 |
| 4 | NO3K2 | + | real: rate multiplier corresponding to NO3T2 |

CARD RN

| <u>Field</u> | <u>Parameter</u> | <u>Value</u> | <u>Description</u> |
|--------------|------------------|--------------|--|
| 0 | AID | RN | character: card identifier |
| 1 | ADSRBP | + | real: adsorption coefficient for phosphorus, $m^3 g^{-1}$ |
| 2 | ADSRBN | + | real: adsorption coefficient for ammonia-nitrogen, $m^3 g^{-1}$ |
| 3 | ADMAXP | + | real: maximum mass of phosphate absorbed per mass of solids |
| 4 | ADMAXN | + | real: maximum mass of ammonia-nitrogen absorbed per mass of solids |

CARD RO

| <u>Field</u> | <u>Parameter</u> | <u>Value</u> | <u>Description</u> |
|--------------|------------------|--------------|--|
| 0 | AID | RO | character: card identifier |
| 1 | O2NH3 | + | real: oxygen stoichiometric equivalent for ammonia-nitrogen decay |
| 2 | O2DET | + | real: oxygen stoichiometric equivalent for detritus decay |
| 3 | O2RESP | + | real: oxygen stoichiometric equivalent for dark respiration |
| 4 | O2FAC | + | real: oxygen stoichiometric equivalent for algal growth |
| 5 | O2DOM | + | real: oxygen stoichiometric equivalent for labile DOM decay |
| 6 | OXYLIM | + | real: lower dissolved oxygen limit for aerobic processes and upper limit for anaerobic processes |

CARD RP

| <u>Field</u> | <u>Parameter</u> | <u>Value</u> | <u>Description</u> |
|--------------|------------------|--------------|--|
| 0 | AID | RP | character: card identifier |
| 1 | TXP4RE | + | real: zero-order sediment anaerobic release rate of phosphorus, as a fraction of SOD |
| 2 | XP04T1 | + | real: lower temperature bound for sediment phosphorus release, °C |

(Continued)

| <u>Field</u> | <u>Parameter</u> | <u>Value</u> | <u>Description</u> |
|--------------|------------------|--------------|---|
| 3 | XP04T2 | + | real: lower temperature bound for maximum release, °C |
| 4 | XP04T3 | + | real: upper temperature bound for maximum release, °C |
| 5 | XP04T4 | + | real: upper temperature bound for anaerobic sediment phosphorus release, °C |

CARD RQ

| <u>Field</u> | <u>Parameter</u> | <u>Value</u> | <u>Description</u> |
|--------------|------------------|--------------|---|
| 0 | AID | RQ | character: card identifier |
| 1 | XP04K1 | + | real: rate multiplier corresponding to XP04T1 |
| 2 | XP04K2 | + | real: rate multiplier corresponding to XP04T2 |
| 3 | XP04K3 | + | real: rate multiplier corresponding to XP04T3 |
| 4 | XP04K4 | + | real: rate multiplier corresponding to XP04T4 |

CARD RR

| <u>Field</u> | <u>Parameter</u> | <u>Value</u> | <u>Description</u> |
|--------------|------------------|--------------|---|
| 0 | AID | RR | character: card identifier |
| 1 | TCNREL | + | real: zero-order sediment anaerobic release rate for ammonia-nitrogen, as a fraction of SOD |
| 2 | CNT1 | + | real: lower temperature bound for sediment ammonia-nitrogen release, °C |
| 3 | CNT2 | + | real: lower temperature bound for maximum release, °C |
| 4 | CNT3 | + | real: upper temperature bound for maximum release, °C |
| 5 | CNT4 | + | real: upper temperature bound for anaerobic sediment ammonia-nitrogen release, °C |

CARD RS

| <u>Field</u> | <u>Parameter</u> | <u>Value</u> | <u>Description</u> |
|--------------|------------------|--------------|---|
| 0 | AID | RS | character: card identifier |
| 1 | CNK1 | + | real: rate multiplier corresponding to CNT1 |
| 2 | CNK2 | + | real: rate multiplier corresponding to CNT2 |
| 3 | CNK3 | + | real: rate multiplier corresponding to CNT3 |
| 4 | CNK4 | + | real: rate multiplier corresponding to CNT4 |

CARD RT

| <u>Field</u> | <u>Parameter</u> | <u>Value</u> | <u>Description</u> |
|--------------|---------------------|--------------|---|
| 0 | AID | RT | character: card identifier |
| 1 | NSOD | + | integer: number of TSOD, ISOD pairs used in mapping sediment oxygen demand |
| 2 | TSOD(1) | + | real: zero-order sediment oxygen demand for segments 2 to ISOD(1), $g\ m^{-2}\ day^{-1}$ |
| 3 | ISOD(1) | + | integer: uppermost segment to which TSOD1 applies |
| 4-9 | TSOD(J) | + | real: sediment oxygen demand for segments I, where $ISOD(J-1) < I \leq ISOD(J)$, $g\ m^{-2}\ day^{-1}$ |
| | ISOD(J) J=2,NSOD | + | integer: uppermost segments to which TSOD(J) applies |

NOTE: if NSOD > 4, the TSOD, ISOD pairs may be continued on additional RT cards beginning in Field 1.

CARD RU

| <u>Field</u> | <u>Parameter</u> | <u>Value</u> | <u>Description</u> |
|--------------|------------------|--------------|--|
| 0 | AID | RU | character: card identifier |
| 1 | SODT1 | + | real: lower temperature bound for sediment oxygen demand, °C |
| 2 | SODT2 | + | real: lower temperature bound for maximum oxygen demand, °C |

(Continued)

| <u>Field</u> | <u>Parameter</u> | <u>Value</u> | <u>Description</u> |
|--------------|------------------|--------------|--|
| 3 | SODT3 | + | real: upper temperature bound for maximum oxygen demand, °C |
| 4 | SODT4 | + | real: upper temperature bound for sediment oxygen demand, °C |

CARD RV

| <u>Field</u> | <u>Parameter</u> | <u>Value</u> | <u>Description</u> |
|--------------|------------------|--------------|--|
| 0 | AID | RV | character: card identifier |
| 1 | SODK1 | + | real: rate multiplier corresponding to SODT1 |
| 2 | SODK2 | + | real: rate multiplier corresponding to SODT2 |
| 3 | SODK3 | + | real: rate multiplier corresponding to SODT3 |
| 4 | SODK4 | + | real: rate multiplier corresponding to SODT4 |
| 5 | SFCO2 | + | real: carbon dioxide production from sediments expressed as a fraction of sediment oxygen demand |

CARD RW

| <u>Field</u> | <u>Parameter</u> | <u>Value</u> | <u>Description</u> |
|--------------|------------------|--------------|--|
| 0 | AID | RW | character: card identifier |
| 1 | BIOP | + | real: stoichiometric equivalent for phosphorus |
| 2 | BIOC | + | real: stoichiometric equivalent for carbon |
| 3 | BION | + | real: stoichiometric equivalent for nitrogen |

NOTES: These stoichiometric equivalents are used for all process transfers, such as phosphate production due to labile DOM decay, detritus decay, etc.

CARD RX

| <u>Field</u> | <u>Parameter</u> | <u>Value</u> | <u>Description</u> |
|--------------|------------------|--------------|--|
| 0 | AID | RX | character: card identifier |
| 1 | TFESET | + | real: total iron settling velocity, m day ⁻¹ |
| 2 | TFEREL | + | real: total iron anoxic sediment release rate, as a fraction of SOD |
| 3 | FEFACT | + | real: adsorption increment for total iron |

Summary of CE-QUAL-W2 input deck

T1
T2
T3
T4
GE IMAX KMAX HIN(1,1) DTM NB IWT
BG IBC(1,JB) IBC(3,JB) ILS(JB) IES(JB) DLX(JB) PHIO(JB) [JB=1,NB]
WP AX DXI DXS CHZY BETA GAMMA
TM NP
DN DLT(J) NIT(J,1) EW(J,JB) [J=1,NP; JB=1,NB]
SN INFORM TBPR FOPR IWRITE(J) [J=1,6]
TW IDIAG IRSW ITSR IVPR ICIRC ICNTR TBPL FOPL TBTS FOTS
VP NOBDAY NOBSTA ITCON
OD TTP(J) [J=1, NOBDAY]
OS ITP(J) [J=1,NOBSTA]
IO IO(J) [J=1,9]
I1 I1(J) [J=1,10]
I2 I2(J) [J=11,17]
IC IRSR ABTM EL TI RIIT
CD NC ICC
CW ICTRIP(JC) [JC=1,NC]
IT ITRIP(JC) [JC=1,NC]
UD NUPDC NUPDRT
CC CI(JC) [JC=1,NC]
MP IEVAP ICE IPRECP
OU NOUT
OJ JBOUT(J) [J=1,NOUT]
OK KOUT(J) [J=1,NOUT]
TR NTRIB IDSTRB
TL ITRIB(J) J=1,NTRIB
WD NWD
WI IWD(J) J=1,NWD
WK KWD(J) J=1,NWD

(Continued)

Summary of CE-QUAL-W2 input deck (Continued)

| | | | | | |
|----|------------|------------------------------|-----------|-----------|--------------|
| BA | B(I,K) | [(K=1,KMAX), I=1,IMAX] | | | |
| TI | TIVP(K) | [K=1,KMAX] | | | |
| CI | CIVP(K,JC) | [(K=1,KMAX), JC=1,NC] | | | |
| RA | Q10COL | TCOLDK | TSSETL | | |
| RB | DMO2 | DMCO2 | | | |
| RC | EXCO | EXTINS | EXTINP | ALDIGO | |
| RD | TPMAX(1) | TSETL(1) | PS2P04(1) | PS2N(1) | |
| RE | PISAT(1) | TPEXCR(1) | TPMORT(1) | TPRESP(1) | |
| RF | ALGIT1 | ALGIT2 | ALGIT3 | ALGIT4 | |
| RG | ALG1K1 | ALG1K2 | ALG1K3 | ALG1K4 | |
| RH | TDSETL | DETT1 | DETT2 | DETK1 | DETK2 |
| RI | TDOMDK | TNH3DK | TN03DK | TDETDK | |
| RJ | TRFRDK | TDOMRF | DOMCNT | TSEDDK | |
| RK | DOMT1 | DOMT2 | DOMK1 | DOMK2 | |
| RL | NH3T1 | NH3T2 | NH3K1 | NH3K2 | |
| RM | N03T1 | N03T2 | N03K1 | N03K2 | |
| RN | ADSRBP | ADSRBN | ADMAXP | ADMAXN | |
| RO | O2NH3 | O2DET | O2RESP | O2FAC | O2DOM OXYLIM |
| RP | TXP4RE | XP04T1 | XP04T2 | XP04T3 | XP04T4 |
| RQ | XP04K1 | XP04K2 | XP04K3 | XP04K4 | |
| RR | TCNREL | CNT1 | CNT2 | CNT3 | CNT4 |
| RS | CNK1 | CNK2 | CNK3 | CNK4 | |
| RT | NSOD | [TSOD(I), ISOD(I), I=1,NOSD] | | | |
| RU | SODT1 | SODT2 | SODT3 | SODT4 | |
| RV | SODK1 | SODK2 | SODK3 | SODK4 | SFCO2 |
| RW | BIOP | BIOC | BION | | |
| RX | TFESET | TFEREL | FEFACT | | |

Coefficients for use in CE-QUAL-W2

239. The following section is intended to provide general guidelines for the constituents and parameters required by CE-QUAL-W2. Many of the water quality coefficients were extracted from the revised CE-QUAL-R1 user's manual (Environmental Laboratory 1985). These coefficients provide only general guidelines for ranges of values found in

the literature. The specific coefficient values used in a particular application are expected to vary with site-specific characteristics. The coefficients are arranged according to the card images described in the preceding section. All coefficients used in CE-QUAL-W2 are in base e and referenced to 20° C.

240. CARD WP.

AX - the horizontal dispersion coefficient for momentum ($m^2 \text{ sec}^{-1}$). This coefficient is dependent upon the space scale for the system. Typical values ranging from 1.0 to 10.0 have been used in previous studies.

DXI - the horizontal dispersion coefficient for heat ($m^2 \text{ sec}^{-1}$). This coefficient is also dependent upon the space scale. Typical values ranging from 1.0 to 10.0 have been used in previous studies.

DXS - the horizontal dispersion coefficient for water quality constituents ($m^2 \text{ sec}^{-1}$). Values near 1.0 have been used in previous studies.

CHZY - the bottom resistance coefficient ($m^{0.5} \text{ sec}^{-1}$). It is space and time invariant. Values near 70.0 have been used in previous studies.

BETA - the fraction of incident solar radiation absorbed at the water surface. In field measurements, it represents the fraction of solar radiation absorbed in a 0.6-m surface layer. It may be obtained from Figure 20 once GAMMA is determined.

GAMMA - the extinction coefficient (m^{-1}) for solar radiation. It can be estimated from Figure 21 if the Secchi disk depth is known, or it can be measured directly with a photometer. This coefficient represents the total extinction coefficient including the effects of dissolved and suspended solids. It is used to determine solar radiation absorption when the first two levels of constituents are not included in simulations. Where they are included, this coefficient is determined from a baseline value (EXCO) incremented by the concentration-dependent effects of inorganic (EXTINS) and organic (EXTINP) solids (card RC). Typical extinction coefficients are provided in Table 4.

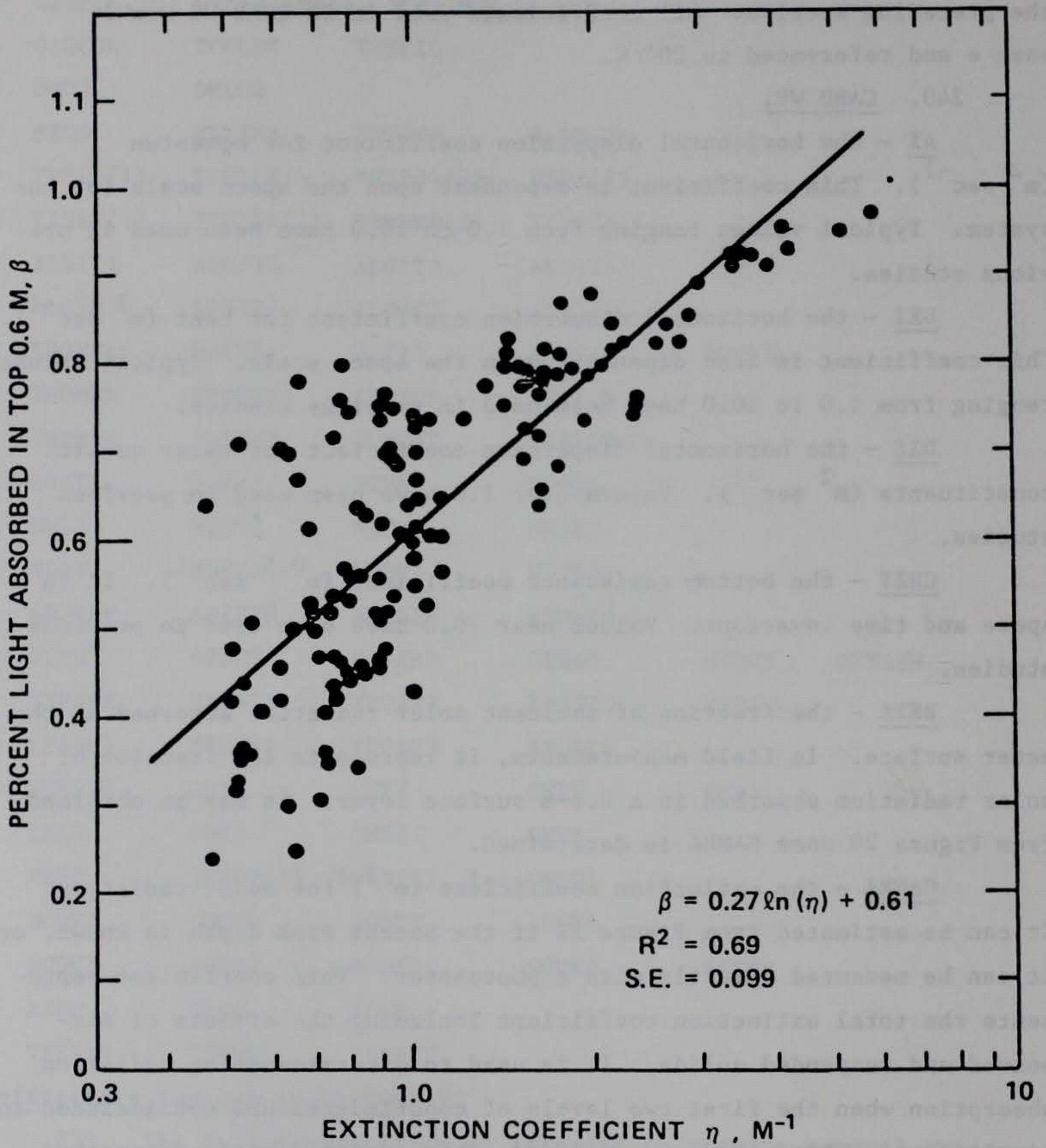


Figure 20. Relationship between the light absorbed in the surface layer and the extinction coefficient

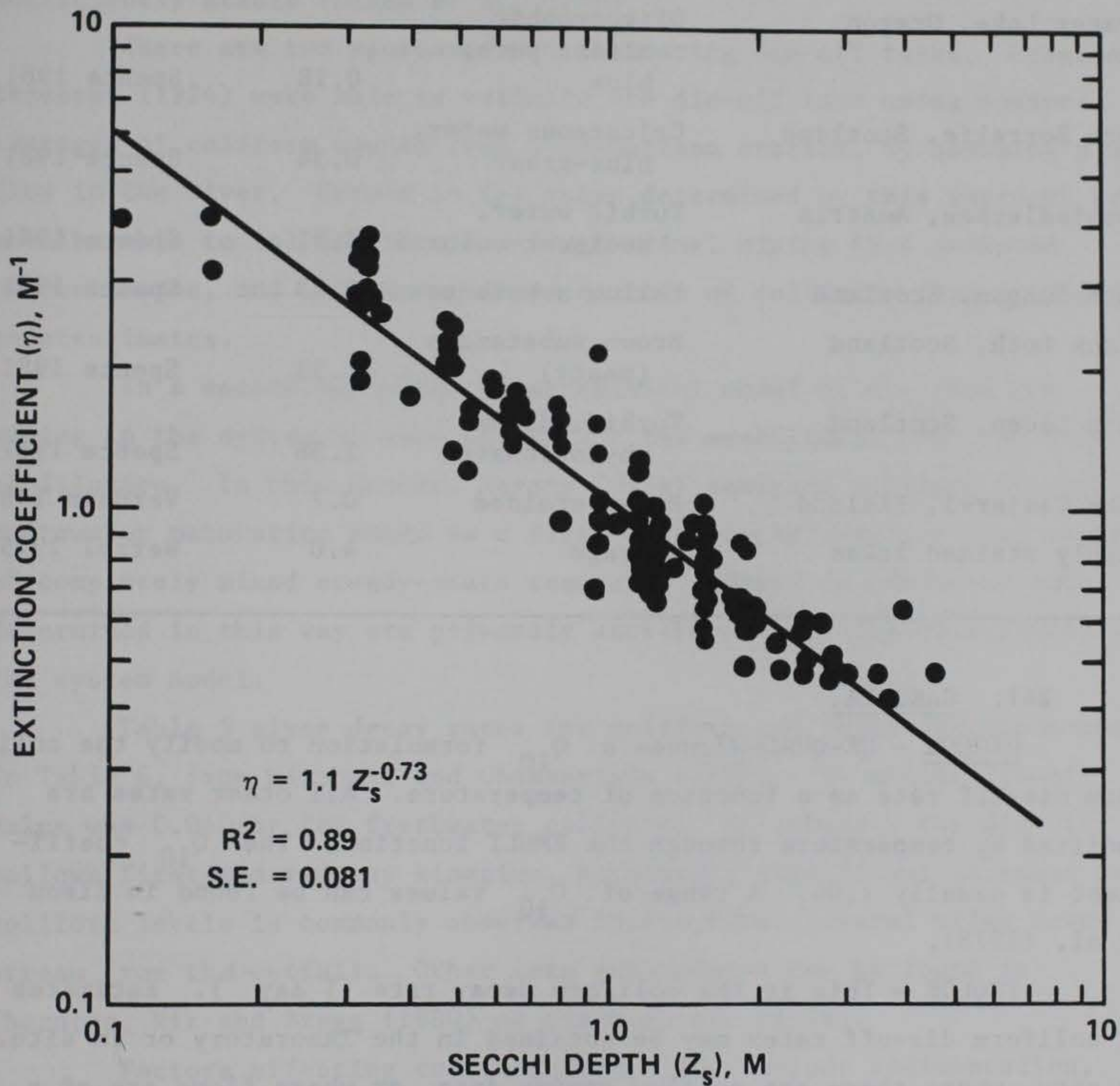


Figure 21. Relationship between the extinction coefficient and the Secchi disk depth (Williams et al. 1980)

Table 4
Extinction Coefficients for Water (1 m^{-1})

| Site | Description | GAMMA | Reference |
|----------------------------|--------------------------------------|-----------|--------------|
| Lake Tahoe, California | Oligotrophic | 0.2 | Wetzel 1975 |
| Wintergreen Lake, Michigan | Eutrophic | 0.46-1.68 | Wetzel 1975 |
| Crystal Lake, Wisconsin | Oligotrophic | 0.2 | Wetzel 1975 |
| Crater Lake, Oregon | Oligotrophic almost pure, blue | 0.18 | Spence 1981 |
| Loch Borrallie, Scotland | Calcareous water, blue-green | 0.34 | Spence 1981 |
| Neusiedlersee, Austria | Turbid water, sediment-colored | 3.31 | Spence 1981 |
| Loch Unagan, Scotland | Yellow substances | 0.93 | Spence 1981 |
| Black Loch, Scotland | Brown substances (peaty) | 1.53 | Spence 1981 |
| Loch Leven, Scotland | Turbid, dense phytoplankton | 2.58 | Spence 1981 |
| Lake Paajarvi, Finland | Brown-stained | 0.7 | Verduin 1982 |
| Highly stained lakes | Average | 4.0 | Wetzel 1975 |

241. CARD RA.

Q10COL - CE-QUAL-W2 uses a Q_{10} formulation to modify the coliform die-off rate as a function of temperature. All other rates are modified by temperature through the RMULT function. The Q_{10} coefficient is usually 1.04. A range of Q_{10} values can be found in Zison et al. (1978).

TCOLDK - This is the coliform decay rate (1 day^{-1}). Estimates of coliform die-off rates may be obtained in the laboratory or in situ. In situ, where there are no flow regime data, or where flows are of a transient nature, a commonly used method is to add a slug of conservative tracer substance (a dye, rate element, or radioisotope) to steady-state discharge. This discharge plume is sampled, dilution is estimated from the concentration of tracer, and the decay rate is estimated from

the dilution-corrected coliform counts. This technique gives misleading results in cases where the tracer is diluted by water heavily contaminated with the same discharge. Since the tracer was introduced as a slug, there is no way to know how many of the surviving coliforms originated in the tracer-dosed effluent and how many came from predosing or postdosing effluent. This problem is reduced where the flow regime is sufficiently stable (Zison et al. 1978).

There are two approaches to estimating die-off rates. Frost and Streeter (1924) were able to estimate the die-off rate using seasonal averages of coliform counts from a downstream station, by assuming plug flow in the river. Errors in the rates determined by this approach are attributable to (a) dilution and longitudinal mixing that produced overestimates, and (b) unconsidered sources of coliforms that produced underestimates.

In a second approach, a mathematical model of the flow and mixing in the system is used to correct the measurements for the effects of dilution. In this manner, Marais (1974) analyzed coliform die-off in wastewater maturation ponds as a first-order decay reaction in a series of completely mixed steady-state reactors. Errors in the decay rates determined in this way are primarily attributable to the reliability of the system model.

Table 5 gives decay rates for coliform and fecal streptococcus. In Table 6, from Mitchell and Chamberlain (1978), the median die-off value was 0.040/hr for freshwater coliform. In general, the die-off follows first-order decay kinetics, although a significant increase in coliform levels is commonly observed in the first several miles downstream from the outfall. Other rate information can be found in Thornton, Nix and Bragg (1980) or Zison et al. (1978).

Factors affecting coliform decay rate include sedimentation, solar radiation, nutrient deficiencies, predation, algae, bacterial toxins, and physiochemical factors.

TSSETL - This is the suspended solids settling velocity (m day^{-1}). The settling rate is dependent on the type of particle, grain size, density temperature, viscosity, and turbulence. Most of the

Table 5

Coliform and Fecal Streptococcus Decay Rates (1 day⁻¹)

| <u>Species</u> | <u>TCOLDK</u> | <u>References</u> |
|--------------------|---------------|---|
| Fecal coliform | 0.048-0.096 | Evans et al. 1968 |
| Fecal streptococci | 0.063 | Evans et al. 1968 |
| Fecal streptococci | 0.004-0.013 | Geldreich et al. 1968 |
| Total coliform | 4.48-5.52 | Kittrell and Furfari 1963 |
| Total coliform | 0.199-0.696 | Klock 1971 |
| Total coliform | 1.99 | Marais 1974 |
| Total coliform | 0.168-1.56 | Geldreich et al. 1968 |
| Total coliform | 0.009-0.028 | Klock 1971 |
| Total coliform | 0.021-0.038 | Evans et al. 1968 |
| Total coliform | 0.045-0.049 | Frost and Streeter 1924 |
| Total coliform | 0.024-0.105 | Hoskins, Ruchhoft, and Williams 1927 |
| Total coliform | 0.48-2.04 | Mitchell and Chamberlain 1978 |

larger particles entering a reservoir settle very quickly and should not be included in the inflow. Lane (1938) gives figures of 0.86 to 860.0 m day⁻¹ for particle diameters of 0.002 to 0.1 mm. Particles found in the main body of a reservoir are usually at the lower end of this scale.

242. CARD RB.

DM02 - the molecular diffusion coefficient for dissolved oxygen across the air/water interface (m² sec⁻¹).

DMC02 - the molecular diffusion coefficient for carbon dioxide across the air/water interface (m² sec⁻¹). The transfer of dissolved oxygen and CO₂ across the air/water interface is determined by an empirical relationship developed by Kanwisher (1963). This relationship requires the molecular diffusivities for O₂ (DM02) and CO₂ (DMC02). Representative values are 0.204 × 10⁻⁹ and 0.204 × 10⁻¹⁰ m² sec⁻¹ at 27° C, respectively. Both values increase with temperature.

243. CARD RC.

EXCO - the extinction coefficient (l m⁻¹) excluding the effects of suspended solids. It can be estimated from Figure 21 if the maximum Secchi depth is known, or it can be measured with a photometer.

Table 6

Freshwater Die-Off Rates of Coliform Bacteria Measured In Situ
(1 day⁻¹) (from Mitchell and Chamberlain 1978)

| Site | Season/ Temperature | Rate | Reference |
|-------------------------------|------------------------|-----------------|--------------------------------------|
| Ohio River | Summer, 20° C | 1.175 | Frost and Streeter 1924 |
| Ohio River | Winter, 5° C | 1.08 | Frost and Streeter 1924 |
| Upper Illinois River | June-Sep. | 2.04 | Hoskins, Ruchhoft, and Williams 1927 |
| Upper Illinois River | Oct.-May | 2.52 | Hoskins, Ruchhoft, and Williams 1927 |
| Upper Illinois River | Dec.-Mar. | 0.567 | Hoskins, Ruchhoft, and Williams 1927 |
| Upper Illinois River | Apr.-Nov. | 1.032 | Hoskins, Ruchhoft, and Williams 1927 |
| Lower Illinois River | June-Sep. | 2.04 | Hoskins, Ruchhoft, and Williams 1927 |
| Lower Illinois River | Oct.-May | 0.888 | Hoskins, Ruchhoft, and Williams 1927 |
| Lower Illinois River | Dec.-Mar | 0.624 | Hoskins, Ruchhoft, and Williams 1927 |
| Lower Illinois River | Apr.-Nov. | 0.696 | Hoskins, Ruchhoft, and Williams 1927 |
| Shallow turbulent stream | Summer | 15.12 | Kittrell and Koschtitzky 1947 |
| Missouri River | Winter | 0.48 | Kittrell and Furfari 1963 |
| Tennessee River (Knoxville) | Summer | 1.03 | Kittrell and Furfari 1963 |
| Tennessee River (Chattanooga) | Summer | 1.32 | Kittrell and Furfari 1963 |
| Sacramento River, Calif. | Summer | 1.752 | Kittrell and Furfari 1963 |
| Cumberland River, Md. | Summer | 5.52 | Kittrell and Furfari 1963 |
| Ground-water stream | 10° C | 0.504 | Wuhrmann 1972 |
| Leaf River, Miss. | N/A | 0.408 | Mahloch 1974 |
| Wastewater lagoon | 7.0-25.5° C | 0.199- 0.696 | Klock 1971 |
| Maturation ponds | N/A | 1.99 | Marais 1974 |
| Maturation ponds | 19° C | 1.68 | Marais 1974 |
| Oxidation ponds | 20° C | 2.59 | Marais 1974 |

However, in situ measurements are likely to overestimate EXCO since they include the effects of particulates, and must be decremented accordingly.

EXTINS - the self-shading coefficient due to particulate inorganic material ($\ell \text{ m}^{-1} \text{ mg}^{-1}$). It should typically be of the same order of magnitude as EXTINP.

EXTINP - the self-shading coefficient due to organic particulate matter in CE-QUAL-W2 ($\ell \text{ m}^{-1} \text{ mg}^{-1}$). The self-shading coefficient represents the decreased light penetration or increased light extinction resulting from phytoplankton and detritus suspended in the water column. The light extinction coefficient is modified as a function of the concentrations of these two constituents. Most measurements of EXTINP refer only to algal biomass; it is assumed in CE-QUAL-W2 that light extinction due to detritus is numerically equivalent to that due to phytoplankton. Megard et al. (1980) and Smith and Baker (1978) determined that each microgram per litre of chlorophyll increased the light extinction coefficient by about 0.022 and 0.016 m^{-1} , respectively. Assuming a ratio of carbon to algal biomass of 0.45 and a carbon/chlorophyll (C/chl) ratio of 50, then algebraically each milligram per litre of algal biomass should increase the light extinction coefficient by about 0.20 to 0.14 m^{-1} , respectively. The range of C/chl ratios, however, varies from 25 to 150, resulting in the range of self-shading coefficients from 0.40 $\ell \text{ m}^{-1} \text{ mg}^{-1}$ to 0.45 $\ell \text{ m}^{-1} \text{ mg}^{-1}$. Values near 0.10 have previously produced reasonable results.

Light extinction by algae is computed from in situ light intensity measurements at depth intervals and in situ determinations of chlorophyll a using the modified Lambert-Bouguer Law (Megard et al. 1980). Bannister (1979) extracted chlorophyll from cell suspensions and measured the absorption spectrum to obtain the mean extinction coefficient. Theoretical estimates of attenuation of photosynthetically active radiation by chlorophyll a in algae range between 0.06 and 0.018, depending on the size and chlorophyll content of cells and colonies (Kirk 1975). The extinction coefficient was determined to range between 0.0066 and 0.0205 $\ell \text{ m}^{-1} \text{ mg}^{-1}$ in laboratory analysis (Bannister 1979).

Values for self-shading coefficients are given Table 7. Values shown in this table have been converted to units used in CE-QUAL-W2 assuming a carbon to chlorophyll ratio of 50 and a carbon to biomass ratio of 0.45.

ALDIGO - the fraction of algal biomass lost by mortality that increments detritus compartment. The remainder of the fraction goes to labile DOM. Otsuki and Hanya (1972) have reported a value of 0.8 for *Scenedesmus* sp.

Algae--general - CE-QUAL-W2 has the capability to simulate a single assemblage of algae. The composition of this group must be determined before any of the required coefficients can be selected.

The first step in selecting the group is to determine the species composition of the reservoir. If the study is of a preimpoundment, then data from surrounding reservoirs with similar land use, morphometry, operation, etc., and local expertise may be helpful. The US Environmental Protection Agency National Eutrophication Survey reports are good references for an initial evaluation since they contain both nutrient information and phytoplankton species enumerations. Attention should be paid to the dominant algal species and the seasonal patterns

Table 7

Self-Shading Coefficients Due to Particulate Matter

($\ell \text{ m}^{-1} \text{ mg}^{-1}$)

| Type | Comment | Value | Reference |
|----------------------------|---|-------|--------------------|
| Suspensoids | Average | 0.12 | Verduin 1982 |
| Suspensoids | Lake Paajarvi Finland | 0.24 | Verduin 1982 |
| Organic matter | Pacific Ocean | 0.047 | Verduin 1982 |
| Phytoplankton | Pacific Ocean | 0.033 | Verduin 1982 |
| Phytoplankton - diatoms | C/chl ratio = 120 dry wt/C ratio = 4 | 0.058 | Verduin 1982 |
| Phytoplankton - diatoms | C/chl ratio = 30 dry wt/C ratio = 4 | 0.014 | Verduin 1982 |
| Phytoplankton - greens | C/chl ratio = 100 dry wt/C ratio = 2 | 0.024 | Verduin 1982 |
| Phytoplankton - greens | C/chl ratio = 30 dry wt/C ratio = 2 | 0.007 | Verduin 1982 |
| Phytoplankton | Shagawa Lake, Minnesota | 0.03 | Megard et al. 1980 |

in phytoplankton succession. Strong seasonal succession patterns may require use of different algal coefficients for different times of the year. In selecting appropriate compartments, specific consideration should be given to:

- a. Study objectives and project purposes.
- b. Problem groups.
- c. Dominant groups.
- d. Environmental requirements (N, P, light).
- e. Similarities in growth response.
- f. Seasonal succession.
- g. Similar morphology
- h. Intradivisional similarity.

Some species will be difficult to incorporate in any assemblage because they exhibit properties that are not simulated by CE-QUAL-W2. *Ceratium* spp., for example, exhibit heterotrophic characteristics, which are not included in the phytoplankton formulations.

244. CARD RD.

TPMAX - the maximum gross photosynthetic or production rate (day^{-1}). CE-QUAL-W2 uses gross production rates to simulate the rate of change of algal biomass through time.

The physiological processes of phytoplankton that are being modeled are gross production and respiration. Gross production is the total rate of photosynthesis, which includes the storage rate of organic matter by the phytoplankton (net production) plus the organic matter used by phytoplankton in respiration. That is,

$$\text{gross production} = \text{net production} + \text{respiration}$$

Net production is the organic matter used for other processes such as sinking, excretion, and mortality. Care must be used in estimating these rates because the rates are often dependent on the experimental design. For example, the maximum growth rate is often used in modeling studies (see, for example, the Preliminary Generalized Computer Program, Water Quality for River-Reservoir Systems, October 1978,

US Army Engineer Hydrologic Engineering Center, Davis, Calif.). The respiration rate is subtracted from the maximum growth rate in order to predict a new mass. However, the values of growth found in the literature are most equivalent to net production in the above equation and have already accounted for respiration; in other words, the model may predict low phytoplankton values because respiration is being accounted for twice. If growth is measured as the difference in mass between two points in time, it must be realized that algae may have been lost to grazing, sinking, etc. Also, the true growth figure may actually be higher than reported. Values are often reported as "production" without mention as to whether the figures represent gross or net production, and the reader may have to evaluate the experimental design to determine the correct value.

There are four general methods used to measure phytoplankton primary productivity (Janik, Taylor, and Lambou 1981). These involve the measurement of (a) changes in the oxygen content of water, (b) changes in the carbon dioxide content of water, (c) incorporation of ^{14}C tracers into the organic matter of phytoplankton, and (d) measures of chlorophyll. Readers should refer to Janik, Taylor, and Lambou (1981) to gain insight into the problems associated with the four methods. For example, the ^{14}C technique gives a measurement that is between net and gross production, depending on the length of the experiment (Whittaker 1975).

The most frequently used method for measuring primary production by phytoplankton has been photosynthetic oxygen evolution and ^{14}C uptake. The light- and dark-bottle ^{14}C technique of Steemann-Nielsen (1952) requires the lowering of pairs of bottles injected with H^{14}CO_3 to fixed depths in the water column for time periods of 1 to 5 hr or the incubation of the bottles under known conditions of light and temperature.

Under optimal conditions, a culture grows so that the rate of addition of cells is proportional to the number present (i.e., exponential growth). Cells divide in a characteristic time called the

division, generation, or doubling time. Population growth follows the solution to the equation

$$dN/dt = k*N$$

where

N = the number or concentration of cells in the culture

t = the time

k = the growth constant - (1/t)

This solution to this equation is

$$k = [\ln (N/N_0)]/(t - t_0)$$

Subscripts denote values at a known initial time, and ln indicates natural logarithms.

The growth constant k is the number of the logarithm (base e) units of increased per day. Growth rate is sometimes expressed as logarithm (base 10) units of increase per day k_{10} , or as logarithm (base 2) units per day k_2 , where

$$k_{10} = \log_{10} (N/N_0)/(t - t_0)$$

$$k_2 = \log_2 (N/N_0)/(t - t_0)$$

Conversions among the expressions are

$$k = 2.3026 k_{10}$$

$$k = 0.6931 k_2$$

where

k = growth rate measured in ln units

k_{10} = growth rate measured in \log_{10} units

k_2 = growth rate measured in \log_2 units

The composite gross production rate for this compartment should also represent a weighted contribution of each species in the assemblage. The maximum gross production rates selected for each species should reflect the range of environmental conditions expected in the simulation. If mixed layer temperatures are expected to reach 25° C, maximum specific gross production rates should be selected that were measured at or near this temperature. These rates will be temperature corrected. Literature values for TP_{MAX} are given in Table 8.

TSETL - phytoplankton settling rate (m day⁻¹). Mechanisms of suspension can influence the settling or sinking rate of algae. Morphological mechanisms include cell size, colony formation, cyclomorphosis, protuberances, and flagella. Physiological mechanisms include fat accumulation; regulation of ionic composition of cell sap; and the response of an organism to light, photoperiod, and nutrient concentration. Physical mechanisms include water viscosity and the role of water movements.

Two methods used to measure sinking rates experimentally are (a) the settling chamber method with or without the use of a microscope, and (b) the photometric technique. In the settling chamber, the descent time is determined (a) by following with a microscope or, in the case of large particles, with the naked eye, the cell trajectory between two marks at a known distance apart; (b) by measuring the time a cell takes to fall to the bottom of a settling chamber of known height placed on the stage of an inverted scope; or (c) using a 1-mm-deep Sedgwick Rafter counting chamber with a compound microscope. Estimation of relative sinking rate has been obtained by placing a well-mixed suspension of phytoplankton into a graduated cylinder and determining the concentration in various layers after a given time. Photometric determination of sinking rate measures changes in optical density of phytoplankton suspension measured at 750 nm after introducing the phytoplankton suspension into a cuvette.

These techniques are influenced by the "wall effect," that is, the effect of the settling chamber wall and convection current on the sinking velocity. To provide adequate fall for attainment of

Table 8
Gross Production Rates of Phytoplankton (day⁻¹)

| Species | TPMAX | Temp. °C | Reference |
|---|-------|----------|--|
| DIATOMS | | | |
| <i>Asterionella formosa</i> | 0.81 | 20 | Holm and Armstrong 1981 |
| <i>Asterionella formosa</i> | 0.69 | 10 | Hutchinson 1957 |
| <i>Asterionella formosa</i> | 1.38 | 20 | Hutchinson 1957 |
| <i>Asterionella formosa</i> | 1.66 | 25 | Hutchinson 1957 |
| <i>Asterionella formosa</i> | 1.71 | 20 | Fogg 1969 |
| <i>Asterionella formosa</i> | 0.28 | 4 | Talling 1955 |
| <i>Asterionella formosa</i> | 0.69 | 10 | Talling 1955 |
| <i>Asterionella formosa</i> | 1.38 | 20 | Talling 1955 |
| <i>Asterionella formosa</i> | 2.2 | 20 | Hoogenhout and Amesz 1965 |
| <i>Asterionella formosa</i> | 1.9 | 18.5 | Hoogenhout and Amesz 1965 |
| <i>Asterionella japonica</i> | 1.19 | 22 | Fogg 1969 |
| <i>Asterionella japonica</i> | 1.3 | 18 | Hoogenhout and Amesz 1965 |
| <i>Asterionella japonica</i> | 1.7 | 25 | Hoogenhout and Amesz 1965 |
| <i>Biddulphia</i> sp. | 1.5 | 11 | Castenholz 1964 |
| <i>Coscinodiscus</i> sp. | 0.55 | 18 | Fogg 1969 |
| <i>Cyclotella meneghiniana</i> | 0.34 | 16 | Hoogenhout and Amesz 1965 |
| <i>Cyclotella nana</i> | 3.4 | 20 | Hoogenhout and Amesz 1965 |
| <i>Detonula confervacea</i> | 0.62 | 2 | Smayda 1969 |
| <i>Detonula confervacea</i> | 1.4 | 10 | Hoogenhout and Amesz 1965 |
| <i>Ditylum brightwellii</i> | 2.1 | 20 | Paasche 1968 |
| <i>Fragilaria</i> sp. | 0.85 | 20 | Rhee and Gotham 1981b |
| <i>Fragilaria</i> sp. | 1.7 | 11 | Castenholz 1964 |
| <i>Melosira</i> sp. | 0.7 | 11 | Castenholz 1964 |
| <i>Navicula minima</i> | 1.4 | 25 | Hoogenhout and Amesz 1965 |
| <i>Navicula pelliculosa</i> | 2.0 | 20 | Hoogenhout and Amesz 1965 |
| <i>Nitzschia palea</i> | 2.1 | 25 | Hoogenhout and Amesz 1965 |
| <i>Nitzschia turgidula</i> | 2.5 | 20 | Paasche 1968 |
| <i>Phaeodactylum tricornutum</i> | 1.66 | 25 | Fogg 1969 |
| <i>Phaeodactylum tricornutum</i> | 2.7 | 19 | Hoogenhout and Amesz 1965 |
| <i>Rhizosolenia fragillissima</i> | 1.20 | 21 | Ignatiades and Smayda 1970 |
| <i>Skeletonema costatum</i> | 1.26 | 18 | Fogg 1969 |
| <i>Skeletonema costatum</i> | 2.30 | 20 | Jorgensen 1968 |
| <i>Skeletonema costatum</i> | 1.52 | 20 | Steemann-Nielsen and Jorgensen 1968 |
| <i>Skeletonema costatum</i> | 1.23 | 20 | Jitts et al. 1964 |
| <i>Synedra</i> sp. | 1.2 | 11 | Castenholz 1964 |
| <i>Thalassiosira</i> <i>nordenskioldii</i> | 0.77 | 13 | Jitts et al. 1964 |
| Natural diatom community | 3.10 | 20 | Verduin 1952 |

(Continued)

(Sheet 1 of 3)

Table 8 (Continued)

| Species | TPMAX | Temp. °C | Reference |
|----------------------------------|-------|----------|---------------------------|
| GREENS | | | |
| <i>Ankistrodesmus braunii</i> | 2.33 | 25 | Hoogenhout and Amesz 1965 |
| <i>Chlamydomonas moewusii</i> | | 4.2 | Hoogenhout and Amesz 1965 |
| <i>Chlorella pyrenoidosa</i> | 2.22 | 28 | Shelef 1968 |
| <i>Chlorella ellipsoidea</i> | 3.6 | 25 | Hoogenhout and Amesz 1965 |
| <i>Chlorella luteoviridis</i> | 0.56 | 22.4 | Hoogenhout and Amesz 1965 |
| <i>Chlorella miniata</i> | 0.87 | 25 | Hoogenhout and Amesz 1965 |
| <i>Chlorella pyrenoidosa</i> | 2.14 | 25 | Fogg 1969 |
| <i>Chlorella pyrenoidosa</i> | 1.95 | 25.5 | Sorokin and Meyers 1953 |
| <i>Chlorella pyrenoidosa</i> | 9.00 | 39 | Castenholz 1969 |
| <i>Chlorella pyrenoidosa</i> | 9.2 | 39 | Hoogenhout and Amesz 1965 |
| <i>Chlorella seccharophilia</i> | 1.2 | 25 | Hoogenhout and Amesz 1965 |
| <i>Chlorella variegata</i> | 0.86 | 25 | Hoogenhout and Amesz 1965 |
| <i>Chlorella vulgaris</i> | 2.9 | 25 | Hoogenhout and Amesz 1965 |
| <i>Chlorella vulgaris</i> | 1.59 | 20 | Goldman and Graham 1981 |
| <i>Dunaliella tertiolecta</i> | 1.0 | 16 | Hoogenhout and Amesz 1965 |
| <i>Dunaliella tertiolecta</i> | 0.77 | 36 | Jitts et al. 1964 |
| <i>Haematococcus pluvialis</i> | 1.2 | 23 | Hoogenhout and Amesz 1965 |
| <i>Nanochloris atomus</i> | 1.0 | 20 | Hoogenhout and Amesz 1965 |
| <i>Platymonas subcordiformia</i> | 1.5 | 16 | Hoogenhout and Amesz 1965 |
| <i>Scenedesmus</i> sp. | 1.34 | 20 | Rhee and Gotham 1981b |
| <i>Scenedesmus costulatus</i> | 2.0 | 24.5 | Hoogenhout and Amesz 1965 |
| <i>Scenedesmus obliquus</i> | 2.11 | 20 | Goldman and Graham 1981 |
| <i>Scenedesmus obliquus</i> | 2.2 | 25 | Hoogenhout and Amesz 1965 |
| <i>Scenedesmus quadricauda</i> | 4.1 | 25 | Hoogenhout and Amesz 1965 |
| <i>Scenedesmus quadricauda</i> | 2.29 | 27 | Goldman et al. 1972 |
| <i>Selenastrum capricornutum</i> | 2.45 | 27 | Goldman et al. 1972 |
| <i>Selenastrum westii</i> | 1.0 | 25 | Hoogenhout and Amesz 1965 |
| <i>Stichococcus</i> sp. | 0.70 | 20 | Hoogenhout and Amesz 1965 |
| GOLDEN-BROWN | | | |
| <i>Botrydiopsis intercedens</i> | 1.5 | 25 | Hoogenhout and Amesz 1965 |
| <i>Bumilleriopsis brevis</i> | 2.9 | 25 | Hoogenhout and Amesz 1965 |
| <i>Cricosphaera carterae</i> | 0.82 | 18 | Fogg 1969 |
| <i>Isochrysis galbana</i> | 0.55 | 20 | Fogg 1969 |
| <i>Isochrysis galbana</i> | 0.80 | 25 | Hoogenhout and Amesz 1965 |
| <i>Monochrysis lutheri</i> | 1.5 | 15 | Hoogenhout and Amesz 1965 |
| <i>Monochrysis lutheri</i> | 0.39 | 24 | Jitts et al. 1964 |
| <i>Monodus subterraneus</i> | 0.93 | 25 | Hoogenhout and Amesz 1965 |
| <i>Monodus subterraneus</i> | 0.39 | 30 | Fogg 1969 |
| <i>Tribonema aequale</i> | 0.70 | 25 | Hoogenhout and Amesz 1965 |

(Continued)

(Sheet 2 of 3)

Table 8 (Concluded)

| Species | TPMAX | Temp. °C | Reference |
|-------------------------------------|----------|----------|---------------------------|
| GOLDEN-BROWN (Continued) | | | |
| <i>Tribonema minus</i> | 1.00 | 25 | Hoogenhout and Amesz 1965 |
| <i>Vischeria stellata</i> | 0.70 | 25 | Hoogenhout and Amesz 1965 |
| <i>Euglena gracilis</i> | 2.2 | 25 | Hoogenhout and Amesz 1965 |
| DINOFLAGELLATE | | | |
| <i>Amphidinium carteri</i> | 1.88 | 18 | Fogg 1969 |
| <i>Amphidinium carteri</i> | 0.32 | 32 | Jitts et al. 1964 |
| <i>Ceratium tropos</i> | 0.20 | 20 | Fogg 1969 |
| <i>Gonyaulax polyedra</i> | 2.1 | 21.5 | Hoogenhout and Amesz 1965 |
| <i>Gymnodinium splendens</i> | 0.92 | 20 | Hoogenhout and Amesz 1965 |
| <i>Peridinium sp.</i> | 0.90 | 18 | Hoogenhout and Amesz 1965 |
| <i>Prorocentrum gracile</i> | 0.83 | 18 | Hoogenhout and Amesz 1965 |
| <i>Prorocentrum micans</i> | 0.71 | 25 | Hoogenhout and Amesz 1965 |
| <i>Prorocentrum micans</i> | 0.30 | 20 | Fogg 1969 |
| BLUEGREENS | | | |
| <i>Agmenellum quadriplaticum</i> | 8.0 | 39 | Hoogenhout and Amesz 1965 |
| <i>Anabaena cylindrica</i> | 0.96 | 25 | Hoogenhout and Amesz 1965 |
| <i>Anabaena variabilis</i> | 3.9 | 34.5 | Hoogenhout and Amesz 1965 |
| <i>Anacystis nidulans</i> | 2.9 | 25 | Hoogenhout and Amesz 1965 |
| <i>Anacystis nidulans</i> | 11.00 | 40 | Castenholz 1969 |
| <i>Chloropseudomonas ethylicum</i> | 3.3 | 30 | Hoogenhout and Amesz 1965 |
| <i>Cyanidium caldarium</i> | 2.4 | 40 | Hoogenhout and Amesz 1965 |
| <i>Cylindrospermum sphaerica</i> | 0.17 | 25 | Hoogenhout and Amesz 1965 |
| <i>Gloeotrichia echinulata</i> | 0.20 | 26.5 | Hoogenhout and Amesz 1965 |
| <i>Microcystis aeruginosa</i> | 0.25 | 20 | Holm and Armstrong 1981 |
| <i>Microcystis aeruginosa</i> | 1.6 | 23 | Hoogenhout and Amesz 1965 |
| <i>Microcystis luminmosis</i> | 1.50 | 40 | Castenholz 1969 |
| <i>Nostoc muscorum</i> | 2.9 | 32.5 | Hoogenhout and Amesz 1965 |
| <i>Oscillatoria principis</i> | 0.50 | 40 | Castenholz 1969 |
| <i>Oscillatoria terebriformis</i> | 3.36 | 40 | Castenholz 1969 |
| <i>Oscillatoria rubescens</i> | 5.04 | 30 | Zimmerman 1969 |
| <i>Rhodopseudomonas sphaeroides</i> | 10.8 | 34 | Hoogenhout and Amesz 1965 |
| <i>Rhodospirillum rubrum</i> | 4.85 | 25 | Hoogenhout and Amesz 1965 |
| <i>Schizothrix calcicola</i> | 3.4 | 30 | Hoogenhout and Amesz 1965 |
| <i>Synechococcus lividus</i> | 4.98 | 40 | Castenholz 1969 |
| <i>Synechococcus sp.</i> | 8.0 | 37 | Hoogenhout and Amesz 1965 |
| <i>Tolypothrix tenuis</i> | 4.0 | 38 | Hoogenhout and Amesz 1965 |
| <i>Leotocylindrus danicus</i> | 0.67-2.0 | 10-20 | Verity 1981 |
| <i>Anabaena variabilis</i> | 0.07-2.0 | 10-35 | Collins and Boylen 1982a |

(Sheet 3 of 3)

terminal velocity and to minimize overcrowding, the selection of chamber size is important.

The sinking rates of natural populations have also been determined by comparing changes in population density with depth and calculating a mean rate of descent. However, determination of sinking rate in situ is complicated by water movements and losses due to grazing. Mathematical expressions may also be used to determine sinking rates (Riley, Stommel, and Bumpus 1949).

The application of experimentally determined sinking rates to natural populations or ecosystem models must be qualified and used with caution. In lakes and reservoirs, vertical gradients of light, temperature, and nutrient concentration contrast with the constancy of the settling chamber and photometer cuvette environments in sinking experiments. The influence of light and nutrients on sinking rates, together with the turbulent motion of the natural environment, suggest that in vitro sinking results may not be particularly representative of natural populations. Values for settling rates are given in Table 9.

PS2P04 - phosphorus half-saturation coefficient (HSC) (mg l^{-1}). In practical terms, the HSC of a nutrient approximately marks the upper nutrient concentration at which growth ceases to be proportional to that nutrient. The modeled uptake of phosphorus by algae follows Monod kinetics. The value of the HSC can be calculated for the hyperbola using the Monod equation. PS2P04 is defined as the concentration phosphorus at which the rate of uptake is one-half the maximum.

The HSCs generally increase with nutrient concentration (Carpenter and Guillard 1971; Hendrey and Welch 1973; and Toetz, Varga, and Loughran 1973). This fact reflects both the change in species composition of the phytoplankton assemblage and the adaptation of the plankton to higher nutrient levels. A reservoir characterized by low nutrient concentrations is generally also characterized by low HSCs.

Nitrogen/phosphorus (N/P) ratios also provide information on the limiting nutrient and should be calculated using N and P concentrations measured in the mixed layer for all sampling dates. Usually, N/P ratios greater than 16:1 indicate phosphorus limitations while ratios

Table 9
Phytoplankton Settling Rates (m day⁻¹)

| Species | TSETL | Reference |
|-----------------------------------|-----------|--------------------------------------|
| DIATOMS - EXPERIMENTAL STUDIES | | |
| <i>Asterionella formosa</i> | 0.26-0.76 | Smayda 1974 |
| <i>Asterionella formosa</i> | 0.4 | Margalef 1961 |
| <i>Bacteriastrum hyalinum</i> | 0.39-1.27 | Smayda and Boleyn 1966 |
| <i>Chaetoceros didymus</i> | 0.85 | Eppley, Holmes, and Strickland 1967b |
| <i>Chaetoceros lauderi</i> | 0.46-1.54 | Smayda and Boleyn 1966 |
| <i>Chaetoceros</i> spp. | 0.25 | Margalef 1961 |
| <i>Chaetoceros</i> spp. | 4.0 | Allen 1932 |
| <i>Coscinodiscus wailesii</i> | 7.0-30.2 | Eppley, Holmes, and Strickland 1967b |
| <i>Coscinodiscus</i> sp. | 1.95-6.83 | Eppley, Holmes, and Strickland 1967b |
| <i>Coscinodiscus</i> sp. | 14.7 | Eppley, Holmes, and Strickland 1967b |
| <i>Cyclotella meneghiniana</i> | 0.08-0.24 | Titman and Kilham 1976 |
| <i>Cyclotella nana</i> | 0.16-0.76 | Eppley, Holmes, and Strickland 1967b |
| <i>Ditylum brightwellii</i> | 0.60-3.09 | Eppley, Holmes, and Strickland 1967b |
| <i>Ditylum brightwellii</i> | 2.0 | Eppley, Holmes, and Strickland 1967b |
| <i>Fragilaria crotonensis</i> | 0.27 | Burns and Rosa 1980 |
| <i>Leptocylindrum danicus</i> | 0.08-0.42 | Margalef 1961 |
| <i>Melosira agassizii</i> | 0.67-1.87 | Titman and Kilham 1976 |
| <i>Nitzschia closterium</i> | 0.52 | Margalef 1961 |
| <i>Nitzschia seriata</i> | 4.0 | Allen 1932 |
| <i>Nitzschia seriata</i> | 0.35-0.50 | Smayda and Boleyn 1965 |
| <i>Phaeodactylum tricornutum</i> | 0.05-0.06 | Riley 1943 |
| <i>Phaeodactylum tricornutum</i> | 0.02-0.04 | Riley 1943 |
| <i>Rhizosolenia hebetata</i> | | Eppley, Holmes and Strickland 1967b |
| <i>f. semispina</i> | 0.22 | Strickland 1967b |
| <i>Rhizosolenia setigera</i> | 0.11-2.23 | Smayda and Boleyn 1966 |
| <i>Rhizosolenia setigera</i> | 0.10-6.30 | Smayda and Boleyn 1966 |
| <i>Rhizosolenia stolterfothii</i> | 1.0-1.9 | Eppley, Holmes and Strickland 1967b |
| <i>Rhizosolenia</i> spp. | 0-0.72 | Margalef 1961 |
| <i>Skeletonema costatum</i> | 0.30-1.35 | Smayda and Boleyn 1966 |
| <i>Stephanopyxis turris</i> | 1.1 | Eppley, Holmes, and Strickland 1967b |

(Continued)

(Sheet 1 of 3)

Table 9 (Continued)

| Species | TSETL | Reference |
|---|-----------|--------------------------------------|
| DIATOMS - EXPERIMENTAL STUDIES (Continued) | | |
| <i>Stephanopyxis turris</i> | 2.1 | Eppley, Holmes, and Strickland 1967b |
| <i>Thalassionema nitzsoides</i> | 0.35-0.78 | Smayda (unpubl.) |
| <i>Thalassiosira fluviatilis</i> | 0.60-1.10 | Eppley, Holmes, and Strickland 1967b |
| <i>Thalassiosira</i> cf. <i>nana</i> | 0.10-0.28 | Smayda and Boleyn 1966 |
| <i>Thalassiosira rotula</i> | 1.15 | Eppley, Holmes, and Strickland 1967b |
| <i>Thalassiosira rotula</i> | 0.39-2.10 | Smayda and Boleyn 1966 |
| <i>Thalassiosira</i> spp. | 0-0.16 | Margalef 1961 |
| THEORETICAL | | |
| <i>Diatoms</i> | 0.3 | Bramlette 1961 |
| DINOFLAGELLATES - EXPERIMENTAL STUDIES | | |
| <i>Gonyaulax polyedra</i> | 2.8-6.0 | Eppley, Holmes, and Strickland 1967b |
| COCCOLITHOPHORIDS - EXPERIMENTAL STUDIES | | |
| <i>Coccolithus huxleyi</i> | 0.28 | Eppley, Holmes, and Strickland 1967b |
| <i>Coccolithus huxleyi</i> | 1.20 | Eppley, Holmes, and Strickland 1967b |
| <i>Cricosphaera carterae</i> | 1.70 | Eppley, Holmes, and Strickland 1967b |
| <i>Cricosphaera elongata</i> | 0.25 | Eppley, Holmes, and Strickland 1967b |
| <i>Cyclococcolithus fragilis</i> | 13.2 | Bernard 1963 |
| <i>Cyclococcolithus fragilis</i> | 13.6 | Bernard 1963 |
| <i>Cyclococcolithus fragilis</i> | 10.3 | Bernard 1963 |
| THEORETICAL | | |
| <i>Coccoliths</i> | 1.5 | Bramlette 1961 |
| MICROFLAGELLATES - EXPERIMENTAL STUDIES | | |
| <i>Cryptomonas erosa</i> | 0.31 | Burns and Rosa 1980 |
| <i>Cryptomonas marsonii</i> | 0.32 | Burns and Rosa 1980 |

(Continued)

(Sheet 2 of 3)

Table 9 (Concluded)

| Species | TSETL | Reference |
|--|-------|--|
| MICROFLAGELLATES - EXPERIMENTAL STUDIES (Continued) | | |
| <i>Rhodomonas minuta</i> | 0.07 | Burns and Rosa 1980 |
| <i>Dunaliella tertiolecta</i> | 0.18 | Eppley, Holmes and Strickland 1967b |
| <i>Monochrysis lutheri</i> | 0.39 | Eppley, Holmes and Strickland 1967b |
| <i>Monochrysis lutheri</i> | 0.39 | Apstein 1910 |
| GREENS EXPERIMENTAL | | |
| <i>Closterium parvulum</i> | 0.18 | Burns and Rosa 1980 |
| <i>Dunaliella tertiolecta</i> | 0.18 | Eppley, Holmes and Strickland 1967b |
| <i>Lagerhaemia quadriseta</i> | 0.08 | Burns and Rosa 1980 |
| <i>Scenedesmus acutiformis</i> | 0.10 | Burns and Rosa 1980 |
| <i>Selenastrum minutum</i> | 0.15 | Burns and Rosa 1980 |
| BLUEGREENS EXPERIMENTAL | | |
| <i>Anabaena spiroides</i> | 0.10 | Burns and Rosa 1980 |
| <i>Gomphosphaeria lacustris</i> | 0.11 | Burns and Rosa 1980 |

(Sheet 3 of 3)

less than 12:1 indicate nitrogen limitation. Intermediate values give indeterminate information, indicating uncertainty over which nutrient may be limiting. Phosphorus is usually the nutrient that limits the growth of algae in lakes and reservoirs.

The procedure of measuring a phosphorus HSC involves the measurement of the net rate of loss of dissolved orthophosphate from the medium in which the experimental population suspended.

Units of measurements must be expressed in terms of the chemical element and not the compound; i.e., the HSC for phosphorus should be specified as milligrams per litre of phosphorus and not milligrams per litre of orthophosphate. Values for the HSC are given in Table 10.

Table 10
Phytoplankton HSCs for P Limitation ($\text{mg } \ell^{-1}$)

| Species | PS2P04 | Reference |
|--|-------------|--|
| <i>Asterionella formosa</i> | 0.002 | Holm and Armstrong 1981 |
| <i>Asterionella japonica</i> | 0.014 | Thomas and Dodson 1968 |
| <i>Biddulphia sinensis</i> | 0.016 | Quasim, Bhattathiri, and Dovassoy 1973 |
| <i>Cerataulina bergonii</i> | 0.003 | Finenko and Krupatkina 1974 |
| <i>Chaetoceros curvisetus</i> | 0.074-0.105 | Finenko and Krupatkina 1974 |
| <i>Chaetoceros socialis</i> | 0.001 | Finenko and Krupatkina 1974 |
| <i>Chlorella pyrenoidosa</i> | 0.38-0.475 | Jeanjean 1969 |
| <i>Cyclotella nana</i> | 0.055 | Fuhs et al. 1972 |
| <i>Cyclotella nana</i> | 0.001 | Fogg 1973 |
| <i>Dinobryon cylindricum</i> | 0.076 | Lehman (unpubl. data) |
| <i>Dinobryon sociale</i> var. <i>americanum</i> | 0.047 | Lehman (unpubl. data) |
| <i>Euglena gracilis</i> | 1.52 | Blum 1966 |
| Freshwater phytoplankton | 0.02-0.075 | Halmann and Stiller 1974 |
| <i>Microcystis aeruginosa</i> | 0.006 | Holm and Armstrong 1981 |
| <i>Nitzschia actinastreoides</i> | 0.095 | Von Muller 1972 |
| <i>Pediastrum duplex</i> | 0.105 | Lehman (unpubl. data) |
| <i>Pithophora oedogonia</i> | 0.98 | Spencer and Lembi 1981 |
| <i>Scenedesmus obliquus</i> | 0.002 | Fogg 1973 |
| <i>Scenedesmus</i> sp. | 0.002-0.05 | Rhee 1973 |
| <i>Thalassiosira fluviatilis</i> | 0.163 | Fogg 1973 |

PS2N - nitrogen (N) HSC ($\text{mg } \ell^{-1}$). Uptake rates of nitrate (NO_3^-) or ammonium (NH_4^+) by algae give hyperbolas when graphed against (NO_3^-) or

NH_4^+ concentrations in the environment. The HSCs (i.e., the concentration of N at which the rate of production is one-half the maximum) can be calculated for the hyperbolas using the Monod equation. This constant reflects the relative ability of phytoplankton to use low levels of nitrogen.

The role of N as a growth-limiting factor has been relatively neglected when compared with phosphorus, presumably because the latter is the growth-limiting factor in most natural fresh waters. However, it has been found that nitrogen becomes the limiting nutrient where phosphorus is abundant because of its release from geological deposits or from external loadings.

There are several methods for measuring HSCs for N limitation. The chemostat method requires the measurement of the remaining nitrogen concentration at a number of fixed dilution rates (i.e., growth rates) in nitrogen-limited chemostat cultures. Culture media are prepared with nitrate or ammonium as the nitrogen source, with one-fifth or less than the usual amount of NO_3^- or NH_4^+ added to the culture media to ensure that, during growth, nitrogen will be depleted before other nutrients. A second, less desirable method is to use nitrogen-starved cells as an inoculum for cultures containing known concentrations of nitrogen and then: (a) measure the concentration of nitrogen in the extracellular fluid at some later time to determine the rate of nitrogen uptake, and (b) measure the increasing cell concentration to determine growth kinetics. The problems associated with this method are that the organisms are poorly adapted to their subsequent growth environment, so growth can occur only after uptake of a substantial amount of nitrogen.

Some trends can be seen in the data for HSCs: (a) organisms with a high HSC for nitrate usually have a high HSC for ammonium uptake as well, (b) large-celled species tend to show higher HSCs, and (c) fast-growing species tend to have lower HSCs than slow growers.

The nitrogen HSC as used in CE-QUAL-W2 should reflect the uptake of both the nitrite plus nitrate and ammonia-nitrogen compartments. Both compounds are taken up for use in production in proportion to their concentration in the layer.

A factor that will lead to selection for a particular functional group or species is the availability of combined nitrogen. In situations where the level of combined nitrogen is relatively low compared with other essential elements like phosphorus, those bluegreen species that can fix nitrogen will be at a selective advantage. Nitrogen fixation is not explicitly included in the model formulation for phytoplankton; however, if bluegreen algae are an important component in one of the compartments, the nitrogen HSC may have to be reduced to a low value to reflect nitrogen fixation. Values for the HSC for nitrogen are given in Table 11.

245. CARD RE.

PISAT - the saturating light intensity at the maximum photosynthetic rate, expressed in watts per square metre. Suspended sediments may exert a significant influence on the light regime in reservoirs. Since phytoplankton adapt to low light regimes, saturation coefficients may be lower than those measured under laboratory conditions. Values reported in the literature may also overestimate this coefficient because they are measured under optimum conditions either in the laboratory or in the field. Literature values are reported in Table 12.

TPEXCR - the maximum excretion rate or photorespiration rate (day^{-1}). TPEXCR is further defined as the rate of extracellular release of organic compounds. In CE-QUAL-W2, this release increments the labile DOM compartment. Wetzel (1975) has stated that these rates can vary from less than 1 percent to the same rate as carbon fixation, but that most values are less than 20 percent of carbon fixation. Literature values can be found in Table 13.

TPMORT - the maximum algal mortality rate (day^{-1}). Values from 0.01 to 0.03 have been used in previous modeling studies.

TPRESP - represents the maximum dark respiration rate of algae (day^{-1}). Respiration rates, in many instances, are expressed as millilitres of oxygen consumed per milligram of organism dry weight per hour. Since the model formulations require units of milligrams per milligram per day or 1 per day, these values must be converted. The

Table 11
Phytoplankton HSCs for N Limitation (mg ℓ^{-1})

| Species | PS2N | N Source | Reference |
|-------------------------------|-------------|-----------------|--------------------------------------|
| DIATOMS | | | |
| <i>Biddulphia aurita</i> | 0.056-0.197 | NO_3^- | Underhill 1977 |
| <i>Chaetoceros gracilis</i> | 0.012 | NO_3^- | Eppley, Rogers, and McCarthy 1969 |
| <i>Chaetoceros gracilis</i> | 0.007 | NH_4^+ | Eppley, Rogers, and McCarthy 1969 |
| <i>Coscinodiscus lineatus</i> | 0.161 | NO_3^- | Eppley, Rogers, and McCarthy 1969 |
| <i>Coscinodiscus lineatus</i> | 0.036 | NH_4^+ | Eppley, Rogers, and McCarthy 1969 |
| <i>Cyclotella nana</i> | 0.025-0.117 | NO_3^- | Carpenter and Guillard 1971 |
| <i>Cyclotella nana</i> | 0.111 | | MacIsaac and Dugdale 1969 |
| <i>Cyclotella nana</i> | 0.027 | | Caperon and Meyer 1972 |
| <i>Cyclotella nana</i> | 0.031 | | Eppley, Rogers, and McCarthy 1969 |
| <i>Cyclotella nana</i> | 0.007 | NH_4^+ | Eppley, Rogers, and McCarthy 1969 |
| <i>Ditylum brightwellii</i> | 0.037 | NO_3^- | Eppley, Rogers, and McCarthy 1969 |
| <i>Ditylum brightwellii</i> | 0.020 | NH_4^+ | Eppley, Rogers, and McCarthy 1969 |
| <i>Dunaliella teriolecta</i> | 0.013 | NO_3^- | Caperon and Meyer 1972 |
| <i>Dunaliella teriolecta</i> | 0.003 | NH_4^+ | Caperon and Meyer 1972 |
| <i>Dunaliella teriolecta</i> | 0.087 | NO_3^- | Eppley, Rogers, and McCarthy 1969 |

(Continued)

(Sheet 1 of 4)

Table 11 (Continued)

| Species | PS2N | N Source | Reference |
|---------------------------------------|-------------|------------------------------|--------------------------------------|
| <i>Fragilaria pinnata</i> | 0.037-0.100 | NO ₃ ⁻ | Carpenter and Guillard 1971 |
| <i>Leptocylindrous danicus</i> | 0.078 | NO ₃ ⁻ | Eppley, Rogers, and McCarthy 1969 |
| <i>Leptocylindrous danicus</i> | 0.013 | NH ₄ ⁺ | Eppley, Rogers, and McCarthy 1969 |
| <i>Navicula pelliculosa</i> | 0.923 | NO ₃ ⁻ | Wallen and Cartier 1975 |
| <i>Phaeodactylum tricornutum</i> | 0.161 | NO ₃ ⁻ | Ketchum 1939 |
| <i>Rhizosolenia robusta</i> | 0.186 | NO ₃ ⁻ | Eppley, Rogers, and McCarthy 1969 |
| <i>Rhizosolenia robusta</i> | 0.135 | NH ₄ ⁺ | Eppley, Rogers, and McCarthy 1969 |
| <i>Rhizosolenia stolterfothii</i> | 0.105 | NO ₃ ⁻ | Eppley, Rogers, and McCarthy 1969 |
| <i>Rhizosolenia stolterfothii</i> | 0.009 | NH ₄ ⁺ | Eppley, Rogers, and McCarthy 1969 |
| <i>Skeletonema costatum</i> | 0.027 | NO ₃ ⁻ | Eppley, Rogers, and McCarthy 1969 |
| <i>Skeletonema costatum</i> | 0.014 | NH ₄ ⁺ | Eppley, Rogers, and McCarthy 1969 |
| BLUEGREENS | | | |
| <i>Anabaena cylindrica</i> | 4.34 | NO ₃ ⁻ | Hattori 1962 |
| <i>Anabaena cylindrica</i> | 2.48 | NO ₂ ⁻ | Hattori 1962 |
| <i>Asterionella formosa</i> | 0.074-0.093 | NO ₃ ⁻ | Eppley and Thomas 1969 |
| <i>Asterionella formosa</i> | 0.062 | NH ₄ ⁺ | Eppley and Thomas 1969 |

(Continued)

(Sheet 2 of 4)

Table 11 (Continued)

| Species | PS2N | N Source | Reference |
|------------------------------|-------------|-----------------|--|
| <i>Oscillatoria agardhii</i> | 0.22 | NO_3^- | van Lierre, Zevenboom, and Mur 1977 |
| MICROFLAGELLATES | | | |
| <i>Bellochia</i> sp. | 0.001-0.016 | NO_3^- | Carpenter and Guillard 1971 |
| <i>Monochrysis lutheri</i> | 0.026 | NO_3^- | Caperon and Meyer 1972 |
| <i>Monochrysis lutheri</i> | 0.052 | NH_4^+ | Caperon and Meyer 1972 |
| <i>Monochrysis lutheri</i> | 0.037 | NO_3^- | Eppley, Rogers, and McCarthy 1969 |
| <i>Monochrysis lutheri</i> | 0.007 | NH_4^+ | Eppley, Rogers, and McCarthy 1969 |
| COCCOLITHOPHORIDS | | | |
| <i>Coccolithus huxleyi</i> | 0.006 | NO_3^- | Eppley, Rogers, and McCarthy 1969 |
| <i>Coccolithus huxleyi</i> | 0.002 | NH_4^+ | Eppley, Rogers, and McCarthy 1969 |
| <i>Coccochloris stagnina</i> | 0.019 | NO_3^- | Caperon and Meyer 1972 |
| GREENS | | | |
| <i>Chlorella pyrenoidosa</i> | 0.006-0.014 | | Pickett 1975 |
| <i>Chlorella pyrenoidosa</i> | 1.15 | NO_2^- | Knudsen 1965 |
| <i>Pithophora oedogonia</i> | 1.236 | NO_3^- | Spencer and Lembi 1981 |
| DINOFLAGELLATES | | | |
| <i>Gonyaulax polyedra</i> | 0.589 | NO_3^- | Eppley, Rogers, and McCarthy 1969 |
| <i>Gonyaulax polyedra</i> | 0.099 | NH_4^+ | Eppley, Rogers, and McCarthy 1969 |

(Continued)

(Sheet 3 of 4)

Table 11 (Concluded)

| Species | PS2N | N Source | Reference |
|------------------------------|-------|------------------------------|--------------------------------------|
| <i>Gymnodinium splendens</i> | 0.235 | NO ₃ ⁻ | Eppley, Rogers, and McCarthy 1969 |
| <i>Gymnodinium splendens</i> | 0.019 | NH ₄ ⁺ | Eppley, Rogers, and McCarthy 1969 |
| <i>Gymnodinium wailesii</i> | 0.223 | NO ₃ ⁻ | Eppley, Rogers, and McCarthy 1969 |
| <i>Gymnodinium wailesii</i> | 0.088 | NH ₄ ⁺ | Eppley, Rogers, and McCarthy 1969 |
| CHRYSOPHYTES | | | |
| <i>Isochrysis galbana</i> | 0.006 | NO ₃ ⁻ | Eppley, Rogers, and McCarthy 1969 |

Table 12

Values of Light Intensity at the Maximum Photosynthetic Rate ($W m^{-2}$)

| <u>Species</u> | <u>PISAT ($W m^{-2}$)</u> | <u>Reference</u> |
|--------------------------------|--------------------------------------|-------------------------------------|
| <i>Oscillatoria agardhii</i> | 10.3 | van Lierre, Zevenboom, and Mur 1978 |
| <i>Scenedesmus protuberans</i> | 24.7 | van Lierre, Zevenboom, and Mur 1978 |
| Mixed diatoms | 86 | Belay 1981 |
| Mixed plankton | 36 | Belay 1981 |
| Shade-adapted | 18 to 29 | Belay 1981 |
| <i>Oscillatoria rubescens</i> | 36 to 61 | Konopka 1983 |
| <i>Cryptomonas ovata</i> | 12 to 36 | Cloern 1977 |

Table 13

Maximum Extracellular Release Rate of Algae (day^{-1})

| <u>Species</u> | <u>TPEXCR</u> | <u>Reference</u> |
|--------------------------------|---------------|------------------|
| <i>Actinastrum hantzschii</i> | 0.044 | Nalewajko 1966 |
| <i>Ankistrodesmus falcatus</i> | 0.031 | Nalewajko 1966 |
| <i>Asterococcus superbis</i> | 0.036 | Nalewajko 1966 |
| <i>Chlorella pyrenoidosa</i> | 0.032 | Nalewajko 1966 |
| <i>Eudorina elegans</i> | 0.023 | Nalewajko 1966 |
| <i>Micractinium pusillum</i> | 0.014 | Nalewajko 1966 |

following is one approach for converting millilitres of oxygen uptake to milligrams of biomass respired.

- a. Compute the molecular weight equivalents of gas volume @ STP

$$1 \text{ mole } O_2 = 22.1 \text{ l at } 32 \text{ g/l, } \frac{32 \text{ g}}{22.1} = 1.45 \text{ mg } O_2/\text{ml } O_2$$

$$1 \text{ mole } CO_2 = 22.1 \text{ l at } 44 \text{ g/l, } \frac{44 \text{ g}}{22.1} = 2.0 \text{ mg } CO_2/\text{ml } CO_2$$

- b. Assume a Respiratory Quotient $\frac{CO_2}{O_2}$ of 0.9 for general

metabolism or $1 \text{ ml } O_2 \rightarrow 0.9 \text{ ml } CO_2$. Therefore, for each millilitre O_2 consumed,

$$\frac{12 \text{ (mol. wt. C)}}{44 \text{ (mol. wt. } CO_2)} \cdot 1.8 \text{ mg } CO_2 = 0.49 \text{ mg C respired.}$$

- c. Assume a C/biomass stoichiometric equivalent of 0.45. Then, for each millilitre O_2 consumed/milligram dry weight

$$\frac{0.49 \text{ mg C}}{0.45} = 1.08 \text{ mg biomass}$$

- d. However, milligrams O_2/l are consumed in the model, not millilitres. Therefore, for each millilitre of O_2 consumed

$$1.45 \text{ mg } O_2 \text{ consumed} = 1.08 \text{ mg biomass respired}$$

or

$$1 \text{ ml } O_2 = 0.74 \text{ mg biomass respired/mg } O_2 \text{ consumed}$$

- e. This relationship may be used to convert millilitres O_2 to milligrams dry weight per unit time.

Literature values of dark respiration can be found in Table 14.

246. Card RF.

ALG1T1 - lower temperature bound ($^{\circ}\text{C}$) at which phytoplankton metabolism continues.

ALG1T2 - lowest temperature ($^{\circ}\text{C}$) at which processes are occurring near the maximum rate.

ALG1T3 - upper temperature ($^{\circ}\text{C}$) at which processes are occurring at the maximum rate.

ALG1T4 - upper lethal temperature ($^{\circ}\text{C}$). Biological temperature curves are generally asymmetrical, with the maximum rates occurring nearer the upper lethal temperatures than the lower temperatures.

The temperature coefficients for algal production are dependent upon the acclimation temperature and the length of time of exposure to this temperature (Collins and Boylen 1982b). For example, algae growing in the northern reservoir will have a lower optimum temperature (ALG1T2 and ALG1T3) than algae growing in a southern reservoir because the northern algae have become acclimated to different climatic regimes. The lower and upper temperature boundaries (ALG1T1 and ALG1T4) will also be affected by acclimation and will differ substantially among different functional groups of algae.

Table 14
Phytoplankton Dark Respiration Rates (day^{-1})

| <u>Species</u> | <u>TPRESP</u> | <u>Reference</u> |
|---|---------------|--------------------------|
| <i>Mesodinium rubrum</i> | 0.05 | Smith 1979 |
| <i>Thalassiosira allenii</i> small cells | 0.14-0.59 | Laws and Wong 1978 |
| <i>Thalassiosira allenii</i> large cells | 0.05-0.42 | Laws and Wong 1978 |
| <i>Monochrysis lutheri</i> | 0.15-0.32 | Laws and Wong 1978 |
| <i>Dunaliella teriolecta</i> | 0.12-0.46 | Laws and Wong 1978 |
| <i>Anabaena variabilis</i> | 0.10-0.92 | Collins and Boylen 1982a |
| <i>Coscinodiscus excentricus</i> | 0.075-0.11 | Riley and von Aux 1949 |
| <i>Chlorella pyrenoidosa</i> | 0.01-0.03 | Myers and Graham 1961 |
| Phytoplankton | 0.05-0.10 | Ryther 1954 |

Unfortunately, there is no set rule to determine these coefficients based upon site-specific temperature regimes. One can estimate these values for a given species or functional group based upon reported experimental conditions or in situ study conditions. Several investigators have determined these values based upon studies where several physical factors such as light intensity, temperature, and day length have been varied simultaneously. Often the algae were preconditioned at a specific combination of these factors, which may help in parameter estimation for a particular site. Values for the temperature coefficients are given in Table 15.

247. CARD RG.

ALG1K1 - value of the temperature rate multiplier corresponding to the lower temperature, ALG1T1. Typical values are near 0.1.

ALG1K2 - value of the temperature rate multiplier corresponding to ALG1T2. Typical values are near 0.98.

ALG1K3 - value of the temperature rate multiplier corresponding to ALG1T3. Typical values are near 0.98.

ALG1K4 - value of the temperature rate multiplier corresponding to ALG1T4. Typical values are near 0.1.

248. CARD RH.

TDSETL - detrital settling velocity (m day^{-1}). Detrital settling velocities vary from 0.001 to over 20 m day^{-1} depending on the detrital characteristics and reservoir hydrodynamics. Settling rates should be obtained from quiescent settling chamber studies because advective and turbulent forces in the mixed layer that can reduce settling in a reservoir are modeled separately. For most studies, settling velocities are in the range of 0.05 to 1.0 m day^{-1} . Much higher values are often reported for fecal pellets; however, such high settling coefficients may be questionable because they produce unrealistically low detritus values in modeling studies. Values for detritus settling velocities are given in Table 16.

DETT1 - lower temperature bound at which detritus decomposition continues, °C.

Table 15

Temperature Coefficients for Phytoplankton (°C)

| <u>Species</u> | <u>ALG1T1</u> | <u>ALG1T2</u> | <u>ALG1T3</u> | <u>ALG1T4</u> | <u>Reference</u> |
|---|---------------|---------------|---------------|---------------|---|
| <i>Amphidinium carteri</i> | 18 | 24 | | 35 | Jitts et al. 1964 |
| <i>Anacystis nidulans</i> | | 38 | 40 | | Castenholz 1969 |
| <i>Asterionella formosa</i> | | 25 | 25 | | Rhee and Gotham 1981a |
| <i>Asterionella formosa</i> | | 25 | 29 | | Hutchinson 1957 |
| <i>Asterionella formosa</i> | 4 | 20 | 25 | | Talling 1955 |
| <i>Chlorella</i> <i>pyrenoidosa</i> | 1 | 28 | 38 | 40 | Clendenning, Brown, and Eyster 1956 |
| <i>Chlorella</i> <i>pyrenoidosa</i> | 7 | 38 | 40 | 42 | Sorokin and Krauss 1962 |
| <i>Chlorella</i> sp. | | 20 | 25 | | Tamiya et al. 1965 |
| <i>Detonula</i> <i>confervacea</i> | 0 | 10 | 12 | 16 | Guillard and Ryther 1962 |
| <i>Detonula</i> <i>confervacea</i> | 1 | 10 | 13 | 15 | Smayda 1969 |
| <i>Ditylum</i> <i>brightwellii</i> | 5 | 23 | 26 | 30 | Paasche 1968 |
| <i>Dunaliella</i> <i>teriolecta</i> | 8 | 31 | 33 | 36 | Eppley and Sloan 1966 |
| <i>Dunaliella</i> <i>teriolecta</i> | 12 | 26 | 28 | 36 | Jitts et al. 1964 |
| <i>Microcystis</i> <i>aeruginosa</i> | | 38 | 40 | | Castenholz 1969 |
| <i>Monchrysis lutheri</i> | 9 | 19 | 22 | | Jitts et al. 1964 |
| <i>Nostoc muscorum</i> | 1 | 31 | 33 | 36 | Clendenning, Brown, and Eyster 1956 |
| <i>Oscillatoria</i> <i>terebriformis</i> | | 38 | 40 | | Castenholz 1969 |
| <i>Phaeodactylum</i> <i>tricornutum</i> | 0 | 20 | 21 | 30 | Li and Morris 1982 |
| <i>Rhizosolenia</i> <i>fragillissima</i> | 7 | 21 | | | Ignatiades and Smayda 1970 |
| <i>Scenedesmus</i> sp. | | 19 | 20 | 21 | Rhee and Gotham 1981a |
| <i>Skeletonema</i> <i>costatum</i> | 1 | 20 | | | Jorgensen 1968 |
| <i>Skeletonema</i> <i>costatum</i> | 2 | 20 | | | Steemann-Nielsen and Jorgensen 1968 |
| <i>Thalassiosira</i> <i>nordenskioldii</i> | 4 | 13 | 14 | 16 | Jitts et al. 1964 |

Table 16
Detritus Settling Velocities (m day⁻¹)

| Source | TDSETL | Reference |
|---|-----------|--------------------------------------|
| <i>Ceratium balticum</i> | 9.0 | Apstein 1910 |
| <i>Chaetoceros borealis</i> | 5.0 | Apstein 1910 |
| <i>Chaetoceros didymus</i> | 0.85 | Eppley, Holmes, and Strickland 1967b |
| <i>Cricosphaera carterae</i> | 1.70 | Eppley, Holmes, and Strickland 1967b |
| <i>Ditylum brightwellii</i> | 2.0 | Apstein 1910 |
| Fecal pellets: <i>Acartia clausii</i> | 116.0 | Smayda 1971 |
| Fecal pellets: <i>Euphausia krohnii</i> | 240.0 | Fowler and Small 1972 |
| Fecal pellets: <i>Euphausia pacifica</i> | 43.0 | Osterberg, Casey, and Curl 1963 |
| Fecal pellets: <i>Pontella meadii</i> | 54.0-88.0 | Turner 1977 |
| <i>Phaeodactylum tricorutum</i> | 0.02-0.04 | Riley 1943 |
| <i>Rhizosolenia herbetata</i> | 0.22 | Eppley, Holmes, and Strickland 1967b |
| <i>Stephanopyxis tunis</i> | 2.1 | Eppley, Holmes, and Strickland 1967b |
| <i>Tabellaria flocculosa</i> | 0.46-1.5 | Smayda 1971 |
| <i>Thalassiosira psuedonana</i> | 0.85 | Hecky and Kilham 1974 |

DETT2 - temperature at which decomposition occurs near the maximum rate, °C.

DETK1 - rate multiplier corresponding to the lower temperature. Values should be near 0.1.

DETK2 - rate multiplier corresponding to DETT2 . Values should be near 0.98.

Detritus temperature coefficients are listed in Table 17.

249. CARD RI.

TDOMDK - decomposition rate (day⁻¹) of labile DOM. Dissolved organic matter in natural waters is one organic substrate for heterotrophic metabolism. The composition of natural DOM is highly variable and little understood, but its sources are generally grouped into

Table 17
Temperature Coefficients for Decomposition (°C)

| Substrate or Site | DETT1 | DETT2 | Reference |
|--|-------|-------|------------------------------|
| <i>Pseudomonas fluorescens</i> : natural substrate | 0 | 25-30 | Tison and Pope 1980 |
| <i>E. coli</i> : natural substrate | 0 | 37 | Tison and Pope 1980 |
| Glucose: Lake George, New York | 0 | 25 | Tison, Pope, and Boylen 1980 |
| Glucose | 0 | 20-30 | Bott 1975 |
| Glucose: Lake Wingra, Wisconsin | 0 | 25-30 | Boylen and Brock 1973 |

(a) excretion from phytoplankton and macrophytes, (b) decomposition of phytoplankton and macrophytes, (c) excretion by animals, and (d) allochthonous drainage (e.g., humic compounds from upstream sources).

Aquatic bacteria appear to be chiefly responsible for the removal of DOM compounds from the water; they are the major agents for bacterial mineralization of organic solutes in fresh water (Wright 1975) using organic matter as an energy source. Various methods have been tested to determine the decay rate of DOM in water. Modification of the basic Parson and Strickland (1963) technique have been developed to quantify the kinetics.

DOM decomposition rates have been represented by filtered carbonaceous biochemical oxygen demand (BOD) decay rates. If sufficient oxygen is available, the aerobic biological decomposition of organics will continue until all the DOM is consumed. In the standard test for BOD, a sample is diluted with water containing a known amount of oxygen. The loss of oxygen after the sample has been incubated for 5 days at 20° C is known as the 5-day BOD. The value of the first-order decay rate is generally about 0.05 to 0.20 per day.

The BOD test suffers from several serious deficiencies. The test has no stoichiometric validity, for example, the arbitrary 5-day period usually does not correspond to the point where all the organic matter is consumed.

Values for DOM decay rates are presented in Table 18.

Table 18
DOM Decay Rates (day⁻¹)

| <u>Compound</u> | <u>Decay Rate</u> | <u>Reference</u> |
|-----------------|-------------------|-------------------------------------|
| Acetate | 0.2 | Wright 1975 |
| Amino acids | 0.64 | Williams, Yentsch, and Yentsch 1976 |
| Glucose | 0.24 | Williams, Yentsch, and Yentsch 1976 |
| Glucose | 0.32-0.50 | Toerien and Cavari 1982 |
| Glucose | 0.111 | Wright 1975 |
| Glutamate | 0.11-0.625 | Carney and Colwell 1976 |
| Glycine | 0.312-0.45 | Vaccaro 1969 |
| Glycine | 0.048 | Vaccaro 1969 |
| Glycolate | 0.024-0.432 | Wright 1975 |
| Glycolate | 0.012-0.25 | Wright 1975 |
| Glycolic acid | 0.004 | Tanaka, Nakanishi, and Kadota 1974 |

TNH3DK - ammonia decay rate (i.e., the rate at which ammonia is oxidized to nitrite plus nitrate) (day⁻¹). Ammonia is generated by heterotrophic bacteria as the primary end product of decomposition of organic matter, either directly from proteins or from other nitrogenous organic compounds. Although ammonia is a major excretion product, this nitrogen source is minor in comparison to decomposition.

Nitrification is the biological conversion of organic and inorganic N compounds from a reduced state to a more oxidized state (Alexander 1965), although only inorganic N is included for this process in CE-QUAL-W2. The nitrifying bacteria capable of oxidation of NH_4^+ to NO_2^- are largely confined to the species *Nitrosomonas*, bacteria which are mesophilic (1-37° C).

Nitrification rates can be determined by a number of different techniques. Courchaine (1968) has plotted nitrogenous BOD on a logarithmic scale and determined the decay rate from the slope of the line. Thomann et al. (1971) used a finite-difference approximation to solve a set of simultaneous linear equations.

Laboratory measurements for the ammonia decay rate can produce results that differ from what might be measured in situ. Several environmental factors can influence the rate of nitrification, including pH, temperature, suspended particulate concentration, hydraulic

parameters, and benthos, although only temperature modifies this rate in CE-QUAL-W2.

Nitrification can be measured as a one- or two-step process. In the one-step method, only the end product of the entire reaction, nitrate, is measured. In the two-step method, (a) nitrite accumulation is measured as ammonia is oxidized to nitrite, and (b) nitrate accumulation is measured as nitrite is oxidized to nitrate. Because nitrite plus nitrate nitrogen is modeled as one compartment, rates for the one-step method should be used. Literature values are given in Table 19.

Table 19
Ammonia Oxidation Rates (day⁻¹)

| Site | TNH3DK | Reference |
|--------------------------------|-------------|-----------------------------------|
| Wastewater treatment plant | 0.05-0.30 | Wild, Sawyer, and McMahon 1971 |
| Grand River, Illinois | 0.80 | Bansal 1976 |
| Grasmerer Lake, United Kingdom | 0.001-0.013 | Hall 1982 |
| Truckee River, Nevada | 0.09-1.30 | Bansal 1976 |
| Upper Mohawk River, New York | 0.23-0.40 | Bansal 1976 |
| Middle Mohawk River | 0.30 | Bansal 1976 |
| Lower Mohawk River | 0.30 | Bansal 1976 |
| Ohio River | 0.25 | Bansal 1976 |
| Big Blue River, Nebraska | 0.17-0.25 | Bansal 1976 |
| Flint River, Michigan | 0.76-0.95 | Bansal 1976 |

TN03DK - denitrification rate of the nitrite plus nitrate-nitrogen compartment. Denitrification only takes place in cells that are considered anaerobic. Values used in previous modeling studies have been near 0.05.

TDETDK - detritus decay rate (day⁻¹). Detritus, as defined by Wetzel et al. (1972), consists of organic carbon lost from an organism by nonpredatory means (including egestion, excretion, secretion, etc.) from any trophic level component, or input from sources external to the ecosystem that enter and cycle in the system (i.e., allochthonous organic carbon). For CE-QUAL-W2, this should be considered to be particulate material only.

The rate of detritus decay can be determined by measuring the use of oxygen during decomposition, with results expressed as a first-order decay coefficient (k base e = milligrams oxygen used/milligram/day). Many workers have measured rates of oxygen uptake by detritus, suggesting that oxygen uptake is related to the organic matter available for decomposition. Odum and de la Cruz (1967) and Fenchel (1970), for example, demonstrated an inverse relation between detritus particle size and oxygen consumption. Oxygen uptake is an integrative measure of all oxidative processes occurring in the sample, both chemical and biological: reduced substances are usually rapidly oxidized; respiration of the organisms associated with detritus is primarily bacterial, although algae, protozoa, and fungi may also contribute. Measurement of the oxygen uptake reflects the metabolism of communities of microorganisms involved in the decomposition of natural substances.

As a detrital particle decomposes with time, there is a decline in oxygen uptake accompanied by succession of communities of microorganisms. This decline occurs as matter changes from labile to refractory, and refractory matter often accumulates in the sediment. Rates of decay are generally high initially and slow down as the material becomes refractory; the rate is influenced by temperature, detrital composition, and age of the detritus. Macrophyte communities are the primary source of detritus in many systems. Submersed and floating macrophytes generally decay more rapidly than highly lignified emergent species. Particulate organic matter of dead bluegreen algae decomposes much faster than that derived from green algae diatoms and desmids. Particulate organic matter (POM) is especially resistant (Gunnison and Alexander 1975). As detritus decays, there is a decrease in the C:N ratio as a result of a buildup of microbial protein (Mann 1972). A 1-g sample of detritus at 20° C consumes about 1 mg oxygen/hr (Hargrave 1972a).

Decay rates can also be measured by suspending a nylon mesh bag of detrital material in situ or under controlled conditions and determining weight loss with time. This actually measures weight loss due to enzymatic decomposition by bacteria and fungi, solution of soluble

substances, and loss of fragments through the container pores.

Decay rates have also been determined by measuring the mineralization rates of carbon, nitrogen, and phosphorus (Otsuki and Hanya 1972). Decomposition of detritus generated from planktonic communities of surface lake water occurs at rates on the order of 10 percent per day (Saunders 1972), based upon radioactive carbon tracer studies.

Consideration should be given to the primary or expected sources of detritus. Decomposition rates for allochthonous detrital sources are generally lower than for autochthonous sources to reflect the more refractory nature of allochthonous material after its transport through the upper portions of the reservoir. Much of the decomposition in the prototype reservoir system occurs in the headwater area. The labile fraction of autochthonous detritus produced in the pelagic zones of the lower reservoir will decompose more rapidly in the water column and should have a higher decomposition rate than allochthonous detritus. However, in a stratified reservoir the POM in the hypolimnion may not be exchanged with the epilimnetic waters. The POM becomes more refractory with time, and rates of decomposition decrease.

Microbial decomposition of detritus can be represented by three stages: a very quick solution of soluble organic components, a relatively rapid decomposition of labile organic constituents, and slow decomposition of refractory organic constituents. Detritus decay rates are given in Table 20.

250. CARD RJ.

TRFRDK - decomposition rate (day^{-1}) of refractory DOM. Contributing to the errors involved in measuring decay rates of DOM is the extensive variability in the composition and stage of decomposition of DOM. Allochthonous inputs of DOM are likely to be more refractory than autochthonous inputs and, as a result, decomposition rates will be slower and decay may be incomplete; therefore, the length of time the organic matter is available for decomposition is important. This is the main reason this version of the model includes two DOM compartments. Values for DOM decay rates are presented in Table 18.

Table 20
Detritus Decay Rates (day⁻¹)

| Detritus Source | TDETDK | Reference |
|--------------------------------|-------------|---------------------------------|
| Beech | 0.001-0.004 | Hanlon 1982 |
| <i>Cladophora glomerata</i> | 0.007 | Piecznska 1972 |
| Dead green algae | 0.016-0.076 | Otsuki and Hanya 1972 |
| Dead mixed algae | 0.007-0.111 | Jewell and McCarty 1971 |
| Dead mixed algae | 0.007-0.06 | Fitzgerald 1964 |
| <i>Gloeotrichia echinulata</i> | 0.001-0.007 | Piecznska 1972 |
| <i>Isoetes lancustris</i> | 0.003-0.015 | Hanlon 1982 |
| Leaf packs | 0.005-0.017 | Sedell, Triska, and Triska 1975 |
| Osier | 0.001-0.005 | Hanlon 1982 |
| <i>Potamogeton crispus</i> | 0.002-0.004 | Rogers and Breen 1982 |
| <i>Potamogeton perfoliatus</i> | 0.002-0.007 | Hanlon 1982 |

TDOMRF - process by which labile DOM becomes refractory DOM (day⁻¹) and should be viewed as part of the decomposition process. Values near 0.01 to 0.1 have been used in previous modeling studies.

DOMCNT - fraction of allochthonous DOM that is labile, with the remainder being refractory. This variable is used in subroutine TVDS to partition influent total DOM. Values near 0.3 have been used in previous modeling studies.

TSEDDK - sediment decomposition rate (day⁻¹). While sediment consists primarily of settled organic detritus, the decomposition rate should reflect the more refractory nature of the detritus as it reaches the sediment. The labile portion of organic detritus may be readily decomposed as it settles through the water column. In addition, the weight of sediment, along with TSEDDK, will affect the amount of decomposition. If high initial values are used for sediment, TSEDDK may have to be lowered since only the top few millimetres of sediment are usually involved in aerobic decomposition. Because sediment decay can be a major factor causing anaerobic conditions, the flux of oxygen at the sediment/water interface caused by sediment decay should be compared to measured values.

In general, sediment values (g m⁻²) times TSEDDK times a stoichiometric equivalent (1.4) should yield oxygen consumption rates at

the sediment/water interface which can be compared with measured rates or literature values (in grams of oxygen utilized per square metre per day). This value may be reduced in CE-QUAL-W2 due to temperature effects. Other information can be found in Gunnison, Chen, and Brannon (1983) and Chen, Brannon, and Gunnison (1984).

251. CARD RK.

DOMT1 - lower temperature bound at which DOM decays ($^{\circ}\text{C}$).

DOMT2 - lowest temperature at which decomposition is occurring near the maximum rate ($^{\circ}\text{C}$).

DOMK1 - rate multiplier corresponding to DOMT1 (dimensionless). Values should be near 0.1.

DOMK2 - rate multiplier corresponding to DOMT2. Values should be near 0.98.

Temperature coefficients for DOM can be found in Table 21.

Table 21

Temperature Coefficients for DOM Decay ($^{\circ}\text{C}$)

| <u>Substrate</u> | <u>DOMT1</u> | <u>DOMT2</u> | <u>Reference</u> |
|---------------------------------|--------------|--------------|------------------------------|
| Glucose | 5.0 | 35.5 | Toerien and Cavari 1982 |
| Glucose: Lake George, New York | 0 | 25 | Tison, Pope, and Boylen 1980 |
| Glucose | 0 | 20-30 | Bott 1975 |
| Glucose: Lake Wingra, Wisconsin | 0 | 25-30 | Boylen and Brock 1973 |

252. CARD RL.

NH3T1 - lower temperature bound at which ammonium nitrification continues (°C).

NH3T2 - lowest temperature at which nitrification is occurring near the maximum rates (°C).

NH3K1 - rate multiplier corresponding to NH3T1 (dimensionless). Values should be near 0.1.

NH3K2 - rate multiplier corresponding to NH3T2. Values should be near 0.98.

Values for these temperature coefficients are located in Table 22.

Table 22

Temperature Coefficients for Ammonia Oxidation (°C)

| <u>Species or Site</u> | <u>NH3T1</u> | <u>NH3T2</u> | <u>References</u> |
|----------------------------|--------------|--------------|------------------------------------|
| <i>Nitrosomonas</i> | 5 | 30 | Knowles, Downing, and Barrett 1965 |
| Wastewater treatment plant | 5 | 25 | Wild, Sawyer, and McMahon 1971 |
| Ann Arbor, Mich. | 2 | 20 | Borchardt 1966 |

253. CARD RM.

NO3T1 - lower temperature bound at which denitrification continues (°C). The value should be near zero.

NO3T2 - lowest temperature at which denitrification occurs at its maximum rate (°C). Values near 25° C have been used in previous modeling studies.

NO3K1 - rate multiplier corresponding to NO3T1 (dimensionless). Values should be near 0.1.

NO3K2 - rate multiplier corresponding to NO3T2. Values should be near 0.98.

254. CARD RN.

ADSRBP - adsorption coefficient of phosphorus for use in the Langmuir isotherm ($\text{m}^3 \text{g}^{-1}$).

ADSRBN - adsorption coefficient of nitrogen for use in the Langmuir isotherm ($\text{m}^3 \text{g}^{-1}$).

ADMAXP - maximum amount of phosphate adsorbed per gram of solids ($\text{g P m}^{-3} / \text{g solid m}^{-3}$).

ADMAXN - maximum amount of ammonia adsorbed per gram of solids ($\text{g N m}^{-3} / \text{g solid m}^{-3}$).

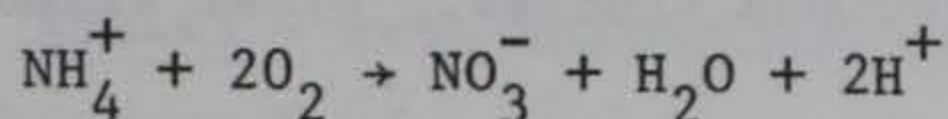
The coefficients ADSRBP and ADSRBN are related to the energy of adsorption. They are equal to the adsorption coefficient divided by the desorption coefficient in the Langmuir isotherm. Variables $1/\text{ADSRBP}$ and $1/\text{ADSRBN}$ equal the concentration at one-half ADMAXP or ADMAXN. The value of ADSRBP was found to be between 1.2 and 33.3 by Ku, Di Giano, and Feng (1978). Values for ADMAXP are given in Table 23.

Table 23
Values of ADMAXP ($\text{g P m}^{-3} / \text{g solid m}^{-3}$)

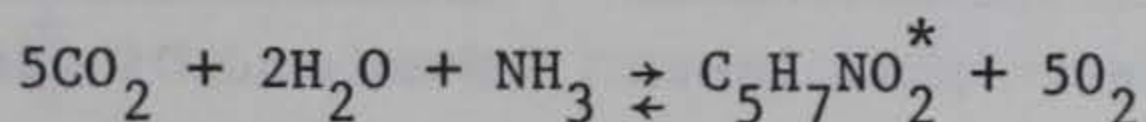
| <u>ADMAXP (g/g)</u> | <u>Site</u> | <u>Reference</u> |
|---------------------|--|-------------------------------|
| 0.0021 to 0.002 | Maumee River Basin Soils | Green, Logan, and Smeck 1978 |
| 0.0004 to 0.0005 | Maumee River Basin - clay fractions | Green, Logan, and Smeck 1978 |
| 0.0007 to 0.001 | Maumee River Basin - suspended sediments | Green, Logan, and Smeck 1978 |
| 0.0002 to 0.0003 | Maumee River Basin - bottom sediments | Green, Logan, and Smeck 1978 |
| 0.001 to 0.002 | Lake Warner | Ku, Di Giano, and Feng 1978 |
| 0.001 | Lake Wyola | Ku, Di Giano, and Feng 1978 |
| 0.0002 to 0.0005 | Blackstrap Lake | Hwang, Lackie, and Huang 1976 |

255. CARD RO.

O2NH3 - number of grams of oxygen required to oxidize 1 g of NH_4^+ (as N) to NO_3^- . The value is 4.57 as derived from the following reaction.

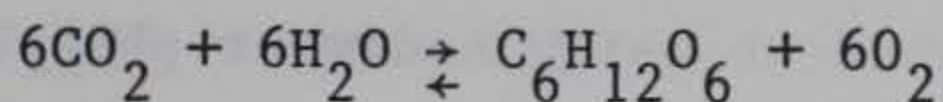


O2DET - stoichiometric requirement for oxygen during the decomposition of detritus and organic sediment, assuming a constant organic composition--1.4.



Where * refers to an average algal and bacterial composition (Golterman 1975, Wang et al. 1978).

O2RESP - oxygen requirement for biological respiration (conversion of carbohydrate to CO_2 and H_2O)--1.1.



O2FAC - stoichiometric equivalent for oxygen production during photosynthesis, taking into account the formation of proteins, etc.

(1.4). This value is derived from the reaction described under O2DET.

O2DOM - stoichiometric requirement for oxygen in the decomposition of DOM, assumed to be the same as for detritus (1.4).

OXYLIM - dissolved oxygen concentration in milligrams per litre which triggers anaerobic processes in the model. When the concentration is less than OXYLIM, anaerobic processes predominate. When dissolved oxygen exceeds OXYLIM, oxidation processes predominate. Setting OXYLIM = -1.0 will effectively prevent the anaerobic processes from occurring. Experience suggests an initial value of 0.5.

256. CARD RP.

TXP4RE - value, as a fraction of the specified sediment oxygen demand in grams per square metre per day which represents the rate at which $\text{PO}_4^{-3}\text{-P}$ is released from sediments under anaerobic conditions.

Values up to 0.3 have been used in previous studies. Other values are listed in Table 24.

Table 24
Phosphorus Release Rates from the Sediment
During Anaerobic Conditions

| <u>TXP4RE (g m⁻² day⁻¹)</u> | <u>Sites</u> | <u>Reference</u> |
|---|---|-----------------------------|
| 0.001; 0.01-0.150 | Shallow eutrophic lakes | Snow and Di Giano 1976 |
| 0.018-0.020 | Lake Glaninger, Sweden Lake Ramsjon, Sweden Lake Ryssbysjon, Sweden | Ryding and Forsberg 1977 |
| 0.013 | Lake Erie | Burns 1976 |
| 0.017 | Lake Fureso | Kamp-Nielsen 1974 |

XP04T1 - lower temperature bound at which sediment phosphorus release continues (°C). Values near 0° C have been used in previous studies.

XP04T2 - lower temperature bound at which sediment phosphorus release is occurring near the maximum rate (°C). Values near 5° C have been used in previous studies.

XP04T3 - upper temperature bound at which sediment phosphorus release is occurring near the maximum rate (°C). Values near 35° C have been used in previous studies.

XP04T4 - upper temperature bound at which sediment phosphorus release continues (°C). Values near 40° C have been used in previous studies.

NOTE: The wide range of temperature values suggested here will result in temperature rate multipliers of near 1 for the majority of conditions expected to occur in reservoirs.

257. CARD RQ.

XP04K1 - rate multiplier that corresponds to XP04T1 . Values should be near 0.1.

XP04K2 - rate multiplier that corresponds to XP04T2 . Values should be near 0.98.

XP04K3 - rate multiplier that corresponds to XP04T3 . Values should be near 0.98.

XP04K4 - rate multiplier that corresponds to XP04T4 . Values should be near 0.1.

258. CARD RR.

TCNREL - value, as a fraction of the specified sediment oxygen demand in grams per square metre per day, which represents the rate at which NH_4^+ -N is released from sediments under anaerobic conditions.

Values of up to 0.4 have been used in previous modeling studies.

CNT1 - lower temperature bound for sediment ammonia-nitrogen release ($^{\circ}\text{C}$). Values near 0°C have been used in previous studies.

CNT2 - lower temperature bound for sediment ammonia-nitrogen release to continue near the maximum rate ($^{\circ}\text{C}$). Values near 5°C have been used in previous studies.

CNT3 - upper temperature bound for sediment ammonia-nitrogen release to occur near the maximum rate ($^{\circ}\text{C}$). Values near 35°C have been used in previous studies.

CNT4 - upper temperature bound for sediment ammonia-nitrogen release to continue. Values of 40°C have been used in previous studies.

NOTE: The wide range of temperature values provided above results in temperature rate multipliers of near unity for the majority of conditions expected to occur in reservoirs.

259. CARD RS.

CNK1 - rate multiplier that corresponds to CNT1 . Values should be near 0.1.

CNK2 - rate multiplier that corresponds to CNT2 . Values should be near 0.98.

CNK3 - rate multiplier that corresponds to CNT3 . Values should be near 0.98.

CNK4 - rate multiplier that corresponds to CNT4 . Values should be near 0.1.

260. CARD RT.

TSODx - value ($\text{g m}^{-2} \text{ day}^{-1}$) which represents the maximum rate of sediment oxygen demand. Sediment oxygen demand is known to vary spatially in reservoirs due to differences in sedimentation patterns. CE-QUAL-W2 allows the specification of up to three different maximum rates of sediment oxygen demand for different longitudinal sections of the grid. Rates of sediment oxygen demand typically range from 0.1 to $1.0 \text{ g O}_2 \text{ m}^{-2} \text{ day}^{-1}$ but may go higher (Newbold and Liggett 1974). Other information may be found in Gunnison, Chen, and Brannon (1983), in Chen, Brannon, and Gunnison (1984), and in Table 25.

Table 25
Sediment Oxygen Demand ($\text{g m}^{-2} \text{ day}^{-1}$)

| <u>Site</u> | <u>Sediment Oxygen Demand</u> | <u>Reference</u> |
|-------------------------------|-------------------------------|--------------------------|
| Cayuga Lake, New York | 0.32-0.98 | Newbold and Liggett 1974 |
| Lake Sammamish, Washington | 1.0 | Bella 1970 |
| Lake Lyndon B. Johnson, Texas | 1.7-5.8 | Schnoor and Fruh 1979 |
| Saginaw River, Michigan | 0.10-5.3 | Chiaro and Burke 1980 |

261. CARD RU.

SODT1 - lower temperature bound for sediment oxygen demand ($^{\circ}\text{C}$). Values near 0°C have been used in previous studies.

SODT2 - lower temperature bound for sediment oxygen demand to continue near the maximum rate ($^{\circ}\text{C}$). Values near 5°C have been used in previous studies.

SODT3 - upper temperature bound for sediment oxygen demand to occur near the maximum rate ($^{\circ}\text{C}$). Values near 35°C have been used in previous studies.

SODT4 - upper temperature bound for sediment oxygen demand to continue ($^{\circ}\text{C}$). Values of near 40°C have been used in previous studies.

NOTE: The wide range of temperature values provided above result in temperature rate multipliers of near unity for the majority of conditions expected to occur in reservoirs.

262. CARD RV.

SODK1 - rate multiplier that corresponds to SODT1 . Values should be near 0.1.

SODK2 - rate multiplier that corresponds to SODT2 . Values should be near 0.98.

SODK3 - rate multiplier that corresponds to SODT3 . Values should be near 0.98.

SODK4 - rate multiplier that corresponds to SODT4 . Values should be near 0.1.

SFCO2 - fraction relating sediment oxygen demand to inorganic carbon production. Values near 1.4 have been used in previous modeling studies.

263. CARD RW.

All of the mass that leaves one compartment by way of a particular process does not necessarily enter one other compartment. For example, the products of algal respiration are assumed to increment the carbon, ammonia, and orthophosphate compartments. For this reason, stoichiometric equivalents are needed.

BIOP - stoichiometric equivalent between organic matter and orthophosphate.

BIOC - stoichiometric equivalent between organic matter and carbon.

BION - stoichiometric equivalent between organic matter and nitrogen.

These equivalents represent the fraction of each element that comprises organic matter. To aid in keeping a mass balance for

different elements, the simplifying assumption is made that all organic matter is made up of the same fraction of different elements. Representative values are 0.005 for BIOP, 0.45 for BIOC, and 0.08 for BION.

264. CARD RX.

TFEREL - value, as a fraction of the specified sediment oxygen demand ($\text{g m}^{-2} \text{ day}^{-1}$), which represents the rate at which iron is released from sediments under anaerobic conditions. Values between 0.3 and 0.5 have been used in previous modeling studies.

TFESET - value (m day^{-1}) which represents the rate at which particulate iron settles in the water column. Values from 0.5 to 2.0 have been used in previous modeling studies.

FEFAC - factor used to increase (or decrease) ADSRBP and ADSRBN due to differential effects of iron versus adsorption by other suspended solids. Values near 1.5 have been used in previous modeling studies.

Calibration Procedures

265. Calibration consists of comparing predictions with historical field data in order to estimate model parameters. While estimates of model parameters may be available from the literature, this manual, or from previous applications, determination of the "best" values for a particular application often requires subjective adjustment of the parameters until an "adequate" fit of the simulation data is obtained.

266. No definite guidelines are provided for data necessary for calibration. A complete calibration would require that everything be known about the system. This is not possible due to the nonavailability of historical data and uncertainties in the systems behavior. However, the data set should be as complete as possible. At a minimum, vertical profiles of temperatures and constituent concentrations of interest should be available at several points along the reservoir over a period of time.

267. A logical sequence for calibration of CE-QUAL-W2 is to first check the water balance, then calibrate the hydrodynamics and temperature, and finally calibrate the water quality compartments. The user typically will specify $ICC = 0$ on the CD card during initial simulations, which allows simulation of hydrodynamics and temperature independently of water quality constituents. The user may also find it necessary to modify hydrodynamic parameters as more information becomes available during water quality simulations. Care should be exercised that all model parameters remain within reasonable ranges and that simulated trends are reasonable.

Water budget

268. The overall water budget of a reservoir is determined by the cumulative effects of inflows, outflows, precipitation, and evaporation. The predicted water body area and capacity relationships should be compared to known relationships to ensure that the geometric schematization accurately represents relationships among pool elevation, volume, and surface area. The water budget may be checked by comparing the predicted reservoir elevation with the recorded or routed reservoir elevation. The difference over the simulation should be less than 0.5 m. Comparisons may also be made between known reservoir volumes and predicted volumes.

269. If there is an error in the water budget, it should first be determined whether the difference results from storm events or is a gradual cumulative error. This is easily checked by comparing predicted with measured elevations using time series plots.

270. Errors in the water budget due to storm events can often be traced to precipitation or errors in inflow measurements. If precipitation is found to be significant, it can be included in water budget (and also heat and water quality) simulations by specifying $IPRECP = 1$ on the MP card and providing values of $PRECIP$ (and $TPRECP$, $CPRECP$) in the TVDS files. Errors concerning inflow measurements may be more complicated. The model CE-QUAL-W2 allows inclusion of effects of upstream inflows and one or more tributaries on water, heat, and constituent balances. Each of these must have a specified flow which could

be in error. More commonly, gaged flows may not account for all of the total inflows to a reservoir. Hydrologic modeling may be required to provide estimates of ungaged flows.

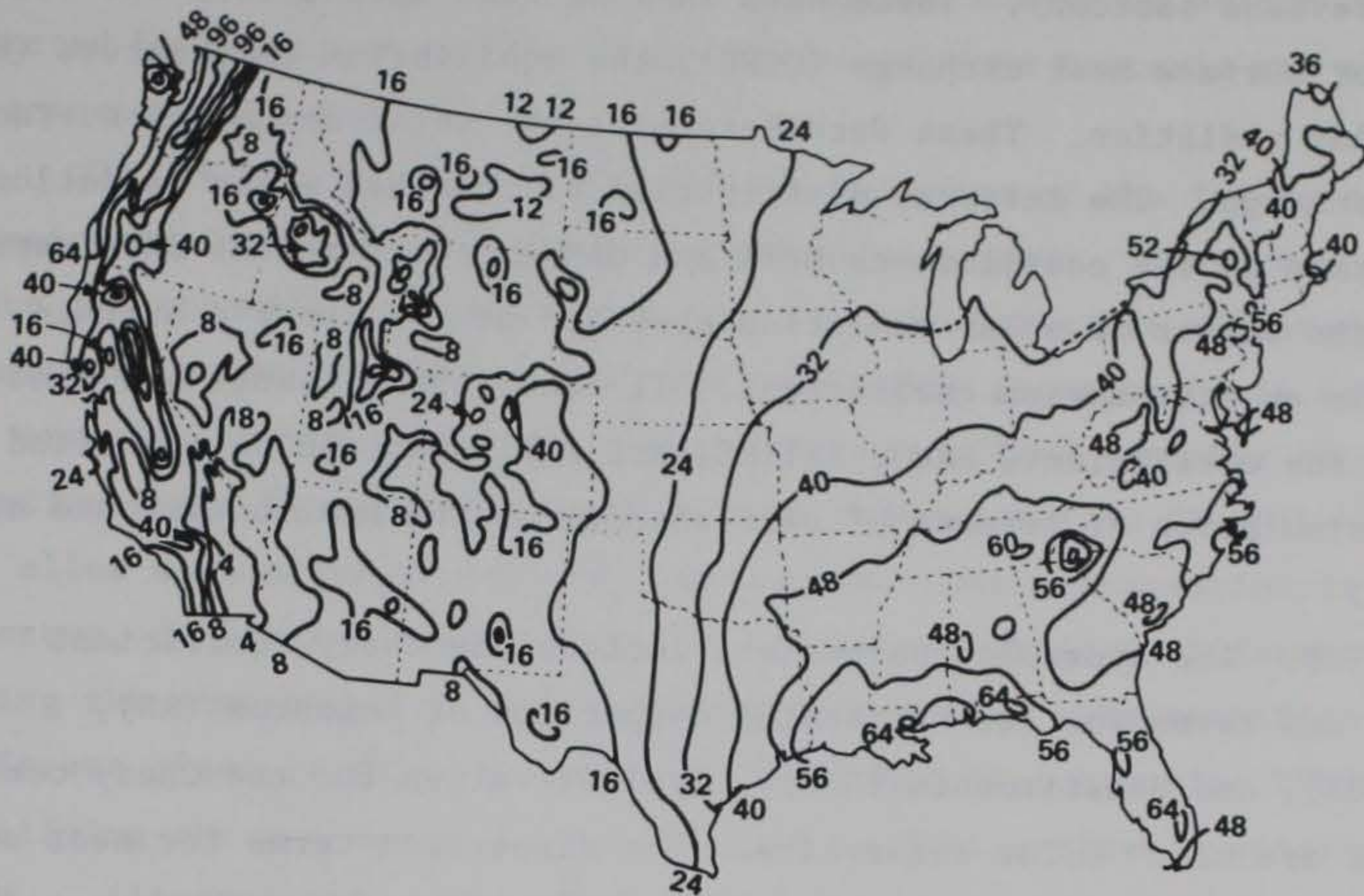
271. Gradual, cumulative errors in the water budget may often be attributed to evaporation, outflows, or seepage. Evaporation is always included in heat budget calculations. Its inclusion in the water budget is specified by setting IEVAP = 1 on the MP card. Evaporative flow and cumulative evaporation are provided in Tape 6 (GRID) data, which can be compared with evaporation data for the area or with average evaporation rates expected for the region (Figure 22). External outflows due to release through structures or withdrawals may be included in water, heat, and constituent balances. Errors due to outflows and seepage need to be checked by investigating outflow measurements.

Thermal structure

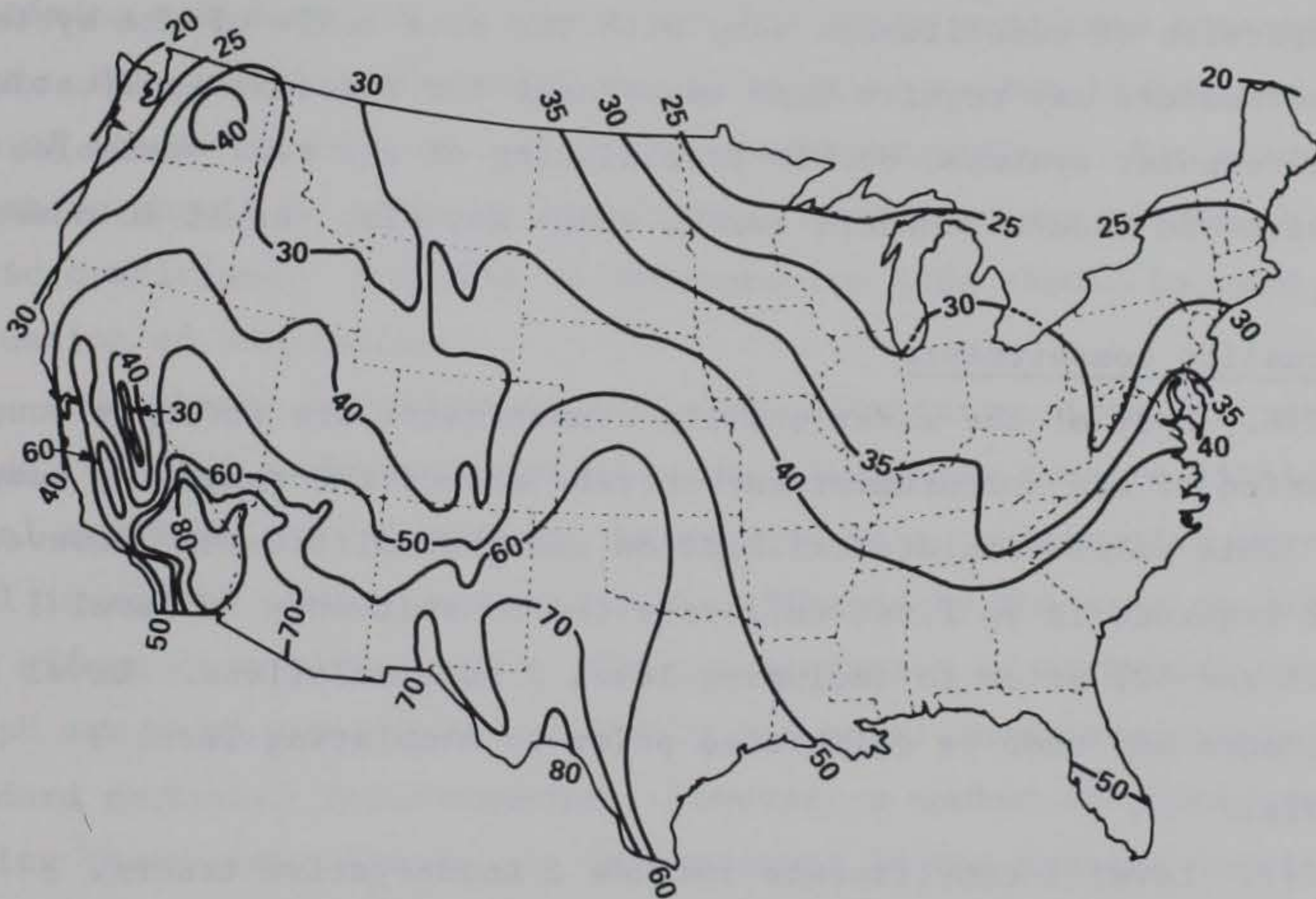
272. The thermal structure is calibrated by comparing predictions with measured profiles. Emphasis should be placed on the timing of the onset of stratification, thermocline depth, gradient in the metalimnion, hypolimnetic temperatures, epilimnetic temperatures, and time and temperature of fall overturn where seasonal stratification patterns are simulated. Calibration of hydraulic parameters is also required at this time to adequately depict temperature variations. However, temperature is not an ideal variable for mixing calibration. Temperature is nonconservative and is affected by surface heat exchange and flows. The hydraulic parameters may require some recalibration when other constituents are included in simulations.

273. Heat contributions due to inflows, tributaries, and precipitation may be included in the heat budget by specifying a flow rate and corresponding temperature. Outflows and withdrawals may also be included in the heat budget computations by specifying their locations and flow rates through TVDS. Ice effects may also be included in simulations.

274. The model CE-QUAL-W2 utilizes the equilibrium temperature approach in computing surface heat exchanges. This requires that time-varying meteorological data be supplied through the TVDS subroutine



a. AVERAGE ANNUAL PRECIPITATION (NWS), INCHES



b. AVERAGE ANNUAL LAKE EVAPORATION (NWS), INCHES

Figure 22. Isoplots of annual precipitation and lake evaporation (National Weather Service) (to convert inches to centimetres, multiply by 2.54)

(see previous section). These data include wind speeds (W), the coefficient of surface heat exchange (CSHE), the equilibrium temperature (ET), and solar radiation. These data determine the total amount of surface heat exchange. The internal distribution of absorbed solar radiation is determined by the coefficients BETA and GAMMA. Coefficient BETA represents the amount of solar radiation absorbed at the water's surface, and GAMMA is an attenuation coefficient. If other constituents are simulated, the coefficients EXCO, EXTINS, and EXTINP should be specified to allow simulation of effects of self-shading on the heat budget and algal growth.

275. The hydraulic parameters include the Chezy coefficient (CHZY) and terms for the horizontal dispersion of momentum (AX), heat (DX), and constituents (DXC). Typical values for the Chezy coefficient are near 70 for reservoirs. The dispersion terms for heat and possibly momentum may have to be arbitrarily high to prevent excessive vertical mixing due to discretization anomalies (Martin 1985). Values for dispersion of constituents vary with the size scale of the system. These parameters may require some adjustment for specific applications. On some computer systems, double-precisioning of all real variables may be required to reduce roundoff error, which may also result in numerical mixing.

Water quality compartments

276. Many of the water quality compartments are strongly coupled. Calibration of one compartment may thereby affect the remaining compartments. This makes complete calibration somewhat difficult. However, a logical sequence is to first calibrate the constituents in level 1 (see pages 11 and 12) prior to including level 2 in simulations. Level 2 constituents may then be calibrated prior to simulating level 3 materials.

277. Level 1 constituents include a conservative tracer, inorganic suspended solids, coliform bacteria, and total dissolved solids (or salinity). The conservative tracer allows comparison of results of tracer studies or simulation of movements of conservative materials through the reservoir. Total dissolved solids are also

treated as a conservative material. Inorganic suspended solids are only affected by transport and settling, while coliform bacteria are affected by transport and die-off.

278. Level 2 constituents allow simulation of the interactive dynamics of dissolved oxygen-phytoplankton-nutrients. These compartments are strongly coupled. Before any coefficients are adjusted, it is important to identify the cause of a particular phenomenon, if possible. For example, changes in algal populations may affect a number of other constituents. However, the single algal compartment in CE-QUAL-W2 does not allow simulation of seasonal succession. Where succession is known to occur, different algal parameters may be required at different times during the simulation to represent the assemblage. The specification of different algal parameters may be accomplished in subroutine TVDS by specifying the appropriate computational variables after a specific ABTM. Alternatively, the simulation may be broken into units by employing the restart option. Particular attention should be given to the timing and duration of events as well as to predicted concentrations. For example, attention should be given to the timing and duration of events as well as to predicted concentrations. For example, attention should be given to the timing, duration, and placement of anoxic conditions. A number of interpretive aids should be used in evaluation of simulations.

279. Level 3 constituents include alkalinity, total inorganic carbon, pH, and carbonate species. This level may require little additional calibration. Alkalinity is treated as a conservative material. Total inorganic carbon is essentially affected by the same processes that affect dissolved oxygen. The concentration of carbonate species and pH are calculated from alkalinity and total inorganic carbon using standard carbonate relationships. However, a number of processes affecting these constituents are not included in the present model structure. For example, carbonate precipitation is not included in formulations. Model limitations must be evaluated in terms of known processes affecting, or expected to affect, the system.

Confirmation

280. Confirmation consists of application of the model to a second, independent data set to determine if the model will yield reliable and informative predictions. Proper confirmation of the model reduces the risks associated with its use in evaluating management or design alternatives. Prior to confirmation, the users must identify the criteria that will be used to indicate successful confirmation.

281. Data may not exist for calibration/confirmation, such as for a preimpoundment study. A nearby reservoir with similar characteristics for which data are available may then be used for this purpose. If calibration/confirmation cannot be accomplished, it is desirable to conduct sensitivity analyses for major variables of interest to place a range or bounds on model predictions.

Output Interpretation

282. The model CE-QUAL-W2 can very quickly produce an overwhelming quantity of data. A variety of numerical, statistical, and graphical tools have been provided to aid the user in interpretation of data. However, output interpretation is a major task which can largely affect the success of, and expense involved in, applications.

283. The interpretation of model results must be based on a thorough knowledge of the limitations and assumptions of CE-QUAL-W2, as well as site-specific characteristics. This interpretation should involve interactions with a multidisciplinary group. This is essential because the model incorporates physical, biological, and chemical considerations. The users should interpret the results in terms of what is known about the system and determine if the model predictions are realistic. The users should also determine what criteria will be used to determine successful completion of calibration and confirmation.

284. No single aid should be used exclusively in interpreting results. For example, comparisons of predicted and simulated vertical profiles should not be the sole criteria to evaluate the success of

simulations. Differences may result from longitudinal displacements of predicted and observed profiles, which may only be detected using other output aids. Errors in circulation patterns may be detected using vector plots. Additionally, no single compartment or variable should be used in interpreting results of simulations. Many of the compartments are strongly coupled, and their interactions must be considered.

REFERENCES

- Alexander, M. 1965. Microbial Ecology, John Wiley and Sons, New York.
- Allen, W. E. 1932. "Marine Plankton Diatom of Lower California in 1931," Botanical Gazette, Vol 95, pp 485-492.
- Apstein, C. 1910. "Hat ein Organisms in der Tiefe Gelebt, in der er gefischt ist?" Internat. Rev. Ges. Hydrobiol. Hydrograph, Vol 3, pp 17-33.
- Ashton, G. D. 1979. "Suppression of River Ice by Thermal Effluents," CRREL Report 79-30, US Army Engineer Cold Regions Research and Engineering Laboratory, Hanover, N. H.
- Bannister, T. T. 1979. "Quantitative Description of Steady State, Nutrient-Saturated Algal Growth, Including Adaptation," Limnology and Oceanography, Vol 24, pp 76-96.
- Bansal, M. K. 1976. "Nitrification in Natural Streams," Water Pollution Control Federation Journal, Vol 48, pp 2380-2393.
- Belay, A. 1981. "An Experimental Investigation of Inhibition of Phytoplankton Photosynthesis at Lake Surfaces," New Phytologist, Vol 89, pp 61-74.
- Bella, D. 1970. "Dissolved Oxygen Variations in Stratified Lakes," ASCE Journal of the Sanitary Engineering Division, Vol 96, No. SA5, pp 1129-1146.
- Bernard, F. 1963. "Vitesses de chute chez *Cyclococcolithus fragilis* Lohm," Consequences Pour le Cycle Vital Des Mers Chaudes.
- Bloss, S., and Harleman, D. R. F. 1979. "Effect of Wind Mixing on the Thermocline Formation in Lakes and Reservoirs," R. M. Parsons Laboratory Report 249, Department of Civil Engineering, Massachusetts Institute of Technology, Cambridge, Mass.
- Blum, J. J. 1966. "Phosphate Uptake by Phosphate-Starved *Euglena*," Journal of General Physiology, Vol 49, pp 1125-1137.
- Bohan, J. P., and Grace, J. L., Jr. 1973. "Selective Withdrawal from Man-Made Lakes: Hydraulic Laboratory Investigation," Technical Report H-73-4, US Army Engineer Waterways Experiment Station, Vicksburg, Miss.
- Borchardt, J. A. 1966. "Nitrification in the Activated Sludge Process," The Activated Sludge Process, Division of Sanitary and Water Resources Engineering, University of Michigan, Ann Arbor.
- Bott, T. L. 1975. "Bacterial Growth Rates and Temperature Optima in a Stream with a Fluctuating Thermal Regime," Limnology and Oceanography, Vol 20, pp 191-197.
- Boylen, C. W., and Brock, T. D. 1973. "Bacterial Decomposition Processes in Lake Wingra Sediments During Winter," Limnology and Oceanography, Vol 18, pp 628-634.

- Brady, D. K., Graves, W. L., and Geyer, J. C. 1969. "Surface Heat Exchange at Power Plant Cooling Lakes," Cooling Water Discharge Project No. 5, Publication No. 69-901, Edison Electric Institute, New York.
- Bramlette, M. N. 1961. (In) Oceanography, No. 67, pp 345-366, M. Sears, ed., American Association of Science, Washington, DC.
- Buchak, E. M., and Edinger, J. E. 1982a. "Hydrothermal Simulation of Quabbin Reservoir Using Longitudinal-Vertical Hydrodynamics, Interim Report," prepared for Wallace, Floyd Associates, Inc., Cambridge, Mass.
- _____. 1982b. "User's Guide for LARM2: A Longitudinal-Vertical, Time Varying Hydrodynamic Reservoir Model," Instruction Report E-82-3, US Army Engineer Waterways Experiment Station, Vicksburg, Miss.
- _____. 1984. "Generalized Longitudinal-Vertical Hydrodynamics and Transport: Development, Programming and Applications" (Contract No. DACW39-84-M-1636), prepared for US Army Engineer Waterways Experiment Station, Vicksburg, Miss.
- Burns, N. M. 1976. "Nutrient Budgets for Lake Erie," Journal of the Fisheries Research Board of Canada, Vol 33, pp 520-536
- Burns, N. M., and Rosa, F. 1980. "In situ Measurement of Settling Velocity of Organic Carbon Particles and 10 Species of Phytoplankton," Limnology and Oceanography, Vol 25, pp 855-864.
- Caperon, J., and Meyer, J. 1972. "Nitrogen-Limited Growth of Marine Phytoplankton; I. Changes in Population Characteristics with Steady-State Growth Rate," Deepsea Research with Oceanography, Vol 9, pp 601-618.
- Carney, J. F., and Colwell, R. R. 1976. "Heterotrophic Utilization of Glucose and Glutamate in an Estuary: Effect of Season and Nutrient Load," Applied and Environmental Microbiology, Vol 31, pp 227-233.
- Carpenter, E. J., and Guillard, R. R. L. 1971. "Intraspecific Differences in Nitrate Half-Saturation Constants for Three Species of Marine Phytoplankton," Ecology, Vol 52, pp 183-185.
- Castenholz, R. W. 1964. "The Effect of Daylength and Light Intensity on the Growth of Littoral Marine Diatoms in Culture," Physiological Plant, Vol 17, pp 951-963.
- _____. 1969. "The Thermophilic Cyanophytes of Iceland and the Upper Temperature Limit," Journal of Phycology, Vol 5, pp 360-368.
- Chapra, S. C., and Reckhow, K. W. 1983. Engineering Approaches for Lake Management, Vol 12: Mechanistic Modeling, Butterworth Publishers, Boston, Mass.
- Chen, R. L., Brannon, J. M., and Gunnison, D. 1984. "Anaerobic and Aerobic Rate Coefficients for Use in CE-QUAL-R1," Miscellaneous Paper E-84-5, US Army Engineer Waterways Experiment Station, Vicksburg, Miss.

- Chiaro, P. S., and Burke, D. A. 1980. "Sediment Oxygen Demand and Nutrient Release," ASCE Journal of the Environmental Engineering Division, Vol 106, No. EE1, pp 177-195.
- Clendenning, K. A., Brown, T. E., and Eyster, H. C. 1956. Canadian Journal of Botany, Vol 34, pp 943-966.
- Cloern, J. E. 1977. "Effects of Light Intensity and Temperature on *Cryptomonas* (Cryptophyceae) Growth and Nutrient Uptake Rates," Journal of Phycology, Vol 13, pp 389-395.
- Collins, C. D., and Boylen, C. W. 1982a. "Physiological Responses of *Anabaena variabilis* (Cyanophyceae) to Instantaneous Exposure to Various Combinations of Light Intensity and Temperature," Journal of Phycology, Vol 18, pp 206-211.
- _____. 1982b. "Ecological Consequences of Long-Term Exposure of *Anabaena variabilis* to Shifts in Environmental Conditions," Applied and Environmental Microbiology, Vol 44, pp 141-148.
- Courchaine, R. J. 1968. "Significance of Nitrification in Stream Analysis--Effects on the Oxygen Balance," Journal of the Water Pollution Control Federation, Vol 40, p 835.
- Edinger, J. E., Brady, D. K., and Geyer, J. C. 1974 (Nov). "Heat Exchange and Transport in the Environment," Report No. 14, prepared for Electric Power Research Institute, Cooling Water Discharge Research Project (RP-49), EPRI Publication No. 74-049-00-3, Palo Alto, Calif.
- Edinger, J. E., and Buchak, E. M. 1975 (Sep). "A Hydrodynamic, Two-Dimensional Reservoir Model: The Computational Basis," prepared for US Army Engineer Division, Ohio River, Cincinnati, Ohio.
- _____. 1978 (Sep). "Reservoir Longitudinal and Vertical Implicit Hydrodynamics," Environmental Effects of Hydraulic Engineering Works, Proceedings of an International Symposium, Knoxville, Tenn.
- _____. 1980. "Numerical Hydrodynamics of Estuaries," Estuarine and Wetland Processes with Emphasis on Modeling, P. Hamilton and K. B. Macdonald, eds., Plenum Press, New York, pp 115-146.
- _____. 1983. "Developments in LARM2: A Longitudinal-Vertical, Time Varying Hydrodynamic Reservoir Model," Technical Report E-83-1, US Army Engineer Waterways Experiment Station, Vicksburg, Miss.
- Edinger, J. E., Buchak, E. M., and Merritt, D. H. 1983. "Longitudinal-Vertical Hydrodynamics and Transport with Chemical Equilibria for Lake Powell and Lake Mead," Salinity in Watercourses and Reservoirs, R. H. French, ed., Butterworth Publishers, Stoneham, Mass., pp 213-222.
- Edinger, J. E., and Geyer, J. C. 1965. "Heat Exchange in the Environment," Publication No. 65-902, Edison Electric Institute, New York, N. Y.

Environmental Laboratory. 1985. "CE-QUAL-R1: A Numerical One-Dimensional Model of Reservoir Water Quality; User's Manual," Instruction Report E-82-1 (Rev. Ed.), US Army Engineer Waterways Experiment Station, Vicksburg, Miss.

Eppley, R. W., Holmes, R. W., and Strickland, J. D. H. 1967b. "Sinking Rates of Marine Phytoplankton Measured with a Fluorometer," Journal of Experimental Marine Biology and Ecology, Vol 1, pp 191-208.

Eppley, R. W., Rogers, J. N., and McCarthy, J. J. 1969. "Half-Saturation Constants for Uptake of Nitrate and Ammonia by Marine Phytoplankton," Limnology and Oceanography, Vol 14, pp 912-920.

Eppley, R. W., and Sloan, P. R. 1966. "Growth Rates of Marine Phytoplankton: Correlation with Light Adsorption by Cell Chlorophyll-a," Physiological Plant, Vol 19, pp 47-59.

Eppley, R. W., and Thomas, W. H. 1969. "Comparison of Half-Saturation Constants for Growth and Nitrate Uptake of Marine Phytoplankton," Journal of Phycology, Vol 5, pp 375-379.

Evans, F. C., Goldreich, E. C., Weibel, S. R., and Robeck, G. G. 1968. "Treatment of Urban Storm Runoff," Journal of the Water Pollution Control Federation, Vol 40, pp 162-170.

Fenchel, T. 1970. "Studies of the Decomposition of Organic Detritus Derived from Turtle Grass *Thalassia testudinum*," Limnology and Oceanography, Vol 15, pp 14-20.

Finenko, Z. Z., and Krupatkina-Aki-Nina, D. K. 1974. "Effect of Inorganic Phosphorus on the Growth Rate of Diatoms," Marine Biology, Vol 26, pp 193-201.

Fitzgerald, G. P. 1964. "The Effect of Algae on BOD Measurements," National Pollution Control Federation Journal, Vol 36, pp 1524-1542.

Fogg, G. E. 1969. "The Physiology of an Algal Nuisance," Proc. R. Soc. B., Vol 173, pp 175-189.

_____. 1973. "Phosphorus in Primary Aquatic Plants," Water Research, Vol 7, pp 77-91.

Ford, D. E., and Johnson, M. C. 1983. "An Assessment of Reservoir Density Currents and Inflow Processes," Technical Report E-83-7, US Army Engineer Waterways Experiment Station, Vicksburg, Miss.

Fowler, S. W., and Small, L. F. 1972. Limnology and Oceanography, Vol 17, pp 293-296.

Frost, W. H., and Streeter, H. W. 1924. "Bacteriological Studies," Public Health Bulletin 143, US Public Health Service, Washington, DC.

Fuhs, G. W., Demmerle, S. D., Canelli, E., and Chen, M. 1972.

"Characterization of Phosphorus-Limited Plankton Algae," Limnol. Oceanogr. Special Symposia, Vol 1, pp 113-133.

- Geldreich, E. E., Best, L. C., Kenner, B. A., and Van Donsel, D. J. 1968. "The Bacteriological Aspects of Stormwater Pollution," Journal of the Water Pollution Control Federation, Vol 40, p 1861.
- Giese, A. C. 1968. Cell Physiology, 3d ed., W. B. Saunders Co., Philadelphia, Pa.
- Gill, A. E. 1982. "Appendix 3, Properties of Seawater," Atmosphere-Ocean Dynamics, Academic Press, New York, pp 599-600.
- Goldman, J. C., and Graham, S. J. 1981. "Inorganic Carbon Limitation and Chemical Composition of Two Freshwater Green Microalgae," Applied and Environmental Microbiology, Vol 41, pp 60-70.
- Goldman, J. C., Porcella, D. B., Middlebrooks, E. J., and Toerien, D. F. 1972. "The Effects of Carbon on Algal Growth--Its Relationship to Eutrophication," Water Research, Vol 6, pp 637-679.
- Golterman, H. L. 1975. Physiological Limnology, Elsevier, Amsterdam.
- Gordon, J. A. 1980. "An Evaluation of the LARM Two-Dimensional Model for Water Quality Management Purposes," Proceedings of the Symposium on Surface-Water Impoundments, Minneapolis, Minn., June 2-5, 1980, Vol 1, Paper 4-34, pp 518-527, American Society of Civil Engineers, New York.
- _____. 1981. "LARM Two-Dimensional Model: An Evaluation," ASCE Journal of the Environmental Engineering Division, 107(E5), pp 877-886.
- _____. 1983. "Short-Term Hydrodynamics in a Stratified Reservoir," Environmental Engineering, Proceedings of the ASCE Specialty Conference, Hilton Harvest House, Boulder, Colo., July 6-8, 1983, pp 524-531, American Society of Civil Engineers, New York.
- Green, D. B., Logan, J., and Smeck, N. E. 1978. "Phosphorus Adsorption-Desorption Characteristics of Suspended Sediments in the Maumee River of Ohio," Journal of Environmental Quality, Vol 7, pp 208-212.
- Guillard, R. R. L., and Ryther, J. H. 1962. "Studies on the Marine Planktonic Diatoms; I. *Cyclotella nana* Hustedt and *Detonula confervacea* (Cleve)," Canadian Journal of Microbiology, Vol 8, pp 229-239.
- Gunnison, D., and Alexander, M. 1975. "Resistance and Susceptibility of Algae to Decomposition by Natural Microbial Communities," Limnology and Oceanography, Vol 20, pp 64-70.
- Gunnison, D., Chen, R. L., and Brannon, J. M. 1983. "Relationship of Materials in Flooded Soils and Sediments to the Water Quality of Reservoir; I. Oxygen Consumption Rates," Water Research, Vol 17, No. 11, pp 1609-1617.
- Hall, G. H. 1982. "Apparent and Measured Rates of Nitrification in the Hypolimnion of a Mesotrophic Lake," Applied and Environmental Microbiology, Vol 43, pp 542-547.

- Halmann, M., and Stiller, M. 1974. "Turnover and Uptake of Dissolved Phosphate in Freshwater; A Study in Lake Kinneret," Limnology and Oceanography, Vol 19, pp 774-783.
- Hanlon, R. D. G. 1982. "The Breakdown and Decomposition of Allochthonous and Autochthonous Plant Litter in an Oligotrophic Lake (Llyn Frongoch)," Hydrobiologia, Vol 88, pp 281-288.
- Harbeck, G. E., Koberg, G. E., and Hughes, G. H. 1959. "The Effect of Addition of Heat...on Lake Colorado City, Texas," USGS Professional Paper 272-B, US Government Printing Office, Washington, DC.
- Hargrave, B. T. 1972a. "Aerobic Decomposition of Sediment and Detritus as a Function of Particle Surface Area and Organic Content," Limnology and Oceanography, Vol 17, pp 582-597.
- _____. 1972b. "Oxidation-Reduction Potentials, Oxygen Concentration and Oxygen Uptake of Profundal Sediments in a Eutrophic Lake," Oikos, Vol 23, pp 167-177.
- Hattori, A. 1962. "Light-Induced Reduction of Nitrate, Nitrite and Hydroxylamine in a Blue-green Alga, *Anabaena cylindrica*," Plant Cell Physiology, Vol 3, pp 355-369.
- Hecky, R. E., and Kilham, P. 1974. "Environmental Control of Phytoplankton Cell Size," Limnology and Oceanography, Vol 19, No. 2, pp 361-365.
- Hendry, G. R., and Welch, E. 1973. "The Effects of Nutrient Availability and Light Intensity on the Growth Kinetics of Natural Phytoplankton Communities," Presentation, American Society for Limnology and Oceanography, 36th Annual Meeting, Salt Lake City, Utah.
- Holm, N. P., and Armstrong, D. E. 1981. "Role of Nutrient Limitation and Competition in Controlling the Populations of *Asterionella formosa* and *Microcystis aeruginosa* in Semicontinuous Culture," Limnology and Oceanography, Vol 26, pp 622-634.
- Hoogenhout, H., and Amesz, J. 1965. "Growth Rates of Photosynthetic Microorganisms in Laboratory Studies," Archives of Microbiology, Vol 50, pp 10-24.
- Hoskins, J. K., Ruchhoft, C. C., and Williams, L. G. 1927. "A Study of the Pollution and Natural Purification of the Illinois River; I. Surveys and Laboratory Studies," Public Health Bulletin No. 171, Washington, DC.
- Hutchinson, G. E. 1957. A Treatise on Limnology; I. Geography, Physics and Chemistry, John Wiley and Sons, New York.
- Hwang, C. P., Lackie, T. H., and Huang, P. M. 1976. "Adsorption of Inorganic Phosphorus by Lake Sediments," Journal of the Water Pollution Control Federation, Vol 48, pp 2754-2760.
- Ignatiades, L., and Smayda, T. J. 1970. "Autecological Studies on the Marine Diatom *Rhizosolenia fragilissima* Bergon; I. The Influence of Light, Temperature, and Salinity," Journal of Phycology, Vol 6, pp 332-229.

- Jacoby, G. C., Jr., et al. 1977. "Evaporation, Bank Storage and Water Budget at Lake Powell," Lake Powell Research Project Bulletin No. 48, Institute of Geophysics and Planetary Physics, University of California, Los Angeles, Calif.
- Janik, J. J., Taylor, W. D., and Lambou, V. W. 1981. "Estimating Phytoplankton Biomass and Productivity," Miscellaneous Paper E-81-2, US Army Engineer Waterways Experiment Station, Vicksburg, Miss.
- Jeanjean, R. 1969. "Influence de la Carence en Phosphore sur les Vitesses d'Absorption du Phosphate Par les Chlorelles," Bull. Soc. Fr. Physiol. Veg., Vol 15, pp 159-171.
- Jewell, W. J., and McCarty, P. L. 1971. "Aerobic Decomposition of Algae," Environment Science and Technology, Vol 5, pp 1023-1031.
- Jitts, H. R., McAllister, C. D., Stephens, K., and Strickland, J. D. H. 1964. "The Cell Division Rates of Some Marine Phytoplankton as a Function of Light and Temperature," Journal of the Fisheries Research Board of Canada, Vol 21, pp 139-157.
- Johnson, M. C., et al. 1981 (Oct). "Analyzing Storm Event Data from DeGray Lake, Arkansas Using LARM," presented at the American Society of Civil Engineers 1981 Convention and Exposition, St. Louis, Mo.
- Jorgensen, E. G. 1968. "The Adaptation of Plankton Algae; II. Aspects of the Temperature and the Temperature Adaptation of *Skeletonema costatum*," Physiological Plant, Vol 21, pp 423-427.
- Kamp-Nielson, L. 1974. "Mud-Water Exchange of Phosphate and Other Ions in Undisturbed Sediment Cores and Factors Affecting Exchange Rates," Archives of Hydrobiologia, Vol 73, pp 218-237.
- Kanwisher, J. 1963. "On the Exchange of Gases Between the Atmosphere and the Sea," Deepsea Research with Oceanography, Vol 10, pp 195-207.
- Ketchum, B. H. 1939. "The Absorption of Phosphate and Nitrate by Illuminated Cultures of *Nitzschia closterium*," American Journal of Botany, Vol 26, pp 399-407.
- Kinsman, B. 1979. Wind Waves: Their Generation and Propagation, Prentice-Hall, Englewood Cliffs, N. J.
- Kirk, J. T. O. 1975. "A Theoretical Analysis of the Contribution of Algal Cells to the Attenuation of Light Within Natural Waters; I. General Treatment of Suspensions of Pigmented Cells," New Phytology, Vol 75, pp 11-20.
- Kittrell, F. W., and Furfari, S. A. 1963. "Observations of Coliform Bacteria in Streams," Journal of the Water Pollution Control Federation, Vol 35, p 1361.
- Kittrell, F. W., and Koschtitzky, O. W., Jr. 1947. "Natural Purification Characteristics of a Shallow Turbulent Stream," Sewage Works Journal, Vol 19, p 1031.

- Klock, J. W. 1971. "Survival of Coliform Bacteria in Wastewater Treatment Lagoons," Journal of the Water Pollution Control Federation, Vol 43, p 2071.
- Knowles, G., Downing, A. L., and Barrett, M. J. 1965. "Determination of Kinetic Constants for Nitrifying Bacteria in Mixed Culture, with the Aid of an Electronic Computer," Journal of General Microbiology, Vol 38, pp 263-278.
- Knudsen, G. 1965. "Induction of Nitrate Reductase in Synchronized Cultures of *Chlorella pipenodosa*," Biochem. Biophys. Acta., Vol 103, pp 495-502.
- Konopka, A. 1983. "The Effect of Nutrient Limitation and Its Interaction with Light upon the Products of Photosynthesis in *Merismopedia tenuissima* (Cyanophyceae)," Journal Phycology, Vol 19, pp 403-409.
- Ku, W. C., Di Giano, F. A., and Feng, T. H. 1978. "Factors Affecting Phosphate Adsorption Equilibria in Lake Sediments," Water Research, Vol 12, pp 1069-1074.
- Lane, E. W. 1938. "Notes on Formation of Sand," Transactions of the American Geophysical Union, Vol 18, pp 505-508.
- Laws, E. A., and Wong, D. C. 1978. "Studies of Carbon and Nitrogen Metabolism by Three Marine Phytoplankton Species in Nitrate-Limited Continuous Culture," Journal of Phycology, Vol 14, pp 406-416.
- Leendertse, J. J., and Liu, S-K. 1977. "Turbulent Energy for Computation; Volume IV, A Three-Dimensional Model for Estuaries and Coastal Seas," Report No. 2-2187-OWRT, The Rand Corporation, Santa Monica, Calif.
- Li, W. K. W., and Morris, I. 1982. "Temperature Adaptation in *Phaeodactylum tricornutum* Bohlin: Photosynthetic Rate Compensation and Capacity," Journal of Experimental Marine Biology and Ecology, Vol 58, pp 135-150.
- MacIsaac, J. H., and Dugdale, R. C. 1969. "The Kinetics of Nitrate and Ammonia Uptake by Natural Populations of Marine Phytoplankton," Deepsea Research with Oceanography, Vol 16, pp 16-27.
- Mackay, D. 1980. "Solubility, Partition Coefficients, Volatility, and Evaporation Rates," Vol 2, Part A, Reactions and Processes Handbook, Springer Verlag, New York.
- Mahloch, J. L. 1974. "Comparative Analysis of Modeling Techniques for Coliform Organisms in Streams," Applied Microbiology, Vol 27, p 340.
- Mann, K. H. 1972. "Ecology Energetics of the Seaweed Zone in a Marine Bay on the Atlantic Coast of Canada; I. Zonation and Biomass of Seaweeds," Marine Biology (Berlin), Vol 12, pp 1-10.
- Marais, G. V. R. 1974. "Faecal Bacterial Kinetics in Stabilization Ponds," ASCE Journal of the Sanitation Engineering Division, Vol 100, No. EE1, p 119.

- Margalef, R. 1961. "Velocidad de Sedimentation de Organismos Pasivos del Fitoplancton," Investigacion Pesq., Vol 18, pp 3-8.
- Martin, J. L. 1986. "Application of a Two-Dimensional Model of Hydrodynamics and Water Quality (CE-QUAL-W2) to DeGray Lake, Arkansas," Technical Report in preparation, US Army Engineer Waterways Experiment Station, Vicksburg, Miss.
- Megard, R. O., Comles, W. S., Smith, P. D., and Knoll, A. S. 1980. "Attenuation of Light and Daily Integral Rates of Photosynthesis Attained by Planktonic Algae," Limnology and Oceanography, Vol 24, pp 1038-1050.
- Meyer, A. F. 1928. The Elements of Hydrology, John Wiley and Sons, New York.
- Mitchell, R., and Chamberlain, C. 1978. "Survival of Indicator Organisms," Indicators of Enteric Contamination in Natural Waters, G. Berg, ed., Ann Arbor Science Publ., Inc., Ann Arbor, Mich., pp 15-38.
- Mortimer, C. H. 1981. "The Oxygen Content of Air Saturated Fresh Waters over Ranges of Temperature and Atmospheric Pressure of Limnological Interest," International Vereinigung Theoretische and Angewandte Limnologie, Vol 22, pp 2-23.
- Morton, F. I. 1965. "Potential Evaporation and River Basin Evaporation," ASCE Journal of the Hydraulics Division, Vol 91, No. HY6, pp 67-97.
- Myers, J., and Graham, J. 1961. "On the Mass Culture of Algae; III. Light Diffusers: High vs. Low Temperature Chlorellas," Plant Physiology, Vol 36, pp 342-346.
- Nalewajko, C. 1966. "Photosynthesis and Excretion in Various Planktonic Algae," Limnology and Oceanography, Vol 11, pp 1-10.
- Newbold, J. D., and Liggett, D. S. 1974. "Oxygen Depletion Model for Cayuga Lake," ASCE Journal of the Environmental Engineering Division, Vol 100, No. EE1, pp 41-59.
- Odum, E. P., and de la Cruz, A. A. 1967. "Particulate Organic Detritus in a Georgia Salt Marsh-Estuarine Ecosystem," Estuaries, G. H. Lauff, ed., American Association for the Advancement of Sciences, Washington, DC, pp 383-388.
- Osterberg, C., Casey, A. G., and Curl, H. 1963. (In) Nature, Vol 200, pp 1276-1277.
- Otsuki, A., and Hanya, T. 1972. "Production of Dissolved Organic Matter from Dead Green Algal Cells; I. Aerobic Microbial Decomposition," Limnology and Oceanography, Vol 17, pp 248-257.
- Paasche, E. 1968. "Marine Plankton Algae Grown with Light-Dark Cycles; II. *Ditylum brightwellii* and *Nitzschia turgidula*," Physiological Plant, Vol 21, pp 66-77.

- Parson, T. R., and Strickland, J. D. H. 1963. "On the Production of Particulate Organic Carbon by Heterotrophic Processes in Sea Water," Deepsea Research with Oceanography, Vol 8, pp 211-222.
- Pickett, J. M. 1975. "Growth of *Chlorella* in a Nitrate-Limited Chemostat," Plant Physiology, Vol 55, pp 223-225.
- Piecznska. 1972. Wiadomosci Ekologiczne, Vol 18, pp 131-140.
- Quasim, S. Z., Bhattathiri, P. M. A., and Dovassoy, V. P. 1973. Marine Biology, Vol 21, pp 299-304.
- Rhee, G-Yull. 1973. "A Continuous Culture Study of Phosphate Uptake, Growth Rate and Polyphosphate in *Scenedesmus* sp.," Journal of Phycology, Vol 9, pp 495-506.
- Rhee, G-Yull, and Gotham, I. J. 1981a. "The Effects of Environmental Factors on Phytoplankton Growth: Temperature and the Interaction of Temperature with Nutrient Limitation," Limnology and Oceanography, Vol 26, pp 635-648.
- _____. 1981b. "The Effects of Environmental Factors on Phytoplankton Growth: Light and the Interaction of Light with Nitrate Limitation," Limnology and Oceanography, Vol 26, pp 649-659.
- Riley, G. A. 1943. Bulletin of the Bingham Oceanography College, Vol 8, Art. 4, p 53.
- Riley, G. A., Stommel, H., and Bumpus, D. F. 1949. "Quantitative Ecology of the Plankton of the Western North Atlantic," Bulletin of the Bingham Oceanography College, Vol 12, pp 1-169.
- Riley, G. A., and von Aux, R. 1949. (In) Journal of Marine Research, Vol 8, No. 11, pp 60-72.
- Roache, P. J. 1982. Computational Fluid Dynamics, Hermosa Publishers, Albuquerque, N. Mex.
- Rogers, K. H., and Breen, C. M. 1982. "Decomposition of *Potamogeton crispus*; I. Effects of Drying on the Pattern of Mass and Nutrient Loss," Aquatic Botany, Vol 12, pp 1-12.
- Ryding, S. O., and Forsberg, C. 1977. "Sediments as a Nutrient Source in Shallow Polluted Lakes," H. L. Golterman, ed., Interactions Between Sediments and Freshwater, Junk, The Hague.
- Ryther, J. H. 1954. "Inhibitory Effects of Phytoplankton upon the Feeding of *Daphnia magna* with Reference to Growth, Reproduction, and Survival," Ecology, Vol 35, pp 522-533.
- Saunders, G. W. 1972. "The Transformation of Artificial Detritus in Lake Water," Mem. Ist. Ital. Idrobiol. Dott Marco de Marchi, Pallanza, Italy 29 (Suppl), pp 261-288.
- Sawyer, C. N., and McCarty, P. L. 1967. Chemistry for Sanitary Engineers, 2d ed., McGraw-Hill, St. Louis, Mo.

- Schindler, D. W. 1971. "Food Quality and Zooplankton Nutrition," Journal of Animal Ecology, Vol 40, pp 598-595.
- Schindler, D. W., et al. 1973. "Eutrophication of Lake 227 by Addition of Phosphate and Nitrate: The Second, Third and Fourth Years of Enrichment, 1970, 1971, 1972," Journal of the Fisheries Research Board of Canada, Vol 30, pp 1415-1428.
- Schnoor, J. L., and Fruh, E. G. 1979. "Dissolved Oxygen Model of a Short Detention Time Reservoir with Anaerobic Hypolimnion," Water Resources Bulletin, Vol 15, No. 2, pp 506-518.
- Sedell, J. R., Triska, F. J., and Triska, N. S. 1975. "The Processing of Conifer and Hardwood Leaves in Two Coniferous Forest Streams; I. Weight Loss and Associated Invertebrates," Verh. Internat. Verein. Limnol., Vol 19, pp 1617-1627.
- Shelef, G. 1968. "Kinetics of Algal Systems in Waste Treatment; Light Intensity and Nitrogen Concentration as Growth-Limiting Factors," Ph. D. Thesis, University of California, Berkeley.
- Smayda, T. J. 1969. "Experimental Observations on the Influence of Temperature, Light, and Salinity on Cell Division of the Marine Diatom *Detonula confervacea* (Cleve) Gran," Journal of Phycology, Vol 5, pp 150-157.
- _____. 1971. "Normal and Accelerated Sinking of Phytoplankton in the Sea," Marine Geology, Vol 11, pp 105-122.
- _____. 1974. "Some Experiments on the Sinking Characteristics of Two Freshwater Diatoms," Limnology and Oceanography, Vol 19, No. 4, pp 628-635.
- Smayda, T. J., and Boleyn, B. J. 1965. "Experimental Observations on the Flootation of Marine Diatoms; I. *Thalassiosira* cf. *nana*, *Thalassiosira rotula* and *Nitzschia seriata*," Limnology and Oceanography, Vol 10, pp 499-509.
- _____. 1966. "Experimental Observations on the Flootation of Marine Diatoms; III. *Bacteriastrium hyalinum* and *Chaetoceros lauderi*," Limnology and Oceanography, Vol 11, pp 35-43.
- Smith, W. O. 1979. "A Budget for the Autotrophic Ciliate *Mesodinium rubrum*," Journal of Phycology, Vol 15, pp 27-33.
- Smith, R. C., and Baker, K. S. 1978. "The Bio-optical State of Ocean Waters and Remote Sensing," Limnology and Oceanography, Vol 23, pp 247-259.
- Snow, P. D., and Di Giano, F. A. 1976. "Mathematical Modeling of Phosphorus Exchange Between Sediments and Overlaying Water in Shallow Eutrophic Lakes," Report 54-76-3, Department of Civil Engineering, University of Massachusetts, Amherst.
- Sorokin, C., and Krauss, R. W. 1962. "Effects of Temperature and Illumination on *Chorella* Growth Uncoupled from Cell Division," Plant Physiology, Vol 37, pp 37-42.

- Sorokin, C., and Meyers, J. 1953. "A High Temperature Strain of *Chlorella*," Science, Washington, D. C., Vol 117, pp 330-331.
- Spence, D. H. N. 1981. "Light Quality and Plant Responses Underwater," Plants and the Daylight Spectrum, H. Smith, ed., Academic Press, New York, pp 245-276.
- Spencer, D. F., and Lembi, C. A. 1981. "Factors Regulating the Spatial Distribution of the Filamentous Alga *Pithophora oedoga* (Chlorophyceae) in an Indiana Lake," Journal Phycology, Vol 17, pp 168-173.
- Steele, J. H. 1962. "Environmental Control of Photosynthesis in the Sea," Limnology and Oceanography, Vol 7, pp 137-150.
- Steedmann-Nielsen, E. 1952. "On Detrimental Effects of High Light Intensities on the Photosynthetic Mechanism," Physiological Plant, Vol 5, pp 334-344.
- Steedmann-Nielsen, E., and Jorgensen, E. G. 1968. "The Adaptation of Plankton Algae; I. General Part," Physiological Plant, Vol 21, pp 401-413.
- Stumm, W., and Morgan, J. J. 1981. Aquatic Chemistry, Wiley Interscience, New York.
- Talling, J. F. 1955. "The Relative Growth Rates of Three Plankton Diatoms in Relation to Underwater Radiation and Temperature," Ann. Bot. N. S., Vol 19, pp 329-341.
- Tamiya, H. T., Sasa, T., Nikei, T., and Ishibashi, S. 1965. "Effects of Variation of Daylength, Day and Night Temperatures, and Intensity of Daylight on the Growth of *Chlorella*," Journal of General and Applied Microbiology, Vol 4, pp 298-307.
- Tanaka, N., Nakanishi, M., and Kadota, H. 1974. "Nutritional Interrelation Between Bacteria and Phytoplankton in a Pelagic Ecosystem," Effects of the Ocean Environment on Microbial Activities, R. R. Colwell and R. V. Mouta, eds., University Park Press, Baltimore, Md., pp 495-509.
- Thomann, R. V., et al. 1971. "The Effect of Nitrification on the Dissolved Oxygen of Streams and Estuaries," Environmental Engineering and Scientific Program, Manhattan College, Bronx, New York.
- Thomas, W. H., and Dodson, A. N. 1968. "Effects of Phosphate Concentration on Cell Division Rates and Yield of a Tropical Oceanic Diatom," Biological Bulletin, Vol 134, pp 199-208.
- Thompson, J. R., and Bernard, R. S. 1985. "WESSEL: Code for Numerical Simulation of Two-Dimensional Time-Dependent, Width-Averaged Flows with Arbitrary Boundaries," Technical Report E-85-8, US Army Engineer Waterways Experiment Station, Vicksburg, Miss.
- Thornton, K. W., and Lessem, A. S. 1978. "A Temperature Algorithm for Modifying Biological Rates," Transactions of the American Fisheries Society, Vol 107, No. 2, pp 284-287.

- Thornton, K. W., Nix, J. F., and Bragg, J. D. 1980. "Coliforms and Water Quality: Use of Data in Project Design and Operation," Water Resources Bulletin, No. 16, pp 86-92.
- Tison, D. L., and Pope, D. H. 1980. "Effect of Temperature on Mineralization by Heterotrophic Bacteria," Applied and Environmental Microbiology, Vol 39, pp 584-587.
- Tison, D. L., Pope, D. P., and Boylen, C. W. 1980. "Influence of Seasonal Temperature on the Temperature Optima of Bacteria in Sediments of Lake George, New York," Applied and Environmental Microbiology, Vol 39, pp 675-677.
- Titman, D., and Kilham, P. 1976. "Sinking in Freshwater Phytoplankton: Some Ecological Implications of Cell Nutrient Status and Physical Mixing Processes," Limnology and Oceanography, Vol 21, No. 3, pp 109-117.
- Toerien, D. F., and Cavari, B. 1982. "Effect of Temperature on Heterotrophic Glucose Uptake, Mineralization, and Turnover Rates in Lake Sediment," Applied and Environmental Microbiology, Vol 43, pp 1-5.
- Toetz, D., Varga, L., and Loughran, D. 1973. "Half-Saturation Constants for Uptake of Nitrate and Ammonia by Reservoir Plankton," Ecology, Vol 54, pp 903-908.
- Trussell, R. P. 1972. "The Percent Un-ionized Ammonia in Aqueous Ammonia Solutions at Different pH Levels and Temperature," Journal of the Fisheries Research Board of Canada, Vol 29, pp 1505-1507.
- Turner, J. T. 1977. "Sinking Rates of Fecal Pellets from the Marine Copepod *Pontella meadii*," Marine Biology, Vol 40, No. 3, pp 249-259.
- Underhill, P. A. 1977. "Nitrate Uptake Kinetics and Clonal Variability in the Neritic Diatom *Biddulphia aurita*," Journal of Phycology, Vol 13, pp 170-176.
- US Army Engineer District, Baltimore. 1977. "Thermal Simulation of Lakes; User's Manual for Program Numbers 722-F5-E1010 and 722-F5-E1011," Baltimore, Md.
- Vaccaro, R. F. 1969. "The Response of Natural Microbial Populations in Seawater to Organic Enrichment," Limnology and Oceanography, Vol 14, pp 726-735.
- van Lierre, L., Zevenboom, W., and Mur, L. R. 1977. "Nitrogen as a Limiting Factor for the Growth of the Blue Green Alga *Oscillatoria agardhii*," Progressive Water Technology, Vol 8, pp 301-312.
- Verduin, J. 1952. "Photosynthesis and Growth Rates of Live Diatom Communities in Western Lake Erie," Ecology, Vol 33, pp 163-169.
- _____. 1982. "Components Contributing to Light Extinction in Natural Waters: Methods of Isolation," Archives of Hydrobiology, Vol 93, pp 303-312.

- Verity, P. G. 1981. "Effects of Temperature, Irradiance and Daylength on the Marine Diatom *Leptocylindrus danicus* Cleve; I. Photosynthesis and Cellular Composition," Journal of Experimental Marine Biology and Ecology, Vol 55, pp 79-91.
- Vollenweider, R. A. 1968. "Scientific Fundamentals of the Eutrophication of Lakes and Flowing Waters, with Particular Reference to Nitrogen and Phosphorus as Factors in Eutrophication," Tech. Rept. OECD, DAS/CSI/68.27, Paris, France.
- _____. 1976. "Advances in Defining Critical Loading Levels for Phosphorus in Lake Eutrophication," Mem. Inst. Ital. Idrobiol., Vol 33, pp 53-83.
- Von Muller, H. 1972. "Wachstum und Phosphatbedarf von *Nitzschia octinastroides* (Lemm.) V. Goor in Statischer and Homokontinuierlicher Kultur unter Phosphatlimitierung," Arch. Hydrobiol. Suppl., Vol 38, pp 399-484.
- Wallen, D. G., and Cartier, L. D. 1975. "Molybdenum Dependence, Nitrate Uptake and Photosynthesis of Freshwater Plankton Algae," Journal of Phycology, Vol 11, pp 345-349.
- Wang, L. K., Poon, C. P., Wang, M. H., and Bergenthal, J. 1978. "Chemistry of Nitrification-Denitrification Process," Journal of Environmental Sciences, Vol 21, pp 23-28.
- Wetzel, R. G. 1975. Limnology, W. B. Saunders, Philadelphia, Pa.
- Wetzel, R. G., Rich, P. H., Miller, M. C., and Allen, H. L. 1972. "Metabolism of Dissolved Particulate Detrital Carbon in a Temperate Hardwater Lake," Mem. Ist Ital. Idrobiol. Suppl., Vol 29, pp 185-243.
- Whittaker, R. H. 1975. Communities and Ecosystems, MacMillan, New York.
- Wiegel, R. L. 1964. Oceanographical Engineering, Prentice-Hall, Englewood Cliffs, N. J.
- Wild, H. E., Sawyer, C. N., and McMahon, T. C. 1971. "Factors Affecting Nitrification Kinetics," Journal of the Water Pollution Control Federation, Vol 43, pp 1845-1854.
- Williams, D. T., et al. 1980. "Determination of Light Extinction Coefficients in Lakes and Reservoirs," Surface Water Impoundments, Proceedings of the Symposium on Surface Water Impoundments, American Society of Civil Engineers, H. G. Stefan, ed.
- Williams, P. J., Yentsch, L. B., and Yentsch, C. S. 1976. "An Examination of Photosynthetic Production, Excretion of Photosynthetic Products and Heterotrophic Utilization of Dissolved Organic Compounds with Reference to Results from a Coastal Subtropical Sea," Marine Biology, Vol 35, pp 31-40.
- Wright, R. T. 1975. "Studies on Glycolic Acid Metabolism by Freshwater Bacteria," Limnology and Oceanography, Vol 20, pp 626-633.

Wuhrmann, K. 1972. "Stream Purification," Water Pollution Microbiology, R. Mitchell, ed., Interscience, New York.

Zimmerman, U. 1969. "Okologische and Physiologische Untersuchungen an der Planktonischen Blaugale *Oscillatoria Rubescens*, D. C., unter Besonderer Beruchischtigung von Licht and Temperatur," Schweiz. Z. Hydrol., Vol 31, pp 1-58.

Zison, S. W., Mills, W. B., Deimer, B., and Chen, C. W. 1978. "Rates, Constants, and Kinetics Formulations in Surface Water Quality Modeling," EPA-600/3-68-105, US Environmental Protection Agency, Washington, DC.

APPENDIX A: PROGRAMMING ASPECTS

1. Parts I and II of the main text of this user's guide describe the basic structure of CE-QUAL-W2. Examination of the basic relationships and auxiliary functions in Part III of this manual should allow the user to easily follow his FORTRAN representation. However, many of the aspects involved in translating the computational basis into an efficient and maintainable FORTRAN program are only apparent through a detailed examination of the code itself. This detailed analysis may not be necessary for the "casual" user. However, a description of the code is provided for those desiring a detailed knowledge of its structure. Additionally, while the code is generalized, allowing its application to a variety of situations, specific applications may require some modifications. Modifications to the code should be made only after the user is completely familiar with its structure.

2. This section consists of two parts. First, outlines are provided which emphasize various aspects of the code. The outline is also imbedded in the code itself to aid the users. Secondly, a narrative description of various programming aspects and algorithms is provided.

Outline of the Program

3. The outline, or sequence of computations, of CE-QUAL-W2 comes directly from the solution technique presented in Part III. The central task in the solution is the calculation of the water surface elevation. Preceding elements of code evaluate the variables necessary to compute the water surface elevation; those following use the newly computed elevation to calculate the circulation fields and constituent concentrations. This sequence is repeated in order to step the computations through time. This integration sequence is thus a representation of the time-varying nature of the water body simulation problem. There is a second aspect of the water body simulation problem which also has a representation in the program. This aspect is the mapping of the water

body onto a finite difference grid. The resulting hierarchy of grid points, cells, segments and layers, branches, and the water body as a whole requires coding to identify and operate on these components. These basic operations, which are used throughout the program, are described following the presentation of the program outline.

4. Table A1 is a general outline of CE-QUAL-W2. The program consists of three parts, the setup of the computation, the integration through time, and termination. Because the integration is repeated for each time step required by the simulation, this part of the code accounts for nearly all the computational effort. The computation of the hydrodynamics (surface elevation, horizontal and vertical velocities) and constituent concentrations (temperature and other constituents) is the major component of the integration. The component is shown in task 2.4 in the outline. Most of the coding for this task is derived directly from the solution technique and the fundamental equations and auxiliary relationships of Part III. Much of the rest of the program is built around the algorithms, procedures, and nomenclature required to support this task.

Setting up the computation

5. Table A2 a more detailed outline of the first part of the program, setup of the computation. Besides the mathematically mandated task of establishing the initial conditions, the first part of CE-QUAL-W2 also performs the more prosaic tasks of beginning a FORTRAN computation, creating the finite grid, reading the simulation control parameters, and writing all this information for review by the user. It is at this point that many of the algorithms discussed later in this appendix are introduced.

6. The program starts with a list of comments regarding the title, current version, implementation notes, and list of input and output files. The comment section will supplement the user's guide in later versions by documenting specific changes and generic updates since the most recently published user's guide. This comment section is followed by an INCLUDE statement for the external commons file. This statement specifies that the contents of the external commons module is

Table A1
Overall Outline of CE-QUAL-W2

1. Set up the computation
 - 1.1 Introduce the computation
 - 1.2 Read control and geometric data, initialize variables
 - 1.3 Read detailed initial condition data
 - 1.4 Write control data
 - 1.5 Complete geometric computations
 - 1.6 Initialize variables and arrays branch by branch
 - 1.7 Write initial condition data to TAPE 6 (through subroutine GRID)
 2. Integrate the equations through time
 - 2.1 Access time-varying boundary condition data
 - 2.2 Update hydrodynamic and transport source arrays for the entire grid
 - 2.3 Compute hydrodynamic and transport source for each branch
 - 2.4 Compute hydrodynamics and transport, branch by branch
 - 2.4.1 Compute branch-related constants
 - 2.4.2 Compute longitudinal momentum terms
 - 2.4.3 Compute the water surface elevation
 - 2.4.4 Compute longitudinal velocities
 - 2.4.5 Compute vertical velocities
 - 2.4.6 Transport heat
 - 2.4.7 Compute constituent sources and sinks
 - 2.4.8 Transport constituents
 - 2.4.9 Compute densities (through function DNST)
 - 2.4.10 Record the maximum value of Z1
 - 2.5 Perform layer and segment additions and subtractions
 - 2.6 Exchange time-dependent variables and arrays
 - 2.7 Summarize and write results
 3. Terminate the computation
-

Table A2

Detailed Outline of CE-QUAL-W2, Emphasizing
the Setup of the Computation

1. Set up the computation
 - 1.1 Introduce the computation
 - 1.1.1 Title
 - 1.1.2 Current version and changes from previous version
 - 1.1.3 Implementation notes
 - 1.1.4 Input and output files list
 - 1.1.5 INCLUDE statement
 - 1.1.6 DIMENSION statements
 - 1.1.7 DATA statements
 - 1.1.8 OPEN statements
 - 1.2 Read control and geometric data, initialize variables
 - 1.2.1 Read control data and compute derived constants
 - 1.2.2 Read geometric data and compute derived constants
 - 1.2.3 Initialize time variables
 - 1.2.4 Initialize variables and arrays for the entire grid
 - 1.3 Read detailed initial condition data and constituent parameters
 - 1.3.1 Read initial constituent profiles
 - 1.3.2 Read constituent parameters
 - 1.3.3 Read restart data
 - 1.4 Write control data
 - 1.4.1 Write identifying information to auxiliary tapes (TAPE 61 to TAPE 66)
 - 1.4.2 Write control parameters to TAPE 6
 - 1.5 Complete geometric computations
 - 1.5.1 Write geometry
 - 1.5.2 Read time-varying boundary condition data (through subroutine TVDS)
 - 1.5.3 Close Input Files
 - 1.5.4 Complete geometric initialization
 - 1.5.5 Compute and write volume-area-elevation table to TAPE 6
 - 1.6 Initialize variables and arrays branch by branch
 - 1.6.1 Initialize temperature fields
 - 1.6.2 Initialize vertical dispersion coefficient field
 - 1.6.3 Initialize constituent fields for each branch
 - 1.6.4 Compute densities (through function DNST)
 - 1.7 Write initial condition data to TAPE 6 (through subroutine GRID)
 - 1.8 Set update counter and convert rate terms
 2. Integrate the equations through time
 3. Terminate the computation
-

to be incorporated in the FORTRAN compilation directly following this statement. The external file allows all storage shared between the main program and various subroutines to be designated in a single area of code. The INCLUDE statement is also found at the beginning of the majority of subroutines.

7. A PARAMETER statement is found at the beginning of the external commons file and allows adjustment of array dimensions to meet the needs of particular applications. A PARAMETER statement is also found in the subroutine TRIDAG which should match the dimension in the commons file. Following the PARAMETER statement, all real variables are double-precisioned by use of the IMPLICIT and REAL statements. Where double-precisioning is not required, statements in the subroutines TRIDAG and RMULT and function DNST as well as in the commons file must be modified. The commons file is then arranged into a series of areas, each dimensioned to the same size or with similar functions to provide an internal documentation. For example, variables with the dimension IMAXP,KMAXP are grid-wide variables, those with dimension NBP have a value for each branch only, while those with dimension NBP,NCP have values for each branch and each water quality constituent.

8. A series of dimension statements follow the INCLUDE statement in the main program. These variables are either required only in the main program or are passed in argument lists. Data statements then follow which assign character values to variables used to ensure the proper sequencing of cards in the control file. Data statements are also found here which assign values of certain numeric variables at computation time, such as ice constants. These are normally not changed by the user, but remain accessible in this section of the code. All other variables are assigned or derived from READ statements in tasks 1.2 and 1.3 of the program.

9. Input-output files are also opened as required in this section of the code. These files include the control file (TAPE 5), TAPE 6 (GRID), and time-varying data files (site specific). Other files are opened as indicated by parameters assigned in READ statements. For example, file 65 for vector plots is opened in task 1.3.3 if the

parameter ICIRC is equal to one. Following the OPEN statements are a series of READ statements.

10. The first group of READ statements (task 1.2.1) inputs control variables from the control file (TAPE 5) which are loosely defined as all variables read except for cell widths, constituent parameters, detailed (gradients) initial condition data, and time-varying boundary condition data. Variables required at this stage for the computation are multiuse in nature and do not fall into simple categories. The data are organized as logically as possible subject to the constraint that the values of some variables are required prior to the reading of others. An algorithm is then included which maps the simulation time step onto a recognizable time scale and computes time constants. The time scale is referred to as the simulation clock and consists of years, days, and fractions of days. Among considerations built into this algorithm are consideration of variable time step sequences and anticipation of simulation clock time in order to select snapshots for printing. Portions of this algorithm appear throughout the program. Variables and arrays for the entire grid are then initialized, which completes task 1.2.

11. Task 1.3 consists of reading detailed initial condition data and constituent parameters. The constituent parameters include stoichiometric coefficients, decay rates, temperature constants, and numerous other rates and constants that affect constituent reactions and interactions. The majority of these parameters are not expected to vary with applications.

12. The writing of the control parameters for inspection by the user takes place as soon as the complete set of control and initial condition data is read. Task 1.4 shows that the control parameters are written to TAPE 6, the primary written file, after identifying information has been written to the auxiliary tapes. The object of these writes is to give the user the opportunity to review his input data as early in the run as possible. The program has a simple input checking routine that screens card images for the correct identifier and some values of the control parameters. On failing any of these tests, the

program writes the suspect card on TAPE 6 and terminates the computation. The writes that are done in task 1.4 are more formal in that variable and units are shown with each value read in.

13. Task 1.5 includes the computations necessary to complete construction of the finite difference grid, that is, its internal representation among the variables and arrays that define the dimensions and sizes. The order of the computations within this task is important. The first is the writing of the geometry for the entire grid, represented by the widths of each active cell and the derived map of active and inactive cells. This geometry is fixed without regard to the location of the water surface at the start of the simulation. The second computation shown within this task at first appears incorrectly located. However, the reading of the time-varying boundary condition data through the use of the subroutine TVDS (Time-Varying Data Selector) provides initial water surface elevation information for the open boundary condition case. The boundary elevation is received from TVDS in the form of an elevation referenced to a datum. This section of the program decomposes this elevation into a top layer number (KT) and a deviation from the top of that layer (Z). This is the same information derived from the simple initial elevation case.

14. With the initial elevation established, the program goes on to complete the geometric initialization. This completion includes the important task of abstracting positional variables from the grid for later use in the computations. These include the current upstream segment number for each branch, the segment number for the upstream and downstream active cells in each layer, and the layer number of the bottom-most active cell in each segment. Other variables related to the geometry of the grid filled to the starting elevation are also initialized.

15. Task 1.5 ends with the computation and printing of the volume-area-elevation table, as well the initial branch-by-branch and overall volumes. These are particularly important in the volume balance algorithm which is discussed separately.

16. Once the water body geometry and its simulation-specific initial condition are established, the last of the variables can be initialized. These are primarily the constituent fields. The reason that the constituent field initialization must follow the water surface and volume initialization is that one must know where to assign the properties of temperature and constituent concentration. The source for these initial conditions may be the longitudinally and vertically homogeneous (water body-wide) values given on the IC and CC cards. A second source would be the vertical profiles for each of the constituents that may be specified in the input deck. The initial conditions, including segment-by-segment water surface elevations, and constituents may also be read from restart data (task 1.3.3), which is the product of a previous simulation. The density field is initialized from the constituent fields using the function DNST. The location of this computation here allows a new density function to be inserted that considers constituents beyond the temperature and solids dependency currently in DNST. This task is also the proper place to initialize the vertical dispersion terms for the longitudinal momentum computations.

17. Task 1.7 consists of writing initial condition data to TAPE 6 for inspection by the user. Here the subroutine GRID is used and longitudinal-vertical snapshots of velocities and constituent concentrations are made.

18. The final step in this part of the code is to set the counters for updating the constituent internal sources and sinks and the temperature rate multipliers. All rate coefficients are then converted from units of per day to per second.

Integrating the equations - preliminary calculations

19. This part of the code is an initialization area which is repeated for each time integration and consists of the first three of the seven tasks in Part 2 of the code. Table A3 shows the detailed structure of these tasks.

20. The purpose of task 2.1 is to provide the user-specified time-varying boundary condition data through the subroutine TVDS. This

Table A3

Detailed Outline of CE-QUAL-W2, Emphasizing the Coding
Preliminary to the Hydrodynamic and
Transport Computation

1. Set up the computation
 2. Integrate the equations through time
 - 2.1 Access time-varying boundary condition data
 - 2.1.1 Find correct Δt and compute related variables
 - 2.1.2 Get time-varying boundary condition data (through subroutine TVDS)
 - 2.2 Update hydrodynamic and transport source arrays for the entire grid
 - 2.2.1 Reset arrays to zero
 - 2.2.2 Tributaries
 - 2.2.3 Withdrawals
 - 2.2.4 Branches (upstream and downstream internal)
 - 2.3 Calculate hydrodynamic and transport source for each branch
 - 2.3.1 Evaporation
 - 2.3.2 Ice
 - 2.3.3 Solar radiation and surface heat exchange
 - 2.3.4 Precipitation
 - 2.3.5 Distributed tributaries
 - 2.4 Compute hydrodynamics and transport, branch by branch
 - 2.5 Perform layer and segment additions and subtractions
 - 2.6 Exchange time-dependent variables and arrays
 - 2.7 Summarize and write results
 3. Terminate the computation
-

subroutine is essentially an interface that matches the notation required by the program to that with which the user is familiar. In order to acquire the correct data for a particular time, that time must be presented to TVDS in recognizable units of years, days, and fractions of a day. This section of the program uses the fundamental simulation timekeepers, the delta-t and interaction number, to produce the more sophisticated simulation clock. TVDS is to be written by the user who is familiar with the structure of the time-varying boundary condition data. (The structure of this subroutine is discussed in Part IV of the manual.)

21. With the possibility of a variable delta-t, this algorithm requires a look-up function to find the current delta-t. Since both the current and next simulation times are required by the coding that selects snapshots for printing, this algorithm is built around computing the next simulation time. The current time is found by simply equating the previous next time to it. A number of derived variables, such as the time of day, are also computed here.

22. The call to TVDS is the final coding in this task.

23. Tasks 2.2 and 2.3 operate on a set of arrays known as the source arrays. These are dimensioned as IMAXP,KMAXP, which are the maximum segment and layer indices, respectively, and therefore apply to the entire grid. There is a source array for mass (Q), heat (HNT), and other constituents (HNC). The latter is further dimensioned (IMAXP, KMAXP,NCP) to accommodate a variable number of user-specified constituents. The units used are mass rates, e.g., cubic metres per second for Q and grams per second for HNC. These arrays are reset to zero and loaded with current values at the beginning of each integration step.

24. Task 2.2 is concerned with updating these arrays for functions related to the entire grid. These include resetting the arrays to zero and accounting for tributaries, withdrawals, and branches. The latter three are grid-wide functions in the following sense: each consists of a list of locations which are given as segments and layers and are therefore independent of the branch notation. The reference to branches in this task is to the segments which they join,

not to the end of branch calculations which are done in task 2.4. The DO-loops which make up this task process the list of tributaries, for example, placing the correct flow and heat and the constituent fluxes for this simulation time (obtained from TVDS) into the source arrays at the proper grid location. The grid location can be fixed throughout the simulation time for withdrawals or, as in the case of tributaries, the segment can be fixed but the layer may vary in response to its density relative to that of the layers in the segment it enters. The detailed coding for this computation is part of task 2.2.

25. The time-lagged nature of the branch computations is explicitly stated in this section of coding. The outflows from a particular branch that were computed on the previous time step are used to account for the flows into the segment that the branch joins. On the first time step of a simulation, therefore, no flow from the branch is available (it not being computed yet), although later in the time step this flow is computed. This lag is equal to the length of the time step.

26. In assembling the source terms, a related computation is also performed. The time-integrated, overall volume accounting is maintained for new inflows to or outflows from the water body. The accounting is performed on tributaries and withdrawals but not branch flows, as the latter are transfer volumes only.

27. Task 2.3 performs a function similar to task 2.2 but is built around the branches rather than the entire grid. Task 2.3 consists of a single DO-loop that accesses each branch, retrieves branch-specific variables from storage, and then processes a number of internal DO-loops that run over the branch from the current upstream segment to its downstream boundary. This task is the natural location of a number of branch-specific manipulations of the source arrays including chemical interactions, evaporation and precipitation, ice thickness calculations, solar radiation and surface heat exchange, and distributed tributaries. The latter is a good example of the coding mechanism that typifies this task.

28. Distributed tributaries allow the user to specify an inflow to be applied to the entire branch, which is then distributed to each

segment in proportion to its area. This algorithm would be used to model a watershed with a large number of small, ungaged tributaries instead of a single large inflow. Quabbin Reservoir (Buchak and Edinger 1982a) was of this type and had the further advantage of excellent water balances that permitted branch-by-branch evaluations of ungaged tributaries. Another use for this feature would be in representing nonpoint sources for detailed nutrient cycle simulations.

29. The presence of the evaporation computation in this task was originally for the simple reason of maintaining branch-by-branch accounting of evaporation rates. However, this computation, like others in this task, have the common thread that each segment in each branch must be processed. The evaporation function is also the site for five different evaporative wind functions. The formulation of Brady, Graves, and Geyer (1969) is the default. Other formulations by Meyer, Morton, Jacoby, and Harbeck (as reported in Edinger, Brady, and Geyer 1974) appear as comment FORTRAN statements. To activate any of them, the default equation would be commented out and the new equation used instead.

30. The ice computation also provides a default value for the exchange coefficient for water-to-ice heat transfer (h_{wi}). A second formulation for computing h_{wi} for riverine conditions (Ashton 1979) is also shown, but commented out, as it has not proved to provide realistic values for ice onset, growth, and decay in the few ice test cases to which the GLVHT code, on which CE-QUAL-W2 is based, has been applied.

31. The precipitation routine is a very simply application of total precipitation (given as length) applied to the particular branch. When used, the temperature and constituent concentrations of the precipitation must be provided.

32. The attenuation of solar radiation requires an evaluation for each cell. The absorption in the upper portion of the water column is indicated by the parameter BETA. The attenuation coefficient for solar radiation is given by the parameter GAMMA. Where constituents are not simulated, GAMMA represents the attenuation coefficient due to all factors. Where constituents are simulated, a baseline attenuation

coefficient (EXCO) is specified, to which the effects of suspended solids (including phytoplankton and detritus) are added. Their effects on the attenuation coefficient are specified by the parameters EXTINS and EXTINP.

33. As with task 2.2, task 2.3 also performs the volume accounting as required for inflows and outflows.

Hydrodynamic computations

34. The most complex and frequently accessed coding in CE-QUAL-W2 is task 2.4, the computation of the hydrodynamics and transport for each branch. It is this task that derives directly from the solution technique and finite difference equations presented in Part III. Although the bulk of the branch is represented on the finite difference grid by the segments from the upstream to downstream boundaries, a computationally important element is the boundary segment of each branch, which lies outside and adjacent to the branch proper. This boundary segment is used to apply the fundamental boundary conditions to each branch.

35. There are three types of boundary conditions: the flow, external head, and internal head types. An example of a flow-specified boundary condition is a known outflow at a dam through a port or an upstream inflow into reservoir backwater. An open boundary that terminates the modeled section of an estuary is an external head type. The word "external" refers to the fact that elevation and vertical profiles of temperature, salinity, and constituent concentrations are required from an external data set. The internal junction in which a branch joins another in the finite difference grid is an example of the internal head type. In this case, the needed elevation and vertical profiles are internally generated. This accounting is done by the program. The head type boundary conditions require the use of the boundary segment to incorporate these conditions in the computation. Each of these types may occur at the upstream (left) or downstream (right) boundaries. Much of the coding in this task supports either the computations of the segments and layers in the branch proper or the segments of the branch boundaries.

36. This task is conveniently discussed in two parts: the hydrodynamic computation and the transport computation. They are in a sense independent, linked only by the density field computed from the constituent concentrations and this field's contribution to the horizontal pressure gradient.

37. Table A4 shows an outline of the hydrodynamic computation in relation to the remainder of the program. The significant tasks are the computation of the longitudinal momentum terms, water surface elevation, and velocity fields. This sequence is followed for each branch through the transport computations. Thus, each branch's value for surface elevation, velocities, and constituent concentrations are updated for the current integration step prior to the same computations for the next branch. The branch computations are completed in the order in which they appear on the finite difference grid. Accordingly, the first task for the hydrodynamic computations is to retrieve and compute branch-specific variables.

38. These variables include the positional descriptors for the branch's location on the finite difference grid and derivatives of those descriptors, the branch delta-x and derivatives, and wind stress-related variables. The latter are branch-specific values because each branch has a unique orientation.

39. The computation of the longitudinal momentum terms follows. This computation is broken into three parts to cover the three geometric elements noted previously: the branch, the left branch boundary, and the right branch boundary. The right branch boundary coding is similar to the left boundary coding and will be described as a single entity. The common elements in these three computations are the density pressure and density pressure gradient, vertical dispersion, and stress calculations. The general branch longitudinal momentum coding also includes the computation of additional momentum terms--advection and longitudinal dispersion of momentum. These terms are not included in the branch boundary computations because these terms require three consecutive cells in a layer for their evaluation. The branch boundary computation

Table A4

Detailed Outline of CE-QUAL-W2, Emphasizing
the Hydrodynamic Computation

1. Set up the computation
2. Integrate the equations through time
 - 2.1 Access time-varying boundary condition data
 - 2.2 Update hydrodynamic and transport source arrays for the entire grid
 - 2.3 Calculate hydrodynamic and transport source for each branch
 - 2.4 Compute hydrodynamics and transport, branch by branch
 - 2.4.1 Compute branch-related constants
 - 2.4.2 Compute longitudinal momentum terms
 - Longitudinal momentum terms for each branch
 - Density pressures and horizontal density pressure gradients
 - Vertical dispersion coefficients
 - Stresses
 - Remaining momentum terms - advection and longitudinal dispersion of momentum
 - Left boundary longitudinal momentum terms
 - Boundary elevation and constituent boundary profiles--internal
 - Boundary elevation and constituent boundary profiles--external
 - Density boundary profile (through function DNST)
 - Longitudinal momentum terms
 - Density pressures and horizontal density pressure gradients
 - Vertical dispersion coefficients
 - Stresses
 - Right boundary longitudinal momentum terms
 - Boundary elevation and constituent boundary profiles--internal
 - Boundary elevation and constituent boundary profiles--external
 - Density boundary profile (through function DNST)
 - Longitudinal momentum terms
 - Density pressures and horizontal density pressure gradients
 - Vertical dispersion coefficients
 - Stresses

(Continued)

Table A4 (Concluded)

-
- 2.4.3 Compute the water surface elevation
 - Compute D and F arrays for the branch
 - Augment D and F for the branch boundaries
 - Upstream flow
 - Downstream flow
 - Upstream head
 - Downstream head
 - Assemble tridiagonal coefficients and right-hand side and solve for Z (through subroutine TRIDAG)
 - Update geometry in top layer
 - 2.4.4 Compute longitudinal velocities
 - Compute pressure and horizontal pressure gradients
 - For the branch
 - For the branch boundaries (upstream and downstream head)
 - Reset boundary U to zero
 - Compute branch boundary U and flow
 - Upstream flow
 - Downstream flow
 - Upstream head and downstream flow
 - Upstream flow and downstream head
 - Upstream head and downstream head
 - Compute U for the branch
 - 2.4.5 Compute vertical velocities
 - Compute W
 - Compute W for the top layer
 - Compute vertical momentum terms for use on next integration step
 - 2.4.6 Transport heat
 - 2.4.7 Compute constituent sources and sinks and transport constituents (through various subroutines)
 - 2.4.8 Compute densities (through function DNST)
 - 2.4.9 Record the maximum value of Z1
 - 2.5 Perform layer and segment additions and subtractions
 - 2.6 Exchange time-dependent variables and arrays
 - 2.7 Summarize and write results
 - 3. Terminate the computation
-

is limited to the interface between the branch proper and the boundary segment, and therefore has only two cells available.

40. The branch boundary computations have three elements that are not required of the branch proper coding. These are the retrieving of the boundary condition data and placing of these values in the boundary segment. For example, the water surface deviation from the local datum Z at the adjacent boundary segment (ILC-1 or IR+1) is retrieved either from the time-varying data or the segment which the branch joins. The former case is the external head condition and the latter the internal head condition. This same procedure is followed in obtaining the vertical profiles of temperature, salinity, and constituent concentrations for insertion in the boundary segment. The last computation prior to computing the longitudinal momentum terms is the calculation of the boundary density profile using function DNST.

41. Since task 2.4.2 makes available the longitudinal momentum terms throughout the branch, the calculation of the water surface elevation can proceed. This calculation is shown in Table A4 as task 2.4.3. It follows directly from the equations shown in Part III. The segment-related variables BHRSUM, D , and F are computed for the branch proper. These are then augmented to account for the flow or head type boundary conditions at each end of the branch. Following assembly of the tridiagonal coefficients from these variables, the subroutine TRIDAG is called to solve the equations for Z . This new water surface deviation is then used to update the derived geometry variables in the top layer.

42. The computation can then proceed to the calculation of the longitudinal velocities. The first step is to compute the pressures and horizontal pressure gradients. These terms are computed for the branch proper and its boundaries in the case that these are of the head type. The next step is to set the boundary U 's. This step is accomplished by resetting the left and right boundary velocities to zero and computing current values for this integration step. The simplest case is for the flow type boundary conditions. Here the specified flows and their

locations are used to compute U 's as simple flows divided by cross-sectional areas at the boundary.

43. The head type boundary U specification is more complex. These U 's are computed from the limited set of longitudinal momentum terms computed prior to the surface elevations. However, in order that these U 's perfectly satisfy the continuity principle, they are then slightly modified to balance the change in storage indicated by the computed surface elevations which are held constant. There are three cases for which this rebalancing must be done: upstream head and downstream flow, upstream flow and downstream head, and upstream head and downstream head. In each case, the difference between the surface elevation-based change in storage and the computed net outflow is reconciled by modifying the head-based U 's.

44. The final calculation of task 2.4.4 is to compute U 's for the branch proper.

45. The hydrodynamic calculation is completed with the evaluation of the vertical velocities W . These are computed from continuity, beginning at the bottom cell of each segment and using the known U 's and bottom W to compute the W at the top of each cell. A contradiction arises at the surface layer, where the existence of the previously computed water surface elevation creates an overdetermined water budget. This contradiction is resolved by computing a surface layer W that perfectly satisfies continuity but which disagrees with the previously computed W by a small amount. The balanced W , known as WKT , is used in the transport calculation.

Transport computations

46. With the evaluation of the velocity fields complete, the program can proceed to transport the constituents. Task 2.4 is shown in detail in Table A5. The transport calculations are similar from constituent to constituent, except that the first one, which is heat transfer, is used to evaluate and save some common coefficients.

47. The heat transport calculation begins with the specification of heat sources for three boundary conditions: upstream head, downstream head, and upstream flow. The specification of the fluxes into

Table A5

Detailed Outline of CE-QUAL-W2, Emphasizing the
Transport Computation

-
1. Set up the computation
 2. Integrate the equations through time
 - 2.1 Access time-varying boundary condition data
 - 2.2 Update hydrodynamic and transport source arrays for the entire grid
 - 2.3 Calculate hydrodynamic and transport source for each branch
 - 2.4 Compute hydrodynamics and transport, branch by branch
 - 2.4.1 Compute branch-related constants
 - 2.4.2 Compute longitudinal momentum terms
 - 2.4.3 Compute the water surface elevation
 - 2.4.4 Compute longitudinal velocities
 - 2.4.5 Compute vertical velocities
 - 2.4.6 Transport heat
 - Heat source specifications--upstream head, downstream head, and upstream flow
 - Derive transport vertical dispersion coefficients from momentum vertical dispersion coefficients
 - Explicit calculation
 - Compute left and right coefficients
 - Compute top and bottom coefficients
 - Compute centered coefficients and solve for temperatures
 - 2.4.7 Transport other constituents
 - Compute transport coefficients
 - Compute left and right coefficients
 - Compute centered coefficients
 - Compute temperature rate multipliers
 - Compute external source specifications--upstream head, downstream head, upstream flow
 - Compute internal source specifications using subroutines where required
 - Solve for constituent concentrations
 - 2.4.8 Compute densities (through function DNST)
 - 2.4.9 Record the maximum value of Z1
 - 2.5 Perform layer and segment additions and subtractions
 - 2.6 Exchange time-dependent variables and arrays
 - 2.7 Summarize and write results
 3. Terminate the computation
-

the branch from these boundary conditions is done by augmenting the source array HNT. This augmentation is done here, rather than in task 2.2, for the reason that the velocities that drive these fluxes are only computed at this stage. The fluxes out of the branch do not need to be accounted for in the HNT array, as the upstream difference operator automatically includes them.

48. A short section of coding precedes the heat transport calculation. This coding evaluates the vertical dispersion coefficients over the branch by using a fraction of the corresponding longitudinal momentum dispersion coefficients. Since the latter are located at the corners of the cells, spatial averages (equivalent to linear interpolation) are taken to correct the locations to the cell's bottom faces.

49. The explicit heat transport calculation is based on the adjacent-cell transport coefficient notation and therefore has a flux value for the four adjacent cells and the one centered cell. The equations are solved explicitly, and transport coefficients for the top (TCT) and bottom (TCB) cells are saved for use in the remaining constituent transport routines. Separate computations for the top layer are maintained.

50. The transport computations for the remaining constituents begin with a check to see if constituents are to be included in simulations, as indicated by the parameter ICC. If constituents are to be included, the transport coefficients for the right (TCR) and left (TCL) adjacent and centered (TCC) cells are recomputed to allow a different longitudinal dispersion term for constituents (DXC) from heat (DX). Almost all constituents are affected by temperature, and that effect is included in a series of temperature rate multipliers. These rate multipliers are updated at this point, with the frequency of updating specified by the parameter NUPDRT. A DO-loop then allows evaluation of flux terms and transport computations to be repeated for each specified constituent. The constituents included in these computations are indicated by the parameter NC and the index ITRIP.

51. The constituent transport calculations include the specification of sources for three boundary conditions: upstream head,

downstream head, and upstream flow. The specification of the fluxes into the branch from these boundary conditions is done by augmenting the source array HNC. This augmentation is done here, rather than in task 2.2, for the same reason as for heat transport. The fluxes out of the branch do not need to be accounted for in the HNC array, as the upstream difference operator automatically includes them.

52. Constituent fluxes may also occur due to internal sources and sinks, such as settling, decay, production, and other reactions and interactions. The specification of the fluxes from these internal sources and sinks is done by computing values for the array CSS in a series of subroutines. Subroutines are only required for nonconservative materials, that is, those having internal sources and sinks. These internal sources and sinks are only updated at a frequency specified by the parameter NUPDC. The total sources and sinks for each constituent in the transport computation is then the sum of the external (HNC) and internal (CSS) source and sinks. The constituents are then transported using an explicit scheme.

53. Transport computations are not required for pH or the carbonate species. These constituents are calculated in the subroutine PHCO2 from total inorganic carbon concentrations and alkalinity using standard carbonate relationships. The constituent sediment is also not subject to transport. Its concentrations are updated in the subroutine SEDIMENT using Euler's method.

54. The final task in the hydrodynamic and transport computation is the recording of the maximum value of Z . Although this search is done on a branch-by-branch basis, the water body maximum is the sought-after value. The maximum represents the lowest water surface elevation and is used in deciding whether to activate the top layer addition or subtraction algorithm.

Completion of the integration and termination of the computation

55. After performing the hydrodynamic and transport computation for each branch, new values of the surface elevation, velocity, and transport fields exist throughout the finite difference grid

representing the water body. At this point it is natural to examine the water surface elevation to determine if the current active cells are appropriate to the new volume. The single variable needed to trigger the operation of the layer addition/subtraction and upstream segment addition/subtraction algorithms is the maximum value of Z . This variable was computed as the last step in task 2.4 and represents the lowest water surface elevation anywhere on the grid.

56. While this water surface protrudes less than 0.8 of the way into the next higher layer or extends less than 0.25 of the way into the current surface layer, no action is taken. However, when the water surface extends beyond the upper limit, a layer is added in order to better resolve the current very thick top layer. Note that the water surface position is not changed but that a thick layer is divided into two. This layer addition may, in turn, permit the addition of upstream segments to the active computational grid for a particular branch. As in the case of layer additions, the segment additions operate using a rule that reflects the computational capabilities of the program. The rule states that each segment must be at least two cells deep. If the layer addition fills previously inactive segments to a depth equal to two layers, these are incorporated into the computation. In this fashion, the active grid expands upward and upstream in response to a filling branch condition. This expansion is not done smoothly in the upstream direction, however, because of the two cell-depth requirement. This algorithm is shown in task 2.5.2 in Table A6.

57. Conversely, when the current surface layer is less than 75 percent full at the segment where the water surface elevation is lowest, the variable locations on the finite difference grid no longer fall in a regular spacing and the current surface layer needs to be incorporated in the next lower layer. This vertical contraction of the grid in turn forces the examination of the upstream boundary to determine whether the two cell-depth requirement is satisfied. If not, the current active upstream segment number (ILC) is adjusted. The layer and segment subtraction routines are shown as task 2.5.3 in Table A6.

58. Following the adjustment of the active finite difference grid

Table A6

Detailed Outline of CE-QUAL-W2, Emphasizing Coding to
Complete the Integration and Terminate
the Computation

1. Set up the computation
2. Integrate the equations through time
 - 2.1 Access time-varying boundary condition data
 - 2.2 Update hydrodynamic and transport source arrays for the entire grid
 - 2.3 Calculate hydrodynamic and transport source for each branch
 - 2.4 Compute hydrodynamics and transport, branch by branch
 - 2.5 Perform layer and segment additions and subtractions
 - 2.5.1 Check for layer addition or subtraction condition
 - 2.5.2 Add a layer
 - Initialize variables in new layer
 - Check for segment addition
 - Compute new upstream segment number and compare to current value
 - Initialize variables in newly active segments
 - 2.5.3 Subtract a layer
 - Reinitialize variables in subtracted layer
 - Initialize variables in newly active layer
 - Check for segment subtraction
 - Compute new upstream segment number and compare to current value
 - Reinitialize variables in newly inactive segments
 - 2.6 Exchange time-dependent variables and arrays
 - 2.7 Summarize and write results
 - 2.7.1 Compute outlet and withdrawal constituent concentrations
 - 2.7.2 Compute cumulative evaporation
 - 2.7.3 Check volume balances for each branch and the overall grid
 - Compute spatial integral
 - Compute temporal integral
 - Compute spatial and temporal integrals
 - 2.7.4 Write results
 - Daily
 - Diagnostics to TAPE 61
 - Time series results to TAPE 63

(Continued)

Table A6 (Concluded)

2.7.4 Write results (Cont'd)

Vertical profile results to TAPE 64 for observation days and stations

Plotting frequency

Circulation data to TAPE 65

Contour data to TAPE 66

Snapshots to TAPE 6 (through subroutine GRID) at printing frequency

2.7.5 Increment constituent update check

3. Terminate the computation

3.1 Write restart data to TAPE 62 (through subroutine RSRTWR)

3.2 Write termination message to TAPE 6, TAPE 61, TAPE 63, TAPE 64

to the newly computed water surface elevation, the time integration is essentially done. It remains only to prepare for the next time step (task 2.6) and to write whatever results are desired and to derive statistics that monitor the simulation's performance (task 2.7).

59. The variables that represent the water surface elevation and constituent concentrations as well as the variables dependent on the elevation, such as surface layer cross sections and volume variables, always exist at two time levels. At the start of the integration, the current values (time step n) are located in arrays suffixed "2" and previous values (time step $n-1$) in arrays suffixed "1." As new values (time step $n+1$) are computed, they are placed in the arrays suffixed "1," and thereby old values ($n-1$) are discarded. Task 2.6 functions to exchange the contents of the "1" and "2" arrays so that arrays suffixed "2" contain time step $n+1$ values and those suffixed "1" contain time step n values. This order is correct for referencing on the next integration step. An additional step in task 2.6 is to prevent constituent concentrations from falling below a specified minimum value (XPP). If the newly computed concentrations are less than XPP, they are set equal to XPP. This prevents instability due to generation of negative numbers or division by zero.

60. Task 2.7 provides the opportunity to communicate results to the user. Three subtasks extract summaries from the basic record of gridwide variables. The first of these summaries is outlet and withdrawal constituent concentrations. These are simply a look up of constituent concentration values corresponding to the outlet and withdrawal locations and renaming for easy use in WRITE statements. The second summary is the derivation of cumulative evaporation as a length. This variable is of interest in evaporation studies, and its units are comparable to those developed from observations. The final summary is the overall volume balance for each branch and the water body as a whole. The volume balances are constructed as both spatial and temporal integrals. The spatial integral is developed as the sum of the individual cell volumes for each branch and compared to the temporal integral. The latter is based on the initial volume plus net addition to that

volume due to externally applied inflows and outflows. This temporal integral can be derived for each branch and the water body as a whole.

61. The final element before going to the next integration step is to write out results as required. The fundamental results generated by CE-QUAL-W2 are time-varying, longitudinal-vertical grids of velocities and constituents and longitudinal profiles of surface elevations. These results are produced at each time step. In order to examine in detail portions of this immense record, several types of summaries can be made. A widely used summary is the snapshot, produced by the subroutine GRID. The snapshot provides numerical values on a longitudinal-vertical grid for selected segments at some useful frequency (e.g., every 2 weeks for a simulation period of 1 year). Graphical representations of longitudinal data are also available through the subroutine for contours, as well as longitudinal-time and vertical-time representations. Other summaries available are values through time of a particular parameter at a specific location or time-series data. An example would be daily temperatures at the reservoir outlet. Vertical profiles are also available at specified frequencies. Selected dates may be specified for which profile data will be printed (such as at times field data are available) to allow users to compare predicted and field results. Various profiles may be overlaid for comparison. Grids of velocities at convenient frequency may also be saved for vector plots of circulation fields. The statistical routines provided use the same output file as the profile routines.

62. Task 3 is very short and has two functions, both related to writing of results. The last elevation, velocity, and constituent fields can be saved for use as initial conditions for an additional simulation that continues from the current one. The final program step is to write a termination message to the user-read output files.

Algorithms

63. The algorithms presented here are the final elements required to complete the program as a unified expression of the solution to the

time-varying, two-dimensional water body simulation problem. Their classification as algorithms rather than fundamental equations does not derive from their being any less rigorous in a mathematical sense, but from being formulated later, during the writing of the program. The algorithms selected for discussion here are the most complex and important among the hundreds coded into the program. As with the outline of the program, the algorithms are described in a narrative form and organized by topics.

Basic operations

64. The most repeated computation in the program is the calculation of a particular variable for all active cells in a branch. This computation is organized as a double DO-loop, with the outer loop sweeping all active segments in the branch. The active segments are within the range from the current upstream (or left) segment ILC to the downstream (or right) segment IR (Figures 1 and 2, main text). As shown before, the location of the upstream segment varies with the upstream extent of the backwater, while the downstream boundary remains fixed. The segment boundaries are stored in an array and retrieved by referencing the branch number.

65. The inner loop sweeps the branch from the current top layer KT to the bottom active cell of each segment KB. The bottom active cell can occur in a different layer for each segment. The list of bottom cells by segment and layer is computed in the first section of the program (task 1.5.3), stored in an array ISC and referenced thereafter as needed.

66. As example of the resulting FORTRAN statements that are used to construct the double DO-loop is the following:

```
DO 13810 I=ILC,IR
  KB=ISC(I)
  DO 13810 K=KT,KB
    .
    .
13810 CONTINUE
```


The array ISC is used to hold the layer number of the bottom-most active cell and is retrieved as KB for the inner loop. The ellipses represent whatever computations are required. This particular element accesses every active cell in the branch. This operation is used to compute variables located at the center of cells, e.g., temperature or width-related variables, since there is exactly one of these for every cell.

67. Variations of this operation exist for computations that are done at cell interfaces. To access the right-hand side of each cell, for example to compute U , the segment index range is ILC,IRMI where $IRMI = IR - 1$. To access the bottom of each cell to compute W , for example, the layer index limits are KT,KBMI with $KBMI = KB - 1$.

68. Other variations on this basic operation include those DO-loops that access only the top layer, or those that access all the cells in a particular segment. In these cases, only one of the loops is used. An example of the layer-only access is the surface heat exchange computations; an example of the segment-only access is the branch boundary computations.

69. On a coarser scale, this operation is also done on an entire branch, regardless of current volume of water. Here the outer loop sweeps from IL (the ultimate upstream boundary) to IR. The inner loop ranges from $K = 2$ to KB. To access the entire grid, the boundaries would be $I = 1, IMAX$ and $K = 1, KMAX$. These computations are more generally used in the first section of the code prior to initializing the grid.

Volume balance variables

70. One of the properties of a successful finite difference representation of a water body is conservation of mass. For very simple cases with constant flows, an inspection of the water surface elevation can reveal if a particular computation is maintaining continuity. For complex cases with time-varying flows, precipitation, and evaporation with several branches, an algorithm must be designed to continually monitor the computation's performance.

71. The volume balance algorithm compares at each time step the current water body volume to the initial volume plus the net inflow over the simulation. The current water body volume is assessed as the sum of each cell's volume throughout the grid. This spatial integral is thus dependent on the extreme details of the computation, as it directly reflects the solution to the surface elevation equation. The time-integrated volume, on the other hand, can be reproduced from the boundary condition data, although certain program-generated variables such as evaporation rate are utilized.

72. This double-entry accounting is applied to each individual branch as well as the overall water body. The time-integrated branch volumes are dependent on the simulation-generated end-of-branch flows.

73. The ratio of spatially and temporally integrated volumes for each branch and the water body as a whole is compared to the perfect balance ratio of one. If a significant deviation occurs, the computation is stopped. During the development of a new algorithm or some other extension of the coding, an error in the volume balance ratio indicates an error in that extension. Diagnosing and correcting this error can be accomplished by monitoring the ratio.

74. During operational simulations, the volume ratio can vary smoothly from its ideal value of one. There are two reasons for this deviation. After long simulation periods represented by thousands of time steps, small errors due to limited accuracy in the central processing unit can occur. The severity and time to buildup vary with the number of digits with which a particular processor works. A second reason for the deviation is the branch-by-branch water surface solution and its inherent lag. The solution technique simultaneously solves the longitudinal momentum and continuity equations for a particular branch. Thus, the net outflow from a branch, for example, is in perfect agreement with the change in storage for that branch. However, that outflow is not used in computing the hydrodynamics for the branch into which the outflow is discharged until the next step. This lag introduces a small error in the overall volume balance, which is more pronounced in rapidly changing flows or long time steps. The error is not cumulative but is

self-compensating. In the case of a rising hydrograph at the head of a branch, the error increases to the peak and then decreases as flows recede.

75. The volume balance variables are the arrays VOLS, VOLT, and VRATIO, dimensioned to the number of branches, and VOLSW, VOLTW, and VRTIOW. The first three variables are the spatially integrated volume, temporally integrated volume, and their ratio for each branch. The latter three are the same variables for the water body as a whole. For the single branch case, the branch and water body variables are identical.

76. The spatially integrated volumes are computed near the end of the time step in a straightforward manner in task 2.7.3 of the program. A DO-loop sweeps across and down the segments and layers for each branch, accumulating VOLS as the sum of $DLX * BH2$ (the length times the cross-sectional area) at each cell. The water body spatially integrated volume is computed as the sum of the branch volumes.

77. The temporally integrated volumes VOLT and VOLTW are more complex. They are initialized in task 1.5.3 as the sum of the $DLX * BH1$ for each cell over each branch. The water body volume is the sum of the branch volumes. This computation is similar to the spatially integrated volume described above. These are the same volumes written to TAPE 6 in task 1.7 and noted as the initial branch and water body volumes.

78. During the integration but prior to its completion, manipulations of the VOLT and VOLTW variables are made in the case of segment additions and subtractions (tasks 2.5.2 and 2.5.3). When a segment is added, for example, an additional volume is brought into the computation, and VOLT and VOLTW must be increased to reflect this larger "initial" volume. The computation is simply an increment equal to the sum of the volumes of the cells added. A similar computation is done to decrease VOLT and VOLTW during segment subtraction.

79. At the completion of the time step, VOLT and VOLTW are incremented by the net inflow. There are two components: the boundary inflows and outflows that enter the computation through the array Q

and those that enter the x-direction momentum equation directly through the application of boundary U's .

80. The array Q is central to the computation of the time-integrated volumes. It is an array dimensioned to IMAXP,KMAXP . It is assembled in tasks 2.2 and 2.3 of CE-QUAL-W2, that is, within the time integration prior to the hydrodynamic and transport calculations. For each of the water body-wide and branch-specific boundary conditions, Q is incremented by the amount of inflow and decremented by the outflow at each cell. The water body-wide boundary conditions are tributaries, withdrawals, and flows from or to branches that join the cells under consideration. The branch-specific boundary conditions are evaporation, precipitation, and distributed tributaries. The presence of these flows in the array Q makes their net addition to the branch and water body volumes easy to account for. In the same coding that integrates the volume in task 2.7.3, the Q's are added to VOLT .

81. It remains only to add to VOLT the inflows and outflows that enter the computation as applied boundary U's . These are QIN and QOUT , the applied boundary flows, and QBLR and QBLL , the computed end-of-branch flows. These increments are also done in task 2.7.3. With the completion of the VOLT (branch values), the water body total VOLTW can be generated. Then the ratio of each pair, VOLS and VOLT , as well as VOLSW and VOLTW , are compared with unity. If any ratio exceeds a present tolerance (variable TOL), currently set at 5 percent, the computation is stopped.

Top layer continuity expression

82. The hydrodynamic and transport solution through time proceeds from the solution of the surface elevation (deviation from the local datum of the top of layer KT) equation to the calculation of U's and W's and thence to the computation of constituent concentrations. Although the continuity and x-momentum equations have been combined to produce an implicit solution, the required order of the computations leaves the vertical velocity calculation as the last element in the hydrodynamics. Thus, both the surface elevations and horizontal

velocities for the new time step are known when the vertical velocities are computed.

83. The fundamental basis for computing W is the continuity expression. Beginning at the bottom active cell at each segment, the net advection through the sides and any sources or sinks (through reference to the Q array) can be computed. This horizontal advection term is called $WT2$. Since the volume of the cell does not change and there is no flow across the bottom boundary, the velocity at the top boundary of the bottom cell is easily computed as the new flow divided by the area of the top boundary. The velocity at the top of the next cell up the segment is computed similarly, except that the bottom velocity is nonzero, but known. In this case, the advection across the bottom boundary is computed as the velocity times the area and is designated $WT1$. The latter case is the more general one, and the computation proceeds in this manner to the cell just beneath the top layer. The vertical velocity at the top boundary of this cell is computed as in the general case. However, since the cell above in the top layer has a zero vertical velocity at its top boundary, a second determination of the vertical velocity at this interface can be made. This computation is based on information in the surface layer, but a new term is introduced. Given the name $WT3$, this term represents the change in volume since the last time step due to a surface elevation change. A second estimate of the vertical velocity at the boundary between the top and next lower cell, known as WKT , is made using $WT2$, the net horizontal advection, and $WT3$. Both these estimates perfectly balance the volumes in the cells from which they are computed. However, they differ by a small amount. This difference is not noticeable in the x -momentum terms in which these vertical velocities are used. However, in the transport equation, the violation of continuity that would occur if a vertical velocity were used which does not perfectly maintain the computed volumes soon manifests itself. The solution is to use the vertical velocity WKT in computing the surface layer temperatures and constituents, and the more general velocity W elsewhere.

84. This method solves a major problem but introduces one of a secondary nature. For example, heat is advected out of the top layer at the rate of $WKT * T * BB$, where BB is the bottom area. Heat arrives at the next lower layer at the rate $W * T * BB$, so that a loss of the amount $T * BB(WKT - W)$ is indicated. The size of this error is very small, since tests have shown that $WKT - W$ is barely detectable. Also, there is no systematic error in that the sign of the difference varies randomly.

Branch boundary velocity computations - open boundary

85. The main features of the branch boundary velocity computations for the head boundary conditions are the abbreviated form of the longitudinal momentum equation at the boundary and the correction of the computed velocity profile by reference to the branch water budget.

86. The individual terms in the longitudinal momentum equation are computed in task 2.4.2 for use in the solution to the surface elevation equation and later in the determination of longitudinal velocities. Because of the availability of only one boundary segment representing the extension of the water body into an area beyond the modeled portion or representing its connection to another branch, two of the terms in the general longitudinal equation cannot be evaluated. These terms are the advection and dispersion of momentum. Computationally, these terms depend on values of U at three cells to correctly assess the velocity gradient; therefore, the ordinary computation cannot be used at an open branch boundary. For the case of an internal head boundary condition, the axis of the branch which the branch in question joins is presumably at an angle approaching 90 deg to the axis of the latter. This condition means that there is no longitudinal momentum to be transferred into the branch and the elimination of terms is justified.

87. For an external head boundary condition (open water boundary), the rationale for elimination of these two terms depends on the geometry beyond the model boundary. In the event this continuation of the water body is narrow and in the same general direction as the modeled portion, the geometric representation is faulty and should be extended to include

this continuation. When the geometric properties beyond the boundary change to a large, open area, the assumption of no momentum transfer to the branch is more realistic.

88. Other than the elimination of these two terms, the remaining longitudinal momentum terms for the branch boundary are identical to those for the more general computation in the branch proper. Task 2.4.2, shown in Table A4, shows that these terms are computed in the order of the branch proper, then for the left boundary, followed by those for the right boundary.

89. The branch boundary velocity computations resume following the computation of the water surface elevation. The availability of the surface elevation for the branch permits the evaluation of the pressures and horizontal pressure gradients, first for the branch and then for the branch boundaries (task 2.4.4). These terms are evaluated identically for the branch proper and its boundaries.

90. The calculation of the branch boundary horizontal velocities for the open boundary case is a straightforward sum of previously computed terms and the velocity at the old time step. As in the case of the top layer vertical velocity computation, however, there is an inconsistency in resulting overall water balance. Under ideal conditions, the computed boundary U 's would complete the water budget for the branch. Tributary inflows, withdrawals, and other applied sources are well known and supplied with the time-varying boundary condition data; they represent the net inflow. The surface elevation, computed from newly evaluated longitudinal momentum terms, provides the change in storage term for the branch water balance. The computed boundary U 's, however, do not provide a perfect closure to the water balance.

91. The impact of this error can be serious. For a single branch with an open boundary (for example, an estuary), the volume balance variables have a continuing deviation of the spatially and temporally integrated volumes. This deviation results from the inexact accounting based on the computed branch boundary velocities. The single branch itself maintains continuity, as the branch boundary velocities are not used directly in the surface elevation solution. For a multibranch

water body, however, the computed branch boundary velocities at the junction of the branch in question and the segment in the branch that it joins are used in the continuity expression for the latter branch. If these velocities do not perfectly satisfy continuity as determined by the change in storage and net inflow from other sources to the branch, the water body volume balance as a whole suffers. For example, a branch joining a main stem may have an outflow determined by integrating the computed branch boundary velocities for $49 \text{ m}^3 \text{ sec}^{-1}$ in comparison to an outflow computed from the net inflow and change in storage of $50 \text{ m}^3 \text{ sec}^{-1}$. The branch would have a perfect water balance, as the computed net outflow of $49 \text{ m}^3 \text{ sec}^{-1}$ is used only in the volume balance accounting. The main stem, on the other hand, would see an inflow of $49 \text{ m}^3 \text{ sec}^{-1}$ and, although it would maintain a perfect water balance based on this flow, $1 \text{ m}^3 \text{ sec}^{-1}$ would be missing from the overall water budget. The result is a steady deviation in the ratio of the temporally integrated volumes for the latter.

92. The solution to this problem is to increment the U's computed at the boundary from the longitudinal momentum terms by an amount that would satisfy continuity based on the change in storage computation. This adjustment is done in task 2.4.4.

93. There are three cases for the open boundary condition: upstream head and downstream flow, upstream flow and downstream head, and upstream head and downstream head. These cases are done separately because the velocity profiles that must be adjusted are in different locations. The fundamental computations can be demonstrated by examining the case of upstream flow and downstream head.

94. The current volume of the branch (VOL1) is computed as the sum of $DLX * BH1$. In the same DO-loop that sweeps the branch, the current net inflow is computed in QBLRNO as the sum of the entries in Q, the water mass source array. The variable QBLRNO is finalized by adding the QIN (the inflow at the head of the branch) and subtracting the change in storage over the integration time step.

Thus,

$$QBLRNO = \Sigma Q - dV/dt$$

and $QBLRNO$ is the net flow at the branch boundary that perfectly satisfies continuity with respect to the given inflows and previously computed surface elevations.

95. The next stage in the computation is to compute the net flow $QBLRN1$, from the computed boundary velocity profile. This integration is performed over the boundary segment as the sum of $U * BHR1$, where the latter term is the cross-sectional area at the right boundary of each cell. In this process, the layer-by-layer flows are also saved as $QBLR$. Finally, in the DO-loop that runs from the top to the bottom of the boundary segment, the difference between $QBLRNO$ and $QBLRN1$ is apportioned to the individual $QBLR$ by dividing the differences among the layers weighted by layer cross-sectional area. From these corrected $QBLR$'s, the corrected Q 's are computed.

96. The upstream head-downstream flow computations are done in a manner similar to the method discussed above, except that the left boundary flows and velocities are used. The upstream and downstream head case is similar, but more complex because of having to compute and correct flow balances at both ends.

97. Note that the array Q , which is used primarily in the volume balance accounting, is used here to total conveniently the net inflow to the branch.

Directly applied boundary velocities

98. The simpler, directly applied boundary velocities are also computed in task 2.4.4 prior to computing the open boundary velocity profiles. The downstream flow boundary condition is easily translated into a velocity by dividing the given flow by the cross-sectional area. The location in the vertical for the flow is fixed and given in the input record. This type of boundary condition is typically used to represent a port or other opening in a dam.

99. The upstream flow boundary condition is in principle a simple application of flows and cross-sectional areas to obtain the needed U at the boundary. However, in the absence of a detailed solution to the hydraulics of the inflow, the program must proportion the inflow in the vertical. This proportion is currently done as the ratio of a specific cell's cross-sectional area to the entire cross-sectional area of the inflow segment. Thus, the assumption of constant velocities in the vertical is made. This result follows from

$$Q_k = Q_{in} * A_k / A_{in}$$

and

$$U_k = Q_k / A_k$$

so that

$$U_k = Q_{in} / A_{in}$$

for every layer k , with A being the cross-sectional area. Rather than use the last relationship directly, the individual areas, flows, and proportions are computed. The proportions are saved so that the corresponding constituent fluxes (temperature and other constituents) can be evaluated correctly for the transport calculations.

100. The inflow cross-sectional area is taken as the BHI summed over the ILC segment, without regard for the depth at the ILC-1 segment. If the latter segment is currently inactive and shallower, a drawing of the inflow velocities would show inflows apparently originating from permanently inactive cells at the bottom of the ILC-1 segment. The use of these cells is an arbitrary convention that permits the distribution of the inflow over more cells and results in lower velocities. These lower velocities contribute to the stability of the computation with regard to the Torrence restriction ($\Delta t < V/Q$).

Geometric variables

101. The fundamental geometric variables describe the length, thickness, and width of each cell in the finite difference grid using the variables DLX , H , and B . Variable DLX is the cell length and is fixed in time and constant over the segments in each branch; B is the cell width and is fixed for each cell; H is fixed for each layer, although in the top layer (KT), H may vary in time. Two kinds of derivatives of these fundamental variables exist. The first kind permits these variables to exist at several time levels. For example, the layer thickness H takes the form of H_1 , H_2 , and H_{IN} . The first two are the layer thicknesses on two consecutive time steps. The latter is the initial layer thickness. A second derivative of the fundamental variables is the various products that can be formed to represent areas or interpolated dimensions, useful in later computations. These products may exist also in several time levels. These include BH_1 and BH_2 , which are the product of the width and thickness at the two time levels; BHR_1 and BHR_2 , which are the product of B times H and are located at and averaged to the right-hand boundary at two time levels; BR , which is B averaged to the right-hand boundary; and BB , which is B averaged to the bottom boundary.

102. The overall finite difference grid is $IMAX$ long and $KMAX$ deep. Onto this grid is mapped each branch of the water body. As few as one branch may be used to represent the water body. The upstream boundary of a branch is given the segment number IL and downstream boundary IR . The downstream boundary is fixed. This assumption handles most cases, as the downstream areas are almost always the deepest. The upstream boundary, however, may change in response to rising and falling water levels. The current upstream boundary is designated ILC . The computations on any particular step, therefore, begin at ILC and go to IR . Surface water levels rise or fall and therefore fluctuate on the grid. The upper layer boundary is designated KT . The bottom boundaries remain fixed and vary by segment. This assumption does not permit changes in bottom boundaries due to the scouring or deposition of sediments. In order to maintain computational

efficiency, the lower segment boundaries are computed in the initialization portion of the code and referenced whenever computation begins at KT and goes to the bottom. These coordinates are placed in the array ISC and referenced as KB .

103. Numerous ancillary variables are derived from this basic grid structure. For example, elevation is computed for each branch at segment IR by adding to the depth at that segment a position variable that relates the grid to a universal datum. Also the elevation-area-volume table for each branch and for each overall water body is derived from these basic variables.

Expansion and contraction of the finite difference grid

104. The rationale and outline for layer and segment additions and subtractions are given earlier in this appendix. This section describes the details of the coding that implements this algorithm.

105. A basic notational premise in this section of the program (tasks 2.5.2 and 2.5.3) is that the grid location variables KT (the current surface layer) and ILC (the current upstream segment) are not changed in value until the algorithm is nearly complete. The new values for these variables are given separate names early in the computation, and these values are then assigned to the more general names at the close of the algorithm. For example, the variable ILCP contains the new upstream segment and is used to reset variables in the upstream area during segment addition or subtraction. Following the resetting, ILC is set equal to ILCP , and the computation proceeds to task 2.6.

106. The addition of a layer occurs when the lowest water surface elevation on the entire grid is such that the Z in that segment protrudes more than 0.8 of the way into the next layer. The layer addition algorithm has the very mundane mission of resetting the geometric variables in the former surface layer (still called KT) to values based on the general layer thickness HIN . Thus H1 and H2 , BH1 and BH2 , and BHR1 and BFH2 are returned to their nonvarying layer thickness values. Likewise, these same variables in the new surface layer

(referred to as KTMI) acquire values based on a new surface elevation deviation, computed as

$$Z' = HIN - Z$$

where HIN is the general layer thickness (H IInitial), and Z' and Z are the new and old deviations, respectively.

107. A second kind of computation involves assigning values to the variables U , T , S , C , and AZ in the new layer (KTMI) equal to the values of the variables in the old layer (KT). The theoretical basis for making these values equal to the values in the layer KT is clear: the original thick layer is divided into two with no change in properties. All these computations are done for each segment in each branch.

108. The final computation is to proportion the end-of-branch flow arrays (QBLL and OBLR) such that there is a value for the new layer and a new value for the previous surface layer. Ice thickness is not changed as it is assumed to continually ride on the water surface, whatever its location.

109. The coding for the addition of segments is more complex. After determining that upstream segments can be added--that is, that the additional layer permits an upstream segment or segments to contain water such that at least two layers are active--variables need to be initialized in the new segments. The range of segments and layers to be processed are ILCP (the new upstream segment) to ILCM1 (the segment just upstream of the previous boundary) and KTMI to KB , the bottom active segment in each layer. Note that segments can be neither added nor subtracted for the upstream head boundary condition and that correctly constructed geometry and flow records will prevent this possibility.

110. The geometric variables in the surface layer of the new upstream active segments are updated in a manner similar to those in the layer addition coding. In addition, however, the values of U , T , C , AZ , DX , and RHO are also required in the newly added segments.

Variables AZ and DX are set to their initial values as they are updated before their next use; U is reset to zero for the same reason. Values of T and C are more difficult to obtain, and the best available estimate is that they are equal to the values for the upstream inflow. For example, the values of T for the newly active upstream segments are set equal to the inflow temperature. The last calculation before completing this part of the algorithm is to reassign the variable names ILC = ILCP and related variables and to update the boundary geometric variables as outlined earlier. Finally, the variable KT - KTMI is set and the layer addition is complete.

111. The details of the layer subtraction and concomitant segment subtraction are similar. Instead of extending properties into newly active cells, the task here is to reset these values to zero in order to avoid use of the wrong values should the volume expand once again. On subtracting a layer, the constituent properties of the upper layer are not discarded but are mixed calorimetrically with those in the lower (now surface) layer. This procedure ensures, for example, that warm epilimnetic water is not artificially stripped from the water body. This same procedure, however, is not used in the subtraction of segments. The difference is that the discarded surface layer is not lost to the computation but is merely reassigned in the grid indexing scheme, while the subtracted segments continue to function outside the active finite difference grid. These are not included in the computation that proceeds and, therefore, their constituent properties are not of direct interest.

APPENDIX B: GLOSSARY OF VARIABLES

A(IMAXP)--The A vector contains subdiagonal coefficients for the tridiagonal algorithm solutions for Z. (TRIDAG)

AB--Upstream differencing operator used in the computation of ADMZ.

ABTM, year/days--Absolute Time, the basic CE-QUAL-W2 clock. It consists of the year as the first two digits, the Julian day as the next three, and the fraction of a Julian day to the right of a decimal point. ABTM is incremented by one delta-t each time step and correctly accounts for leap years and transitions to the beginning of the next year.

ABTMN, year/days--ABTM for the Next time step; equal to ABTM plus one delta-t.

ADMAXN, g N/g solids--Maximum mass-specific adsorption coefficient for ammonia-nitrogen.

ADMAXP, g N/g solids--Maximum mass-specific adsorption coefficient for orthophosphorus.

ADMZ(IMAXP, KMAXP, $(u_b w_b b)_{k+1/2} - (u_b w_b b)_{k-1/2}$, $m^3 \text{ sec}^{-2}$)--ADvection of Momentum in the z-direction.

ADMX(IMAXP, KMAXP), $\partial/\partial x (U^2 B h)$, $m^3 \text{ sec}^{-2}$ --ADvection of Momentum in the x-direction.

ADSRBN, m^3/g --Adsorption coefficient for ammonia-nitrogen.

ADSRBP, m^3/g --Adsorption coefficient for orthophosphorus.

AEXCR(IMAXP, KMAXP, 1) sec^{-1} --Calculate excretion, or photorespiration, rate of algae.

AID--Alphanumeric Identifier. The character variable AID is used to hold the alphanumeric ID read from the input cards for comparison to the card titles held by the code. (INPUT)

AL--Alpha Left; an upstream differencing operator used in the computation of ADMX.

ALB(KMAXP, NBP), m^2 --Area by Layer by Branch; contains the area of each layer in each branch.

ALDIGO--Fraction of algal mortality going to detritus, with the remaining fraction going to labile dissolved organic matter.

ALG1K1--Rate multiplier corresponding to ALG1T1.

ALG1K2--Rate multiplier corresponding to ALG1T2.

ALG1K3--Rate multiplier corresponding to ALG1T3.

ALG1K4--Rate multiplier corresponding to ALG1T4.

ALG1T1, °C--Lower temperature bound for algal growth.

ALG1T2, °C--Lower temperature bound for maximum algal growth.

ALG1T3, °C--Upper temperature bound for maximum algal growth.

ALG1T4, °C--Upper temperature bound for algal growth.

ALW(KMAXP), m^2 --Area by Layer by Water body; contains the sum of the areas of each layer for all branches.

AMU(IMAXP,KMAXP,1), sec^{-1} --Calculated algal gross production rate.

ANPM(IMAXP,KMAXP,1), sec^{-1} --Calculated algal mortality rate.

ARR--Alpha Right; an upstream differencing operator used in the computation of ADMX.

ART(IMAXP,KMAXP,1), sec^{-1} --Calculated algal dark respiration rate.

ASPMPO--Absolute value of the Sign of Phi Minus Phi zero; a computational variable.

AX, A_x , $m^2 sec^{-1}$ --x-direction momentum diffusion coefficient.

AZ(IMAXP,KMAXP), A_z , $m^2 sec^{-1}$ --Stores the z-direction momentum diffusion coefficients.

AZO, $m^2 sec^{-1}$ --Base value used in the AZ computation.

AZMAX, $m^2 sec^{-1}$ --AZ's MAXimum permitted value; a function of the grid size and time step.

AZMIN, $m^2 sec^{-1}$ --AZ's MINimum permitted value; the molecular value of vertical diffusion.

B(IMAXP,KMAXP), m--Bathymetry. The B array is loaded with cell widths for the grid. (INPUT)

BB(IMAXP,KMAXP), m--B at the Bottom. B contains the cell widths at the cell centers. BB is located at the vertical cell interfaces and is the vertical average of B.

BETA, β --Contains the fraction of incident solar radiation absorbed at the water surface.

BGAID--Character variable that contains the character string "BG"; used in conjunction with AID to check the Branch Geometry input card alphanumeric identifier.

BH1(IMAXP,KMAXP), m^2 --BH at time level 1. BH1 stores cross-sectional areas computed at the center of each cell.

BH2(IMAXP,KMAXP), m^2 --BH at time level 2. BH2 stores cross-sectional areas computed at the center of each cell.

BHR1(IMAXP,KMAXP), m^2 --BH right time level 1. BHR1 stores the geometric average cell width times layer thickness averaged to the right-hand boundary.

BHR2(IMAXP,KMAXP), m^2 --BH right time level 2. BHR2 stores the geometric average cell width times layer thickness averaged to the right-hand boundary.

BHRSUM(IMAXP), $m^5 \text{ kg}^{-1}$ --BHRhoSUM.

BIOC--Stoichiometric equivalent coefficient for carbon.

BION--Stoichiometric equivalent coefficient for nitrogen. (INPUT)

BIOP--Stoichiometric equivalent coefficient for phosphorus. (INPUT)

BIOSUM, $g \text{ m}^3$ --Computational variable containing the sum of concentrations of detritus and algae, at a particular time; used to modify the light extinction coefficient.

BLANK--Character variable that contains seven blanks; used to mask unused grid cells for the snapshot output. (GRID)

BR(IMAXP,KMAXP), m--Geometric averaging width variable; location at right-hand side of cell.

BTA, $\text{mm Hg } ^\circ\text{C}^{-1}$ --BeTA; the vapor pressure-temperature gradient.

BUOY, $\text{kg m}^3 \text{ m}^{-1}$ --BUOYancy.

C(IMAXP)--C vector that contains subdiagonal coefficients for the tridiagonal algorithm solution of Z.

C1(IMAXP,KMAXP,NCP), $g\ m^{-3}$ --Constituent concentration, time level 1.

C2(IMAXP,KMAXP,NCP), $g\ m^{-3}$ --Constituent concentration, time level 2. (GRID)

CCAID--Character variable that contains the character string "CC"; used in conjunction with AID to check the Constituent Concentration input card alphanumeric identifier.

CDAID--Character variable that contains the character string "CD"; used in conjunction with AID to check the Constituent Definition input card alphanumeric identifier.

CDSTRB(NBP,NCP), $g\ m^{-3}$ --Concentration DiStributed TRiButary; contains the constituent concentration of inflows due to distributed tributaries by branch. (TVDS)

CEVAP, m --Cumulative EVAPoration; the total evaporation throughout the simulation for the water body.

CHZY, $m^{1/2}\ sec^{-1}$ --CHeZY resistance coefficient.

CI(NCP) $g\ m^{-3}$ --Constituent Initialization. The CI vector contains one initial constituent value for each constituent. Any of its values may be set to -1 to indicate initialization as a vertical profile. (INPUT)

CIN(NBP,NCP), $g\ m^{-3}$ --Constituent upstream INflow concentration. (TVDS)

CIVP(KMAX,NCP), $g\ m^{-3}$ --Constituent Initial Vertical Profile; stores initial vertical profile values layer by layer for each constituent. (INPUT)

CKL, sec^{-1} --Computed interfacial exchange rate for carbon dioxide.

CL(KMAXP,NBP,NCP), $g\ m^{-3}$ --Constituent profile Left; stores time-varying values for constituents at the left-hand open boundary. (TVDS)

CNH3DK, sec^{-1} --Maximum decay (nitrification) rate of ammonia.

CNK1--Rate multiplier corresponding to CNT1.

CNK2--Rate multiplier corresponding to CNT2.

CNK3--Rate multiplier corresponding to CNT3.

CNK4--Rate multiplier corresponding to CNT4.

CNO3DK, sec^{-1} --Maximum decay (denitrification) rate of nitrate-nitrogen.

CNREL--Computational variable representing the zero-order rate of ammonia-nitrogen release under anaerobic conditions, expressed as a fraction of sediment oxygen demand.

CNT1, $^{\circ}\text{C}$ --Lower temperature bound for sediment ammonia-nitrogen release.

CNT2, $^{\circ}\text{C}$ --Lower temperature bound for maximum rate of sediment ammonia-nitrogen release.

CNT3, $^{\circ}\text{C}$ --Upper temperature bound for maximum rate of sediment ammonia-nitrogen release.

CNT4, $^{\circ}\text{C}$ --Upper temperature bound for sediment ammonia-nitrogen release.

CNTOT(IMAXP,KMAXP) g m^{-3} --Contains total nitrogen (ammonia-nitrogen + nitrate-nitrogen) used in computing nitrogen limitation of algal growth.

COLIDK, sec^{-1} --Maximum coliform decay rate.

CONV(17,KMAXP)--CONVert. The CONV character array contains the grid values written in alphanumeric format. (GRID)

COUT(10,NCP), g m^{-3} --Concentration of OUTflow; contains the outflow constituent concentrations for the flow boundary conditions.

COUTAV(NCP), g m^{-3} --Concentration of OUTflow, Average; contains the flow-weighted average of outflow constituent concentrations.

CPRECP(NCP), g m^{-3} --Concentration of PREciPitation; contains the constituent concentrations for inflows due to precipitation. (TVDS)

CR(KMAXP,NBP,NCP), g m^{-3} --Constituent profile Right; stores time-varying values for constituents at the right-hand open boundary. (TVDS)

CSHE, m sec^{-1} --Coefficient of Surface Heat Exchange. (TVDS)

CSPMPO--CoSine of Phi Minus Phi zero.

CSS((IMAXP,KMAXP,NCP), g sec^{-1} --Internal source and sink array for constituents.

CTRIB(10,NCP), g m^{-3} --Constituent concentration for TRIButaries. (TVDS)

CVLB(KMAXP,NBP), m^3 --Cumulative Volume by Layer by Branch.

CVLW(KMAXP), m^3 --Cumulative Volume by Layer by Water body.

CWD(10,NCP), $g\ m^3$ --Concentration of Withdrawals; contains the constituent concentrations of withdrawals.

CZ--Wind resistance coefficient; value varies with wind speed.

D(IMAXP)--D contains right-hand side values for the tridiagonal algorithm solution of Z. (TRIDAG)

DEPTH, m--Computational variable.

DETK1--Rate multiplier corresponding to DETT1.

DETK2--Rate multiplier corresponding to DETT2.

DETUDK, sec^{-1} --Maximum detritus decay rate.

DETT1, $^{\circ}C$ --Lower temperature bound for detritus decay.

DETT2, $^{\circ}C$ --Lower temperature bound for maximum detritus rate of decay.

DF--Depth Factor; a computational variable.

DFC--Depth Factor Coefficient; a computational variable.

DLT, sec --DeLta-T; the computation time step.

DLTO(50), sec --DeLta-T zero. This array contains the list of up to 50 different delta-t's used in the computation. (INPUT)

DLTM, sec --DeLta-T Minimum; used to compute AZMAX.

DLTMAX, sec --DeLta-T MAXimum; the maximum permissible delta-t. Its value is based on the minimum of V/Q for each cell.

DLTN, sec --DeLta-T Next; the next computational time step.

DLTVQ(IMAXP,KMAXP), sec --DeLta-T based on Volume and flow (Q); the maximum allowable delta-t for each cell.

DLX(NBP), m--DeLta-X, m. The DLX vector stores one cell length value for each branch. (INPUT)

DLX2, m^2 --DeLta-X².

DLXR--1/DeLta-X/Rho; a computational variable.

DM(IMAXP,KMAXP), $A_x [\partial^2 / \partial x^2 (UBh)]$, $m^3 \text{ sec}^{-2}$ --Diffusion of Momentum.

DMCO2, $m^2 \text{ sec}^{-1}$ --Molecular diffusion coefficient for carbon dioxide. Used to compute interfacial exchange.

DMO2, $m^2 \text{ sec}^{-1}$ --Molecular diffusion coefficient for dissolved oxygen. Used to compute interfacial exchange.

DNAID--Character variable that contains the character string "DN"; used in conjunction with AID to check the Delta-t Number of interactions input card alphanumeric identifier.

DOMCNT--DOM CoNTent; represents the fraction of influent DOM that occurs as labile DOM with the remainder being refractory. It is used in the subroutine TVDS to partition the two components of total DOM. (INPUT)

DOMDK, sec^{-1} --Maximum decay rate of labile dissolved organic matter.

DOMK1--Rate multiplier corresponding to DOMT1.

DOMK2--Rate multiplier corresponding to DOMT2.

DOMRFR, sec^{-1} --Maximum decay rate from labile to refractory dissolved organic matter.

DOMT1, $^{\circ}\text{C}$ --Lower temperature bound for dissolved organic matter decay.

DOMT2, $^{\circ}\text{C}$ --Lower temperature bound for maximum dissolved organic matter decay rates.

DSETL, $m \text{ sec}^{-1}$ --Detritus settling rate.

DTM, m --Distance from reference DaTuM. DTM is a fixed, grid-positional value that assigns the distance from a reference datum, mean sea level, to the lower grid boundary. (INPUT)

DX(IMAXP,KMAXP), D_x , $m^2 \text{ sec}^{-1}$ --Dispersion coefficient X-direction; used in the heat balance equation.

DXC(IMAXP,KMAXP), $m^2 \text{ sec}^{-1}$ --Dispersion coefficient, X-direction. DXC is used in the constituent balance equation.

DXI, $m^2 \text{ sec}^{-1}$ --Initial value for DX.

DXS, $m^2 \text{ sec}^{-1}$ --Initial value for DXC.

DZ(IMAXP,KMAXP), D_z , $m^2 \text{ sec}^{-1}$ --Dispersion coefficient,
Z-direction. DZ is used in the heat and constituent balance equation.

EL, m--Elevation. (INPUT)

ELL(NBP), m--Elevation Left. The ELL vector contains external boundary condition elevation values. ELL is used with open water boundary conditions. (TVDS)

ELR(NBP), m--Elevation Right. The ELR vector contains external boundary condition elevation values. ELR is used with open water boundary conditions. (TVDS)

ELT, m--Elevation Top. ELT is used to determine the initial value of KT in the estuary case.

ET, °C--Equilibrium Temperature of surface heat exchange.

ETM, °C--Equilibrium Temperature daily Mean value. (TVDS)

EW(10,NBP)--Effective Wind coefficient. EW contains the factor by which wind speeds supplied by TVDS are multiplied for use in wind shear computations. A different EW may be used for each branch, each DLTO. (INPUT)

EWC(NBP)--Effective Wind Coefficient; factor applied to the wind as supplied by TVDS for use in the wind shear computations. One EWC is assigned for each branch, each DLTO.

EWCN(NBP)--Effective Wind Coefficient Next. Computational variable containing the effective wind coefficient for the next time step.

EXPDF--EXP(DF); a computational variable.

EXPRAZ--Computational variable.

EXTINS, $m^2 g^{-1}$ --Coefficient relating inorganic suspended solids concentrations to light attenuation.

EXTINP, $m^2 g^{-1}$ --Coefficient relating organic suspended solids (algae + detritus) concentrations to light attenuation.

EXCO, m^{-1} --Light attenuation coefficient excluding solids effects.

F(IMAXP)--The F vector contains values for simultaneous implicit solution of the x-momentum and continuity equations.

FEFACT--Factor by which ADSRBP and ADSRBN are multiplied to adjust for iron adsorption. (INPUT)

FEREL, $g\ m^{-2}\ sec^{-1}$ --Sediment release rate of iron under anaerobic conditions.

FESETL, $m\ sec^{-1}$ --Settling velocity for iron.

FETCH, m --One-half of branch length.

FOPL, hr --Frequency Of PLOtting. Postprocessing information is printed every FOPL hours, beginning at TBPL. (INPUT)

FOPR, hr --Frequency Of PRinting. Snapshots are printed every FOPR hours, beginning at TBPR. (INPUT)

FOTSR--Frequency Of Time SeRies. FOTSR specifies the frequency at which time series, that is information to TAPE 63, is written. (INPUT)

FW, $W\ m^2\ mm^{-1}\ Hg$ --Function of Wind speed.

G, $m^1\ sec^{-1}$ --Gravitational constant.

GAMMA, $l\ m^{-1}$ --Exponential decay constant for absorption of solar radiation with depths.

GC2--Computational variable; value determined by $G/CHZY^2$.

GDT2DX-- $G\Delta T^2/2 * \Delta X$; a computational variable.

GEAID--Character variable that contains the character string "GE"; used in conjunction with AID to check the GEometry input card alphanumeric identifier.

H1(IMAXP,KMAXP), m --Stores layer thicknesses at time level 1.

H2(IMAXP,KMAXP), m --Stores layer thicknesses at time level 2.

HIA--Heat-Ice-Atmosphere; the coefficient of surface heat exchange for ice to the atmosphere.

HIN(IMAXP,KMAXP), m --Heat-INitial; stores the original value of grid layer thickness. It is used to compute varying H in the top layer of cells. (HIN(1,1) is INPUT)

HNC(IMAXP,KMAXP), $g\ m^{-3}\ m^3\ g^{-1}\ sec^{-1}$ --External source and sink array for the constituent computation.

HNT(IMAXP,KMAXP), $^{\circ}C\ m^3\ sec^{-1}$ --Source and sink array for the heat balance computation.

HPG(IMAXP,KMAXP)--Horizontal Pressure Gradient.

HWI--Heat-Water-Ice; exchange coefficient for water to ice computations.

I--DO-loop index used for grid segments.

I0(9)--I0 contains the segment numbers for segments that are to be written to the snapshots. I0 is in effect only if IFORM = 0.
(INPUT,GRID)

I0AID--Character variable that contains the character string "I0"; used in conjunction with AID to check the I0 input card alphanumeric identifier.

I1(17)--Contains the segment numbers for segments that are to be written to the snapshots. I1 is in effect only if IFORM = 1.
(INPUT,GRID)

I1AID--Character variable that contains the character string "I1"; used in conjunction with AID to check the I1 input card alphanumeric identifier.

I2AID--Character variable that contains the character string "I2"; used in conjunction with AID to check the I2 input card alphanumeric identifier.

IB--I-Begin; locates the first active cell in each layer for use in the tridiagonal solution of the heat balance and constituent transport equations. (TRIDAG)

IBC(3,NBP)--I-BranC Controller. This array contains for each branch the segment number for the most upstream segment, the segment number for the current upstream segment, and the segment number for the most downstream segment. The second term, the segment number for the current upstream segment, is the only value which varies during the computation. (INPUT)

ICAID--Character variable that contains the character string "IC"; used in conjunction with AID to check the InItial Conditions input card alphanumeric identifier.

ICC--(Integer) Constituent Computation flag; turns the constituent transport computations on or off. (GRID,INPUT)

ICE--ICE flag; turns the ice computations on or off. (GRID,INPUT)

ICIRC--(Integer); used for turning the writing information used for velocity vector plots on and off.

ICKUD--I Check UpDates; computational variable that is used, along with NUPDRT, to determine if the temperature rate multipliers are to be updated.

ICKUDC--I Check UpDates for Constituents; computational variable that is used, along with NUPDC, to determine if the constituent source and sink array, CSS, is to be updated.

ICNTR--(Integer) CoNTOuR plotter flag; turns the contour information writing option on or off. (INPUT)

ICTRIP(NCP)--Specifies which of the constituent results are to be written to TAPES 63, 64, and 66. If ICTRIP(J) = 1, results concerning constituent J are written to tape. (INPUT)

IDIAG--(Integer) DIAGNostic flag; turns the writes to TAPE 61 on or off. (INPUT)

IDM--I Delta-t Maximum; stores the segment location for the cell at which the delta-t on a particular time step is at its maximum according to the V/Q criterion.

IDSTRB--(Integer) DiStributed TRiButary flag; turns the distributed tributary computation on or off. If IDSTRB = 1, QDSTRB, TDSTRB, and CDSTRB(NCP) must be provided via the subroutine TVDS. (INPUT)

IEPR--I-End Print; has a value of either 9 or 17. It controls which and how many segments are written in the snapshots. (GRID)

IES(NBP)--I-Enter Segment. The IES value, read for each branch, contains the boundary value for the right-hand side of that branch. IES can be either the segment where the branch enters the main stem or another branch, or user can specify one of the two other possible boundary conditions: downstream head (internal) or downstream flow (external). (INPUT)

IEVAP--(Integer) EVAPOration flag; turns the evaporation computation on or off. (INPUT)

IFLAG--(Integar) FLAG. IFLAG is transmitted to the time-varying data selector (TVDS) subroutine. If IFLAG equals to zero, TVDS performs the initialization function. If IFLAG is equal to one, TVDS returns to the main code with the correct values for the current ABTM.

IFORM--(Integer) FORM. IFORM is set to either zero or one, depending on the snapshot column width desired. When IFORM = 0, output is shortened and compressed to fit an 8-1/2-in. page width. When IFORM = 1, output includes the volume-area-elevation table and is for the 17 segments specified on the I1 and I2 cards. (GRID,INPUT)

I1--Computational variable.

IL--I-Left; used to store the segment number at the most upstream or left-hand segment for a particular branch. It is the same as the first parameter in the IBC array.

ILC--I-Left Current; current upstream boundary for each branch and the same as the second parameter in the IBC array. (TRIDAG)

ILCM1--I-Left Current Minus 1; current upstream boundary minus one for each branch.

ILCP--I-Left Current Prime; computational variable used to hold a new value for ILCP in the layer addition/subtraction, upstream cell addition/subtraction algorithm.

ILCP1--I-Left Current Plus 1; computational variable.

ILCPM1--I-Left Current Prime Minus 1; computational variable.

ILM1--I-Left Minus 1; computational variable.

ILS(NBP)--I-Leave-Segment. The ILS value for each branch contains the boundary value for the left-hand side of that branch. ILS can be either the segment number where the branch leaves the main stem or another branch, or can be set to one of two other boundary conditions: upstream flow (external) or upstream head external. (INPUT)

IMAX--I-MAXimum, stores the number of segments in the grid. (INPUT)

IMAXM1--I-MAXimum Minus 1; computational variable.

IMAXP--I-MAXimum Parameter; used to establish the segment dimensions of all the vectors and arrays in the code.

IPLLOT--(Integer) PLOT; used for turning the writing of information used for the velocity vector plots on or off. (INPUT)

IPRECP--(Integer) PRECiPitation flag; turns the precipitation computation on or off. If IPRECP = 1, PRECIP, TPRECP, and CPRECP(JC) must be provided via the subroutine TVDS. (INPUT)

IR--I-Right; used to store the segment number of the most downstream or right-hand active segment for each branch. It is the same as the third parameter in the IBC array. (TRIDAG)

IRM1--I-Right Minus 1; a computational variable.

IRP1--I-Right Plus 1; computational variable.

IRSR--(Integer) ReStart Read; turns the reading of the restart information option on or off. (INPUT)

IRSW--(Integer) ReStart Write; turns the writing of the restart information at the end of a simulation on or off. (INPUT)

ISC(IMAXP)--(Integer) Segment Coordinate; stores the layer number of the bottom-most active cell for each segment. (GRID)

ISODx--Specifies the largest segment number for which SODx applies (x = 1, NSOD). (INPUT)

ITCON--Specifies whether profiles and contour results, that is, writes to TAPE 64 and TAPE 66, are to occur at FOPL intervals (ITCON = 1) or only on OD dates (ITCON = 0). (INPUT)

ITP(10)--I-Temperature Profiles; stores the segment numbers for which temperature and constituent profiles are written out. (INPUT)

ITRIB(10)--I-TRIButary; stores the segment numbers at which tributaries are located. (INPUT)

ITRIP(NCP)--Specifies which of the constituents (totaling NC) is to be included in simulations. If ITRIP(J) = 1, constituent J is included. (INPUT)

ITSR--(Integer) Time Series Results; turns the writing of time series results to TAPE 61 switch on or off. (INPUT)

IVPR--(Integer) Vertical Profile Results; turns the writing of vertical temperature or constituent profiles to TAPE 64 switch on or off. (INPUT)

IWD(10)--I-WithDrawal; stores the segments at which withdrawals are located. (INPUT)

IWRITE(6)--(Integer) WRITE; contains six flags for writing U, W, T, Rho, C, and limiting factor values to the snapshots. (INPUT, GRID)

IWT--(Integer) Water body Type. If IWT = 0, total dissolved solids are simulated. If IWT = 1, the simulation includes salinity in computations. (INPUT, GRID)

IY--(Integer) Year; contains the two year-digits from the ABTM.

IZ1MAX--I-Z1-MAXimum; contains the segment number at which Z1 is at its maximum. It is used in deciding whether to add or subtract a layer.

J--DO-loop index used for tributaries, withdrawals, or outlets.

J1 --Alternative DO-loop index.

J2--Alternative DO-loop index.

JB--J-Bbranch; DO-loop index used for branches.

JBOUT(10)--J-Bbranch OUTlet; contains the branch number for each outlet. (INPUT)

JBT--J-Bbranch Top; computational variable used in determining the initial value of KT in the open boundary case.

JBTRIB(10)--J-Bbranch TRIButary; contains the branch number corresponding to each tributary.

JC--J-Constituent; DO-loop index that counts the number of constituents.

K--DO-loop index used for grid layers.

KBM1--K-Bottom Minus 1.

KBPR--K-Bottom Print; contains the deepest active layer to be printed. (GRID)

KBPRM1--K-Bottom Print Minus 1. (GRID)

KDM--K-Delta-t Maximum; stores segment number for the cell at which the delta-t on a particular time step is at its maximum according to the V/Q criterion.

KDT--K-Distributed Tributary; stores the layer at which distributed tributaries enter.

KMAX--K-Maximum; stores the number of layers in the grid. (INPUT)

KMAXM1--KMAX Minus 1.

KMAXP--Maximum Parameter; used to establish the segment dimensions of all the layers in the code.

KOUT(10)--K-OUTlet; stores the layer numbers for each outlet specified in the input listing. (INPUT,TVDS)

KT--K-Top; current layer number for the top active layer cells. (GRID)

KTm1--K-Top Minus 1.

KTP1--K-Top Plus 1.

KTRIB(10)--K-TRIButary; stores the layer at which tributaries enter.

KWD(10)--K-WithDrawal; contains the layer numbers at which withdrawals are located. (INPUT,TVDS)

L(IMAXP,KMAXP)--L is an integer array which stores the grid's active (L = 1) or inactive cells (L = 0).

LC(NBP*KMAXP,3,NCP)--L-Coordinate; contains the layer number (first position), the first active segment in that layer (second position), and the last active segment in that layer (third position).

LIMIT(IMAXP,KMAXP,1)--LIMITing factor; character variable that contains the factor limiting to algal growth. LIMIT contains P, N, or L corresponding to phosphorus, nitrogen, or light limitation as determined by the minimum of XP, XN, or XL.

M--DO-loop index.

MPAID--Character variable that contains the character string "MP"; used in conjunction with AID to check the Meteorological Parameter input card alphanumeric identifier.

N--DO-loop index used for program time steps.

NB--Number of Branches; stores the number of branches in the reservoir. (INPUT)

NBKMAX--Number of Branches * KMAX; a computational variable.

NBP--Number of Branches Parameter; used to establish the segment dimensions of all the branches in the code.

NC--Number of Constituents. (INPUT,GRID)

NCCLB(KMAXP,NBP)--Number of Cumulative Cells by Layer by Branch.

NCCLW(KMAXP)--Number of Cumulative Cells by Layer by Water body.

NCP--Number of Constituents Parameter; used to establish the segment dimensions of all the constituents in the code.

NH3K1--Rate multiplier corresponding to NH3T1.

NH3K2--Rate multiplier corresponding to NH3T2.

NH3T1, °C--Lower temperature bound for ammonia decay (nitrification).

NH3T2, °C--Lower temperature bound for maximum rate of ammonia decay.

NIT(50,2)--Number of Iterations; controls the total number of time steps for which the computation is performed. (INPUT)

NK--Number of K-layers; computational variable that counts the number of layers in each segment and is used in determining ILC and LCB.

NLC(NBP)--Number of Layer Coordinates. This variable contains the number of continuous layers in each branch and is a function of the branch number. There can be more than one continuous layer in each layer if, for instance, there is a submerged rise in the bottom of the reservoir, breaking the layer into two discrete strings. This variable is used in the tridiagonal algorithm solution for Z.

NLCW--Number of Layer Coordinates by Water body; stores the sum of the number of layer coordinates for the entire grid.

NLR--Computational variable used to determine placement of inflows at the left branch boundary. Contains the layer number for density matched inflows.

NMAX--Number of time steps MAXimum; the upper limit in the time step DO-loop.

NOBDAY--Number of Observation DAYS; stores the number of days for which survey observations are available. (INPUT)

NOBSTA--Number of Observation STATIONS; stores the number of segments for which survey observations are available. (INPUT)

NOUT--Number of OUTlets. (INPUT)

NO3K1--Rate multiplier corresponding to NO3T1.

NO3K2--Rate multiplier corresponding to NO3T2.

NO3T1, °C--Lower temperature bound for nitrate-nitrogen decay (denitrification).

NO3T2, °C--Lower temperature bound for maximum rate of nitrate-nitrogen decay.

NP--Number of Periods; number of delta-t time step periods to be read in. (INPUT)

NSOD--Number of Sediment Oxygen Demands; number of TSOD, ISOD pairs used in mapping SOD.

NTPS--Number of Time Periods; computational variable that determines when to print the vertical temperature and constituent profiles to TAPE 63.

NTPSP--Number of Time Periods Prime; computational variable related to NTPS.

NTRIB--Number of TriButaries. (INPUT)

NUMLNS--Number of LineS; computational variable that controls spacing in writes to TAPE 6.

NUPDC--Number of UPDates for Constituents; specifies the number of iterations between updates of the constituent internal source and sink array, CSS. (INPUT)

NUPDRT--Number of UPDates for RaTes; specifies the number of iterations between updates of the temperature rate multipliers. (INPUT)

NWD--Number of WithDrawals. (INPUT)

O2DET--Stoichiometric equivalent between detritus and oxygen for decomposition.

O2DOM--Stoichiometric equivalent between dissolved organic matter and oxygen for decomposition.

O2FAC--Stoichiometric equivalent between algae and oxygen for photosynthesis.

O2NH3--Stoichiometric equivalent between ammonia-nitrogen and oxygen for oxidation.

O2RESP--Stoichiometric equivalent between algal respiration and oxygen.

OJAID--Character variable that contains the character string "OJ"; used in conjunction with AID to check the Outlet J-branch input card alphanumeric identifier.

OKAID--Character variable that contains the character string "OK"; used in conjunction with AID to check the Outlet K-layer input card alphanumeric identifier.

OKL, sec^{-1} --Computed interfacial exchange rate for dissolved oxygen.

OUID--Character variable that contains the character string "OU"; used in the conjunction with AID to check the Oulet input card alphanumeric identifier.

OXYLIM, g m^{-3} --OXYgen LIMit; upper limit of dissolved oxygen for anaerobic processes. (INPUT)

P(IMAXP,KMAXP), pascals--Pressure.

PALT--Altitude correction factor for gas partial pressures; used to correct saturation concentrations of carbon dioxide and dissolved oxygen in computing interfacial exchange.

PEXCR(1), sec^{-1} --Maximum excretion (Photorespiration) rate for algae.

PHI, radians--Phi; wind direction. (TVDS)

PHI0(NBP), radians--Phi0; branch direction relative to the north. (INPUT)

PISAT(1), W m^{-2} --Light at maximum photosynthesis for algae.

PLT--PLoT; computational variable used to determine the time at which the next plotting information is written to TAPE 65 and TAPE 66.

PMAX(1), sec^{-1} --Maximum rate for algal production.

PMORT(1), sec^{-1} --Maximum rate for algal mortality.

PRECIP, m sec^{-1} --PRECIPitation; rate of precipitation over the entire water body. (TVDS)

PRESP(1), sec^{-1} --Maximum rate of algal respiration.

PRT--Computational variable used to determine the next time at which snapshot is written to TAPE 6.

PS2P04(1), g m^{-3} --Phosphorus half-saturation coefficient for algal growth.

PS2N(1), g m^{-3} --Nitrogen half-saturation coefficient for algal growth.

Q10COL--The Q_{10} formulation for coliform die-off.

Q(IMAXP,KMAXP), $\text{m}^3 \text{sec}^{-1}$ --Q is the source and sink array for the water budget. Almost all of the source and sink flows are either added to or subtracted from this array.

QBLL(KMAXP,NBP)--Q-Branch by Layer, Left; holds the upstream inflows to an outflow from the left side for each branch layer by layer.

QBLLNO(NBP)--Q-Branch by Layer, Left Net-0; stores the total inflow to or outflow from the upstream end of each branch.

QBLLN1(NBP), $m^3 \text{ sec}^{-1}$ --Q-Branch by Layer, Left Net-1; stores the total inflow to or outflow from the upstream end of each branch.

QBLR(KMAXP,NBP), $m^3 \text{ sec}^{-1}$ --Q-Branch by Layer, Right; holds the upstream inflows to or outflows from the right side for each branch layer by layer.

QBLRNO(NBP), $m^3 \text{ sec}^{-1}$ --Q-Branch by Layer, Right Net-0; stores the total inflow to or outflow from the upstream end of each branch.

QBLRN1(NBP), $m^3 \text{ sec}^{-1}$ --Q-Branch by Layer, Right Net-1; stores the total inflow to or outflow from the upstream end of each branch.

QDSTRB(NBP), $m^3 \text{ sec}^{-1}$ --Q-DiStributed TRiButary; contains the inflow rates for distributed tributaries. (TVDS)

QDT, $m^3 \text{ sec}^{-1}$ --Q-Distributed Tributary; contains the portion of the QDSTRB, or distributed tributary flow, proportioned to each segment of the branch by its area in relation to the total branch area at a particular layer.

QE(IMAXP), $m^3 \text{ sec}^{-1}$ --Q-Evaporation; contains the evaporation rate segment by segment.

QET(NBP), $m^3 \text{ sec}^{-1}$ --Q-Evaporation Total; contains the total evaporation rate for each branch.

QIN(NBP), $m^3 \text{ sec}^{-1}$ --Q-INflow; specifies the upstream inflow to each branch. (TVDS)

QOUT(10)--Q-OUTflow; specifies downstream outflow rates for the flow boundary conditions. (TVDS)

QPRECP, $m^3 \text{ sec}^{-1}$ --Q-PRECiPitation; computational variable used to temporarily hold the precipitation rate for each segment.

QPRCPS(NBP), $m^3 \text{ sec}^{-1}$ --Q-PRECiPitation Sum; stores the total precipitation into each branch.

QSUM, $m^3 \text{ sec}^{-1}$ --Q-SUM; contains the total outflow for the right boundary flow condition case.

QTOT, $\text{m}^3 \text{sec}^{-1}$ --Q-TOTAL; computational variable used to aggregate tributary inflows that are above the current upstream segment (ILC) into the upstream inflow.

QTRIB(10), $\text{m}^3 \text{sec}^{-1}$ --Q-TRIButary; contains the inflow rates for tributaries. (TVDS)

QWD(10), $\text{m}^3 \text{sec}^{-1}$ --Q-WithDrawal; contains withdrawal rates. (TVDS)

RFRDK, sec^{-1} --Maximum decay rate for refractory dissolved organic matter.

RHO(IMAXP,KMAXP), kg m^{-3} --Rho(ρ); density. (GRID)

RHOA, 1.25 kg m^{-3} --Rho Air (ρ_a); density of air, assumed constant.

RHOI, $1,000 \text{ kg m}^{-3}$ --Rho-Initial (ρ_i); initial density. RHOI is used to set the boundary cell densities and has no effect on the computation.

RHOICE, kg m^{-3} --Rho-ICE; density of ice.

RHOIN--Rho-INflow; computational variable that holds the density of the inflow so that it can be compared with the density profile where the tributary enters the reservoir.

RI--Richardson number.

RIABTM--(Real) (Integer) ABSolute TIme; the year plus day portion of the computation clock.

RIAZO--Richardson AZO; the Richardson number derived from the ratio of AZO to AZMAX.

RIAZ1--Richardson AZ1; the computed Richardson number.

RIIT, m--(Real) Initial Ice Thickness. (INPUT)

RIMT, $^{\circ}\text{C}$ --(Real) Ice Melt Temperature; used in the ice computation.

RIS--(Real) Ice Switch; used to turn off the wind stress computation when ice covers the water body.

RIT(IMAXP), m--(Real) Ice Thickness; stores ice thickness for each segment. (GRID)

RK1--Ice computational variable.

RL1--Ice computational variable.

RLISCS(KMAXP)--(Real) Layer Inflow Segment Cross Section; computational variable used in proportioning the upstream inflow across all the layers of the inflow segment.

RTMLT1(J,IMAXP,KMAXP)--Temperature rate multiplier for the ascending portion of the temperature curve. An index of J terms is provided in the subroutine RMULT.

RTMLT2(J,IMAXP,KMAXP)--Temperature rate multiplier for the descending portion of the curve. An index of J terms is provided in the subroutine RMULT.

SB(IMAXP,KMAXP), $m^3 \text{ sec}^{-2}$ --Stress at the Bottom.

SEDDK, sec^{-1} --Maximum sediment decay rate.

SETL(1), $m \text{ sec}^{-1}$ --Algal settling rate.

SFCO2--Sediment production rate of carbon dioxide expressed as a fraction of sediment oxygen demand.

SHEARS, sec^{-2} --Vertical velocity gradient.

SNAID--Character variable that contains the character string "SN"; used in conjunction with AID to check the Snapshot input card alphanumeric identifier.

SOD(IMAXP), $g \text{ m}^{-2} \text{ sec}^{-1}$ --Maximum zeroth-order sediment oxygen demand.

SODK1--Rate multiplier corresponding to SODT1.

SODK2--Rate multiplier corresponding to SODT2.

SODK3--Rate multiplier corresponding to SODT3.

SODK4--Rate multiplier corresponding to SODT4.

SODT1, °C--Lower temperature bound for sediment oxygen demand.

SODT2, °C--Lower temperature bound for maximum sediment oxygen demand.

SODT3, °C--Upper temperature bound for maximum sediment oxygen demand.

SODT4, °C--Upper temperature bound for sediment oxygen demand.

SODx, $\text{g m}^{-2} \text{sec}^{-1}$ --Sediment Oxygen Demand; rate of sediment oxygen demand in segments specified by ISODx. Up to three values for SODx may occur.

SRM, W m^{-2} --Incident solar radiation for computing algal growth.

SRO, $^{\circ}\text{C m sec}^{-1}$ --Solar Radiation. (TVDS)

SSC, $\text{m}^2 \text{sec}^{-1}$ --Surface Stress Coefficient.

SSETL, m sec^{-1} --Settling rate of inorganic suspended solids.

SSSUM, g m^{-3} --Suspended Solids SUM; contains the sum of inorganic suspended solids and is used to modify the light extinction coefficient. (INPUT)

ST(IMAXP,KMAXP), $\text{m}^3 \text{sec}^{-2}$ --Stress Top. The ST array contains stresses at the top of each cell.

SUM, m^2 --Represents the total cross-sectional area at the boundary and is used in the open boundary computation.

T1(IMAXP,KMAXP), $^{\circ}\text{C}$ --Temperature time level 1.

T2(IMAXP,KMAXP), $^{\circ}\text{C}$ --Temperature time level 2. (GRID)

T1AID--Character variable that contains the character string "T1"; used in conjunction with AID to check the first Title input card alphanumeric identifier.

T2AID--Character variable that contains the character string "T2"; used in conjunction with AID to check the second Title input card alphanumeric identifier.

T3AID--Character variable that contains the character string "T3"; used in conjunction with AID to check the third Title input card alphanumeric identifier.

T4AID--Character variable that contains the character string "T4"; used in conjunction with AID to check the fourth Title input card alphanumeric identifier.

TA, $^{\circ}\text{C}$ --Air temperature. (TVDS)

TBPL, year/days--Time to Begin Plotting; specifies the time that plotting, that is, writing to TAPE 65 and TAPE 66, is started. (INPUT)

TBPR, year/days--Time to Begin Printing; specifies the time that printing, that is, writing to TAPE 65 and TAPE 66, is started. (INPUT)

TBTSR--Time to Begin Time Series; specifies the time that time series, that is, writing to TAPE 63, is started. (INPUT)

TCB(IMAXP,KMAXP)--Transport Coefficient Bottom; bottom coefficient for the explicit transport of heat and constituents.

TCC(IMAXP,KMAXP)--Transport Coefficient Centered; centered coefficient for the explicit transport to heat and constituents.

TCL(IMAXP,KMAXP)--Transport Coefficient Left; left coefficient for the explicit transport of heat and constituents.

TCNREL, $\text{g m}^{-2} \text{ day}^{-1}$ --Specifies the zero-order rate of sediment ammonia-nitrogen release under anaerobic conditions. (INPUT)

TCOLDK, day^{-1} --Rate of coliform bacteria mortality. (INPUT)

TCR(IMAXP,KMAXP)--Transport Coefficient Right; right coefficient for the explicit transport of heat and constituents.

TCT(IMAXP,KMAXP)--Transport Coefficient Top; top coefficient for the explicit transport of heat and constituents.

TD, $^{\circ}\text{C}$ --Dew point temperature. (TVDS)

TDETDK, day^{-1} --Rate of detritus decay. (INPUT)

TDOMDK, day^{-1} --Upper limit of the rate of labile DOM decay. (INPUT)

TDOMRF, day^{-1} --Specifies the rate of transfer from labile to refractory DOM. (INPUT)

TDSETL, m day^{-1} --Settling rate of detritus. (INPUT)

TDSTRB(NBP), $^{\circ}\text{C}$ --Temperature DiStributed TRiButary; the temperature of inflows from distributed tributaries. (TVDS)

TEST1, m^3 --Computational variable corresponding to the volume of inflow during a particular time step.

TEST2, m^3 --Computational variable set to 90 percent of the volume of the vertical cell NLR in the leftmost active segment.

TFEREL--Sediment release rate for iron under anaerobic conditions expressed as a fraction of the sediment oxygen demand. (INPUT)

TFESET, m day^{-1} --Settling velocity for total iron. (INPUT)

TI, °C--Initial temperature. TI can be set to a value to be applied to the entire grid's temperature or to -1. If TI = -1., vertical profiles are read. (INPUT)

TIN(NBP), °C--Temperature IN; stores the temperature of the upstream inflows for each branch. (TVDS)

TISCS, m^2 --Total Inflow Segment Cross Section; computational variable used in conjunction with RLISCS to proportion the upstream inflow according to inflow segment cross-sectional area.

TITLE(4)--Character array that contains the four lines of the simulation text. (INPUT,GRID)

TIVP(KMAXP), °C--Temperature Initial Vertical Profile; used to establish an initial vertical profile for temperature. (INPUT)

TL(KMAXP,NBP), °C--Temperature Left; stores the vertical temperature profile for the open water boundary condition at the upstream end of each branch layer by layer. (TVDS)

TLAID--Character variable that contains the character string "TL"; used in conjunction with AID to check the Tributary Location input card alphanumeric identifier.

TM, °C--Temperature Mean; the average of the surface and dew point temperatures. TM is used in computing data for the evaporation computation.

TMAID--Character variable that contains the character string "TM"; used in conjunction with AID to check the Time input card alphanumeric identifier.

TMD, fraction of a day--Time of Day; derived from the current simulation time by dropping the year and day.

TMY, fraction of a day--Time of Year; derived from the current simulation time and equal to the FLOAT (Julian day).

TNH3DK, day^{-1} --Rate of ammonia decay (nitrification). (INPUT)

TNO3DK, day^{-1} --Rate of nitrate-nitrogen decay (denitrification). (INPUT)

TOL--TOLerance; used in the water budget. TOL is the percent tolerance allowed in the ration of spatially and temporally integrated volumes before computation is halted. (DATA)

TOUT(10), °C--Temperature OUTflow; water temperature of the downstream outflow.

TOUTAV, °C--Temperature OUT AVerage; contains the volume-weighted average outflow temperature for time series results (TAPE 63).

TPEXCR(1), day^{-1} --Maximum excretion (photorespiration) rate of algae. (INPUT)

TPMAX(1), day^{-1} --Maximum growth rate of algae. (INPUT)

TPMORT(1), day^{-1} --Maximum mortality rate of algae. (INPUT)

TPRECP, °C--Temperature PRECiPitation; temperature of inflow due to precipitation. (TVDS)

TR(KMAXP,NBP), °C--Temperature Right. The TR array contains the vertical temperature profile for the open water boundary conditions at the downstream end of each branch layer by layer.

TRAID--Character variable that contains the character string "TR"; used in conjunction with AID to check the TRibutary input card alphanumeric identifier.

TRANS--TRANSfer; holds the most recent value of one of a series of time-dependent variables while the previous value is switched into a former array.

TRFRDK, day^{-1} --Rate of refractory DOM decay. (INPUT)

TSEDDK, day^{-1} --Upper limit of the rate of organic sediment decay. (INPUT)

TSETL(1), m day^{-1} --Settling rate of algae. (INPUT)

TSOD(x), $\text{g m}^{-2} \text{day}^{-1}$ --Rate of sediment oxygen demand for the segments specified by ISODx. For example, TSOD(1) applies from segments 2 to ISOD(1). (INPUT)

TSR--Time Series. TSR is a computational variable used to determine the time at which the next plotting information is written to TAPE 63.

TSSETL, m sec^{-1} --Contains the inorganic suspended solids settling velocity. (INPUT)

TTP(12), year/days --Time of Temperature Profiles; used to specify the time in which the vertical temperature profiles are to be written. (INPUT)

TTRIB(10), °C--Temperature of TRIButaries; contains the temperature of each tributary. (TVDS)

TWAID--Character variable that contains the character string "TW"; used in conjunction with AID to check the Tape Write input card alphanumeric identifier.

TWD(10), °C--Temperature of WithDrawal; contains the water temperature of withdrawals.

TXP4RE--Rate of sediment phosphorus release under anaerobic conditions expressed as a fraction of SOD. (INPUT)

U(IMAXP,KMAXP), m sec⁻¹--x-direction velocity. (GRID)

UL, m sec⁻¹--U Left; mean velocity at the left side of each cell.

UR, m sec⁻¹--U Right; mean velocity at the right side of each cell.

US(IMAXP,KMAXP)--U Sign; upstream difference operator for the x-direction velocity. If that velocity is positive, US is equal to zero. If that velocity is negative, US is equal to one.

V(IMAXP)--Contains the main diagonal coefficients for the tri-diagonal algorithm solutions for Z.

VOL1(NBP), m³--Volume time level 1; used to ensure a perfect water balance in each branch; it is the sum of the B * H * DLX.

VOL2(NBP), m³--Volume time level 2; computed from VOL1 but is the volume for each branch on the previous time step. The change in volume over time for each branch is used with the net inflow or outflow to modify to QBLRNO or QBLLNO such that perfect water balance is maintained for each branch.

VOLS(NBP), m³--VOLume Spatially; used as a check on the overall water budget in the computation. It represents, at any particular time, the total volume in each branch as obtained by B * H * DLX for each cell.

VOLSW, m³--VOLume Spatially integrated for the entire Water body; used as a check on the water budget for the water body as a whole. It represents, at any particular time, the total volume of the water body.

VOLT(NBP), m³--VOLume Temporally; used as a check on the overall water budget. It represents the initial volume in each branch plus the time-integrated inflows minus the time-integrated outflows.

VOLTW, m³--VOLume Temporally integrated for the entire Water body; used as a check on the water budget for the water body as a whole. It represents the initial volume plus the time-integrated inflows minus the time-integrated outflows.

VPAID--Character variable that contains the character string "VP"; used in conjunction with AID to check the Vertical Profile input card alphanumeric identifier.

VRATIO(NBP)--Ratio between the spatially integrated volume and the time-integrated volume for each branch. The computation is halted if VRATIO deviates from 100 percent by more than the specified tolerance.

VRTIOW--Volume RaTIO for the Water body; represents the ratio of the spatially (VOLSW) and temporally (VOLTW) integrated water volumes for the water body as a whole. The computation is halted when VRTIOW deviates from 100 percent by more than the specified tolerance.

W(IMAXP,KMAXP), m sec⁻¹--Vertical velocities, positive down.
(GRID)

WA, m sec⁻¹--Wind speed. (TVDS)

WAS, m sec⁻¹--Wind speed, Shaded; the wind speed times the effective wind coefficient for each branch.

WB, m sec⁻¹--W Bottom; the average vertical velocity at the lower right-hand corner of each cell.

WDAID--Character variable that contains the character string "WD"; used in conjunction with AID to check the WithDrawal I-segment input card alphanumeric identifier.

WKAID--Character variable that contains the character string "WK"; used in conjunction with AID to check the Withdrawal K-layer input card alphanumeric identifier.

WKT(IMAXP), m sec⁻¹--WK Top; the vertical velocity at the bottom of each of the top layer cells. WKT is computed differently from the rest of the vertical velocities in that it is computed from the change in storage in the top layer in order to preserve a perfect water balance. It is used strictly in the temperature and constituent transport equations and differs very little from the W of KT computed in the usual manner.

WS(IMAXP,KMAXP)--Upstream differencing parameter for the vertical velocities. If W is less than zero, WS is equal to zero. If W is greater than zero, WS is equal to one.

WSKT(IMAXP)--Upstream differencing parameter for WKT. If WKT is less than or equal to zero, WSKT is equal to zero. If WKT is greater than zero, WSKT is equal to one.

WT1, $m^2 \text{ sec}^{-1}$ --W Term 1; computational variable used in computing the vertical velocities. WT1 is equal to the vertical transport at the bottom of that cell for which the vertical velocity is being computed.

WT2, $m^2 \text{ sec}^{-1}$ --W Term 2; computational variable used in computing the vertical velocities. WT2 is equal to the net transport through the cell from the left and right boundaries. WT2 also includes any sources or sinks.

WT3, $m^2 \text{ sec}^{-1}$ --W Term 3; computational variable used in computing the balance of W in the top layer. WT3 is equal to the change in storage from one time step to another divided by the Δt .

WWT--Wind Wave period.

YD, days--Year Days; the number of days in a year. It is used in the algorithm for computing ABTM.

XL--Temporary variable for photosynthetic limitation due to light.

XN--Temporary variable for photosynthetic limitation due to total nitrogen (CNTOT(IMAXP,KMAXP)).

XP--Temporary variable for photosynthetic limitation due to orthophosphorus.

XP4REL, $g \text{ m}^{-2} \text{ sec}^{-1}$ --Zeroth-order sediment release rate for phosphorus.

XPO4K1--Rate multiplier corresponding to XPO4T1.

XPO4K2--Rate multiplier corresponding to XPO4T2.

XPO4K3--Rate multiplier corresponding to XPO4T3.

XPO4K4--Rate multiplier corresponding to XPO4T4.

XPO4T1, °C--Lower temperature bound for sediment phosphorus release.

XPO4T2, °C--Lower temperature bound for maximum sediment release rates for phosphorus.

XPO4T3, °C--Upper temperature bound for maximum sediment release rates for phosphorus.

XPO4T4, °C--Upper temperature bound for sediment phosphorus release.

XPP--Computational variable that determines the size of the negative hedge. If a given constituent falls below its corresponding value of XPP at the end of a time step, it is set equal to this value.

Z1(IMAXP), m--Z time level 1; the deviation of the water surface from the top active layer of cells, positive down. (TRIDAG)

Z1MAX, m--Z1's MAXimum value; used in the top layer algorithm that is for adding and subtracting layers.

Z2(IMAXP), m--Z time level 2; stores, in positive down values, the deviation of the water surface from the top active layer of cells. (GRID)

ZI--Z Initial; initial water surface elevation. (INPUT)

ZL(NBP), m--Z Left; time-varying upstream elevation deviation.

ZR(NBP), m--Z Right; time-varying downstream elevation deviation.

APPENDIX C: GRAPHICS AND STATISTICAL ROUTINES FOR CE-QUAL-W2

1. A variety of statistical and graphics routines have been prepared to display output results from CE-QUAL-W2. Several of these packages can also be used to concurrently display calibration and confirmation field measurements for the purpose of evaluating model accuracy and making necessary adjustments to the model parameters.

2. Contour plots (method I) are potentially the most useful means of data display since large amounts of data can be summarized in a relatively few plots and compared with field data. Model output can be viewed from three different perspectives: a reservoir side view, a segment time series view, and a depth time series view (see Figure C1). If a Versatec plotter is available, shaded contour plots (method II) can be produced from the same data set as for the line contour plots; presently, only the reservoir side view is available. Displays of velocity vectors at specified times during a simulation can be produced with method III. Time series displays (method IV) can be produced for surface water elevation and for flow-weighted temperature and constituent concentrations in the main stem outflow. Depth profiles of temperature and constituent concentrations for specified dates and segments can be displayed by method V. The statistical routine compares observed and predicted data for each OD date and provides summary statistics for all sample dates.

3. Instructions for each of these methods are provided on the following pages. Since graphics displays are dependent on specific hardware and software configurations, the instructions and programs will need to be modified for a particular computer system. These instructions and programs were implemented on a DEC VAX 11/750 under the VMS operating system. Graphics devices used on this system with these display programs included a Tektronix 4014 and various 4014 emulating terminals, a Versatec V80 electrostatic plotter, and a Tektronix 4662 pen plotter.

4. Methods I-IV were written using Calcomp/Versatec plotting subroutines. Use of these programs as written will require the subroutine

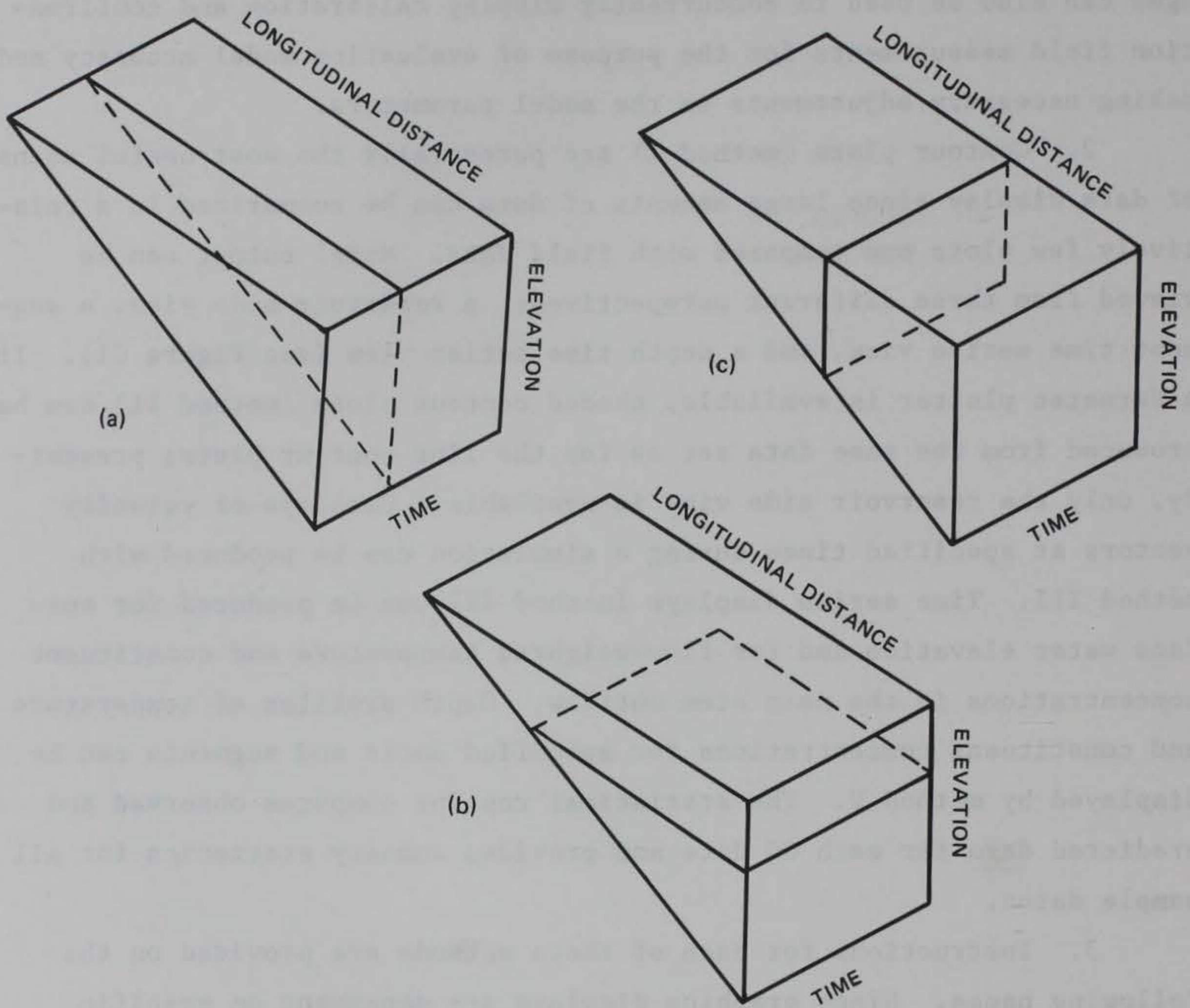


Figure C1. Diagram of contour plots available with QCONTOUR, a contouring package for CE-QUAL-W2, where (a) elevation-longitudinal distance contours at specified times; (b) longitudinal distance-time contours at specified depths, and (c) elevation-time series contours at specified longitudinal distances

packages from either of these vendors for use on their plotters, or the Tektronix Terminal Control System and Preview packages for use on Tektronix terminals or emulators. Method V was written using the Graphics Compatibility System (GCS) and can be used on a Tektronix 4014 terminal or emulator. Depending on the hardware configuration at a particular computer installation, an alternate plotting device may also be used with method V.

Instructions for Contour Plotting

5. Obtain contour output. To obtain contour data from CE-QUAL-W2, turn on switch ICNTR and the ICTRIP switches for the desired constituents. Set the ITCON switch (TW card) for the interval type desired: If ITCON = 1, contour data will be written at FOPL intervals to data set CONTOUR.OTP (TAPE 66); if ITCON = 0, contour data will be written for every OD date. (See Table C1 for contour data set format.)

6. Run UNFORM. Since the contour output data set is potentially quite large, it should be unformatted (binary) for lower storage costs and greater efficiency. This program converts the formatted contour data set from CE-QUAL-W2 into an unformatted one. This step is not necessary if unformatted output is obtained directly from CE-QUAL-W2.

7. Prepare VER1.DAT if desired (optional confirmation data set). (See Table C2 for the format of this data set.)

8. Run QCONTP (linked with Tektronix Preview subroutines) to display the contour plots on a Tektronix 4014 or equivalent. If Preview is not available, skip to paragraph 9.

a. The user is now ready to run the contouring program. Preview options must first be declared. The first question asked is MODE/OPTION? Here the user types "3" to request that each plot be viewed separately. The preview program then prompts the user with: OPTION? (Giving a "?" here will list the options available and a short explanation of each.) Type E,C,C to erase the screen and continue to the contouring program.

b. The next question is:

INPUT DATA FILE NAME?

Table C1

Contour Data Set Format for CE-QUAL-W2

| | |
|--------|---|
| Card 1 | TITLE (A72) title = first title card from input data deck |
| Card 2 | DTM,KMAX,HIN,NB,(DLX(JB),JB=1,NB) (F8.1,I3,F8.1,I3,6F8.1) dtm = elevation at lower grid boundary, m kmax = number of layers in the grid hin = initial grid layer thickness, m nb = number of branches dlx = cell length for branch, km |
| Set 1 | NSEGS,JC,JB,ABTM (3I3,F10.2) nsegs = number of segments in this set jc = constituent number jb = branch number abtm = absolute time (julian date.decimal hour) |
| 1A | I,KT,KTOT (3I3) i = segment number kt = number of first active layer ktot = total number of active layers |
| 1B | (Z(I),I=1,KTOT) (10F8.4) z = constituent value |

NOTE: Set 1 is repeated for each constituent and time specified.

Table C2

Confirmation Data Set Format for Contour Plots

| | |
|--------|---|
| Card 1 | TITLE (A72) title = description of this data set, up to 72 characters |
| Set 1 | NSOD,JCOD,IDATE,NPAIRS,(DEPTH(I),C2(I),I=1,NPAIRS) nsod = segment number jcod = constituent number idate = date (ABTM format without decimal) npairs = number of pairs of depth-constituent values depth = depth, positive down, m c2 = constituent value |

NOTES: Set 1 is repeated for each segment, constituent, and date.

Format for set 1: (2I3,I7,I4,1X,4(F4.1,1X,F9.3,1X),/,
(18X,4(F4.1,1X,F9.3,1X)))

Format specification provided for information only, as the contour program expects to use an unformatted data set for better efficiency.

This corresponds to the name of the data file that contains the contour data set. A two-level VAX name can be supplied, e.g., CONTUNF.DAT, but only the first part is required.

c. The next statement is:

```
SELECT CONTOUR TYPE:
RESERVOIR - SIDE VIEW (0)
SEGMENT TIME SERIES - FRONT VIEW (1)
DEPTH TIME SERIES - TOP VIEW (2) ?
```

Choose the desired contour type (see Figure C1).

(1) If the reservoir side view is chosen, the next request will be

DATE (ABTM FORMAT), CONSTITUENT, BRANCH?

(2) If segment time series is chosen, the next request will be

CONSTITUENT, SEGMENT?

(3) If the depth time series is chosen, the request will be

CONSTITUENT, LAYER, BRANCH?

d. The next question is:

NUMBER OF CONTOUR LEVELS, 1ST LEVEL, LAST LEVEL?

The contour levels are computed by dividing the difference between the first level and the last level equally so as to obtain the requested number of contour levels. Any number of these sets of data can be input by typing a set after each MORE? question. However, the total number of contour levels cannot exceed 50. To go to the next question, type a carriage return.

e. The next question asked is:

```
PLOT OBSERVED NUMBERS (1), SIMULATED
NUMBERS (2), OR NONE (0)?
```

This option allows the user to plot the observed (confirmation) data points or the simulated numbers (Z values) centered at their respective (X,Y) positions

on the contour plot. The user can then check the accuracy of the generated contour lines. (Note: option 1 is not currently available for the depth time series.) If option 1 or 2 is the answer, the question:

NUMBER OF PLACES TO RIGHT OF DECIMAL POINT?

is asked. This allows plotting of the Z values at the proper accuracy.

- f. The next question asked is:

PLOT CONTOUR LABELS?

If "Y" or "YES" is given, contour lines will be labeled with letters, starting with "A." If "N" or "NO" is given, lines will not be labeled but a list of contour levels will still be given.

- g. At this point, if no problems have occurred, the preview program will take over and OPTION ? will appear on the screen. At this point you must set the screen window in which to view the plot. (This can be done any time after mode selection, before the plot appears. It can also be changed for subsequent plots if desired.) The appropriate window setting would be -2,-2 for the origin and 17,12 for the size. Erase (E) and continue (C) as necessary to view the plot and continue with the program. After the contour plot is drawn on the screen, the bell will ring and the program will pause. If a plot has been produced on the screen, the user can then make a hard copy before typing a "C" to go back to the NUMBER OF CONTOUR LEVELS, 1ST LEVEL, LAST LEVEL? question. The user can then type a carriage return and go back one question to SELECT CONTOUR TYPE . In fact, the program is designed to allow the user to return to the previously asked question at any time by hitting a carriage return (except for the MORE? question). To exit the program, continue hitting carriage returns, until OPTION? appears; then type "Q" to quit.
- h. To produce a plot on the Tektronix 4662 pen plotter, use the Tektronix 4014 terminal at 1200 baud, turn the plotter on, load the paper and pen, and then use "P" as the final option before the contour is plotted. The plot will then be produced on the pen plotter directly. Use option "O" to return to previewing on the screen.

9. To produce a plot directly on the Versatec plotter, run QCONTV (linked with Calcomp/Versatec subroutines). Previewing options are not used with this version of the program, so no MODE/OPTION ? prompts

will appear. Instead, enter any Versatec options you would like after each "VPL>." Enter "/E" to use the defaults or after the last option. (One recommended option is SCALE=.5 to reduce the plot to one-half size.) Then follow directions as outlined in paragraph 8c to specify the various contour options. On the VAX, plot files will be created in VECTR1.PLV and PARM.PLV.

10. Send the PLV files to the Versatec plotter. On the VAX, this is done by entering "PH." This logical name executes RASM.EXE through a command procedure PH*ase2.

11. Sample problem. The sample interactive session given below demonstrates use of the program under preview.

To obtain a reservoir side view with observed values plotted:

```
$ ASSIGN VD79R2U.DAT VER1
$ RUN QCONTP
START OF PREVIEW
MODE/OPTION? 3
OPTION? E,C,C
INPUT DATA FILE NAME?
CONTUNF.DAT
SELECT CONTOUR TYPE:
  RESERVOIR - SIDE VIEW (0)
  SEGMENT TIME SERIES - FRONT VIEW (1)
  DEPTH TIME SERIES - TOP VIEW (2)
0
DATE (ABTM FORMAT), CONSTITUENT, BRANCH ?
79163.48 12 1
NUMBER OF CONTOUR LEVELS, 1ST LEVEL, LAST LEVEL?
12 6 28
MORE?
<CR>
PLOT OBSERVED NUMBERS(1), SIMULATED NUMBERS(2), OR NONE(0) ?
1
NUMBER OF PLACES TO RIGHT OF DECIMAL POINT?
1
PLOT CONTOUR LABELS?
Y
```



```

OPTION? E
OPTION? W
WHERE WOULD YOU LIKE ORIGIN?(X,Y) -2,-2
ENTER SIZE (WIDTH,HEIGHT) 17,12
OPTION? E,C
      (plot should now appear on screen)
OPTION? C      (to continue with another plot)
      Q      (to quit the program)

```

12. To produce the same plot directly on the Versatec, but half-size:

```

$ RUN QCONTV
VPL> SCALE=0.5
VPL> /E
INPUT DATA FILE NAME?
CONTUNF.DAT
SELECT CONTOUR TYPE:
  RESERVOIR - SIDE VIEW (0)
  SEGMENT TIME SERIES - FRONT VIEW (1)
  DEPTH TIME SERIES - TOP VIEW (2)
0
DATE (ABTM FORMAT), CONSTITUENT, BRANCH ?
79163.48 21 1
NUMBER OF CONTOUR LEVELS, 1ST LEVEL, LAST LEVEL?
12 6 28
MORE?
<CR>
PLOT OBSERVED NUMBERS(1), SIMULATED NUMBERS(2), OR NONE(0) ?
1
NUMBER OF PLACES TO RIGHT OF DECIMAL POINT?
1
PLOT CONTOUR LABELS?
Y
<CR>
<CR>
<CR>
<CR>

```

Figure C2 shows the resulting plot. Figure C3 shows the results with the no data points plotted; Figure C4 shows the same plot with the simulated numbers plotted for comparison. Figures C5 and C6 show a segment-time series plot, with and without confirmation data for comparison. Figure C7 shows a depth-time series plot.

13. Batch mode. The program can be run in batch mode to produce Versatec plot files, by preparing a command file containing the appropriate answers to the questions asked by the program. The listing below

REGULAR DEGRAY RUN WITH 1979 TVDS DATA

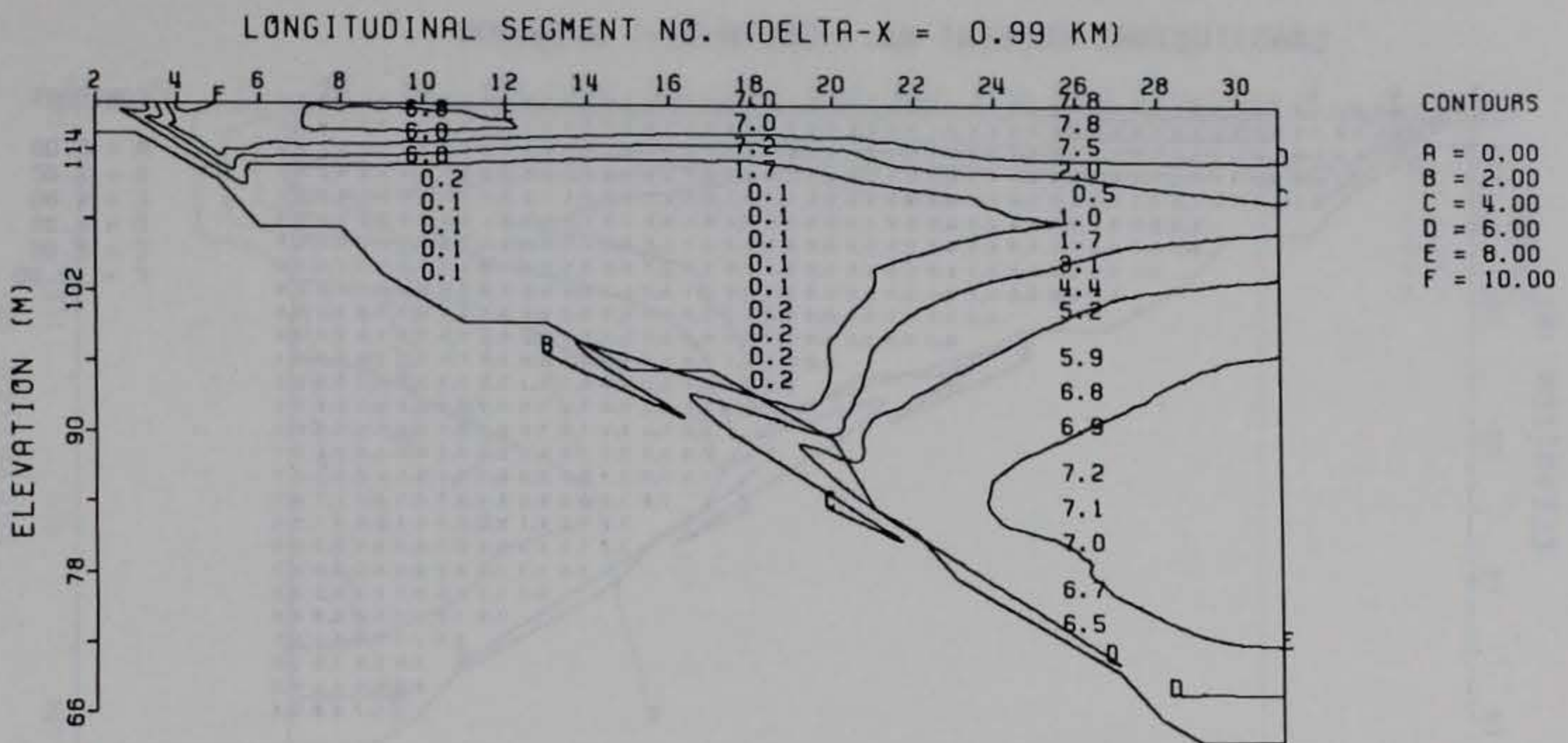


Figure C2. Example of reservoir contour (side view) with observed (confirmation) data

REGULAR DEGRAY RUN WITH 1979 TVDS DATA

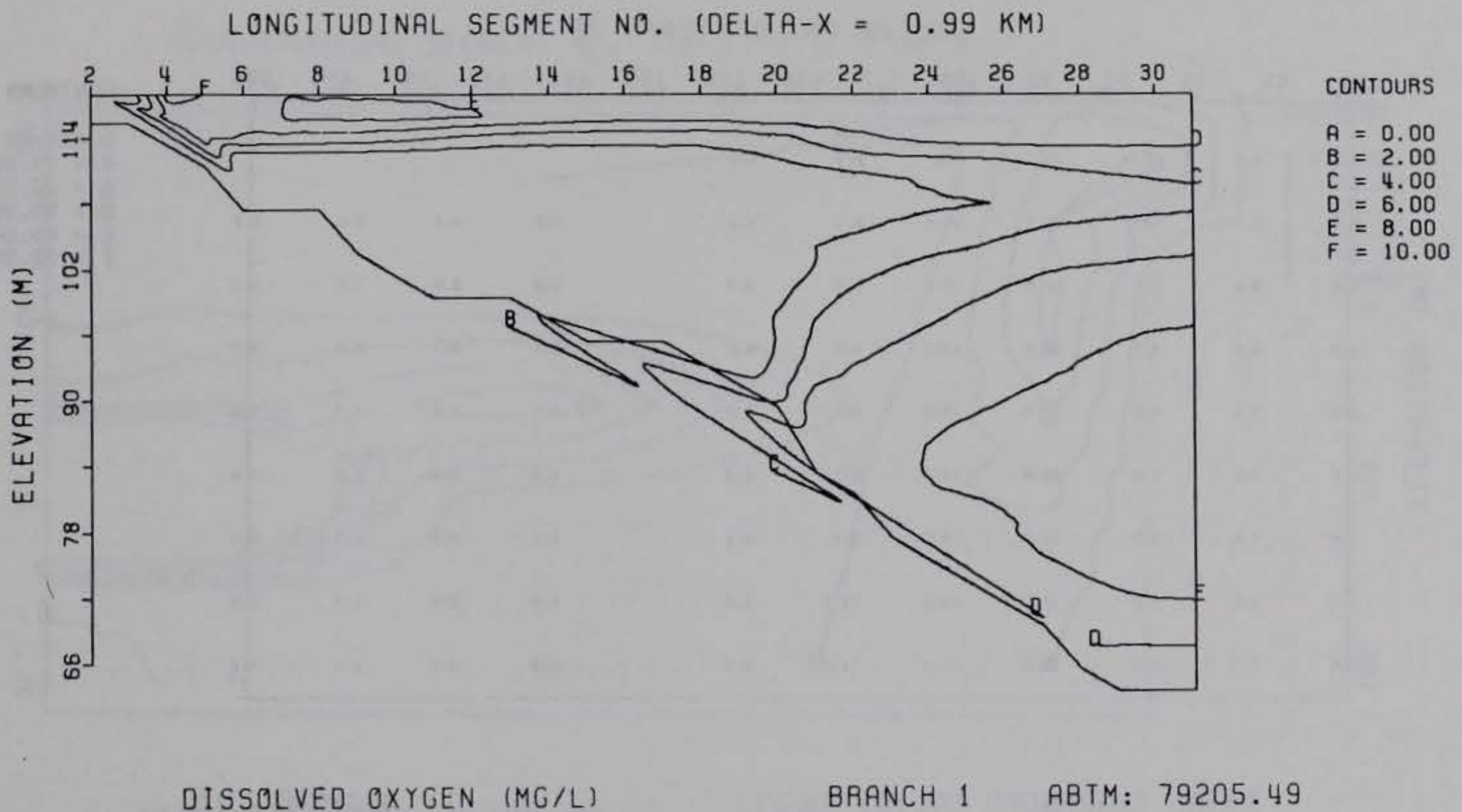
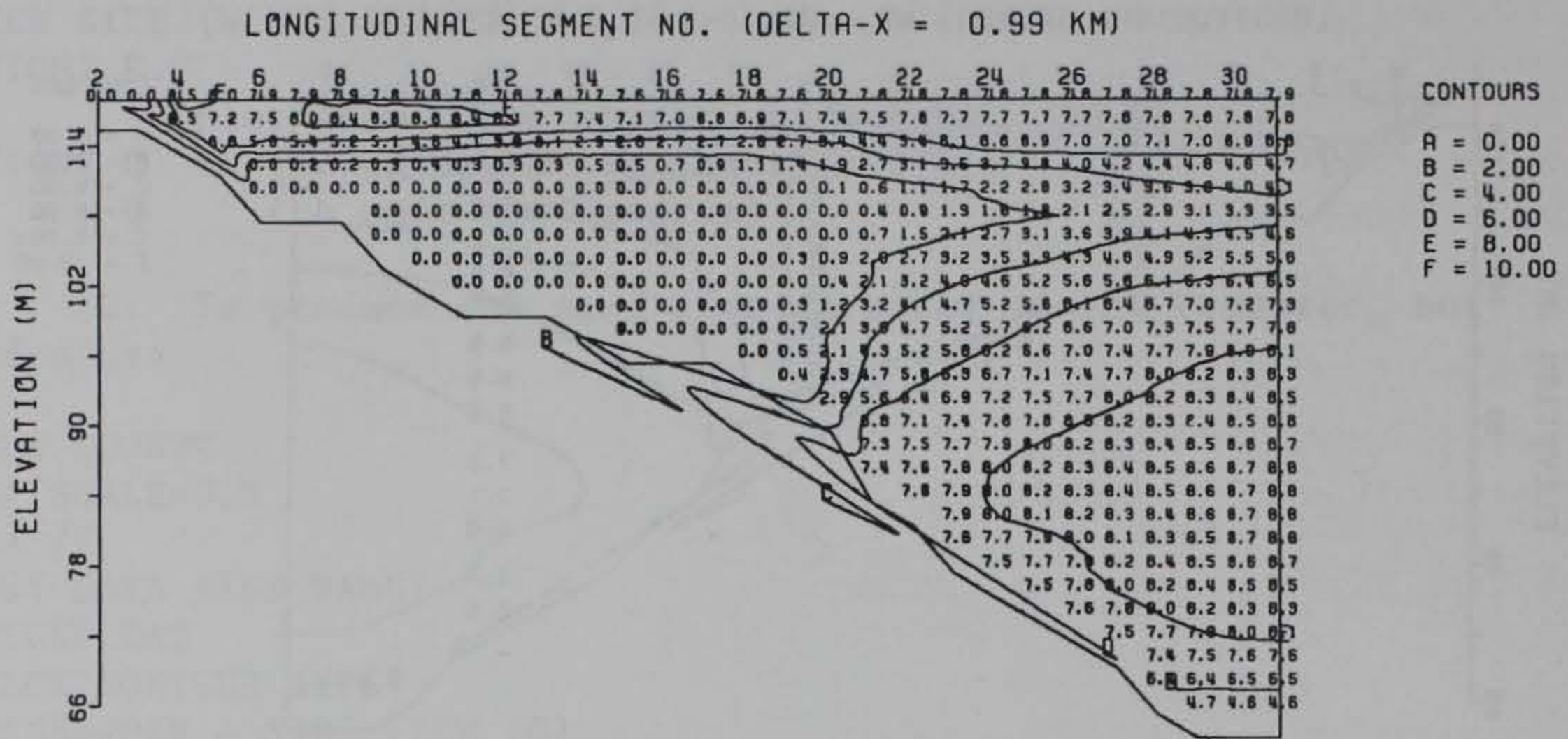


Figure C3. Example of reservoir contour (side view) without observed (confirmation) data

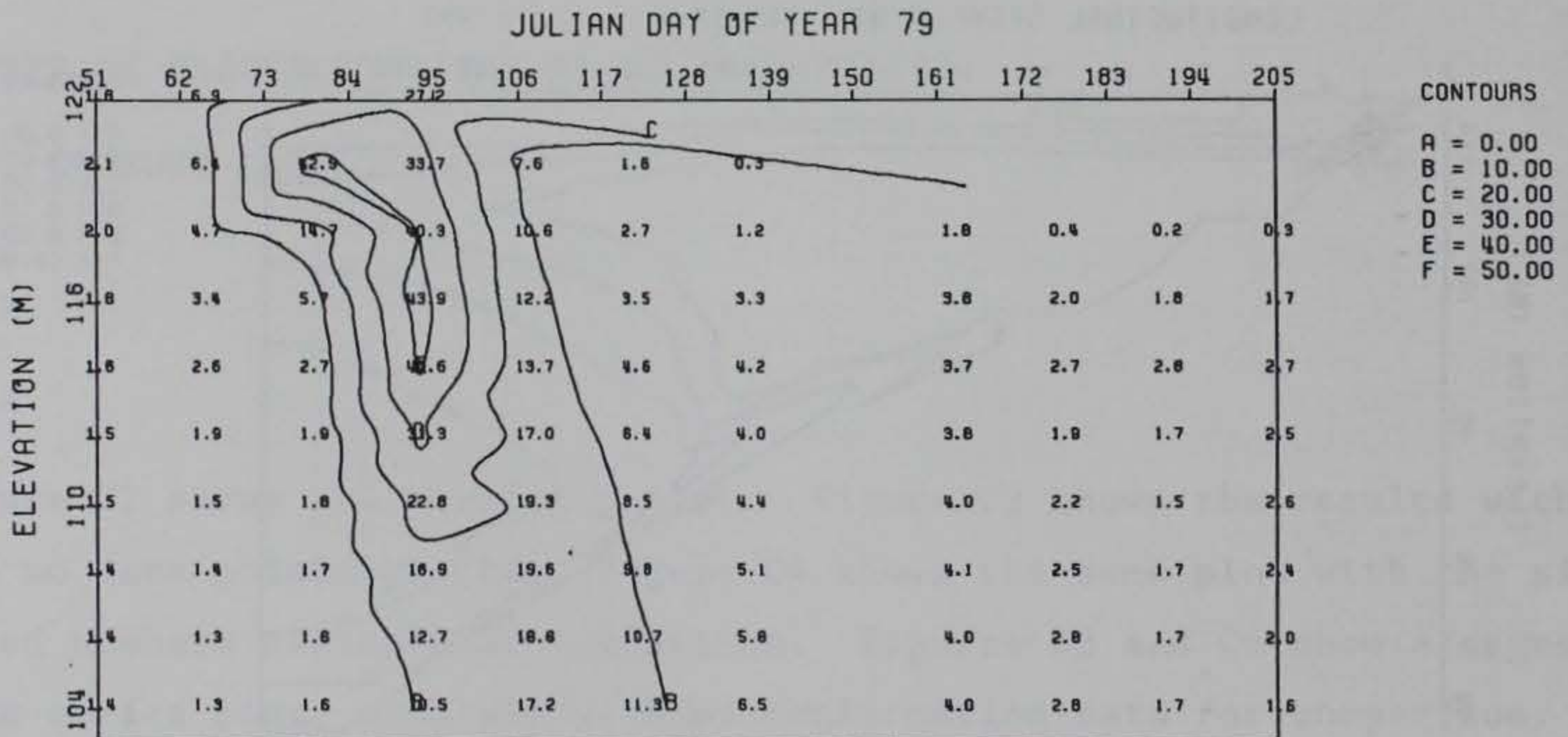
REGULAR DEGRAY RUN WITH 1979 TVDS DATA



DISSOLVED OXYGEN (MG/L) BRANCH 1 ABTM: 79205.49

Figure C4. Example of reservoir contour (side view) with simulated data

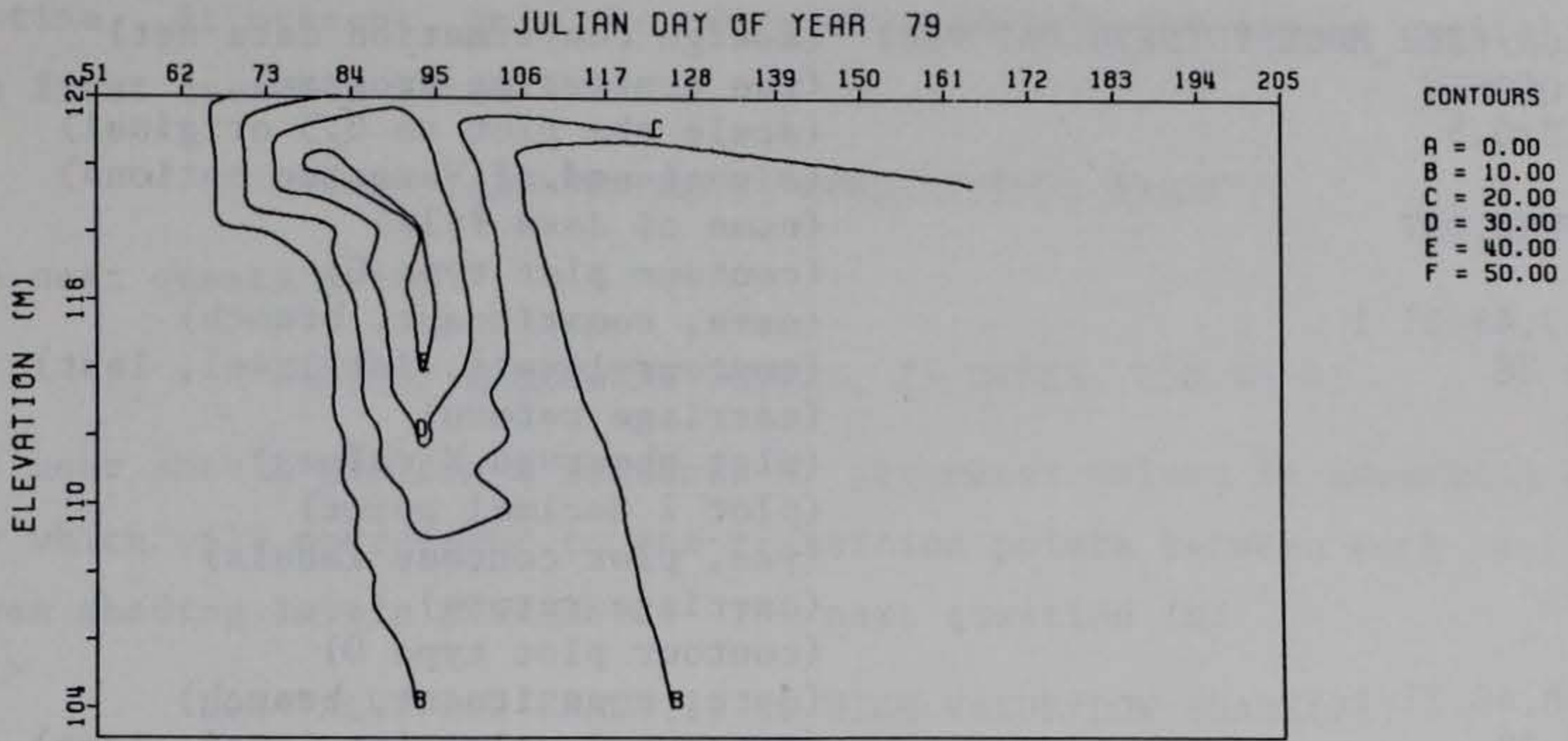
REGULAR DEGRAY RUN WITH 1979 TVDS DATA



TOTAL SUSPENDED SOLIDS (MG/L) SEGMENT: 10

Figure C5. Example of segment-time series contour with observed (confirmation) data

REGULAR DEGRAY RUN WITH 1979 TVDS DATA

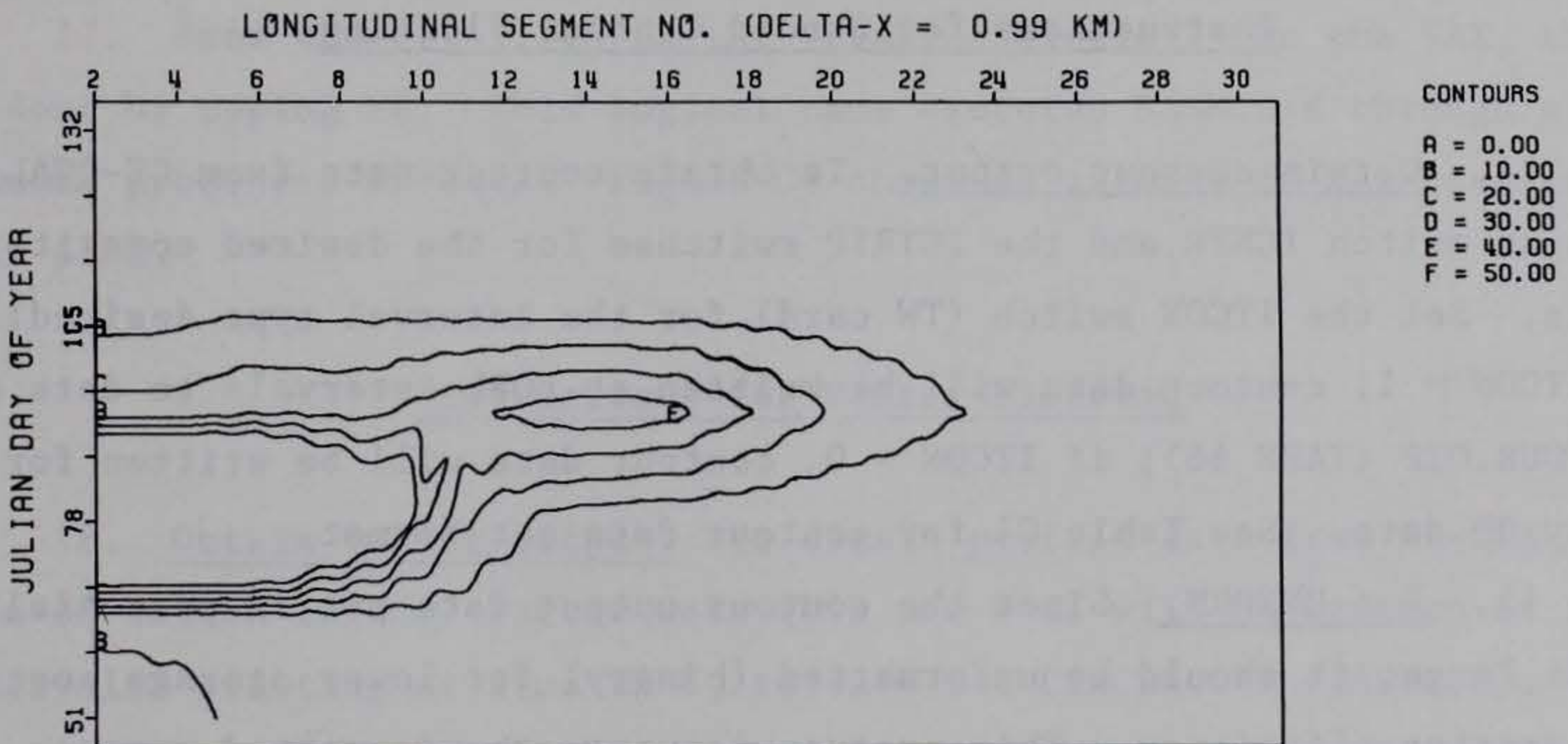


TOTAL SUSPENDED SOLIDS (MG/L)

SEGMENT: 10

Figure C6. Example of segment-time series contour without observed (confirmation) data

REGULAR DEGRAY RUN WITH 1979 TVDS DATA



TOTAL SUSPENDED SOLIDS (MG/L)

BRANCH 1

LAYER 8

Figure C7. Example of reservoir depth-time series contour (top view)

shows an example of such a command file, with an explanation on the right side.

| | | | |
|------------------|-------------|------|-----------------------------------|
| ASSIGN/USER_MODE | VD79R2U.DAT | VER1 | (assign confirmation data set) |
| RUN | QCONTV | | (run contouring program) |
| SCALE= | 0.5 | | (scale the plot to 0.5 original) |
| /E | | | (signal end of Versatec options) |
| CONTUNF.DAT | | | (name of data file) |
| 0 | | | (contour plot type 0) |
| 79163.48 | 21 | 1 | (date, constituent, branch) |
| 12 | 6 | 28 | (contour levels, 1st level, last) |
| <CR> | | | (carriage return) |
| 1 | | | (plot observed Z values) |
| 1 | | | (plot 1 decimal point) |
| Y | | | (yes, plot contour labels) |
| <CR> | | | (carriage return) |
| 0 | | | (contour plot type 0) |
| 79168.48 | 21 | 1 | (date, constituent, branch) |
| 12 | 6 | 28 | (contour levels, 1st level, last) |
| <CR> | | | (carriage return) |
| 1 | | | (plot observed Z values) |
| 1 | | | (plot 1 decimal point) |
| Y | | | (yes, plot contour labels) |
| <CR> | | | |
| <CR> | | | |
| <CR> | | | |
| <CR> | | | (4 carriage returns to exit) |

Instructions for Shaded Contour Plotting

14. Obtain contour output. To obtain contour data from CE-QUAL-W2, turn on switch ICNTR and the ICTRIP switches for the desired constituents. Set the ITCON switch (TW card) for the interval type desired: If ITCON = 1, contour data will be written at FOPL intervals to data set CONTOUR.OTP (TAPE 66); if ITCON = 0, contour data will be written for every OD date. See Table C1 for contour data set format.

15. Run UNFORM. Since the contour output data set is potentially quite large, it should be unformatted (binary) for lower storage costs and greater efficiency. This program converts the formatted contour data set from CE-QUAL-W2 into an unformatted one. This step is not necessary if unformatted output is obtained directly from CE-QUAL-W2.

16. Run QSHADE (linked with Versatec subroutines). This program can only produce output on a Versatec plotter, using the TONE subroutine. At present, only the reservoir side view option is available. The first question asked is:

DATE (ABTM FORMAT), CONSTITUENT, BRANCH?

The next question is:

LIST OF 6 SHADING LEVELS, IN ORDER, LOW TO HI

The user should provide a sequence of parameter values in ascending order which will correspond to the transition points between each of the seven shading levels available. The next question is:

LOW VALUE/LOW SHADE(1) OR HIGH VALUE/LOW SHADE(2)?

Here the user decides whether a low parameter value is associated with a light shade (option 1) or with a dark shade (option 2). The plot will be created and the process repeated if desired by the proper response to the question:

ANOTHER? (Y/N)

On the VAX, plot files will be created in VECTR1.PLV and PARM.PLV.

17. Send the PLV files to the Versatec plotter. On the VAX, this is done by typing PH. This logical name executes RASM.EXE through a command procedure PH*ase2. Figure C8 shows an example of a shaded contour plot.

Instructions for Vector Plotting

18. Obtain vector output. To obtain profile data from CE-QUAL-W2, turn on switch ICIRC. Vector data (U's and W's) will be written at FOPL intervals, starting at time TBPL, to data set CIRCLN.OTP (TAPE 65).

19. Run VECPLOTV (linked with Calcomp/Versatec subroutines) to plot directly to the Versatec. On the VAX, plot files will be created

REGULAR DEGRAY RUN WITH 1979 TVDS DATA

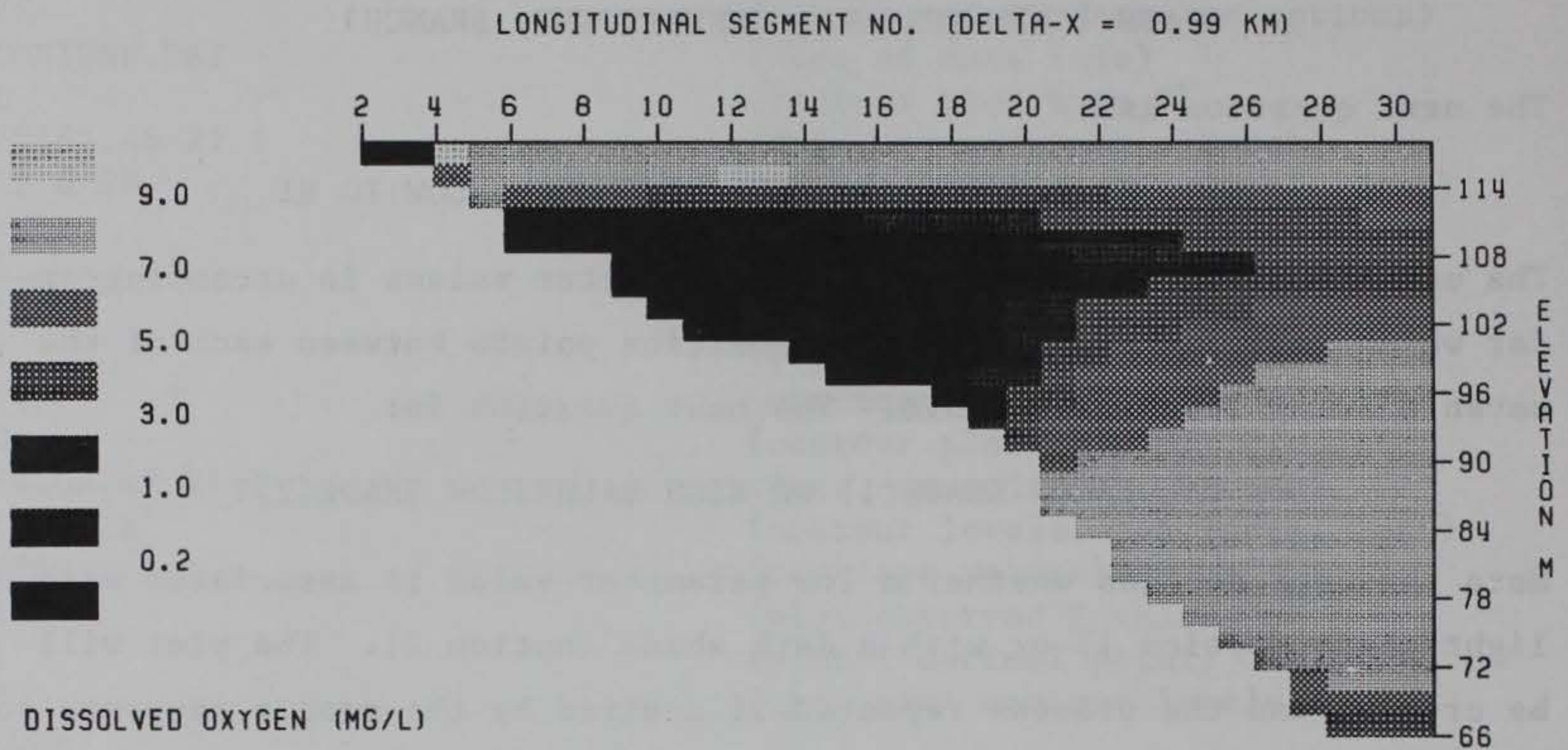


Figure C8. Example of shaded contour plotting

in VECTR.PLV and PARM.PLV. Check for clipped or unplottable vectors, indicating problems with the data or program.

20. Send the PLV files to the Versatec plotter. On the VAX, this is done by typing PH. This logical name executes RASM.EXE through a command procedure PH*ase2. Figure C9 shows an example of a vector plot.

21. Run VECPLOTP (linked with Tektronix Preview subroutines) to preview on a Tektronix 4014 or equivalent. Each plot may be viewed separately on a Tektronix terminal. The previewing software must be set up as follows:

START OF PREVIEW
MODE/OPTION? 3 (mode to view each plot separately)

OPTION? C (continue)
OPTION? W (option to set viewing window,
values in inches)

WHERE WOULD YOU LIKE ORIGIN? (X,Y) -1,-1
ENTER SIZE (WIDTH,HEIGHT) 6,4

OPTION? E,C (erase screen and continue)
(type C to continue as necessary)
(plot should now appear on screen)

OPTION? E,C (to continue with the next plot)
OPTION? Q (to quit the program)

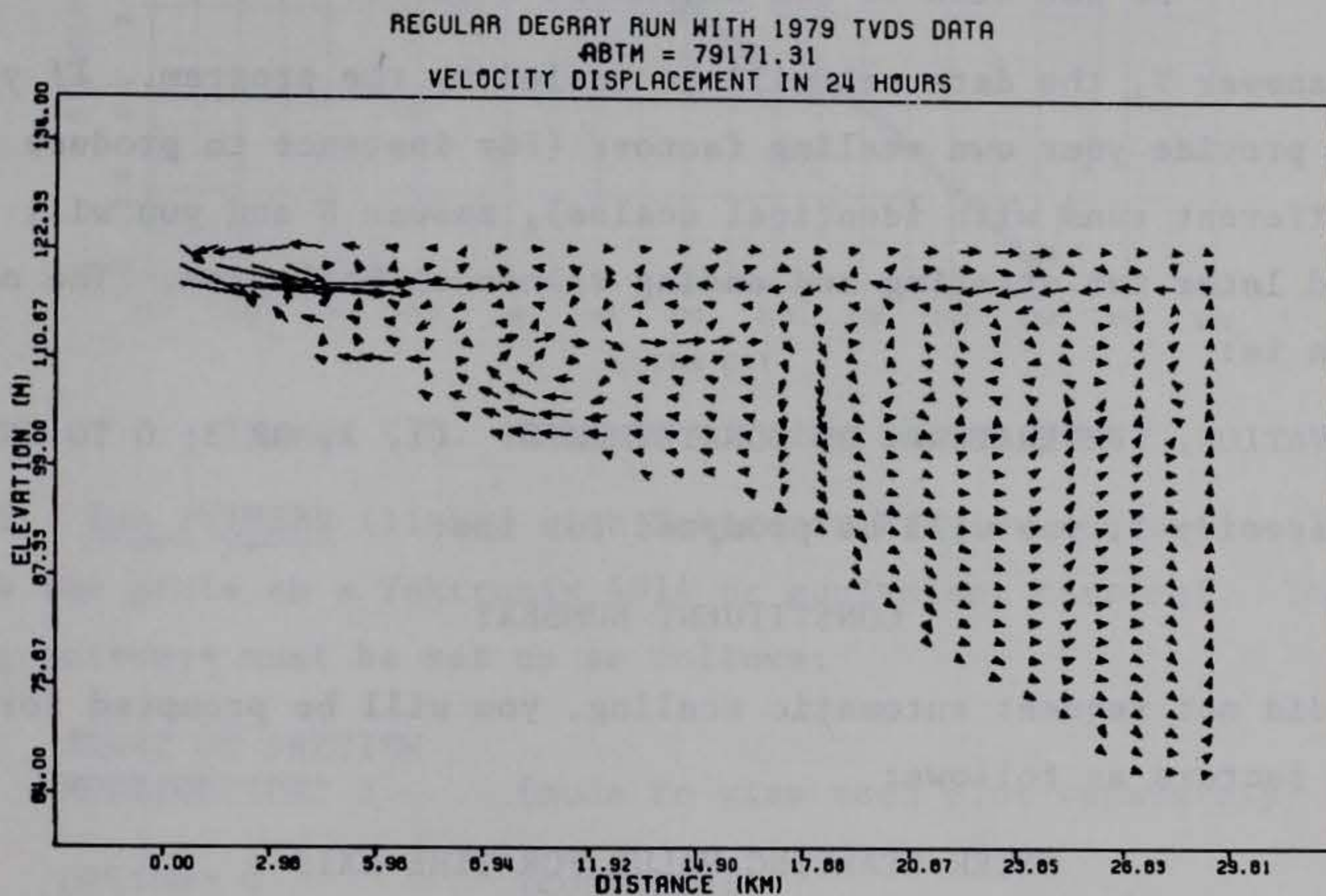


Figure C9. Example vector plot

Vectors are plotted by combining the U and W scalars, with U positive to the right (in kilometres) and W positive upward (in metres). The tail of the arrow is plotted at the segment and layer location, and the head of the arrow is plotted at the end of the velocity displacement from the tail. Vector lengths are scaled for a certain number of hours, depending on the length of the largest vector. If both U and W are zero (less than 0.0001 with a formatted data set), no arrow head will be drawn. Figure C9 shows an example of a vector plot.

Instructions for Time Series Plotting

22. Obtain time series output. To obtain time series data from CE-QUAL-W2, turn on switch ITSR. Data will be written at FOTSR intervals starting at time TBTSR, to data set TIMSER.OTP (TAPE 63). Time series data are provided for surface water elevation and flow-weighted temperature and constituent concentrations in the main stem outflow, for constituents specified on the CW card.

23. Run VTIMSER (linked with Calcomp/Versatec subroutines) to plot directly to the Versatec. The first question asked is:

DO YOU WISH TO USE AUTOMATIC SCALING? (Y/N)

If you answer Y, the data set will be scaled by the program. If you wish to provide your own scaling factors (for instance to produce plots from different runs with identical scales), answer N and you will be prompted later for starting and ending values on both axes. The next question is:

ELEVATION, TEMPERATURE, OR CONSTITUENTS? (1, 2, OR 3; 0 TO END)

If you specify 3, you will be prompted for the:

CONSTITUENT NUMBER?

If you did not request automatic scaling, you will be prompted for the scaling factors as follows:

ENTER STARTING VALUE FOR TIME AXIS

ENTER ENDING VALUE FOR TIME AXIS

ENTER STARTING VALUE FOR PARAMETER AXIS

ENTER ENDING VALUE FOR PARAMETER AXIS

As many plots as desired can be created; enter a zero in response to the ELEVATION... question to terminate plotting. On the VAX, plot files will be created in VECTRI.PLV and PARM.PLV.

24. Send the PLV files to the Versatec plotter. On the VAX this is done by typing PH. This logical name executes a command procedure

PH*ase2 which runs RASM.EXE. Figure C10 shows an example of a time series plot.

REGULAR DEGRAY RUN WITH 1979 TVDS DATA

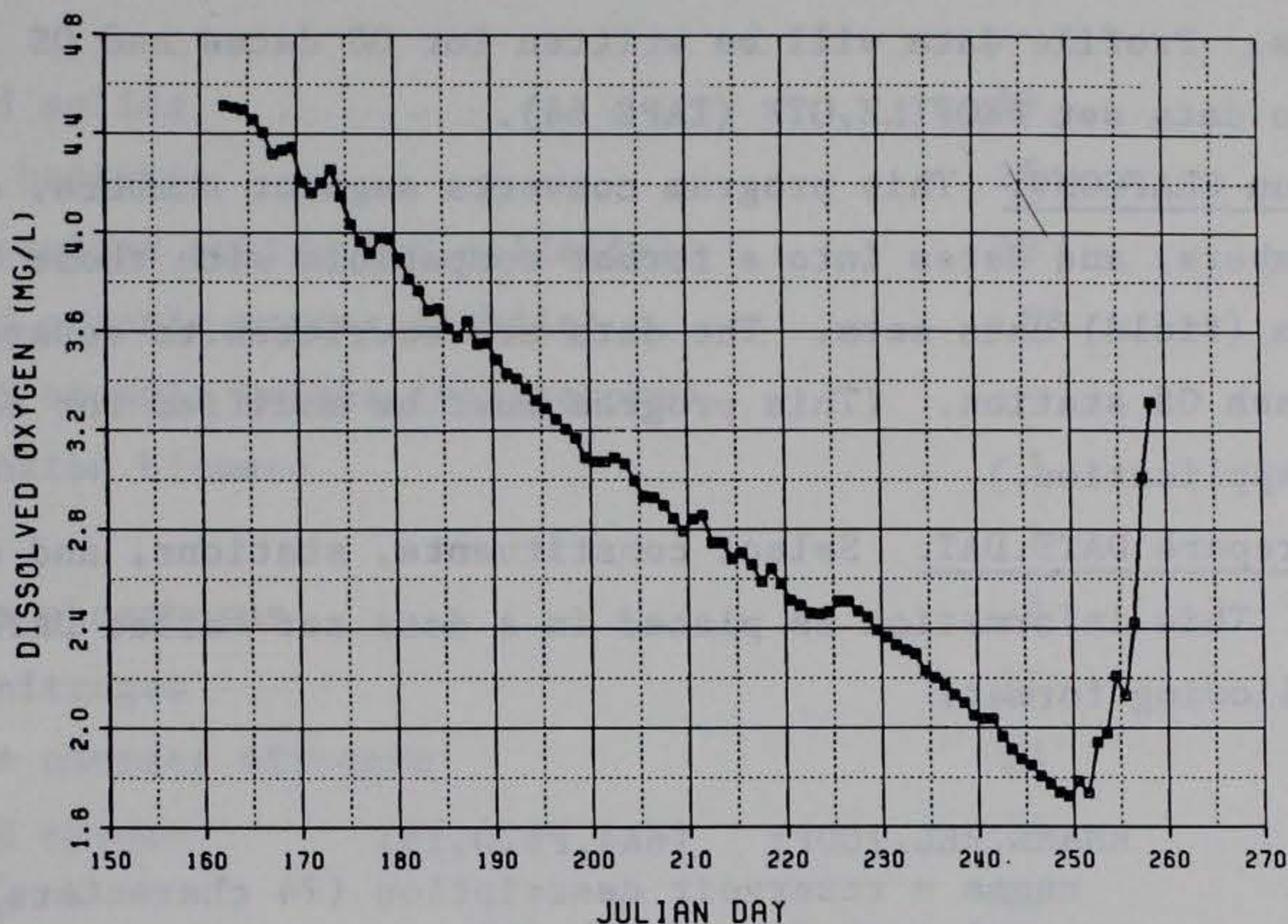


Figure C10. Example of time series plot

25. Run PTIMSER (linked with Tektronix Preview subroutines) to preview the plots on a Tektronix 4014 or equivalent terminal. The pre-viewing software must be set up as follows:

START OF PREVIEW
MODE/OPTION? 3 (mode to view each plot separately)

OPTION? C (continue)
OPTION? W (option to set viewing window,
values in inches)

WHERE WOULD YOU LIKE ORIGIN? (X,Y) -1,-1
ENTER SIZE (WIDTH,HEIGHT) 8,6

OPTION? E,C (erase screen and continue)
(type C to continue as necessary)
(follow directions in step 2 above)

OPTION? E,C (to continue with the next plot)
OPTION? Q (to quit the program)

Instructions for Profile Plotting

26. Obtain profile output. To obtain profile data from CE-QUAL-W2, turn on switch IVPR and ICTRIP switches for the desired constituents. Profile data will be written for OD dates and OS segments, to data set PROFILE.OTP (TAPE 64).

27. Run GRAFCONV. This program converts segment numbers, constituent numbers, and dates into a format compatible with those of the confirmation (field) data sets. The data are rewritten to separate data files for each OS station. (This program must be modified for each particular application.)

28. Prepare DATE.DAT. Select constituents, stations, and dates to be plotted. This information is placed in a data set called DATE.DAT, with the following format:

```
CARD 1      RNAME,REL,ICOPY   (6A4,F6.0,I5)
             rname = reservoir description (24 characters)
             rel  = maximum depth (m)
             icopy = hardcopy switch
                  (0=off, 1=autocopy, 2=versatec direct)
```

```
SET 2      NFD,IFD(I),I=1,NFD (10I8)
           nfd = no. of files to be read
           ifd = file types
                1 = 1st simulation data set (sim1)
                2 = 2nd simulation data set (sim2)
                3 = 3rd simulation data set (sim3)
                4 = 1st confirmation data set (ver1)
                5 = 2nd confirmation data set (ver2)
```

```
SET 3      NC,NDDUM,DATES(NC,N),N=1,NDDUM (10I8)
           nc = constituent number ***
           nddum = no. of dates to be plotted
           dates = dates to be plotted (in YYYYMMDD format)
```

*** Constituent numbers correspond to confirmation numbers used for CE-QUAL-R1 (See Table C3). Set 3 is repeated for each constituent desired. If dates are repeated for subsequent constituents, NDDUM can be set to 1. In this case, the previous set of dates will be used. See example below.

Table C3

Correspondence of Constituent Numbers in CE-QUAL-R1 and CE-QUAL-W2

| <u>Constituent Name</u> | <u>CE-QUAL-R1</u> | <u>CE-QUAL-W2</u> |
|---------------------------------------|-------------------|-------------------|
| Tracer | -- | 1 |
| Suspended solids | 19 | 2 |
| Coliform bacteria | 26 | 3 |
| Total dissolved solids (or salinity) | 18 | 4 |
| Dissolved organic matter (labile) | 8* | 5 |
| Dissolved organic matter (refractory) | -- | 6 |
| Phytoplankton biomass | 3 | 7 |
| Detritus | 7 | 8 |
| Phosphate phosphorus | 9 | 9 |
| Ammonia-nitrogen | 11 | 10 |
| Nitrate + nitrate nitrogen | 12 | 11 |
| Dissolved oxygen | 14 | 12 |
| Sediments | -- | 13 |
| Total inorganic carbon | 10 | 14 |
| Alkalinity | 17 | 15 |
| pH | 16 | 16 |
| Carbon dioxide | 15 | 17 |
| Bicarbonate | -- | 18 |
| Carbonate | -- | 19 |
| Total iron | 20 | 20 |
| Temperature | 1 | (21) |

* Refractory and labile DOM are combined as constituent number 8. The program GRAFCOV combines W2 constituents 5 and 6 as a single parameter for use with confirmation data (R1 constituent 8).

29. @PROGRAF.COM. If you do not want to rename the data sets, use assign statements to connect the actual data set names with the appropriate file name used by the program (see file names above). See example below.

30. Check GRAFDAT.DAT. This file is created to indicate any errors in dates or files. Check it after a run to be sure the data were plotted correctly.

31. Sample of DATE.DAT. Two data files are plotted--one simulation and one confirmation. Two constituents are plotted for seven dates.

| | | | | | | | | | |
|-------|---------|---|--------|--------|--------|--------|--------|--------|--------|
| DG794 | STATION | 4 | 60.00 | 0 | | | | | |
| | 2 | 1 | 4 | | | | | | |
| | 1 | 7 | 790612 | 790626 | 790710 | 790724 | 790807 | 790821 | 790904 |
| | 14 | 1 | | | | | | | |

32. Sample of PROGRAF.COM.

```
ASSIGN/USERMODE VD794.DAT VER1
ASSIGN/USERMODE R2794.DAT SIM1
RUN PROGRAF
```

If Versatec plots were requested, VECTR1.PLV and PARM.PLV plot files will be created. Send these files to the Versatec plotter by typing PH. This executes a command procedure PH*ase2 which runs RASM.EXE. Figures C11 and C12 show examples of profile plots.

Instructions for Statistical Routine

33. Obtain profile output. The statistics routine will utilize the same files as produced for the profile routines. To obtain profile data from CE-QUAL-W2, turn on the switch IVPR and the ICTRIP switches for the desired constituents. Profile data will be written for OD dates and OS segments to data set PROFILE.OTP (TAPE 64).

34. Run GRAFCONV. This program converts segment numbers, constituent numbers, and dates into a form compatible with the confirmation (field) data sets. The data are written to separate files for each OS station.

22-JUL-85 DG794 STATION 4
SOLID LINE = SIMULATION 1

X CONFIRMATION 1

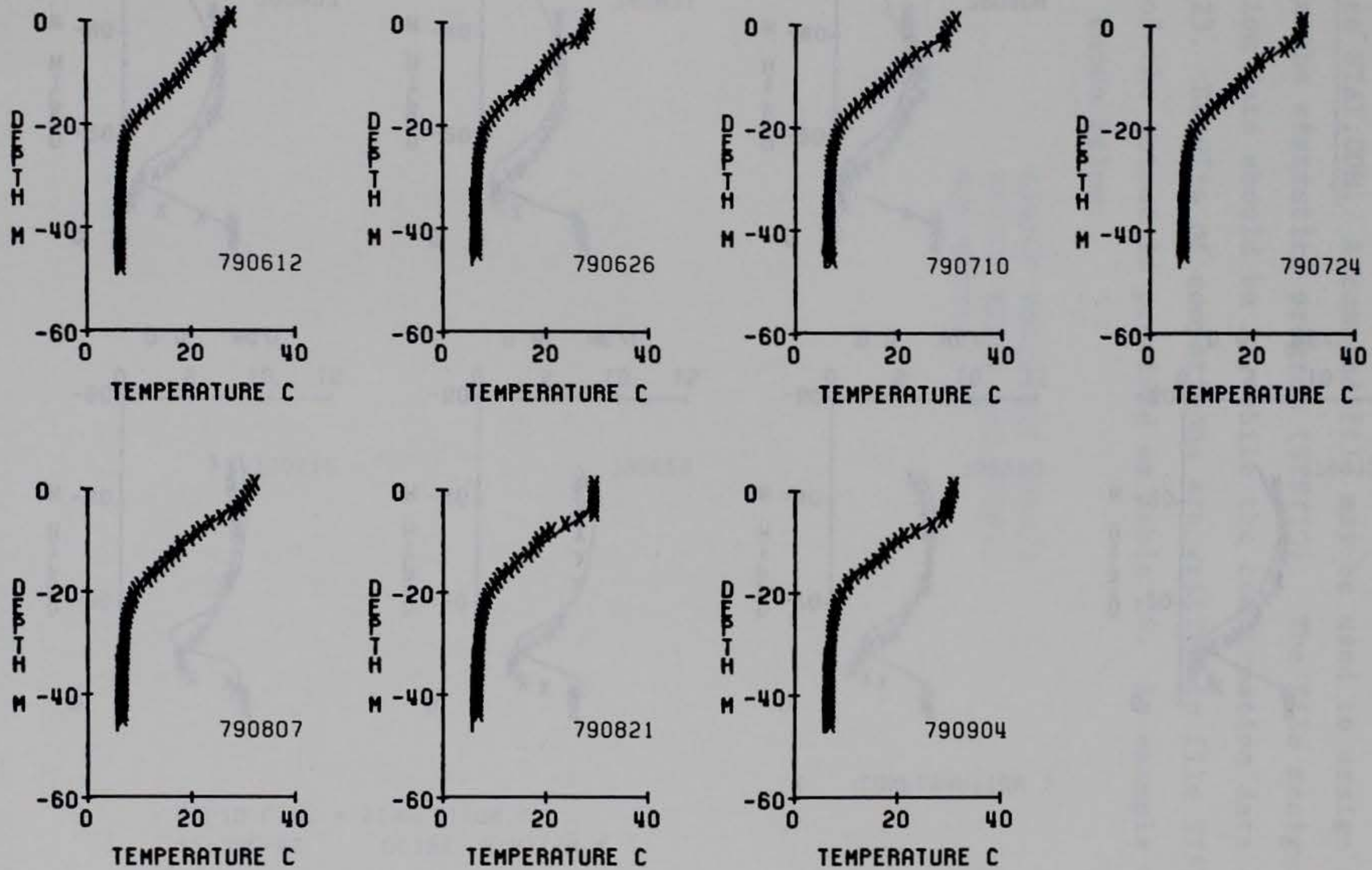


Figure C11. Example of profile plot for water temperature

22-JUL-85 DG794 STATION 4
SOLID LINE = SIMULATION 1

X CONFIRMATION 1

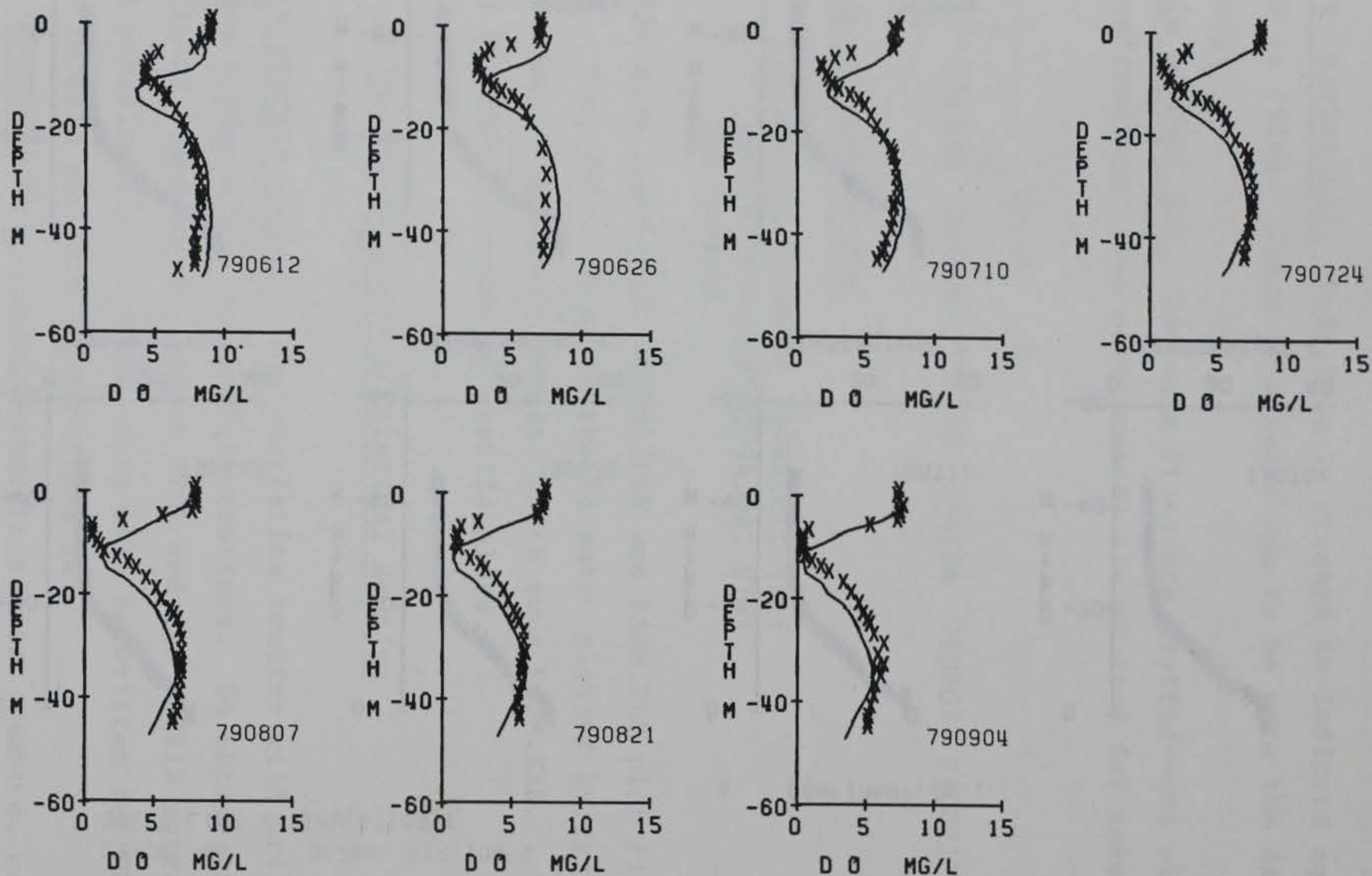


Figure C12. Example of profile plot for dissolved oxygen

35. Prepare STSWICH.DAT. This data set contains a series of flags (1 = on, 0 = off, format 50I1) to indicate which constituents are to be compared in the statistical routine. Constituent numbers correspond to confirmation numbers (see Table C3).

36. Prepare STAT.COM. A command file may be used to assign file names and to run the statistics program (STSTIC). The file assignment for the simulation data should be 22, while the confirmation data are read from file 23. Results of comparisons are written to file STST.OTP, and an example of the output is provided as Table C4. An example of the command file is shown below:

```
ASSIGN VD804.DAT FOR023
ASSIGN R2804.DAT FOR022
RUN STSTIC
```


Table C4

Example Output from Statistical Routine

STATISTICAL PROGRAM FOR CE-QUAL-W2 COMPARING FILES
 REGULAR DEGRAY RUN WITH 1980 TVDS DATA AND DEGRAY 80 ST.4
 VAX VERSION 11-6-84 FOR DEGRAY

RELIABILITY INDEX LEGGETT AND WILLIAMS ECOLOGICAL MODELLING 13(1981)303-312
 PAIRED T TEST FOR MEANS SOKAL AND ROHLF 1969 BIOMETRY W.H.FREEMAN AND COMPANY
 NORMALIZED MEAN ERROR(SUM(ABS(P-O)/O)*100.)/N,
 COEFFICIENTS FOR THE LINEAR REGRESSION EQUATION
 STATISTICS ARE UNDEFINED WHEN .999 IS PRINTED

| VARIABLE | DATE YYMMDD | NO. OF COMPAR | OBSERVED MEAN | PREDICTED MEAN | T STATISTIC | RELIABILITY INDEX | NORMALIZED MEAN ERROR |
|----------|----------------|------------------|------------------|-------------------|----------------|----------------------|--------------------------|
| TEMP | 800304 | 24 | 0.692E+1 | 0.692E+1 | 0.240E-1 | 0.101E+1 | 0.491E+0 |
| TEMP | 800318 | 24 | 0.769E+1 | 0.841E+1 | -0.170E+2 | 0.110E+1 | 0.976E+1 |
| TEMP | 800401 | 24 | 0.852E+1 | 0.920E+1 | -0.882E+1 | 0.110E+1 | 0.895E+1 |
| TEMP | 800415 | 24 | 0.956E+1 | 0.101E+2 | -0.324E+1 | 0.112E+1 | 0.975E+1 |
| TEMP | 800429 | 24 | 0.103E+2 | 0.108E+2 | -0.178E+1 | 0.114E+1 | 0.118E+2 |
| TEMP | 800515 | 24 | 0.108E+2 | 0.114E+2 | -0.281E+1 | 0.112E+1 | 0.104E+2 |
| TEMP | 800610 | 24 | 0.125E+2 | 0.126E+2 | -0.285E+0 | 0.112E+1 | 0.105E+2 |
| TEMP | 800624 | 24 | 0.129E+2 | 0.129E+2 | 0.159E-1 | 0.111E+1 | 0.908E+1 |
| TEMP | 800708 | 24 | 0.135E+2 | 0.135E+2 | 0.123E+0 | 0.110E+1 | 0.811E+1 |
| TEMP | 800722 | 24 | 0.134E+2 | 0.142E+2 | -0.268E+1 | 0.114E+1 | 0.121E+2 |
| TEMP | 800805 | 24 | 0.133E+2 | 0.144E+2 | -0.398E+1 | 0.116E+1 | 0.144E+2 |
| TEMP | 800819 | 24 | 0.135E+2 | 0.148E+2 | -0.417E+1 | 0.118E+1 | 0.162E+2 |
| TEMP | 800902 | 24 | 0.136E+2 | 0.150E+2 | -0.456E+1 | 0.117E+1 | 0.143E+2 |
| TEMP | 800916 | 24 | 0.136E+2 | 0.151E+2 | -0.395E+1 | 0.120E+1 | 0.169E+2 |
| TEMP | 800930 | 24 | 0.127E+2 | 0.144E+2 | -0.431E+1 | 0.121E+1 | 0.176E+2 |
| TEMP | 801014 | 24 | 0.124E+2 | 0.140E+2 | -0.337E+1 | 0.124E+1 | 0.205E+2 |
| TEMP | 801028 | 24 | 0.122E+2 | 0.136E+2 | -0.286E+1 | 0.123E+1 | 0.195E+2 |
| TEMP | ALL DATES | 408 | 0.116E+2 | 0.124E+2 | -0.104E+2 | 0.115E+1 | 0.124E+2 |

A=0.213E+01 B=0.888E+00 T FOR SLOPES=-.996E+01 T FOR INTERCEPTS= 0.143E+02
 R SQUARE=0.939E+00 ST.ERROR OF EST.=0.294E+02